Growth and Differentiation Factor-15 and MicroRNA in Intensive Care Unit Acquired Paresis

Susannah Amelia Alice Bloch

Imperial College London

National Heart and Lung Institute

Submitted for the degree of PhD

January 2015

Declaration of originality

I confirm that this thesis and the data within it are my own work. Where information or data has been used from other members of the group, collaborators or the literature it has been acknowledged accordingly.

Susannah Bloch

Copyright declaration

The copyright of this thesis rests with the author and is made available under a Creative Commons Attribution Non-Commercial No Derivatives licence. Researchers are free to copy, distribute or transmit the thesis on the condition that they attribute it, that they do not use it for commercial purposes and that they do not alter, transform or build upon it. For any reuse or redistribution, researchers must make clear to others the licence terms of this work.

Dedicated to our patients.

Acknowledgements

This PhD has taken the help and support of many people. Firstly, I would like to thank my supervisors Mike Polkey, Paul Kemp and Mark Griffiths. From the beginning of this project with applications for funding in 2009 to the submission of this thesis they have provided careful guidance, practical help and endless support; without them none of this would have been possible and I cannot thank them enough. The Medical Research Council generously funded this PhD and additional financial support has come from the British Lung Foundation and the American Thoracic Society – thank you. Particular thanks go to Thomas Syburra, Ulrich Rosendalh and Trevor Morgan; without the help and support of the surgical, intensive care and biomedical research unit teams this project would not have worked. Thank you to Jen Lee and Amy Lewis who patiently taught me all the molecular biology techniques. Thank you to all the friends I have made in the Critical Care, Muscle and Kemp groups. Most importantly I would like to thank all the patients who were involved in these clinical studies. Thank you for your time and effort, for allowing us to take samples and for your interest and faith in the project. Your contribution was truly altruistic and I am indebted to you.

Thank you to my family, to Neil, to Edie and Milo, to my mum Caroline and sister Claudia. You have supported me through this and make it all worthwhile. I love you and am eternally grateful.

Abstract

Intensive Care Unit Acquired Paresis (ICUAP) is a major health concern facing today's critical care patients. This syndrome of severe muscle wasting and weakness is associated with significant morbidity and mortality, resulting in a substantial clinical and financial burden. However as yet, other than early mobilisation and rehabilitation, there are no available treatments. The aim of this work was to identify molecular mechanisms in the aetiology of ICUAP with a view to finding novel therapeutic targets.

In a prospective study of high-risk elective cardiothoracic patients, prolonged elevation of circulating GDF-15, a stress-induced cytokine and TGF-β family member, was associated with acute muscle wasting. Following on from this work, the hypothesis that GDF-15 might be a driver of muscle wasting in ICUAP was tested in an observational study of 20 ICUAP patients and 7 elective cardiothoracic controls. Both circulating GDF-15 and muscle GDF-15 mRNA expression were elevated in patients compared to controls. In addition microRNAs essential for muscle homeostasis and protection against TGF-β signalling were found to be down-regulated. *In vitro* experiments demonstrated that GDF-15 could increase expression of muscle atrophy-related genes and supress these microRNAs. Increased sensitivity to TGF-β signalling secondary to down-regulation of muscle microRNAs driven by GDF-15 hypothesised as an aetiological mechanism of muscle wasting in critical illness. Supporting this hypothesis, transfection of miR-181a into C2C12 cells reduced the response to TGF-β1 and increased TGF-β signalling was found in the muscle of ICUAP patients.

An interventional study of neuromuscular electrical stimulation (NMES) in ICU demonstrated that although increased mobility in critical care patients can improve outcomes there is a risk that NMES may cause muscle damage. Finally preliminary data, suggested that miR-181a is a potential biomarker for ICUAP.

GDF-15 and microRNAs are potential therapeutic targets and this work supports the need for further investigation into these pathways in ICUAP.

Table of contents

Declaration of originality 2

Copyright declaration 2

Acknowledgements 6

Abstract 8

Table of contents 10

List of figures 17

List of tables 19

Abbreviations 20

Chapter 1 Introduction 22

1.1 Why investigate molecular mechanisms in ICUAP? 22

1.2 Intensive care unit acquired paresis (ICUAP) 23

1.2.1 Background 23

1.2.2 ICUAP from a clinical perspective 25

1.2.2.1 Definition and diagnosis 25

1.2.2.2 Incidence. 30

1.2.2.3 Clinical risk factors 31

1.2.2.4 Outcome and prognosis 34

1.2.2.5 Prevention and treatment strategies 36

1.2.3 ICUAP muscle dysfunction and molecular mechanisms 39

1.2.3.1 Alterations in muscle phenotype and function in ICUAP. 40

1.2.3.2 Muscle Mass in ICUAP 41

1.2.3.2.1 Up-regulation of muscle protein breakdown in ICUAP 42

1.2.3.2.2 Autophagy 43

1.2.3.2.3 Down-regulation of muscle protein synthesis in ICUAP 44

1.2.3.3 TGF-β signalling in muscle atrophy 45

1.2.3.4 Reduction in force generating capacity in ICUAP 48

1.2.3.4.1 Neuropathy and nerve activity. 49
1.2.3.4.2 Myocyte structure and myofilament integrity;..... 50
1.2.3.4.3 Electrical in-excitabiltity..... 51
1.2.3.4.4 Bio-energenetic failure, oxidative stress and glycaemic control: 52
1.3 GDF-15..... 54
1.3.1 Background 54
1.3.2 Rationale for investigation of GDF-15 in muscle wasting and ICUAP 56
1.4 MicroRNA 58
1.4.1 Background 58
1.4.2 Muscle microRNAs 59
1.4.3 Rationale for investigation of MicroRNAs in ICUAP in relation to GDF-15 62
1.5 Summary, aims and hypotheses 64
Chapter 2 Methods 66
2.1 Clinical Methods..... 66
2.1.1 Ethical approval..... 66
2.1.2 Assessment of quadriceps muscle bulk 66
2.1.2.1 Inter-observer variability..... 67
2.1.2.2 Definition of a significant change in US RF_{csa} 68
2.1.3 Assessment of muscle strength 69
2.1.3.1 Medical Research Council - strength score (MRC-SS) 69
2.1.3.2 Quadriceps maximal voluntary contraction (QMVC) 70
2.1.4 Risk Scoring Systems 72
2.1.4.1 European System for Cardiac Operative Risk Evaluation (EuroSCORE) 72
2.1.4.2 Sequential Organ Failure Assessment Score (SOFA) 73
2.1.5 Blood sampling, handling and storage of samples 74
2.1.6 Muscle biopsy, handling and storage of samples 75
2.2 Molecular Methods..... 76

2.2.1 General solutions 76
2.2.2 Cell culture and differentiation 76
2.2.3 Cell stretch experiments 77
2.2.3.1 Cell culture for stretched cells 77
2.2.3.2 Cell stretch using Flexcell® FX-4000™ apparatus 78
2.2.3.3 Cell Viability and damage assays following cell stretch. 78
2.2.3.4 Method development 79
2.2.4 GDF-15, Myostatin and TGF-β treatment 80
2.2.5 Luciferase assays 81
2.2.5.1 Preparation of DNA plasmids 81
2.2.5.2 Transfection of DNA plasmids 83
2.2.5.3 Luciferase assays 83
2.2.5.4 Over-expression of miR-181a 84
2.2.6 RNA extraction 85
2.2.6.1 RNA extraction from Cells 85
2.2.6.2 RNA extraction from Human Tissue 85
2.2.6.3 MicroRNA extraction from Plasma 86
2.2.7 cDNA synthesis and quantative PCR (qPCR) for mRNA 87
2.2.8 qPCR quantification of microRNA. 90
2.2.8.1 Across plate standardisation of microRNA qPCR data. 91
2.2.9 Protein Extraction 91
2.2.9.1 From Cells 91
2.2.9.2 From Human Tissue 91
2.2.9.3 Protein quantification 92
2.2.10 Western Blotting 93
2.2.10.1 Western blotting procedure 93
2.2.10.2 Quantification of protein by Western blot. 95
2.2.11 ELISA 95

2.2.12 Histology of muscle samples 96
2.2.12.1 Muscle fibre diameter 96
2.2.12.2 Immunoflourscencent staining for fibre type 96
2.2.12.3 Localisation of pSMAD-2/3 97
2.3 Statistical methods 98
2.3.1 Statistical handling and analyses of demographic data and results from the clinical studies. 98
2.3.1.1 Analysis of in vitro data. 99
Chapter 3 Investigation of circulating mediators of muscle homeostasis and Growth and Differentiation Factor-15 in acute muscle wasting following high risk cardiothoracic surgery. 100
3.1 Rationale 100
3.2 Hypothesis 101
3.3 Patients studied and study design 102
3.4 Results 103
3.4.1 Patients and change in RF_{csa} 103
3.4.2 Assessment of muscle strength 106
3.4.3 Myostatin 106
3.4.4 IGF-1 107
3.4.5 GDF-15 108
3.5 Discussion 110
3.5.1 Summary of findings 110
3.5.2 Discussion 111
3.5.3 Critique of the method 114
3.5.4 Conclusion 115
Chapter 4 GDF-15 regulation of muscle microRNAs in the pathogenesis of ICUAP . 118
4.1 Rationale 118
4.2 Hypothesis 120

4.3 Patients studied and study design 120
4.4 Results 121
4.4.1 Patients 121
4.4.2 Muscle Layer Thickness (MLT) 124
4.4.3 Histology 124
4.4.4 GDF-15 in the plasma and muscle GDF-15 mRNA expression in ICUAP .. 126
4.4.5 Muscle mRNA expression in ICUAP 127
4.4.6 microRNA expression 128
4.4.7 TGF-β receptor type 2 132
4.4.8 TGF -β signalling in ICUAP muscle 133
4.4.9 GDF-15 effects on *in vitro* C2C12 cells 135
4.4.9.1 GDF-15 did not affect SMAD-dependant luciferase activity 135
4.4.9.2 microRNA array 135
4.4.9.3 mRNA expression in GDF-15 treated myotubes 136
4.4.9.4 microRNA expression in GDF-15 treated myotubes 136
4.4.9.5 TGF-β receptor type 1 and 2 protein concentration in GDF-15 treated myotubes 137
4.4.10 MiR-181a over-expression reduced TGF-β signalling 138
4.4.11 Investigation of the potential relationship between GDF-15 and glucose metabolism 139
4.4.11.1 In ICUAP patients 139
4.4.11.2 Effect of glucose concentration of GDF-15 and miR-181a expression in C2C12 myotubes..... 140
4.4.11.3 Plasma GDF-15 in COPD patients with diabetes mellitus or impaired glucose tolerance. 140
4.5 Discussion 142
4.5.1 Main findings..... 142
4.5.2 Discussion..... 143
4.5.3 Critique of the methods 150

4.5.4 Conclusion 154

Chapter 5 An interventional study of neuromuscular electrical stimulation in patients at risk of acute muscle wasting on the cardiothoracic ICU. 156

5.1 Rationale 156

5.2 Hypotheses 158

5.3 Study design 158

5.3.1 Original protocol 158

5.3.2 Amendments to the protocol 162

5.3.2.1 Feasibility 162

5.3.2.2 Pacemakers 164

5.3.2.3 Recruitment of ICU patients. 165

5.3.2.4 Final protocol 165

5.4 Neuromuscular electrical stimulation 166

5.5 Results 170

5.5.1 Effect of cyclic mechanical stretch on myostatin signalling in confluent C2C12 myoblasts. 170

5.5.2 Patients studied 171

5.5.3 Protocol compliance and adverse events. 174

5.5.4 Primary outcome measure: change in myostatin mRNA expression 175

5.5.5 Secondary outcome measures 175

5.5.5.1 US 175

5.5.5.2 Effect of NMES on mRNA and microRNA expression 177

5.6 Discussion 179

5.6.1 Main findings 179

5.6.2 Comment on Recruitment 180

5.6.3 Critique of the method 182

5.6.4 Significance of the results. 184

5.7 Conclusion 186

Chapter 6 MiR-181a: a potential biomarker of acute muscle wasting following cardiac surgery? 188

6.1 Rationale 188

6.2 Hypothesis 189

6.3 Patients studied 190

6.4 Results 190

6.4.1 Patients 190

6.4.2 Circulating microRNAs in acute muscle wasting. 190

6.4.2.1 MiR-181a 192

6.4.2.2 MiR-1 192

6.4.2.3 MiR-16 193

6.5 Discussion 193

6.5.1 Summary of the findings 193

6.5.2 Clinical perspective 193

6.5.3 Critique of the method 195

6.6 Conclusion 198

Chapter 7 General Discussion 200

7.1 Summary of main findings 200

7.2 General limitations 203

7.3 Future directions. 205

7.4 Implications for the treatment of ICUAP 206

Chapter 8 References 210

Appendixes 236

Appendix A1 – Copy right permissions. 236

Appendix A2 – MicroRNA Array Results 238

Appendix A3 – David analysis of MiRWALK microRNA targets. 243

Appendix A4 – Publications, presentations and prizes. 244

Appendix A5 – Medical Research Council Grant Details 247

List of figures

Figure 1-1 Schematic of the basic molecular pathways balancing muscle protein synthesis and breakdown. 42
Figure 1-2 Representation of potential mechanisms reducing force generating potential of skeletal muscle in ICU- acquired paresis (ICUAP) 48
Figure 1-3 Mitochondrial dysfunction in bio-energenetic failure results in increased free radical production and in turn further mitochondrial damage. 53
Figure 1-4 Schematic representation of the current understanding of the role of microRNAs in muscle homeostasis. 62
Figure 2-1 Assessment of quadriceps muscle size by rectus femoris cross-sectional area (RF_{csa}) and mid-thigh muscle layer thickness (MLT). 67
Figure 2-2 Bland Altman plot of ultrasound rectus femoris cross-sectional area (US RF_{csa}) to assess inter-observer variability. 68
Figure 2-3 Bland Altman plot of ultrasound rectus femoris cross-sectional area (US RF_{csa}) to assess repeatability and define a significant change. 69
Figure 2-4 Bland Altman plot of measurement of quadriceps strength with the quads chair and handheld dynamometer. 71
Figure 2-5 Relative growth of C2C12 cells on uncoated plastic or collagen coated plates. 77
Figure 2-6 Flexcell® FX-4000™ apparatus. 78
Figure 2-7 Example melt curves. 92
Figure 3-1 Change in Rectus Femoris Muscle Cross Sectional Area (RF_{csa}) in high-risk elective cardiothoracic patients following cardiac surgery. 104
Figure 3-2 Plasma Myostatin Concentration. 107
Figure 3-3 Plasma IGF-1 concentration 108
Figure 3-4 Plasma GDF-15 Concentration 109
Figure 3-5 Area under the curve of rise in GDF-15. 110
Figure 3-6 Schematic representation of the imbalance of circulating regulators of muscle mass following cardiothoracic surgery. 111
Figure 4-1 Effect of GDF-15 treatment of C2C12 myotubes. 119
Figure 4-2 Consort diagram of recruitment of ICUAP patients into the observational study. . 122
Figure 4-3 Muscle Layer Thickness (MLT). 124
Figure 4-4 Muscle biopsy specimens from the rectus femoris of ICUAP patients (n=7) and controls (n=4). 125
Figure 4-5 Immunostained muscle biopsy specimens for fibre typing. 126

Figure 4-6 GDF-15 in ICUAP patients and controls. 127
Figure 4-7 Muscle mRNA expression. 129
Figure 4-8 Muscle MHC expression. 130
Figure 4-9 Rectus femoris muscle microRNA expression of different microRNA. 131
Figure 4-10 Muscle TGF-β type-2 receptor (TGFBR2) protein concentration. 132
Figure 4-11 TGF-β Signalling in ICUAP muscle. 134
Figure 4-12 GDF-15 effects on SMAD dependant CAGA-12-driven luciferase activity. 135
Figure 4-13 GDF-15 and myostatin effects on mRNA and microRNA expression in myotubes. 137
Figure 4-14 TGF-β receptor type 1 and 2 protein (TGFBR1 and 2). 138
Figure 4-15 Over-expression of mir-181a reduced TGF-β signalling. 139
Figure 4-16 Correlation of total insulin exposure in ICUAP patients with plasma GDF-15 140
Figure 4-17 Plasma GDF-15 concentration in COPD patients classified according to glucose tolerence. 142
Figure 4-18 Schematic representation of the interaction between microRNAs and TGF-β (transforming growth factor-β) signalling. 148
Figure 5-1 Planned study design for the interventional study of NMES in elective cardiothoracic patients. 160
Figure 5-2 Final protocol for the interventional study of NMES in elective cardiothoracic patients and critically unwell ICU patients. 166
Figure 5-3 Position of electrodes for NMES. 169
Figure 5-4 NMES in healthy volunteers. 169
Figure 5-5 Effect of cyclic mechanical stretch on myostatin signalling in C2C12 cells 171
Figure 5-6 Consort diagram for the interventional study of NMES in patients at risk of acute muscle wasting on the cardiothoracic ICU. 172
Figure 5-7 mRNA expression at baseline (pre) following 1 week (post) of single leg NMES or control. 176
Figure 5-8 Change in US RF_{csa} following 1 week of NMES or control. 177
Figure 5-9 microRNA at baseline (pre) following 1 week (post) of single leg NMES or control. 178
Figure 6-1 Circulating plasma microRNA following cardiothoracic surgery. 191
Figure 6-2 ROC curve analysis for change in circulating miR-181a of >1.7-fold following cardiothoracic surgery. 192
Figure 7-1 Schematic representation of the possible role of Growth and Differentiation Factor-15 (GDF-15) in the development of intensive care unit acquired paresis. 202

List of tables

Table 1-1 Diagnostic criteria for Intensive care unit acquired paresis (ICUAP). 25
Table 1-2 Summary of findings on nerve conduction studies (NCS), electromyography (EMG) and direct muscle stimulation in Critical Illness Neuropathy (CIN) and Myopathy (CIM). 28
Table 1-3 APACHE III score and the presence of SIRS predict the chance of developing ICUAP within 30 days of mechanical ventilation 31
Table 2-1 Medical Research Council Strength Score..... 70
Table 2-2 EuroSCORE calculation. 73
Table 2-3 Sequential Organ Failure Assessment score. 74
Table 2-4 General Solutions 76
Table 2-5 Restriction digests for plasmid identification..... 83
Table 2-6 qPCR Primers 89
Table 2-7 Housekeeping genes. 90
Table 2-8 Solutions for western blotting..... 93
Table 2-9 Antibodies used for western blotting. 95
Table 2-10 Antibodies used for Immuno-flourescence..... 97
Table 3-1 Demographic data: 105
Table 4-1 Demographics and clinical data of patients and controls in the observational study of ICUAP..... 123
Table 4-2 microRNA expression in C2C12 cells treated with GDF-15 or myotatin. 137
Table 4-3 Demographic data of St George's hospital COPD patients. 141
Table 5-1 Inclusion and exclusion criteria for the interventional study of NMES..... 159
Table 5-2 Surgical patients admitted under the care on Mr Petrou to the Royal Brompton Hospital between April and September 2010. 163
Table 5-3 Protocol for NMES and sham-NMES delivery. 170
Table 5-4 Demograpic, intervention and outcome data for patients studied in the interventional study of NMES. 173
Table A-1 Significant hits from differentiating myoblasts - 6 hour microRNA Array results. ... 238
Table 8-2 Significant hits from differentiating myoblasts treated with myostatin - 24 hour microRNA Array results. 241
Table 8-3 4 day GDF-15 treatment of differentiated myotubes – microRNA Array results. 242
Table 8-4 to show results of DAVID analysis. Predicted targets of miRs 1, 133a, 181a and 499 from mirWALK were combined to generate significant analysis for significant pathways 243

Abbreviations

ALK	Activin receptor-Like Kinase
APACHE	Acute Physiology and Chronic Health Evaluation
ARDS	Acute Respiratory Distress Syndrome
ASIS	Anterior Superior Iliac Spine
BMP	Bone Morphogenetic Protein
BSA	Bovine Serum Albumin
CABG	Coronary Artery Bypass Graft
CIM	Critical Illness Myopathy
CIN	Critical Illness Neuropathy
CLP	Caecal Ligation and Puncture
CMS	Cyclic Mechanical Stretch
COPD	Chronic Obstructive Lung Disease
CRP	C-Reactive Protein
CT	Computerised Tomography
CYR61	Cysteine-Rich, Angiogenic Inducer-61
DM	Differentiation Media
DMEM	Dulbecco's Modified Eagle Medium
DMSO	Dimethylsulfoxide
EDTA	Ethylenediaminetetraacetic acid
EMG	Electromyography
FDR	False Detection Rate
FFP	Fresh Frozen Plasma
FoxO	Forkhead box protein
GCS	Glucocorticoids
GDF-15	Growth and Differentiation Factor-15
GM	Growth Media
GSK3β	Glycogen Synthases Kinase 3 Beta
HDAC-4	Histone Deacetylase-4
HDU	High Dependency Unit
HOXA11	Homeobox Protein A11
Hz	Hertz
ICUAP	Intensive Care Unit Acquired Paresis
IGF-1	Insulin-like Growth Factor-1
JNK	c-Jun-N-terminal Kinase
LDH	Lactate Dehydrogenase
LVEF	Left Ventricular Ejection Fraction
mA	milliAmperes
MAPK	Mitogen Activated Protein Kinase
MEF-2	Myocyte Enhancer Factor-2
MIC-1	Macrophage Inhibitory Cytokine-1
MLT	Muscle Layer Thickness
MRC-SS	Medical Research Council strength score
mTOR	mammalian Target of Rapamycin protein
MTT	3-(4, 5-dimethylthiazolyl-2)-2, 5-diphenyltetrazoliumbromide

MuRF-1	Muscle Ring Finger -1 protein
MyoD	Myogenic Differentiation Factor D
NAG-1	non-steroidal anti-inflammatory activated gene-1
NCS	Nerve conduction studies
NHLI	National Heart and Lung Institute
NICE	National Institute for Health and Care Excellence
NIHR	National Institute for Health Research
NMBA	neuromusclular blocking agents
NMES	Neuromusclular electrical stimulation
PA	Pulmonary artery
PCR	Polymerase Chain reaction
PI3K	phosphoinositide 3-kinase
PLAB	Placental TGF-β
QMVC	Quadriceps Maximal Voluntary Contraction
qPCR	quantative PCR
RBHT	Royal Brompron Hospital Trust
RCT	Randomised controlled trial
RF_{csa}	Cross-Sectional Area of the Rectus Femoris
SIRS	Systemic Inflammatory Response Syndrome
SMAD	Small Mothers Against Decapentaplegic
SOFA	Sequential Organ Failure Assessment Score
SRF	Serum Response Factor
TGF	Transforming Growth Factor
TGFBR	TGF-β receptors
TNF	Tumor Necrosis Factor
UK HES	UK Hospital Episode Statistics
UP	Ubiquitin Proteosome
US	Ultrasound
VIDD	Ventilator Induced Diaphragm Dysfunction

Chapter 1 Introduction

1.1 Why investigate molecular mechanisms in ICUAP?

Intensive care unit acquired paresis (ICUAP) is one of the increasingly recognised complications of survival from critical illness. Advances in medical management have improved survival from acute severe illness and multi-organ failure and as a result the sequalae have become important clinical syndromes in their own right. ICUAP is associated with a significant morbidity and mortality independent of the severity of the primary illness (1) but, despite this, our understanding of the aetiology, pathology and potential management options of this disease is limited.

ICUAP is characterised by significant skeletal muscle weakness and wasting and results in a spectrum of physical disability ranging from mild loss of muscle function to complete paralysis and inability to wean from mechanical ventilation (2). The incidence of this condition is not fully described and depends on the cohort of patients examined. However, evidence suggested that more than 25% of patients admitted to ICU developed ICUAP (3, 4) and many more undocumented cases are likely to exist. Although many patients recovered their muscle function, neuromuscular dysfunction was still one of the major burdens affecting survivors of critical illness (5, 6). At discharge from hospital approximately 65% of patients had functional limitation (7) and 30% were left with permanent disability (7). Rehabilitation and weaning of these patients is both lengthy and costly and as yet early mobilisation and rehabilitation are the only treatments available.

ICUAP is likely to result from a complex interplay of many aetiological factors and as a result our understanding of the molecular mechanisms underlying the condition is limited. Patients and clinical circumstances are heterogeneous and much of our current understanding

is extrapolated from animal and *in vitro* studies with limited relevance. Clinical studies in ICU patients are both ethically and logistically challenging but, as highlighted by the NICE (National Institute for Health and Care Excellence) guidance on rehabilitation following critical illness (8), a better understanding of the clinical and molecular factors behind the disease is the key to identifying potential therapeutic targets from which future treatments and prevention can be devised. Therefore, the work in this thesis aimed to investigate potential molecular mechanisms within the complex aetiology of ICUAP with a view to identifying future therapeutic targets.

1.2 Intensive care unit acquired paresis (ICUAP)

1.2.1 Background

Muscle wasting has been a recognised complication of critical illness for more than a century; however, since patients rarely survived severe critical illness, it was not a significant problem. Therefore, it was not until early case studies describing muscle weakness following critical illness were first published in the 1950s (9) that the syndrome began to be formally recognised. Initially the clinical syndrome was attributed to an axonal neuropathy; however, in 1977 a similar myopathic syndrome following treatment for acute severe asthma with corticosteroids and neuromuscular blocking agents was reported (10).

In 1984 Bolton *et al* published a case series of 5 patients who developed a severe motor and sensory polyneuropathy during critical illness. Patients presented with difficulty weaning from mechanical ventilation despite the fact that their critical illness was resolving (11). The authors described the heterogeneous clinical features of the patients' primary illness that all resulted in a common clinical syndrome: a severe bilateral flaccid paralysis affecting all skeletal muscle groups with some sensory involvement. The syndrome became known as Critical Illness Neuropathy (CIN), as an axonal neuropathy of both motor and sensory nerves

with reduced combined muscle and nerve action potentials was revealed by nerve conduction studies (NCS) and electromyography (EMG). Muscle biopsies were also taken from these early cases and demonstrated atrophy of both type 1 and 2 muscle fibres; this was explained as a secondary myopathy (11). Over time it was recognised that neuropathy alone could not account for the extent of muscle wasting and weakness, or the histological changes seen at muscle biopsy, and it was therefore proposed that a primary myopathic process, Critical Illness Myopathy (CIM), must also be present, (12, 13). Electrical in-excitability of muscle, even when stimulated by directly implanted intramuscular electrodes, confirmed that a primary myopathic process was also present (14). Latronico *et al* published the first prospective series in 1996 in which 23 of 24 patients with muscle weakness following critical illness had myopathy on muscle biopsies. Furthermore in 15 of these patients there was no significant neuropathy and thus the paralysis could *only* be explained by myopathy (12). Latronico's study also confirmed the co-existence of neuropathy and myopathy and the clinical overlap of the 2 syndromes.

The term ICUAP (or ICU-acquired weakness), developed in 2009 (15), is now widely accepted and used to reflect the fact that the separation of CIN and CIM is not only clinically difficult, but also that neither term would adequately describe what is probably a heterogeneous spectrum of disease, with significant overlap between the two pathological processes (15, 16). The heterogeneous nature of ICUAP in terms of its clinical aetiology, patient population and severity of clinical features as well as the complex pathological overlap is in part why the current understanding of the molecular pathology of the disease is limited.

In the following sections we will review the current understanding of ICUAP from a clinical and molecular point of view.

1.2.2 ICUAP from a clinical perspective

1.2.2.1 Definition and diagnosis

ICUAP is defined as clinically detectable weakness in critically ill patients in whom there is no other plausible cause for the aetiology other than critical illness (15). In 2009 Stevens *at al* set out the diagnostic criteria for ICUAP from a clinical and pragmatic perspective, these are now widely accepted and used in clinical practice (Table 1-1).

Diagnostic criteria for ICUAP
1) Generalised weakness which develops following critical illness.
2) The weakness is diffuse, symmetrical and flaccid. Cranial nerves are usually spared.
3) MRC-SS <48.
4) Difficulty weaning from mechanical ventilation.
5) Other causes for weakness have been excluded.
For a diagnosis of ICUAP either 1,2 and 3, or 4 and 5 should be present.

Table 1-1 Diagnostic criteria for Intensive care unit acquired paresis (ICUAP).
Adapted from Stevens et al (15) (Crit Care Med. 2009 Oct;37(10 Suppl):S299-308). MRC-SS - medical research council strength score.

ICUAP diffusely affects skeletal muscle so weakness presents in both proximal and distal limb muscles and as well as trunk and respiratory muscles. ICUAP often presents as a recovering critically ill patient who has difficulty weaning from mechanical ventilation, despite only requiring low airway pressures and inspired oxygen content (FiO_2) and the fact that the primary cause for critical illness and cardiopulmonary function are improving (2, 17). The cause for dependence on mechanical ventilation is suggested by signs of respiratory muscle weakness such as weak cough, paradoxical abdominal movement, difficulty clearing secretions, worsening respiratory function on lying flat and absence of inspiratory abdominal expansion (18). Alternatively ICUAP may be first suspected by evidence of reduced limb movements, for example in response to pain (18). Respiratory and peripheral limb muscle dysfunction have been shown to correlate with each other suggesting that, although the diaphragm is also affected by mechanical ventilation and the syndrome of Ventilator Induced Diaphragm Dysfunction (VIDD), the pathology of ICUAP affects the respiratory muscles in the

same way as other skeletal muscle (11, 19, 20). On examination a symmetrical flaccid paresis of the limbs with loss or reduction of the deep tendon reflexes and marked muscle wasting is demonstrated; in severe disease quadriplegia may result leaving the patient completely immobile (2). Facial and ophthalmic muscle involvement is very rare and therefore facial grimacing in response to pain or eye movements on demand are a useful test of awakening and comprehension. However, a sensory component is described with the neuropathic component of the disease (21) and, therefore, the diagnosis should not be rejected in the absence of facial grimacing. If present, sensory involvement is a distal, symmetrical loss of pain, temperature and vibration sense and occurs alongside neuromuscular weakness. Pure sensory critical illness neuropathy is not documented in the literature although the sensory element is less well examined and researched (22). It is essential to exclude other causes of muscle weakness and central nervous and higher functioning should remain unaffected, although of course encephalopathy secondary to critical illness may often be a complicating factor.

In practice the diagnosis of ICUAP is usually made clinically (23). Where possible this should include the accurate quantitative assessment of muscle strength (24). A Medical Research Council strength score (MRC-SS) of less than 48 in the right clinical setting is sufficient to make the diagnosis of ICUAP (15); however the MRC-SS requires alertness, understanding and cooperation from the patient. The reliability and usefulness of the MRC-SS in the ICU setting is discussed further in the Methods Chapter of this thesis. Although the MRC-SS has been shown to be sensitive in describing degrees of muscle weakness in those patients who are unable to lift their limbs against gravity, sensitivity is lost in stronger patients (24, 25). In these circumstances, hand-held dynamometry (for example of elbow flexion) (26, 27) and hand grip dynamometry (26, 28) have been used to detect muscle weakness in alert ICU patients and have been shown to correlate well with the MRC-SS (29). From a research perspective these techniques may be interesting; however, they require the patient to be alert

and cooperative, are not routinely used in clinical practice and clear normal ranges are not yet well established (24). Hand grip strength has probably been the best described (26) and, in combination with an MRC-SS of less than 48, a strength of less than 11kg in men or 7kg in women was useful in aiding diagnosis of ICUAP and was associated with increased in-hospital mortality (30). However, all techniques of hand-held dynamometry are not as sensitive or easy to interpret in patients who are very weak (31) and, although ICUAP affects all muscle groups, measurement of just one muscle does not necessarily truly reflect overall strength (32, 33). Furthermore, relatively large changes in strength are needed to accurately define progression or improvement as the variability is great (26).

The ability to test non-volitional strength in ICU patients would obviously be useful, but again there is not, as yet, a standardised technique for doing this. The ulnar nerve supplies the adductor pollicis muscle of the thumb and is readily accessible and widely used in ICUs to assess the adequacy of neuromuscular blockade in the train-of-four technique. The twitch pressure generated following supra-maximal stimulation of the adductor pollicis has been studied in the ICU setting (34); however, again these techniques are not yet standardised and are also limited by drugs, the temperature of the patient and the presence of oedema and, therefore, cannot be routinely used or currently recommended (24, 31, 35).

Muscle electrophysiology can be assessed by NCS and EMG. In clinical practice these tests are often time consuming and difficult to carry out (35): they require extensive expertise, the ICU is an “electrically unfriendly” setting, they are hampered by oedema, EMG requires patient cooperation and the tests are contraindicated in those with external pacemakers and require extra caution with the use of electrical charge in potentially wet areas (23, 35). The need for these investigations in the diagnosis of ICUAP is debated as, in both clinical practice and research, it is unclear how the results add to the diagnosis (36, 37) or change the

management (23, 37). However, where available and in the research setting they may provide useful insight into the relative contribution of myopathy and neuropathy present.

Table 1-2 describes the changes that reported on NCS, EMG and with direct muscle stimulation with different underlying causes of ICUAP. In reality these often overlap and this further complicates their use (16).

Investigation	CIN	CIM
Nerve Conduction Studies		
CMAP (Motor)	Reduced amplitude (may be the first sign)	Normal (but may be reduced)
SNAP (Sensory)	Reduced amplitude (Nerve conduction velocity should be normal as CIN is an axonal neuropathy)	Normal
EMG		
Step 1: No contraction	Fibrillation (a late sign)	Normal/none
Step 2: Repeated slow contraction	Large, polyphasic MUPs with early recruitment (secondary to axonal loss resulting in collateral recruitment)	Small, polyphasic short duration MUPs (secondary to motor unit loss and dyssynchrony with in motor units)
Step 3: Maximal voluntary contraction	Reduced recruitment and lack of interference	Low amplitude weak signal.
Direct muscle stimulation	Reduced neuronal CMAP Normal muscle CMAP	Reduced or absent CMAP

Table 1-2 Summary of findings on nerve conduction studies (NCS), electromyography (EMG) and direct muscle stimulation in Critical Illness Neuropathy (CIN) and Myopathy (CIM).

CMAP – compound muscle action potential, SNAP – sensory nerve action potential, MUP – motor unit potential. (Adapted from (2, 17, 38)).

Although the use of electrophysiological tests in the diagnosis of ICUAP may be academically interesting and enable the detection of pathology early (39) and in unconscious patients (24, 34), the relevance of early electrophysiological changes in terms of the later development of clinically significant muscle weakness is unclear. However, what is increasingly clear is that the insult that results in ICUAP occurs very early in the course of critical illness (40) and that changes in neuromuscular function can be detected long before clinical presentation of ICUAP (4, 41). This was illustrated by the study by Khan *et al* (39), where 31/48 of patients

(63%) had abnormal nerve conduction studies at day 2-5 of ICU admission but only 10/48 (21%) developed a diagnosis of ICUAP (39). However, even at baseline assessment abnormal nerve conduction studies were associated with increased risk of mortality (39) and at day 7 were predictive of a diagnosis of ICUAP (39).

Although muscle wasting may not be clinically obvious to the observer until marked, it can be detected as early as day 3 on ICU as a downward trend in cross-sectional area of quadriceps muscle measured by ultrasound which becomes statistically significant by day 6 (42). This is a non-invasive technique that is not technically challenging and does not require patient cooperation and quadriceps cross-sectional area has been shown to correlate with muscle strength (42). Therefore, in the future it may be a useful screening tool to identify those patients who are developing wasting and weakness.

Assessment and quantification of respiratory muscle strength is also important but even more challenging and fraught with contentious issues than the testing of peripheral muscle strength. In clinical practice respiratory muscle strength can be estimated in ambulant patients by sniff or maximal voluntary static mouth pressures. The equivalent for ventilated patients would be the maximal inspiratory pressure measured by the ventilator. More detailed tests of diaphragm function, such as the transdiaphragmatic pressure elicited by magnetic stimulation, diaphragm EMG and ultrasound are really only used for research purposes and by a few experienced investigators (38, 43, 44). Pragmatically, respiratory muscle weakness is generally assumed on the grounds of failure to wean associated with limb muscle weakness and wasting.

As the need for accurate diagnosis and documentation of progression of the disease becomes better understood, these techniques may become more widely used and could potentially be useful in predicting outcomes and detecting response to treatment. However, at

present the diagnosis of ICUAP is more pragmatic and, although the MRC-SS is widely used, in non-alert patients the diagnosis relies entirely on the clinical picture.

1.2.2.2 Incidence.

The reported incidence of ICUAP ranges from about 25% to 100% depending on the definition and diagnostic techniques used and the case mix of patients (3, 4, 36, 45). The first large prospective study to examine the incidence of ICUAP found that 25% of unselected patients intubated for more than 7 days had clinically detectable weakness at awakening (3). However, by limiting the definition to those with clinically detectable weakness the study only included patients who were awake and could communicate, potentially missing significant weakness in those patients who were either transferred out of the unit pre-awakening or died prior to assessment (109 out of 206 identified patients) (3). In contrast, studies using EMG criteria identified muscle dysfunction in 49%-59% of unselected patients (46, 47). In a further study, at an average of 28 days on ICU, 70% of patients had electrophysiological evidence of muscle dysfunction, but in only 30% of these was the weakness clinically detectable (19). 46% of patients included in a review of studies including patients with sepsis, multi-organ failure or prolonged mechanical ventilation were diagnosed with ICUAP (by various methods) (48) and of patients with severe sepsis or multi-organ failure 70-100% had abnormal EMGs (4, 19).

In the UK over 230,000 patients a year are admitted to critical care with over 30,000 staying more than 1 week (UK Hospital Episode Statistics (UK HES) adult critical care data 2012-13 (49)); at least 25% of these could be expected to develop ICUAP and at any one time 5% of critical care beds are occupied by weaning patients (50). When combined these data demonstrate that ICUAP is a huge clinical and financial burden.

1.2.2.3 Clinical risk factors

In order to assess the clinical risk factors for the development of ICUAP, studies have typically adopted prospective observational or retrospective case-control designs. These vary further in terms of patient case-mix and sample size and for these reasons the evidence for even the most accepted risk factors is often inconclusive and studies have contradicted each other. It is impossible to design a randomised controlled trial (RCT) in humans to assess the causal effects of clinical exposures and in the case of pharmacological exposures where the use of any drug will be indicated in the management of the patients' critical illness, it would therefore be unethical to do so. Management of hyperglycaemia is the exception and RCTs of intensive insulin therapy have led to the acceptance that hyperglycaemia is an important risk factor for the development of ICUAP (51).

The most established and accepted risk factors for ICUAP are sepsis, systemic inflammatory response syndrome (SIRS) and multiorgan failure (3, 19, 20, 36, 41, 45, 48, 52). These factors have been reliably shown in prospective trials and systematic review to increase the risk of development of ICUAP (48). This is consistent with the finding that, on multivariate analysis, APACHE III score (a score reflective of illness severity and underlying co-morbidity in critically ill patients) was an independent risk factor for ICUAP and, when combined with the presence or absence of SIRS, could be used to predict the risk of ICUAP (36) Table 1-3.

Stratified group	Apache III Score	Presence of SIRS	Risk of ICUAP within 30 days of mechanical ventilation
Low risk	< 70	No	8%
Medium risk	70-85 ***Or*** >85	Yes No	28%
High risk	> 85	Yes	72%

Table 1-3 APACHE III score and the presence of SIRS predict the chance of developing ICUAP within 30 days of mechanical ventilation

Adapted from data from de Letter et al (36).

Hyperglycaemia is an important risk factor for ICUAP and the evidence supporting this is strong; 5 out 6 trials included in the 2007 systematic review found an association between the risk of developing ICUAP and hyperglycaemia (48); on multivariate analysis a 1mmol/l (20mg/dl) increase in blood glucose resulted in an increased odds ratio of 1.24 (95% CI 1.15-1.56) for the development of ICUAP (46, 48). Furthermore, hyperglycaemia is modifiable and two large RCTs of tight glucose control achieved by intensive insulin therapy demonstrated that the incidence of ICUAP was reduced from 49% to 25% (46) and from 50% to 38.9% in surgical and medical ICUs, respectively (51). Intensive insulin therapy was also an independent protector against the need for prolonged mechanical ventilation in both studies.

Other potential independent risk factors for the development of ICUAP that have been identified in prospective studies include renal failure and renal replacement therapy (3, 53), illness severity score (36, 54), duration of vasopressor or catecholamine support (46) and parenteral nutrition (46). One study also suggested an increased risk in women compared to men (3); however, this result has not been reproduced (48). Age also may be a risk factor although this was not demonstrated on multivariate analysis (48). Pharmaceutical exposures that have been implicated include glucocorticoids (GCS) (19) and neuromuscular blocking agents (NMBAs) (48). GCS were associated with an increased risk of ICUAP (3, 55), with an odds ratio of almost 15 (3), but this was not confirmed in other studies (36, 45, 56). A Cochrane review of the treatment options for ICUAP identified one RCT in which the development of ICUAP was assessed with respect to treatment with corticosteroids. The review retrospectively analysed data from the trial comparing three weeks treatment of patients with un-resolving ARDS with methylprednisolone or placebo and no difference in the development of ICUAP was found (57, 58). Furthermore in Hermams' and Van den Berghe's studies GCS were in fact found to be protective against ICUAP, potentially due to their anti-inflammatory properties predominating once their hyperglycaemic effect had been suppressed

by insulin (46, 51). Perhaps clinical studies that have not in the past controlled for insulin therapy, hyperglycaemia or insulin resistance are less relevant to current practice.

Similarly systematic review has disputed the proposed role of NMBAs in the aetiology of ICUAP. This was initially suggested following the observation, in case studies and retrospective analyses, of prolonged neuromuscular dysfunction following long term NMBA use in the ICU (59, 60). Most prospective studies and systematic reviews have not been able to reproduce this association (3, 45, 48, 54, 56, 60, 61); however, some prospective studies do suggest a link (51, 53) and authors have postulated that a combined effect of corticosteroids and high dose prolonged NMBAs may lead to a necrotising myopathy as was described in asthmatic patients in the 1990s (53). A recent randomised controlled trial in ARDS patients demonstrated improved survival and no difference in ICUAP in those treated with NMBAs (in this case cisatricurium) compared to placebo (62). Aminoglycosides have minor effects at the neuromuscular junction (48) and these drugs are contraindicated in myasthenia gravis; an aetiological role in ICUAP was suggested (3, 54) but the majority of studies demonstrated no association (48, 53).

ICUAP develops in patients who are usually immobile as a result of their critical illness and often have impaired consciousness. Although there is a well-recognised syndrome of disuse atrophy resulting in dramatic loss of muscle mass (63) and immobility is often used in animal models of ICUAP (64, 65), the evidence that immobility is a critical factor in ICUAP is indirect. Additionally, models comparing skeletal atrophy in disuse and sepsis show distinct differences (65). However, early mobilisation and attempts to reduce immobility are currently the main components of both prevention and treatment of ICUAP and, therefore, it is plausible that immobility is at least one of the contributing factors in its development (64). It is possible that immobility and inflammation/ systemic stress are synergistic in combination (66).

1.2.2.4 Outcome and prognosis

ICUAP is an independent predictor of poor outcome and is associated with prolonged length of stay on ICU (1, 3) , delayed weaning (1, 3, 61, 67), and increased risk of death (1, 28, 47, 53).

The link between ICUAP and delayed weaning is now well established. Following observations that reduced diaphragmatic compound nerve potentials correlated with peripheral muscle weakness in ICU patients (19), prospective studies demonstrated that ICUAP was associated with prolonged duration of mechanical ventilation (3) and was an independent risk factor for delayed weaning. The first prospective study to demonstrate this was in the cohort of patients described by de Jonghe *et al* where ICUAP was associated on average with a two-fold increase in weaning time (67). Since then several other groups, controlling for other causes of respiratory failure, have continued to demonstrate the same association (1, 61). Respiratory muscle strength (as measured by maximal inspiratory and expiratory force, rather than diaphragm strength) was also predictive of delayed weaning (20) and correlated with peripheral muscle diagnosis of ICUAP. When taken together this evidence suggests that ICUAP, and its involvement of the respiratory muscles, is causally associated with delayed weaning.

Increased dependence on mechanical ventilation naturally leads to increased length of stay in critical care units (3, 61) as, although criteria for ICU admission and discharge vary worldwide, specialist weaning units are rare and the level of support required for a weaning patient is generally only available in the ICU/critical care setting. The increased time on ICU results in increased exposure to ICU-related complications (infection, thromboembolism, pressure areas) and this translates directly into increased costs of health provision. Even when controlled for length of stay, weak patients had increased health care costs compared to matched non-weak patients (1). UK national ICU data reveal that patients with delayed

weaning who are otherwise clinically stable occupy 5% of ICU beds; although the data did not delineate between the causes of difficulty weaning, it can be presumed that a significant percentage of these patients will have some degree of ICUAP (50).

Historically, the association between ICUAP and mortality was debated because several studies did not conclusively demonstrate a link (3, 61) or the authors attributed it to confounding factors such as severity and duration of illness (47). Indeed ICUAP is more common in severe and prolonged illness so increased mortality would be expected and its aetiology difficult to attribute. Risk adjusted for severity of illness and other confounders, ICU mortality in ICUAP patients was not increased in several studies, but later in-hospital and 1 year mortality was increased (1, 28, 61). The reasons for this are as yet unclear but mirror observations in other conditions, for example COPD that muscle weakness is associated with increased mortality (68).

Recovery from critical illness is a lengthy and challenging process (23) although prognosis of recovery from ICUAP is generally reported as good and 70% of patients recovered "fully" (defined as being able to walk and breath independently) (7); follow-up of survivors from Acute Respiratory Distress Syndrome (ARDS) demonstrated that patients only recover to a median of 70% of their baseline performance at 5 years (as measured by 6 minute walk test) (69). 64% of survivors with ICUAP were left with weakness at discharge from hospital (6). Prognosis may be worse in those patients with pure CIN (rather than CIM) (6, 70), although data to support this are limited. At 5 years 30% of patients reported some degree of functional disability that impaired their ability to walk and breath independently (7) and EMG abnormalities were still demonstrated in 90% of individuals with a history of prolonged ICU admission (5). Even in those patients with the most severe forms of ICUAP (tetraparesis) a similar pattern was seen; the majority recovered fully, but 32% remained severely disabled at

2 years (71). Older patients and those with premorbid medical conditions consistently had poorer outcomes and recovery from ICUAP (55, 69, 72, 73).

Thus the data suggest that, while the overall prognosis is good with most patients making a good recovery in the first few months and by 5 years even returning to work (69, 74), about one-third will be left with a severe disability. This has long-term implications not only for individuals but also from the point of view of resource provision for rehabilitation and long term care (1, 69).

1.2.2.5 Prevention and treatment strategies

Unfortunately despite the increased awareness of the impact of ICUAP there are still few rigorously evaluated interventions for either the prevention or treatment of the condition. Aggressive and early treatment of sepsis and multi-organ failure is generally accepted to improve outcomes and would be expected to reduce the risk of ICUAP, but it would be unethical to design a trial to test this hypothesis. As discussed above, some pharmacological exposures may be associated with increased risk of ICUAP; however, the evidence to support this is inconclusive and, therefore, guidelines do not go further than suggesting judicious use of drugs such as GCS and NMBAs and generally trying to limit exposure to potentially harmful medications. However, even this approach is controversial as GCS have been associated with improved outcomes in septic-shock and multi-organ failure (75) and are widely used to treat several medical conditions (e.g. asthma). Indeed, in some studies (62, 75), but not others (76), as with NMBAs, GCS have been shown to improve outcomes in ARDS.

Although it has been accepted since at least 2001 that hyperglycaemia is associated with increased morbidity and mortality in ICU patients (77) and specifically with increased risk of ICUAP (46, 48), tight glucose control with intensive insulin treatment is not without its own risks and controversies. Robust evidence does exist that tight glucose control can reduce the

risk of ICUAP. For example, a Cochrane review of 2 large trials included an intention-to-treat analysis (of all 2748 randomised patients) as well as a combined analysis only including those patients still on ICU at 7 days (n=825) as previously published (51, 78, 79) . The risk of ICUAP was significantly reduced in those treated with intensive insulin therapy in both analyses (RR 0.7 and 0.65 respectively) (46, 51, 57, 80); furthermore, duration of mechanical ventilation, ICU stay and 180-day mortality were also reduced. Intensive insulin therapy aimed to maintain the patients' blood sugar between 4.4 and 6.1mmols/dl (80-110mg/dl); the greatest benefit was seen in those patients who had the best control, but those treated with insulin in whom control was not so well achieved still received a benefit (81). It has therefore been postulated that insulin itself may have positive effects beyond blood glucose control, potentially including endothelial protection as well as anabolic, neuro-protective and anti-inflammatory properties (22). However, other studies in which increased insulin administration was associated with death have refuted this (82). Tight glucose control in the ICU setting has been widely adopted by the ICU medical community (77), but the level of control itself remains contentious because of the associated risks of hypoglycaemic episodes and recurrent hypoglycaemia (57, 77, 80). The risks of hypoglycaemia are thought not to be limited to the severe acute symptoms (reduced consciousness and seizures), but may also include more subtle long-term negative systemic effects (77). Furthermore, some studies have shown that even single episodes of hypoglycaemia were associated with increased risk of death (83-85). Perhaps a more moderate approach of aiming for a controlled level at less than 10mmols/l (180 mg/dl) would be safer, but still deliver a benefit (83, 86); however, the impact of this level of glucose control on ICUAP has not yet formally been assessed.

Over recent years there has been a growing body of evidence to support the use of early rehabilitation and mobilization in the critical care population. This approach challenges the acceptance of the ICU patient as bed-bound and immobile and aims to achieve awakening and mobilisation much earlier than classically accepted. The approach is increasingly

recognised to be safe and feasible (64, 87-92) but, despite this, few ICU units have adopted it (89). Positive outcomes are difficult to assess as the studies have varying protocols and report on different outcome measures (80, 93). Systematic review suggested that studies generally reported improvements in terms of mobility milestones, time to achieve these and improved muscle strength (but only in the chronic/ recovery setting, not on the ICU), but that the evidence to support a reduction in duration of mechanical ventilation or hospital stay, mortality or improvement in quality of life was contradictory and hampered by the variability of patients and protocols (93, 94). Among other things, barriers to early mobilisation include sedation, haemodynamic instability and practical considerations with respect to staffing expertise, time and equipment (64, 89). However, when these factors were addressed with the help of an experienced multidisciplinary team, not only were mobility milestones achieved more quickly (87, 91), but ICU and hospital lengths of stay were also reduced (90). One prospective randomised controlled study addresses the specific risk of developing ICUAP (68). This study combined early mobilisation and rehabilitation with daily interruption of sedation or just interruption of sedation alone (previously shown to be beneficial) (95). The intervention group initiated occupational and physiotherapy at a median of 1.5 days after intubation, compared to 7.4 days in the control group. The risk of ICUAP was significantly reduced (OR 0.62, 95% CI 0.39-0.96) and the authors reported improved physical independence at discharge, reduced duration of mechanical ventilation and shorter duration of delirium. However, there was no effect on length of ICU or hospital stay, or mortality. These results are encouraging and have led researchers to explore further the use of passive exercise (for examples with neuromuscular electrical stimulation (96)) and other modalities such as cycle ergometry (97), some of which show promising results (89). However, overall the data are often contradictory and there is a need for further large, multicentre RCTs with clear and clinically relevant outcome measures before the critical care community will widely adopt this approach.

Other treatments that have been explored include antioxidant therapy, nutritional supplementation (e.g. glutathione and glutamine), hormonal therapy and intravenous immunoglobulins. Little data to date support these interventions and therefore it is difficult to comment further although there are theoretical benefits to these approaches and they warrant further exploration (80).

1.2.3 ICUAP muscle dysfunction and molecular mechanisms

The current understanding of the muscle dysfunction that occurs in ICUAP and the molecular mechanisms behind it are mainly inferred from *in vitro* and animal models of muscle wasting. Predominantly rodent models are used and those commonly cited are denervation, cast immobilisation or hind-limb suspension and models of sepsis induced by endotoxin, pro-inflammatory cytokines or caecal ligation and puncture (CLP). In combination with these, administration of high dose corticosteroids and NMBAs are also often used. Thus, these data should be extrapolated to humans with caution. The aetiology of ICUAP is probably multi-factorial, the syndrome is a spectrum and both neuropathy and myopathy are involved. As a result, ICUAP is unlikely to be due to a single easily targetable molecular mechanism. It is also important to note that some of the data have also been derived from the diaphragm in ventilated animal models and, although ICUAP is thought to affect the diaphragm, the diaphragm is also exposed to the unique insult of mechanical ventilation and VIDD. The translation of data from the laboratory to the clinical condition is difficult and limited, but these models have helped to identify candidate pathways involved in ICUAP, which should be further validated in clinical studies. As discussed above and demonstrated by the variability of the clinical studies to date, well controlled and relevant clinical studies are difficult to carry out successfully and because of this there remains a lack of human data describing the molecular mechanisms of ICUAP.

A range of alterations occur in the muscle of patients with ICUAP and, as previously discussed, both neuropathy and myopathy play a role. It is widely accepted that in the majority of cases these 2 pathological processes overlap and exist simultaneously to a greater or lesser extent (15, 98). Furthermore motor nerve and muscle function are physiologically dependent on each other and, therefore, attributing any one pathological process or feature solely to either neuropathy or myopathy may be an oversimplification. Within these limits and the current understanding of muscle and nerve function, this section will review the data available and the major molecular pathways that are likely to be important in the pathophysiology of ICUAP.

1.2.3.1 Alterations in muscle phenotype and function in ICUAP.

The strength of a muscle depends on both the muscle mass and the force generating capacity of that muscle. ICUAP affects both of these components and clinically manifests initially as abnormal muscle electrophysiology followed by wasting. Disruption of the organised muscle architecture is a key component of the pathophysiology of ICUAP. There is marked loss of thick myosin filaments with disruption of both the actin:myosin ratio (13, 99-101) and myofilament organisation (17, 102) on which healthy force generation is dependant. Histologically, ICUAP muscle demonstrates atrophy of both type 1 and 2 fibres (103) and can be associated with an inflammatory infiltrate and myofibre necrosis (40). A shift towards fast fibres expressing type 2 myosin has been reported in models and early case studies of ICUAP (99, 104); however, unlike in muscle wasting associated with aging and other atrophic states, such as chronic inflammation, starvation or indeed disuse (104, 105), this has not been conclusively demonstrated even in animal models (106). However, type 2 fibres demonstrate greater atrophic changes and are thought to waste more rapidly (99, 107), suggesting potentially increased sensitivity of type 2 fibres to the multifactorial insult of critical illness.

Neuropathy, electrical inexcitability, dysregulation of calcium handling and a reduction in energy generation by the muscle through insulin resistance and mitochondrial dysfunction also contribute to muscle dysfunction in ICUAP and will be considered individually in the coming sections.

1.2.3.2 Muscle Mass in ICUAP

In healthy skeletal muscle a balance exists between muscle atrophy (due to muscle protein breakdown, autophagy and apoptosis) and muscle hypertrophy (muscle protein synthesis). Muscle homeostasis depends on the balance of these factors and in steady state the two processes balance equally with no overall net change in muscle mass/ protein although this can alter in response to changes in demand. For example, in hypertrophic responses both protein synthesis and degradation pathways can be increased with a greater increase in the rate of protein synthesis; similarly during atrophic responses the reverse can be true. The aim of this flexible balance in healthy muscle is to allow for repair of muscle fibres and release of amino acids for gluconeogenesis. A disruption in this balance has been believed to be responsible for the loss of muscle mass in ICUAP since it was first demonstrated in 1968 in response to denervation (108). However, only recently has this been conclusively demonstrated in human critical care patients. Using dynamic markers of muscle synthesis and breakdown, Puthucheary *et al* demonstrated reduced protein synthesis in the initial phase of critical illness followed by a sustained increased in rate of muscle protein breakdown resulting in maintained catabolism over the first week (40). Figure 1-1 summarises the basic molecular mechanisms regulating muscle protein synthesis and breakdown.

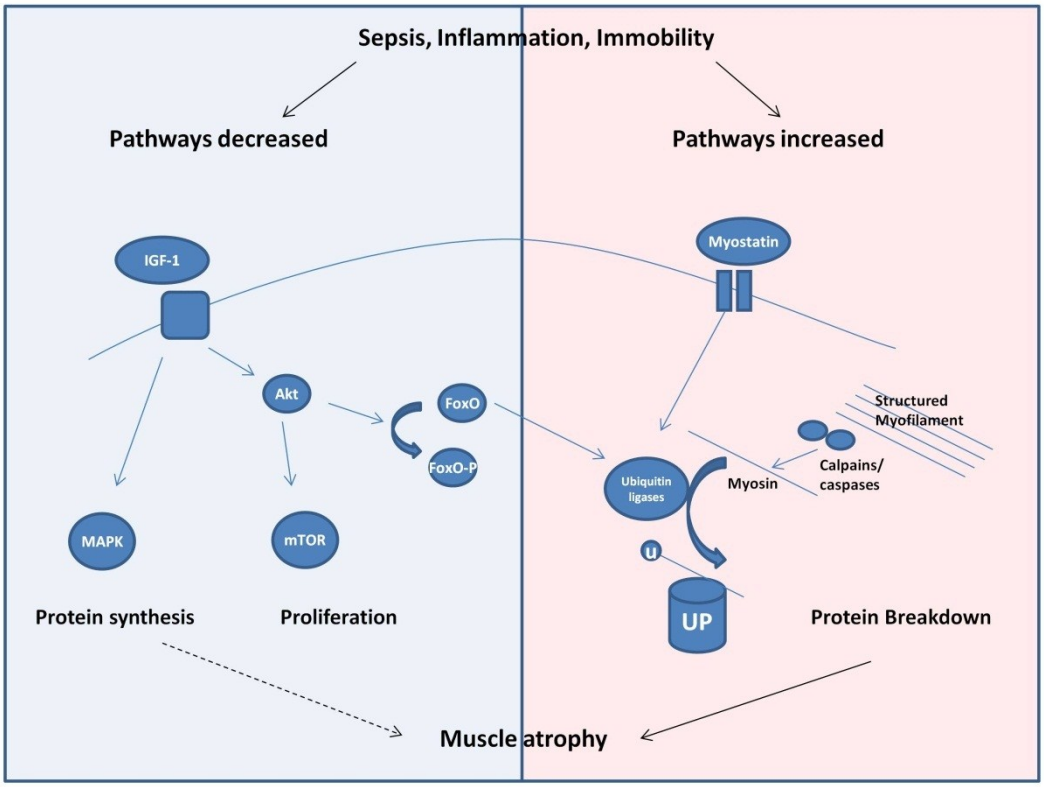


Figure 1-1 Schematic of the basic molecular pathways balancing muscle protein synthesis and breakdown.

In ICUAP sepsis, inflammation and immobility result in muscle atrophy by shifting this balance in favour of muscle protein breakdown. IGF-1 - Insulin like growth factor, MAPK – Mitogen Activated Protein Kinase, mTor – mammalian target of rapamycin, FoxO – Forkhead box protein, FoxO-P – phosphorylated FoxO (inactive), UP – ubiquitin proteosome, U – ubiquitin. Published in Bloch et al ERJ 2012 39 (4): 1000-11 (109) copyright permission granted see appendix A1.

1.2.3.2.1 Up-regulation of muscle protein breakdown in ICUAP

The primary mechanism of proteolysis is thought to be the ubiquitin-protesome (UP) pathway, but caspase and calpain activity, as well as autophagy also play important roles (110). Briefly, the UP pathway involves the specific regulated degradation of proteins by tagging of the targeted proteins with ubiquitin moieties. The tag is recognised by the proteasome, which consists of a multi-protein complex that breaks down the targeted protein into its constituent amino acids. Proteins E1 and E2 activate and carry the ubiquitin molecule, thus preparing it for conjugation. E3, the ubiquitin ligase, then catalyses the ligation to the target protein (110). E3 ligases target specific proteins, and their own expression can be restricted to specific tissues. Atrogin and muscle ring finger-1 (MuRF-1) are muscle-specific (110-112). MuRF-1 is of particular interest in ICUAP as it specifically targeted thick myosin filaments (113, 114), whose

loss is a key feature of ICUAP. However, these ligases not only target contractile and structural proteins, but also those involved in regulation of muscle proliferation and differentiation, such as myogenic differentiation factor D (MyoD) (115, 116). MuRF-1 and atrogin were identified in models of disuse atrophy (111, 112, 117) and knock-out rodents were resistant to denervation-related atrophy (112) and MuRF-1 and atrogin mRNA expression were induced following CLP (118). In addition, inflammation also activated ubiquitination (110). UP and MuRF-1 expression were regulated by the transcription factor nuclear factor kappa-B (NF-κB) which itself was negatively regulated by the inhibitor of NF–κB (IκB) (119-121). Sepsis and inflammation also activated the UP pathway potentially by increased ubiquitination and degradation of IκB induced by Tumour Necrosis Factor (TNF)-α (119). GCS, which are elevated in stress responses including critical illness, were also found to up-regulate the UP pathway (122). Furthermore GCS disruption of the balance between protein synthesis and breakdown can be exacerbated by denervation (108). The clinical relevance of GCS is unclear as there is only inconclusive evidence that GCS are a risk factor for ICUAP at all (48).

In human patients with ICUAP increased protein ubiquitination was demonstrated alongside damage to myosin filament structure (123). In the muscle of septic patients on ICU UP mRNA was increased (124) and increased activity of the proteosome (direct evidence for increased muscle proteolysis) was demonstrated in both respiratory (30% higher than controls) and limb (45-55% higher than controls) muscles (125).

1.2.3.2.2 Autophagy

Autophagy is a major catabolic process by which the cell breaks down its own components within special lysosomes called autophagosomes (98). In animal models sepsis, denervation and GCS all induced autophagy (98, 126) and autophagy has been implicated in congenital human myopathies (127). However, as yet there is not conclusive evidence to suggest a role in ICUAP. For example, despite being implicated in diaphragmatic atrophy in

critically ill patients (128), increased levels of autophagy regulatory proteins in the muscle of critically ill patients was not accompanied by increased mature autophagosomes (129), in fact there was a decrease in mature vesicles. It is possible that defective autophagy is in fact present in ICUAP and that autophagy has a protective role in healthy muscle (98).

1.2.3.2.3 Down-regulation of muscle protein synthesis in ICUAP

As discussed above, it is the overall balance between protein synthesis and breakdown which, when disrupted, results in net catabolism that is important when considering muscle protein balance in ICUAP. Human (and animal) studies show variably decreased or increased muscle protein synthesis at different stages in the clinical course (40, 130-132). However in these studies the rate of protein breakdown still exceeded that of protein synthesis resulting in catabolism. Decreased protein synthesis also occurred in response to sepsis and immobility (133-135) and in healthy volunteers in response to endotoxin infusion (136).

The Insulin-like growth factor-1 (IGF-1)/Akt signalling cascade is recognised as the major molecular pathway driving muscle protein synthesis (137, 138). The binding of IGF-1 to its serine/ threonine kinase receptor activates the Mitogen Activated Protein Kinase (MAPK) cascade, thus increasing myoblast proliferation and/or the Akt pathway. Akt activates protein synthesis via mTOR (the mammalian target of rapamycin protein) and via inhibition of glycogen synthases kinase 3 beta (GSK3β) itself an inhibitor of protein synthesis (137, 139). In addition Akt regulates and inhibits atrophy pathways via phosphorylation of forkhead box (FoxO) proteins and subsequent inhibition of the expression of MuRF-1 and atrogin (140, 141).

Sepsis and mediators of septic inflammation are well documented inhibitors of IGF-1 (133). With respect to ICUAP, examples include IGF-1 reduction in the diaphragm of septic mice (142) and the observation that CLP-induced muscle protein loss in mice can be prevented by implanting a small IGF-1 pellet into the muscle (143). IGF-1 inhibition correlated with

decreased muscle protein synthesis and down-regulation of proteins required for translation (144). In a septic rodent model Akt signalling and FoxO phosphorylation were decreased and MuRF-1 and atrogin expression increased (145).

IGF-1 is also sensitive to muscle activity and was increased by muscle contraction and reduced by disuse (146). Muscle IGF-1 was reduced in human models of sepsis (133, 136), immobility (135), surgery (130) and in critical illness (147). Reduced plasma IGF-1 levels were also observed in acute critical illness (147) and were associated with poor clinical outcome (148) and development of severe ICUAP (149).

Anabolic resistance is a further mechanism that may contribute to the inhibition of protein synthesis. Anabolic resistance describes a syndrome by which, in the setting of critical illness, muscle is unable to respond to anabolic signalling and use the supply of amino acids available and is thus unable to maintain adequate protein synthesis (150). The mechanisms behind this are unclear, but may include damage to the microcirculation secondary to sepsis and an ensuing reduction in the supply of oxygen, nutrients and growth hormones to the muscle (151).

1.2.3.3 TGF-β signalling in muscle atrophy

The Transforming Growth Factor (TGF)-β superfamily is a group of more than 30 cytokines that are involved in regulation of diverse and essential biological processes, including cell proliferation, differentiation and apoptosis (152). The family can be divided broadly into two groups: the TGF-β/ activin/ nodal family and the BMP (Bone Morphogenetic Protein) family. GDFs, Growth and Differentiation Factors, may fall into either group (153). The TGF-β cytokines can have very different functions from each other and their complex interplay, competition for receptor binding and variable effects in different molecular environments make understanding their signalling systems very complicated. Despite this they are all

characterised by some conserved features; these include a “cysteine knot”, a central structure within each monomer. The TGF-β proteins are predominantly secreted in an inactive form and cleaved by proteases to release their active component (153). Activity of the TGF-β ligands is regulated by, amongst other things, ligand traps; these molecules bind and inactivate the ligand often in the circulation or extracellular matrix (152). TGF-β receptors (TGFBR) are comprised of 2 subunits and there are currently 7 type 1 and 5 type 2 recognised receptors known. Ligands are believed to have specific affinity for their type 1 receptor but may have affinity for several different type 2 receptor subunits and competitive binding and partial agonists are thought to exist. On extracellular ligand binding, a dimmer of type I receptors and a dimmer of type 2 receptors aggregate to form a heterotetremer complex. The intracellular component of the type 2 receptors is a constitutively active serine threonine kinase and, when in proximity to the type 1 receptor (also a serine threonine kinase), causes its phosphorylation (152, 153). The phosphorylated type I receptor activates the SMAD pathway. These activated SMAD (small mothers against decapentaplegic) proteins are transcription factors that translocate to the nucleus on phosphorylation where, with other specific co-transcription factors, they then promote transcription of TGF-β responsive genes. TGF-β subfamily ligands activate SMADS 2 and 3, which when phosphorylated bind co-SMAD 4; BMP family members phosphorylate SMADS 1,5,8 and there is competition for co-SMAD 4; SMADs 6 and 7 are R-SMADs, regulatory SMADS that acts as a negative feedback loop to control and regulate signalling (154, 155). The multi-protein complex of phosphorylated SMADs serves as a “hub” for other regulatory factors and co-transcription factors to come together and activate specific signalling pathways. Non-canonical pathways also exist and are activated independently of the SMAD proteins; these include JNK (c-Jun-N-terminal Kinase) and the p38 MAPK/ PI3K (Phosphoinositide 3-kinase) pathways. These may serve to augment or antagonise SMAD-dependant signalling (155).

Myostatin, also known as GDF-8, is a member of the TGF-β family, discovered in 1997 and was found to be a potent negative regulator of muscle mass (156). Myostatin knockout mice exhibited hyper-muscularity (156) and hereditary hyper-muscular conditions have been identified in, amongst others, cattle (157) and humans (158). Myostatin is almost exclusively expressed and secreted from skeletal muscle and, like other TGF-β members, myostatin is translated as an inactive pro-peptide and the active N-terminal domain pro-domain is removed to produce the active C-terminal domain (159). Myostatin has autocrine, paracrine and endocrine functions and is increasingly recognised to be involved in regulation of not only muscle mass but also adipocyte function and glucose metabolism (156, 160). Follistatin is a circulating protein that acts as the ligand trap for myostatin (161). Myostatin preferentially binds the Activin receptor-like kinase (ALK) 4 and 5 type 1 receptors and the Activin 2B type 2 receptor and can activate both SMAD-dependant and independent pathways (161, 162). Activin 2B receptor inactivation reproduced the myostatin knock-out phenotype (163), but follistatin knockout resulted in greater muscle hypertrophy than myostatin knockout alone – suggesting that follistatin regulates other TGF-β ligands involved in the regulation of muscle atrophy (164). Myostatin promoted muscle atrophy through many different pathways including induction of the E3 ligases (165) and autophagy (166), inhibition of myoblast proliferation and differentiation (162), and suppression of IGF-1 signalling via Akt (167, 168). Excessive myostatin activity is implicated in, and has been linked in man to, muscle wasting in cardiac failure, cancer and HIV (169-171). Myostatin signalling was also elevated by GCS (172) and was negatively correlated with daily activity (173). However, currently a role for mysotatin in ICUAP has not been conclusively demonstrated and existing data are contradictory (147, 174, 175).

1.2.3.4 Reduction in force generating capacity in ICUAP

Early in the course of critical illness abnormal muscle electrophysiology was predictive of ICUAP and poor outcomes, and detectable weakness occurred prior to muscle wasting (41). Early weakness also occurred in animal models of sepsis and force-generating capacity of the diaphragm and limb muscles was reduced independent of any muscle wasting (106, 176-178). These changes are likely to be independent of the UP pathway discussed above as they occurred within hours of the onset of sepsis (179). Five major potential mechanisms have been proposed and are likely all to be relevant to a greater or lesser extent across the spectrum of ICUAP: (1) Neuropathy; (2) altered myocyte structure and myofilament integrity; (3) Sarcoplasmic reticulum dysfunction; (4) electrical inexcitability; and (5) bioenergetic failure and oxidative stress (Figure 1-2).

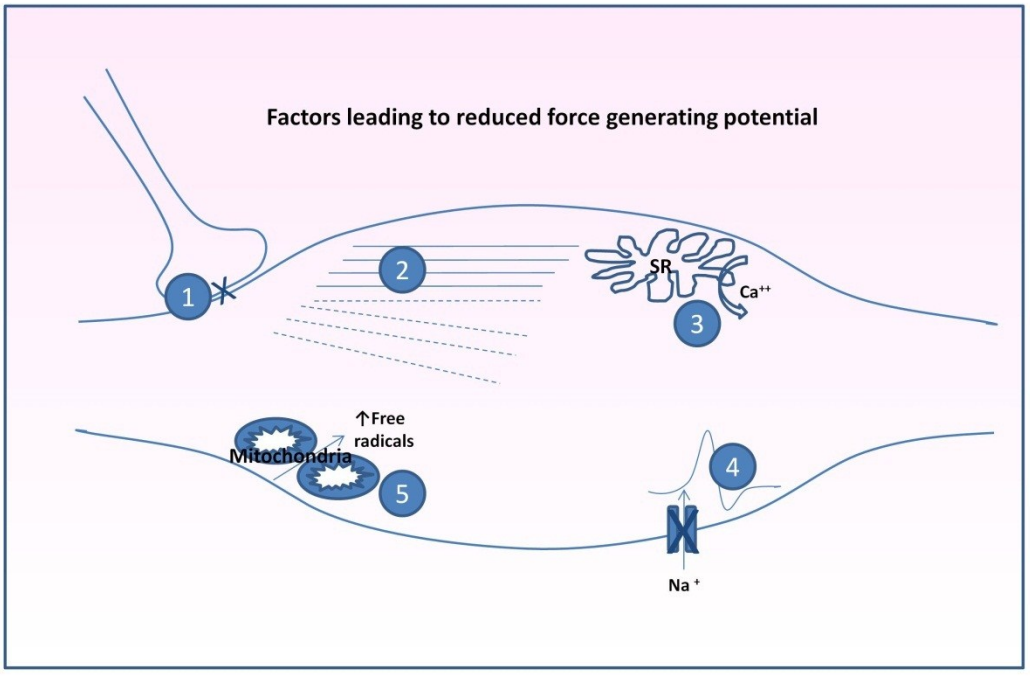


Figure 1-2 Representation of potential mechanisms reducing force generating potential of skeletal muscle in ICU-acquired paresis (ICUAP)

(1) Neuropathy; (2) altered myocyte structure and myofilament integrity; (3) Sarcoplasmic reticulum dysfunction; (4) electrical inexcitability; and (5) bioenergetic failure Published in Bloch *et al* ERJ 2012 39 (4): 1000-11 (109) copyright permission granted see appendix A1.

1.2.3.4.1 Neuropathy and nerve activity.

As discussed above, ICUAP was initially postulated to be a pure neuropathy, CIN (11, 180). The neuropathic component of this disease has been less well studied than the myopathic component and therefore is less well understood. The 2 are difficult to separate as muscle innervation is required for the maintenance of muscle phenotype as well for contraction. Furthermore, denervation increased sensitivity to inflammatory mediators and promoted myosin loss in a rat model of ICUAP (181). Nerve biopsy taken early in the course of ICUAP is often histologically normal, even in severe cases (99) and an axonal neuropathy is not demonstrated until much later (182). However, action potentials in the nerve may be abnormal within hours of the onset of critical illness (183). The mechanisms leading to neuropathy in ICUAP are not well understood or researched. Suggestions include a membrane depolarisation defect that theoretically could occur in a histologically normal nerve; disruption of the blood-nerve barrier, potentially caused by microvascular pathology and inflammatory mediators (including TGF-β), has been postulated to cause the depolarisation defect (98, 184). This is supported by increased activation of endothelial cells in the microcirculation surrounding peripheral nerves of patients with ICUAP (185). Additionally a loss of endoneural membrane potential has been suggested secondary to local hyperkalaemia and possibly linked to renal insufficiency (98, 186). Lastly, the neurotoxicitiy of inflammatory cytokines is well recognised (187).

A full discussion of VIDD is beyond the scope of this thesis and the aetiology and pathology of VIDD and ICUAP are difficult to separate, but it is worth noting that traffic in the nerve is especially relevant to VIDD. One of the aims of ventilatory support is to reduce the work of the respiratory muscles. The diaphragm has a specific and unique phenotype designed to facilitate the fact that it is never immobile and during total mechanical ventilation it is subjected to varying degrees of passive stretch. VIDD has been reviewed recently by Jaber *et al*

(188). We should note that diaphragm weakness occurs commonly in intubated patients (44, 189), and risk of weakness increased with duration of ventilation (190). Furthermore there is increasing evidence that those modes of ventilation that promote continued (191) or, in rodents, intermittent (192) phrenic activity may attenuate VIDD.

1.2.3.4.2 Myocyte structure and myofilament integrity;

The integrity of the myofilament structure, the major components of which are myosin and actin, is essential for maximal force generation. Myofilament structure was disrupted by mediators of sepsis such as TNF-α (193). Calpains facilitate ubiquitination and proteolysis of myofilament components (mainly myosin) by cleavage, acting to provide an amino acid pool. However cleavage of myofilaments disrupts the structure of the myofibrils and thus the force generating capacity of the fibre is also reduced (194, 195). Caspases are involved in the activation of apoptotic pathways; as multinucleate muscle fibres atrophy, apoptosis begins by a slow reduction in number of nuclei (196, 197). There is a convincing body of evidence to suggest a pathological role for both caspases and calpains in muscle atrophy in ICUAP; both were induced in animal models of sepsis and immobility and were shown to be associated with muscle wasting and reduction in the force generating capacity of muscle (196, 198-201). Furthermore calpain 3/p94 was linked to human muscle atrophy (202). However, as yet there are no human ICUAP data and most animal data were derived from diaphragm work. Altered function of the sarcoplasmic reticulum:

Intracellular calcium concentration is critical in regulation of muscle contraction. Calcium has direct effects on the myosin ATPase during the contraction cycle and regulates glycolytic and oxidative energy metabolism. Pathological increases in intracellular calcium during sepsis and immobility were observed in limb skeletal muscle (203, 204), potentially caused by disruption of the sarcoplasmic reticulum (205) (the sarcoplasmic reticulum stores, binds and releases calcium and thus is responsible for calcium homeostasis) resulting in

increased sensitivity of contractile proteins to calcium (206). Furthermore, calcium also regulated protein breakdown, by activating calpains and ubiquitination (203).

As calcium is essential for muscle contraction it might be expected that increased intracellular calcium would increase the force generating potential of muscle; however, this appears not to be the case and this implies that reduced calcium release from the sarcoplasmic reticulum is in fact the dominant effect. Furthermore, serum from critically ill patients who developed ICUAP reduced the calcium-activated force generated in permeabilised muscle fibres. It was suggested that this effect was secondary to blocked calcium release. The serum fraction used was low molecular weight, <30 kDa, suggesting a role for inflammatory cytokines in this process (207).

1.2.3.4.3 Electrical in-excitabiltity

It has been postulated that CIM and CIN coexist as the result of a systemic syndrome of electrical in-excitability (17). Consistent with this hypothesis were the findings that both nerve and muscle tissue were relatively in-excitable in ICUAP models with altered membrane potentials (14, 186, 208, 209) and that nerve histology was often normal, suggesting functional rather than structural abnormalities (12, 17). Furthermore, these membrane alterations resulted in chronic depolarisation and reduced excitability of the nerve (186) and therefore caused functional denervation of the adjacent muscle (22). Cardiac in-excitability in sepsis has also been demonstrated by reduced ECG potentials in septic patients (210) lending weight to the argument for a generalised syndrome of in-excitability. The mechanisms behind the in-excitability have been investigated in animal and *in vitro* models; for example, denervated rat muscle had reduced membrane potential and when also exposed to GCS was unable to produce action potentials at all (211). One potentially unifying mechanism that has been postulated is sodium channel dysfunction and an overall reduction in the availability of sodium channels (212). In denervated, septic and lipopolysaccharide models of ICUAP an embryonic

form of sodium channel was expressed (Nav1.5) in muscle in place of the mature form (Nav1.4) (213-215), this resulted in a more negative depolarisation threshold, consequently 99% of the available sodium channels were inactive (216) and the muscle fibre was unable to produce an action potential. Not all fibres are affected to the same extent and the percentage affected determines the severity of weakness (17).

1.2.3.4.4 Bio-energenetic failure, oxidative stress and glycaemic control:

Bio-energetic failure is an umbrella term for the combination of tissue hypoxia, insulin resistance, and increased oxidative stress resulting from sepsis and critical illness. This combination of factors results in reduced glucose uptake and ATP formation, mitochondrial dysfunction and increased free radical production (217). The primary source of energy used by muscle is glucose and in the absence of a sufficient supply gluconeogenesis is fuelled by muscle proteolysis and amino acids. Glucose uptake in muscle is controlled by GLUT-4 receptors, which are insulin-dependent. Critical illness and sepsis result in insulin resistance and thus glucose uptake is reduced, which results in reduced ATP production and mitochondrial dysfunction.

Bio-energetic failure may be worsened by both hypoxia and hypercapnia. Oxidative stress, in part driven by hypoxia, contributed to muscle wasting (218-220). Hypercapnia resulting in systemic and cellular acidosis may also disrupt metabolic function, causing decreased ATP and increased free radical production and leading to reduced contractile force in both diaphragm and limb skeletal muscle (221-223). However, direct evidence for the relative importance of gas exchange abnormalities in ICUAP is lacking (Figure 1-3). Muscle expression of genes encoding electron transport components, levels of mitochondrial proteins and mitochondrial oxygen consumption were all suppressed in animal models of sepsis (224-226). In human studies of acute critically ill patients with septic shock and ICUAP, mitochondrial dysfunction in limb muscle was an independent risk factor for mortality (227).

However not all studies in humans have shown mitochondrial dysfunction in muscle from critically ill patients (228).

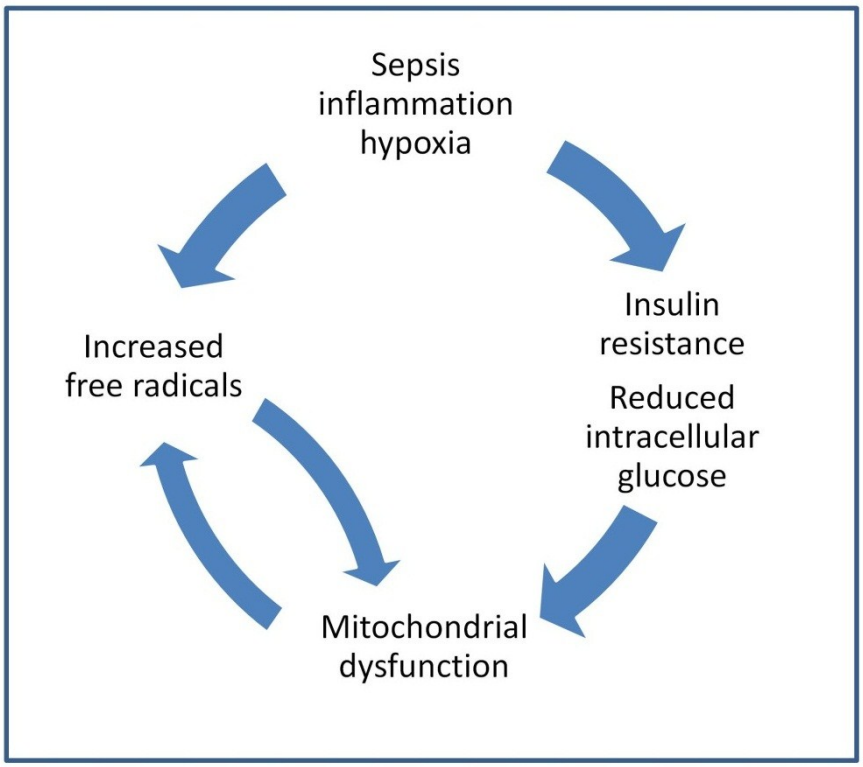


Figure 1-3 Mitochondrial dysfunction in bio-energenetic failure results in increased free radical production and in turn further mitochondrial damage.
Published in Bloch *et al* ERJ 2012 39 (4): 1000-11 (109) copyright permission granted see appendix A1.

Oxidative stress secondary to increased free radicals has been implicated in pathways potentially contributing to ICUAP both via total muscle protein loss (229, 230) and reduced force generating potential (224). For example, oxidative stress activated the UP pathway (231, 232) and calpains and caspases (233-235). Free radicals disrupted the myofilament structure (236) and caused sarcolemmal damage, which was subsequently reduced by inhibition of nitric oxide synthase (209). Free radicals are not only produced in the mitochondria in sepsis but production by sarcolemmal NAPDH oxidase and nitric oxide synthase (NOS) (195, 224) is also increased (237-239). Additionally, pathological effects of sepsis can be reversed with free radical scavengers and inhibitors of free radical production (233, 240-242). To date free radical

inhibition has only been tested in animal models and as yet the potential of antioxidant therapy in human ICUAP is not known (243). Finally, immobility may worsen bioenergetic failure with increased free radical production (244), increased microvascular permeability, increased insulin resistance and decreased antioxidant potential (59).

As discussed above, hyperglycaemia may be an important aetiological factor in ICUAP. The mechanisms for this are unproven, but may include protection against bio-energetic failure via increased controlled uptake of glucose into the skeletal muscle and improved availability for mitochondrial function, in part via regulation of GLUT-4 receptors (217). Furthermore, insulin also had anabolic effects (245), inhibited the UP (246), was potentially anti-inflammatory (247), improved dyslipidaemia (248) and was neuroprotective (249). In a human post-mortem study of critically ill patients, increased skeletal muscle protein concentration was seen in those who were treated with intensive insulin therapy compared to controls (228) and similar results were demonstrated in patients with burns (245) and cancer cachexia (250). A further human study of ICUAP demonstrated increased IGF-1 and net protein synthesis in those treated with intensive insulin therapy compared to controls (147). However the above post-mortem study failed to demonstrate a protective effect of insulin on skeletal muscle mitochondria, only on liver mitochondria (228) again highlighting the difficulties of translating animal and *in vitro* work to human pathology.

1.3 GDF-15

1.3.1 Background

Growth and differentiation factor- 15 (GDF-15) is a member of the TGF-β superfamily of cytokines. In the late 1990s several different groups independently identified GDF-15 in a wide range of different tissues and scenarios (251). As a result GDF-15 is known by several other names, including Macrophage Inhibitory Cytokine-1 (MIC-1) (252), Placental TGF-β

(PTGFB) (253), Placental Bone Morphogenic Protein (PLAB) (254) and non-steroidal anti-inflammatory activated gene-1 (NAG-1) (255), according to how the protein was identified. GDF-15 was cloned from murine cDNA libraries and identified in many tissues, but found in highest levels in macrophages and epithelial cells (256). As a TGF-β family member, GDF-15 has the essential conserved elements, the cysteine rich domains and knot, and is secreted as a pro-peptide then cleaved into its active dimeric form (251). GDF-15 expression has been demonstrated in a wide range of tissues in both human and animal studies; however, it is expressed in the highest levels in embryological and developing tissues (251, 257). It is important to note that, unlike other TGF-β family members, GDF-15 is relatively poorly conserved between species and its expression profile differs in different animals (256, 258). As such it is increasingly recognised to have, diverse and divergent functions, but these are often related to central/ basic cellular function.

Despite being widely expressed, it is thought that GDF-15 is actually only expressed by the placenta in adult normal physiological conditions and otherwise is only expressed in response to stress stimuli including hypoxia, inflammation, sepsis, mechanical stress and tissue damage (257). The physiological role of GDF-15 is therefore not yet fully understood. However, it has been implicated in a wide range of pathological processes and conditions, including cardiovascular (257), pulmonary (259, 260) and renal disease (261), inflammation (252) and solid and haematological cancers (262). Furthermore, GDF-15 is found in the circulation and its circulating concentration is a strong independent predictor of mortality in numerous conditions: for example, acute coronary syndromes and myocardial infarction (257), pulmonary artery hypertension (260), chronic renal disease (261) and malignancy (263). This relationship with mortality in numerous medical conditions was reflected in a recent study where, among elderly individuals followed for 5 years, higher circulatory GDF-15 concentration was related to all-cause mortality with a hazard ration of 4 (95% CI 2.7-6.0) and was specifically associated with worsening renal and cardiovascular function (264).

The mechanism of GDF-15's action and signalling pathways have not yet been fully elucidated. As a member of the TGF-β family, GDF-15 would be expected to activate the well-recognised TGF-β signalling pathways via a combination of type 1 and 2 receptors. However the evidence for this is currently lacking. Mutant TGFBR 1 and 2 cancer cells were resistant to the growth inhibitory effects of GDF-15 (265), GDF-15 induced malignant changes in prostate cells via the ALK 5 receptor (266) and Breit *et al* suggested co-localisation of the TGFBR2 and GDF-15 in the hypothalamus (267). However other groups have not been able to reproduce these results (251). Similarly, there is controversy as to whether GDF-15 activates SMAD-dependant pathways, those independent of the SMAD protein or indeed both; again the data so far are inconclusive. Some data from cardiac myocytes and prostate cancer cells suggest that GDF-15 caused SMAD activation (266, 268). However, other groups suggest signalling to be uniquely via non-canonical pathways including Akt/ ERK (269), p38/MAPK (270) and NFKB (271).

1.3.2 Rationale for investigation of GDF-15 in muscle wasting and ICUAP

As discussed above, TGF-β signalling is one of the central pathways involved in muscle atrophy. However, despite myostatin's potency as a negative regulator of muscle mass, the role of myostatin in ICUAP is unconfirmed and myostatin inhibition has not always been successful in treatment of muscle wasting disease (272). GDF-15 is expressed in human and rodent skeletal muscle (251). However, unlike myostatin, which is largely limited to cardiac and skeletal muscle, GDF-15 is also widely expressed in other tissues (256), raising the possibility of both autocrine and paracrine functional effects. Furthermore, the structure of GDF-15 is predicted to be very similar to that of myostatin, which is also known as GDF-8 (258). Although the regulation of GDF-15 expression is not fully understood, its profile as a stress-induced cytokine is recognised and similar factors (oxidative stress, hypoxia, inflammation) have been demonstrated to induce its expression in various tissues. These factors are importantly also

recognised to be aetiological factors in the development of ICUAP and are known to have detrimental effects of muscle size and function (see above).

The functions of GDF-15 in vivo are likely to be divergent and may depend on the local environment. For example, in cardiac cells GDF-15 has been shown to be hypertrophy limiting and anti-apoptotic *in vitro* (268); however, *in vivo* animals lacking GDF-15 showed increased cardiac hypertrophy in response to vascular stress (273). Similarly GDF-15 may have a protective role by promoting apoptosis in prostate cancer cells (274, 275), conversely it may also enhance metastatic potential and angiogenesis (262). GDF-15 was pro-apoptotic and protective in atheroma, promoting macrophage apoptosis and increasing plaque stability (276, 277), and in acute myocardial infarction by protection of the myocardium from infiltration of polymorphonuclear leukocytes so protecting against post-infarction myocardial rupture (278). However, increasing data support the association between GDF-15 and poor outcomes. For example, with relevance to the topic of this thesis, in ARDS (279) (a leading cause of ICUAP) where higher circulating GDF-15 levels were associated with poor outcome. Furthermore, GDF-15 causes cachexia in murine cancer models (267) and in humans is associated with cachexia of chronic disease and cancer (262, 280). The mechanism of these effects are not fully understood, but it has been suggested that it involves central hypothalamic appetite suppression, and neutralising antibodies to GDF-15 are able to reverse the effects in animals (280).

In summary, therefore, our rationale for investigation of GDF-15 in ICUAP is as follows. Firstly, GDF-15 is expressed in response to aetiological factors thought to be responsible for ICUAP (oxidative stress, inflammation, hypoxia) in many tissues and it is therefore plausible that these factors will also drive expression in muscle. Secondly, at least in some circumstances, GDF-15 is thought to activate TGF-β signalling, promote apoptosis and limit hypertrophy pathways, all of which could contribute to muscle wasting. Thirdly, increased

circulating GDF-15 is generally associated with disease progression outcomes, despite a protective role sometimes being suggested; thus, both circulating and muscle GDF-15 may drive muscle atrophy.

1.4 MicroRNA

1.4.1 Background

MicroRNAs are small non-coding RNAs that regulate mRNA stability and translation. They were discovered in 1993 in the *C-elegans* nematode worm. The microRNA lin-4 was identified and it was recognised that the RNA sequence did not code for a protein, but rather had anti-sense complimentary sequences to the 3'-UTR of the lin-14 gene. It was implied from this that the microRNA (lin-4) had a role in the regulation of transcription of the lin-14 gene (281). Following this let-7 was identified and found to be conserved in many species including humans (282). It is now recognised that microRNAs make up approximately 1% of human predicted genes but, more importantly, that at least 1/3 of all genes are under regulation of microRNAs (283) and that their functions include regulation of most major cellular processes – including proliferation, apoptosis and differentiation (284).

The steps in microRNA biogenesis are complex. Briefly, microRNAs are transcribed from the genome as a pri-microRNA, which may be several thousand bases in length. DNA sequences for microRNAs may have their own promoter or be within the un-translated regions of related genes. Pri-microRNAs contain stem loop sequences encoding the miRNA, which are cleaved into a small hairpin structure known as the pre-microRNA. Cleavage is carried out by a large structure known as the "microprocessor" made up, in part, of Drosha (an RNA polymerase type III like protein). The product pre-microRNA is approximately 70 nucleotides in length and is exported from the nucleus by exportin. In the cytoplasm Dicer protein (an RNAase) is responsible for the final processing and production of the mature, approximately 23

nucleotide, microRNA. Both 3' and 5' strands are produced, although it is thought that one is usually degraded and that this process may be tissue specific. One strand is incorporated into the RISC (RNA-induced silencing complex) where it binds with the target mRNA and acts to inhibit translation or destabilise the mRNA itself (284).

The network of microRNA to mRNA interactions is complex; each microRNA may target several, even hundreds, of mRNAs and, in turn, the expression of microRNAs is regulated by many different factors (285). Seed-sequence recognition of the 2nd to the 8th 5'-nucleotides results in target specificity, but exact sequence specificity beyond this is not required for binding in animals (although it is in plants) and, as a result, target prediction is also complex. Furthermore many microRNAs function together. These features led to the hypothesis that microRNAs fine-tune the balance between transcription and translation and ultimately co-ordinate gene expression networks (286).

1.4.2 Muscle microRNAs

Since their discovery, thousands of microRNAs have been identified in humans and their role in health and disease is a rapidly expanding field of research. The importance of microRNAs to muscle development and function is demonstrated by the fact that tissue specific Dicer knock-out mice (who are unable to produce microRNAs in muscle) develop abnormally in the embryonic and perinatal phase and are unable to survive (287). As in other tissues, microRNAs have been found to be involved in, and essential for, muscle homeostasis, both during embryogenesis and in adult life. Some microRNAs are tissue/ muscle specific and known as myomiRs, but many microRNAs that are expressed in muscle are also ubiquitously expressed (288, 289).

The myomiRs are highly expressed in skeletal (and cardiac) muscle and include mainly miRs 1, 133a, 133b, 206, 208a, 208b and 499. Some of these microRNAs are organised into

clusters which are transcribed together, such as miR-1/133a (actually existing as miR1-1/133a-2 and miR1-2/133a-1) and miR-206/133b (290). MiRs 1 and 206 differ by only 4 nucleotides and miRs 133a and b are identical except for one final nucleotide. MiRs 1 and 133a are expressed in cardiac and skeletal muscle, whereas miR-206 is limited to skeletal muscle and miR-208a to cardiac muscle (289). MiRs 208b and 499 are limited to slow-twitch muscle fibres and coded for within the introns of the MHC type 1 genes (MyH-7 and MyH7B) (291). Co-transcription and sequence similarity indicate that these microRNAs are likely to have similar targets and functions. Although the regulation of expression of these myomiRs is not fully understood, central myogenic factors are thought to activate myomiR expression, including Serum Response Factor (SRF), Myocyte Enhancer Factor-2 (MEF-2), MyoD and myogenin (289).

MiR-1 and 133a fine-tune the balance between proliferation and differentiation. The two processes are exclusive and myoblasts proliferate in the presence of growth factors, but on exiting the cell cycle they fuse and differentiate into multinucleate muscle fibres. In *in vitro* models, miR-1 inhibited HDAC-4 (Histone Deacetylase-4) a potent inhibitor of differentiation; thus, miR-1 promotes differentiation. In contrast, miR-133a inhibited SRF, thus promoting proliferation (290). MiR-206 also promoted differentiation, preventing down-regulation of MyoD (289). MiR-181a is not muscle-specific but is expressed highly in differentiating and regenerating muscle and, by suppression of Homeobox Protein A11 (HOX-A11), promotes muscle differentiation (292). Furthermore, inhibition of these microRNAs resulted in delayed or abnormal proliferation or differentiation (290, 292-294).

Determination of muscle fibre type is also closely controlled and dependant on genetic factors, each specific muscle's function and external factors (for example activity). MicroRNAs 208b and 499 are expressed within the gene encoding slow myosin (Myh7). When expressed, miRs-208 and 499 down-regulate transcriptional repressors, including Sox-6 (which promotes

the type 2 phenotype), and result in promotion and maintenance of the type I phenotype (291).

Our understanding of the role of microRNAs in the maintenance of muscle mass is limited but, by regulating atrophy and hypertrophy pathways, myomiRs have been shown to be involved. MiRs-1, 133 and 206 inhibited IGF-1-driven hypertrophy by targeting IGF-1 itself and its receptor; in turn, IGF-1 and active Akt down-regulated miR-1 potentially via suppression of FoxO (288, 295). However, despite an increase in myofibre size *in vitro* associated with miR-206 inhibition, *in vivo* studies did not demonstrate a significant effect (296). Myostatin is also under regulation of microRNAs and, in turn, regulates their expression. Interestingly, Texel sheep, which have significant muscle hypertrophy, demonstrate a mutation in the 3'-UTR of the myostatin gene; this results in a novel binding site for miRs-1 and 206 resulting in myostatin degradation and increased muscle hypertrophy (297). In normal tissue miR-27, 208b and 499 act to target and inhibit myostatin, thus promoting hypertrophy (293). Myostatin knock-out mice show increased levels of miRs 1, 133 and 206 however a direct link between myostatin and their regulation has not yet been demonstrated (298). Firgure 1-4 summaries a basic understanding of the role of muscle microRNA in muscle homeostasis.

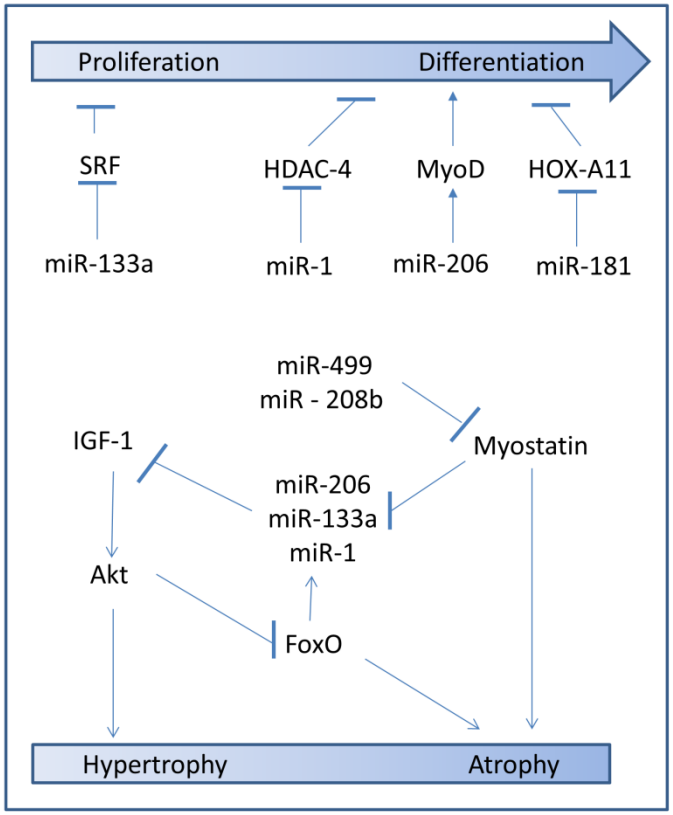


Figure 1-4 Schematic representation of the current understanding of the role of microRNAs in muscle homeostasis.

SFR- serum response factor, HDAC – histone deacetylase, HOX-A11 – Homeobox protein A11, IGF-1 – Insulin-like growth factor-1, FoxO – Forkhead box protein.

1.4.3 Rationale for investigation of MicroRNAs in ICUAP in relation to GDF-15

MicroRNAs have been implicated many muscle diseases (299), including congenital muscle diseases such as Duchene's Muscular Dystrophy (DMD) (300), inflammatory myopathies (301) and secondary muscle diseases such as muscle wasting related to COPD (302). Well-recognised animal models of DMD have been used to investigate the role of microRNAs and, for example, miR-206 was significantly increased in the diaphragm and adductor pollicis of the Mdx mouse model of Duchenne's muscular dystrophy (300, 303) and similar patterns were seen in humans with DMD (303) and myotonic dystrophy type 1 (304); however, results depend on the model used and the muscle sampled (288). Interestingly, circulating miR-206 was found to be a useful biomarker in human patients with DMD (305). In

COPD, Lewis *et al* showed that down-regulation of miR-1 in the quadriceps muscle was associated with muscle atrophy and functional down-regulation of SRF (302). Inflammatory myopathies have been shown to be associated with a general down-regulation of myomiRs and the authors postulated that this would result in generally deranged muscle homeostasis (301). MicroRNAs are essential for muscle regeneration following injury or insult (288, 292) and it is therefore consistent that they should be dysregulated in conditions with abnormal or inadequate regeneration; however, this has not previously been investigated in ICUAP.

Additionally, inflammatory cytokines have been shown to regulate microRNA expression (288, 301) and TGF-β signalling and myostatin, central to muscle atrophy, are increasingly recognised to be under microRNA control (293). Finally, therefore these data led to the hypothesis that muscle microRNAs would be dysregualted in ICUAP and may also be under GDF-15 regulation.

1.5 Summary, aims and hypotheses

Understanding of the molecular mechanisms of ICUAP provides the opportunity to identify potential future therapeutic targets. ICUAP is a common and sometime devastating disease for which there are no pharmacological therapies at present and for which physical rehabilitation currently provides the only potential intervention. Therefore, the aim of this thesis is to investigate the role of GDF-15, a potential novel modulator of muscle mass, in ICUAP. Additionally, with investigation of muscle microRNA expression in ICUAP, the findings may provide insight into the pathological mechanisms of ICUAP. Therefore the main hypotheses of this thesis can be stated as follows:

1. **GDF-15 will be elevated in the blood and muscle of ICUAP patients.**
2. **MicroRNA will be dysregulated in the muscle of ICUAP patients.**
3. ***In vitro*, GDF-15 will regulate expression of muscle atrophy related genes and muscle microRNAs.**

Chapter 2 Methods

2.1 Clinical Methods

2.1.1 Ethical approval

Ethical approval for the clinical studies carried out as part of this thesis was secured either from the National Research Ethics Committee (10/H0722/9) or under a generic permission to draw blood granted to the National Institute for Health Research (NIHR) Biomedical Research Unit at the Royal Brompton Hospital ethical approval (10/H0504/9). Written informed consent was obtained from all participants, except when the participant was unable to consent for themselves, in which case written informed assent was obtained from the participant's next of kin. This only occurred when participants were sedated and ventilated on ICU.

2.1.2 Assessment of quadriceps muscle bulk

Quadriceps muscle size was assessed with B-mode ultrasound (US) imaging using a 10MHz 12L-RS probe (Logiq E, GE Healthcare, UK). US cross-sectional area of the rectus femoris (US RF_{csa}) and mid-thigh muscle layer thickness (MLT) were measured using well established techniques (40, 42, 306, 307) . The patient was positioned supine on the bed with their legs flat and leg muscles relaxed. The anterior superior iliac spine (ASIS) and the point 60% of the distance from the ASIS to the superior border of the patella were identified. The US probe was positioned perpendicular to the axis of the leg and the scanning depth set to visualise the femur in the same image. Where the entire RF_{csa} could not be visualised in a single US image a point 66% or 80% of the distance between the ASIS and patella was also used. The same point was used for follow-up measurements for each patient. MLT was always measured

at the 60% point. Three separate consecutive images were taken and RF_{csa} and MLT estimated using Image-J software (National Institutes of Health, USA). The average of these three measurements was used. To calculate RF_{csa} a line was drawn round the interior echogenic line delineating the RF muscle (42). The area was then calculated using Image-J software (Figure 2-1). The MLT was defined as the depth of a vertical line drawn from the interior edge of the superior aspect of the RF muscle to the upper edge of the femur (Figure 2-1) (306). Inadequate ultrasound images were defined as those where the edges of the RF muscle could not be defined well enough to calculate the RF_{csa} or MLT.

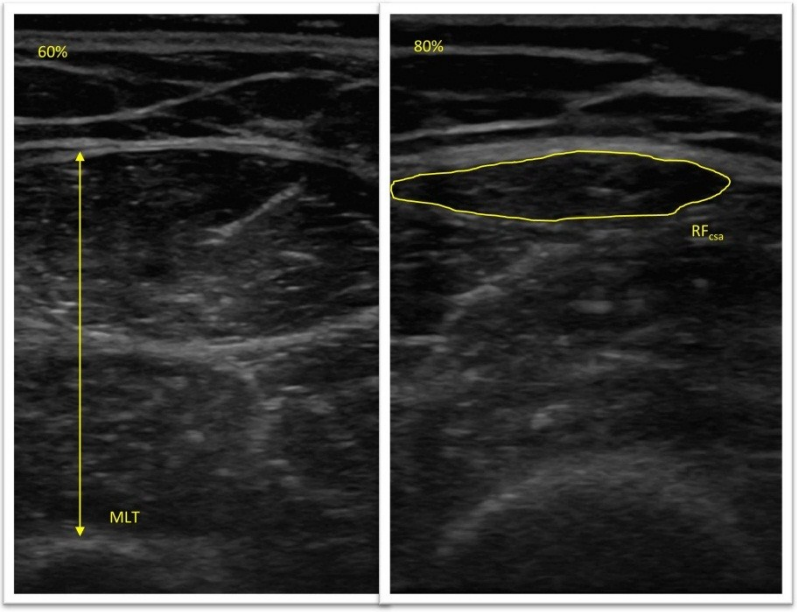


Figure 2-1 Assessment of quadriceps muscle size by rectus femoris cross-sectional area (RF_{csa}) and mid-thigh muscle layer thickness (MLT).

Image on the left taken at 60% of the distance between the anterior superior iliac spine and the superior border of the patella and demonstrates that the whole cross sectional area of the rectus femoris muscle is not visible in a single ultrasound image. The MLT is demonstrated on this image. Image on the right is at 80% and shows the whole cross sectional area at this level and the measurement of the RF_{csa} is illustrated.

2.1.2.1 Inter-observer variability

In collaboration with a colleague in the same group, Dr Dinesh Shrikrishnapalasuriyar, the inter-observer variability of our technique was assessed. The US RF_{csa} of volunteers from the muscle lab was measured by both myself and Dr Shrikrishnapalasuriyar and Graphpad Prisim (GraphPad Software, California, USA) was used to generate a Bland Altman plot of the

results (Figure 2-2). The Bias was found to be 0.1 cm^2 with a standard deviation of 0.29 cm^2 and 95% limits of agreement -0.68-0.46 cm^2.

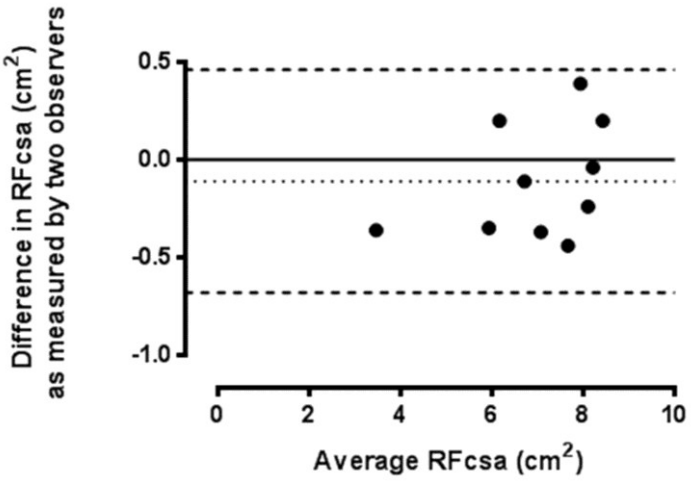


Figure 2-2 Bland Altman plot of ultrasound rectus femoris cross-sectional area (US RF_{csa}) to assess inter-observer variability.

Bland Altman plot of difference between measurements by two observers of RFcsa. Dotted line represents bias -0.11 cm^2, Dashed line represents 95% limits of agreement -0.68-0.46cm^2. n=10

2.1.2.2 Definition of a significant change in US RF_{csa}

In order to define a significant change in RF_{csa} overtime the coefficient of variation for the technique, when carried out by myself on ICU patients, was calculated. To calculate the coefficient of variation the RF_{csa} for the first 10 patients studied was repeated on two separate occasions, on the same day, and a Bland Altman plot was generated (Figure 2-3). The coefficient of variation of the percentage difference was found to be 5.60 and therefore a significant change in US RF_{csa} was defined as greater than 9.24%, based on the assumption that 1.65xCV approximates the 95% confidence limits.

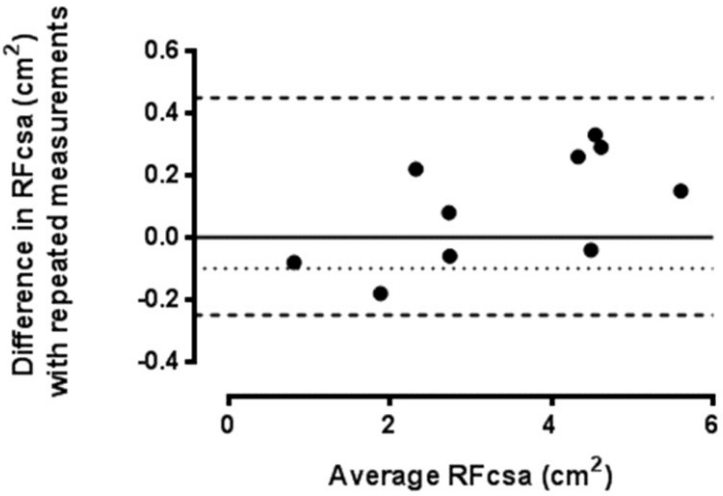


Figure 2-3 Bland Altman plot of ultrasound rectus femoris cross-sectional area (US RF_{csa}) to assess repeatability and define a significant change.

Bland-Altman plot of difference in repeated measurements of RFcsa in ICU patients. Dotted line represents bias -0.1 cm^2. Dashed lines demonstrate limits of agreement -0.25-0.45cm^2. n=10

2.1.3 Assessment of muscle strength

Muscle strength assessment was attempted using two techniques; the Medical Research Council strength score (MRC-SS) and manual muscle testing of maximal voluntary contraction of the quadriceps (QMVC).

2.1.3.1 Medical Research Council - strength score (MRC-SS)

The MRC-SS is a clinical tool used to assess global peripheral muscle strength. It involves the clinical assessment of strength of three muscle groups in each of the four limbs. Each movement's strength is assessed by the assessor and graded 0-5 (Table 2-1). The total score therefore ranges from 0 (complete paralysis) to 60 (normal strength) (3, 18). This test is widely used in both clinical practice and research. It has also been used to define ICUAP; where a score of less than 48 in a patient with the appropriate medical history defines ICUAP (3). The test relies on the cooperation and understanding of the patient and is therefore unsuitable in a large proportion of ICU patients (308). The MRC-SS had good reproducibility and inter-observer variability in the general population (308), however in critical care patients

only moderate consistency was demonstrated for the diagnosis of ICUAP (308). Furthermore the test was not adequately discriminatory in elective cardiothoracic patients recruited for the studies in this thesis – all of whom scored 60 at pre-operative recruitment – and at follow up all but 4 (of whom two were still intubated and ventilated and therefore unable to complete the test) scored 60 despite reportedly feeling weaker and having documented loss of muscle bulk on US.

Strength for each movement tested	Score
Normal Power	5
Active movement against resistance	4
Active movement against gravity	3
Active movement but not against gravity	2
Visible contraction but no limb movement	1
No visible contraction	0
Movements tested on each side: *Arm abduction, Elbow flexion, wrist extension, Hip flexion, Knee extension, Ankle dorsiflexion.*	

Table 2-1 Medical Research Council Strength Score

2.1.3.2 Quadriceps maximal voluntary contraction (QMVC)

The gold standard for assessment of quadriceps strength is the measurement of quadriceps maximal voluntary contraction (QMVC) using the technique described by Edwards et al (309). This involves the measurement of isometric contraction against a non-extendable strap attached to a strain gauge. However this technique requires a significant volume of non-mobile equipment including a modified chair, the strain gauge and the computer equipment to analyse the measurements. Therefore to facilitate measurement of strength at the bedside within the ICU and on the wards, a handheld dynamometer was used instead. This has the advantages of being mobile, quick and easy to carry out in a ward setting. A Lafayette manual muscle tester (device 01163 MMT, Lafayette Instruments Europe Ltd, Leicestershire, UK) was used with the smooth curved attachment. The patient was positioned sitting with the leg flexed at 90 degrees over the edge of the bed or chair. The assessor held the dynamometer in

contact with the patient's mid-shin. The patient was asked to kick out their leg with maximal power which the assessor matched to prevent movement of the leg. The movement was continued for five seconds and the dynamometer recorded the maximal strength in kilograms maintained for one second as per the Lafayette instructions manual.

In a trial of 8 healthy volunteers the quadriceps strength was assessed by both the quads chair and the handheld dynamometer. A Bland Altman analysis of the results showed that the techniques vary significantly with the quads chair always recording a higher strength (Bias 8.5 kg) and the 95% limits of agreement being between -9kg and 26kg (Figure 2-4). However the two techniques did correlate (r=0.75, p=0.03 – Pearson's) and for the purposes of the study assessment of change in strength was required and therefore in view of the logistical issues with using the quads chair, measurement of quadriceps strength was attempted with the hand-held device.

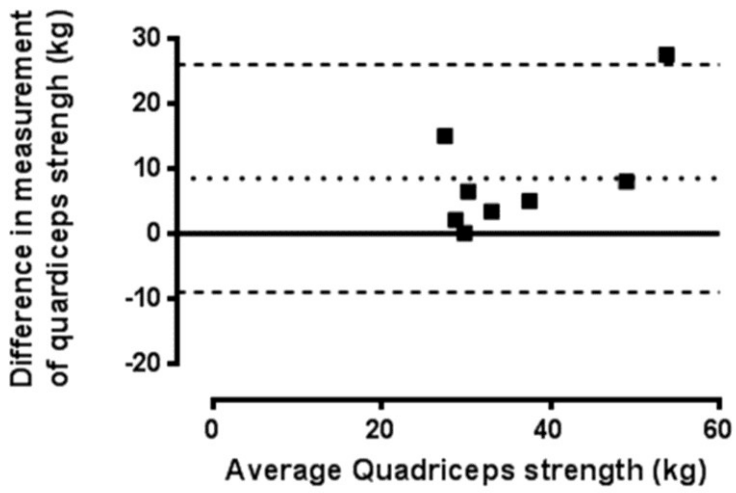


Figure 2-4 Bland Altman plot of measurement of quadriceps strength with the quads chair and handheld dynamometer.

Dashed lines represent 95% limits of agreement -9-26Kg%. Dotted line represents bias 8.5kg (SD 8.9Kg). n=8

This technique clearly involves cooperation and understanding from the patient as well as the ability to sit with the knee flexed over the edge of a bed or chair. Therefore it is unsuitable in many ICU patients and was not attempted on the intensive care unit. The assessment of muscle strength in elective patients was attempted. However repeatability and reliability were found to be poor with a large volitional component. Furthermore for many patients the maximum power of their quadriceps was greater than that which I was able to match with my arm. Finally post operatively patients were unable to complete the test in the majority of cases due to pain from their sternal wounds.

2.1.4 Risk Scoring Systems

2.1.4.1 European System for Cardiac Operative Risk Evaluation (EuroSCORE)

Pre-operative elective cardio-thoracic patients at the Royal Brompton Hospital are routinely scored for operative risk. The EuroSCORE was developed across 128 European cardiothoracic centres with the aim to predict early post operative mortality and complications (310). It has an additive and logistic version both of which have been validated for their ability to predict post-operative mortality, complication and ICU length of stay (311, 312). The additive EuroSCORE was chosen for the purposes of this thesis as it is readily accessible and can be manually calculated. Table 2-1 shows calculation of the additive EuroSCORE, which can also be done online at www.EuroSCORE.org. In the original study in 1999 a score of 0-2 was classified as low-risk, 3-5 medium-risk and > 6 as high-risk. However in a subsequent study the risk of complications and increased length of ICU stay was found to rise at a score of > 5 (311). Therefore we used a cut off of >5 if the surgical team had not already classified the patient as "high-risk" for inclusion into the study discussed in chapters 3 and 6, where larger numbers of patients were required: and >6 for the interventional study (chapter 5) where a longer ICU stay and inpatient stay was essential for the study protocol (predicted ICU stay for a patient with a EuroSCORE > 6 was a mean of 6.1 days in the Messaoudi *et al* study (311)).

Calculation of the additive EuroSCORE		
Patient-related factors		***Score***
Age	(per 5 years or part thereof over 60 years)	**1**
Sex	Female	**1**
Chronic pulmonary disease	Longterm use of bronchodilators or steroids for lung disease	**1**
Extracardiac arteriopathy	Any one or more of the following: claudication, carotid occlusion or >50% stenosis, previous or planned intervention on the abdominal aorta, limb arteries or carotids	**2**
Neurological dysfunction disease	Severely affecting ambulation or day-to-day functioning	**2**
Previous cardiac surgery	Requiring opening of the pericardium	**3**
Serum creatinine	>200 micromol/L preoperatively	**2**
Active endocarditis	Patient still under antibiotic treatment for endocarditis at the time of surgery	**3**
Critical preoperative state	Any one or more of the following: ventricular tachycardia or fibrillation or aborted sudden death, preoperative cardiac massage, preoperative ventilation before arrival in the anaesthetic room, preoperative inotropic support, intraaortic balloon pump or preoperative acute renal failure (anuria or oliguria<10 ml/hour)	**3**
Cardiac-related factors		***Score***
Unstable angina	Rest angina requiring iv nitrates until arrival in the anaesthetic room	**2**
LV dysfunction	Moderate or LVEF30-50%	**1**
	Poor or LVEF <30	**3**
Recent myocardial infarct	(<90 days)	**2**
Pulmonary hypertension	Systolic PA pressure>60 mmHg	**2**
Operation-related factors		***Score***
Emergency	Carried out on referral before the beginning of the next working day	***2***
Other than isolated CABG	Major cardiac procedure other than or in addition to CABG	***2***
Surgery on thoracic aorta	For disorder of ascending, arch or descending aorta	***3***
Post-infarct septal rupture		***4***

Table 2-2 EuroSCORE calculation.
Adapted from www.EuroSCORE.org LVEF – left ventricular ejection fraction, PA – pulmonary artery, CABG –coronary artery bypass graft

2.1.4.2 Sequential Organ Failure Assessment Score (SOFA)

The SOFA score was developed in 1994 as a means of quantifying organ failure in critical care patients (313). Since then it has been widely validated in different ICU populations and has been validated for both sequential use and as a prognostic marker of outcome (314).

This enables the score to be used during ICU admission as a marker of the patient's severity of organ failure/ illness. The SOFA score also has the significant advantage of being easy to use and unlike other scoring systems, for example the acute physiology and chronic health evaluation (APACHE) scores (315), it is possible to manually calculate with data readily available on the intensive care unit. Furthermore despite this it performs almost as well as a prognostic marker for outcome when used as a single time point (314) or when assessing response to treatment (316). Table 2-3 shows how to calculate the SOFA score however there are also free online platforms to facilitate this for example www.mdcalc.com.

SOFA score	1	2	3	4
For respiration with respiratory support PaO_2/FiO_2 (mmHg)	<400	<300	<200	<100
Platelets $x10_3/mm_3$	<150	<100	<50	<20
Bilirubin µmol/L	20-32	33-101	102-204	>204
Cardiovascular hypotension	MAP <70	Dopamine < 5 or Dobutamine any dose	Dopamine >5 or Cathecolamines <0.1	Dopamine >15 or Cathecolamines > 0.1
Glasgow Coma Score	13-14	10-12	6-9	<6
Creatinine µmol/L or (Urine output mls/24 hours)	110-170	171-299	300-400 (<500)	>400 (<200)

Table 2-3 Sequential Organ Failure Assessment score.
Adapted from Crit Care Med. 1998 Nov; 26(11):1793-800. (313)

2.1.5 Blood sampling, handling and storage of samples

Approximately 15mls of blood was collected from the patients using standard techniques; one full serum tube and two EDTA (ethylenediaminetetraacetic acid) tubes. Whole blood was aliquoted and the remaining samples were centrifuged at 1,500x*g* for 10 minutes to enable separation of plasma and serum. To avoid repeated freeze thaw cycles 500µl aliquots were stored at -80^{o}C until required. Samples were processed and frozen within 2 hours of collection.

2.1.6 Muscle biopsy, handling and storage of samples

Quadriceps muscle biopsies were collected from the rectus femoris muscle by two different techniques – Surgical or Bergstrom. Both sets of biopsies were then handled in the same way.

Surgical biopsies were taken by the surgical teams, either at the time of the initial cardiothoracic surgery, a subsequent procedure (for example tracheostomy) or in some cases if the patient was fully anticoagulated on the ICU. This technique involved an open biopsy with direct visualisation of the muscle in order to control bleeding, if it occurred, with diathermy. Open surgical biopsies were taken under full sedation/ anaesthesia, using sterile techniques and only by the surgical team. The wound was closed with sutures and dressed appropriately.

Bergstrom biopsies (317) were taken if the patient did not meet the above criteria. The mid-point of the rectus femoris muscle was identified by ultrasound with the patient supine in bed. Sterile technique was used throughout the procedure. 5-10mls of 1% lignocaine was infiltrated and a small incision with a scalpel made in the skin. The bergstrom needle was then inserted into the muscle and a 50ml syringe used to apply suction. Several small pieces of muscle tissue were biopsied. The wound was then closed with steri-strips and dressed appropriately.

Following collection the biopsies were put into ice-cold saline while the wound was closed and the patient made comfortable. Biopsies, where appropriate, were divided into several pieces and the final biopsy weight size ranged from 10-100mg. Biopsies were then either snap frozen in liquid nitrogen or cork mounted in O.C.T. (VWR International, UK) using isopentane freezing. The biopsies were stored at -80^{o}C until batch processing.

2.2 Molecular Methods

All reagents were supplied by Sigma-Aldrich (Dorset, UK) unless otherwise stated.

2.2.1 General solutions

Solution	Ingredients
PBS (x1)	138mM NaCl, 2.8mM KCl, 8mM NaH_2PO_4, 1.5mM KH_2PO_4 in dH_2O adjusted to pH 7.4
TBE (x10)	890mM Tris-Base, 890 mM Boric Acid, 20mM EDTA adjusted to pH 8 with HCl
2YT	1.6% Bacto-tryptane, 1%Bacto-yeast extract, 0.09% NaCl in dH_2O

Table 2-4 General Solutions

2.2.2 Cell culture and differentiation

Mouse C2C12 skeletal myoblasts were maintained in Dulbecco's Modified Eagle Medium (DMEM) (Life Technologies, Paisley, UK) with Penicillin (100µ/ml) and Streptomycin (100µ/ml) (Life Technologies). DMEM was supplemented with 10% v/v Foetal Calf Serum (GE Healthcare, Little Chalfont, UK) for growth media (GM) and 2% v/v Horse Serum (GE Healthcare) for differentiation media (DM). Stock cells were cultured at 5% CO_2, 37^{o}C and maintained at sub-confluent levels by trypsinisation (Life Technologies) every 2-3 days (split ratio 1:6) for up to 15 passages.

Cells were seeded at 5 x 10^4 cells/ ml in 6 (2mls/ well) or 96 (125µl/ well) well culture plates as appropriate for the experiment. For differentiation purposes C2C12 cells were seeded in 6 well plates and allowed to proliferate in GM until 70-80% confluent (approximately 3 days). They were then transferred to DM which was refreshed every 2-3 days. Differentiated myotubes were clearly visible by day 5-7 and early myotube formation could be seen by day 3.

2.2.3 Cell stretch experiments

2.2.3.1 Cell culture for stretched cells

C2C12 cells were seeded onto 6 well, type I collagen coated, BioFlex® plates (Flexcell International Corporation, USA). These plates have a flexible membrane base to allow extension and stretch of the cell layer which is cultured on them. BioFlex® plates are available with different surface coating on the flexible membrane. The best coating for C2C12 growth was established by testing cell growth on lipopolysaccaride coating, pre-coated collagen plates and re-coated collagen plates against growth on un-coated plastic (standard plates). C2C12 cells grew best on un-coated plastic, they did not thrive at all on lipopolysaccaride or re-coated collagen and they grew more slowly on the collagen coated surface (Figure 2-5), but were able to reach sufficient levels of confluence. Cells were stretched when 100% confluent in DM for 24 hours with or without myostatin treatment at 20ng/ml (R&D systems, UK) and harvested immediately. Stretched cells were both harvested for RNA extraction and used in luciferase assay experiments (see below for methodology).

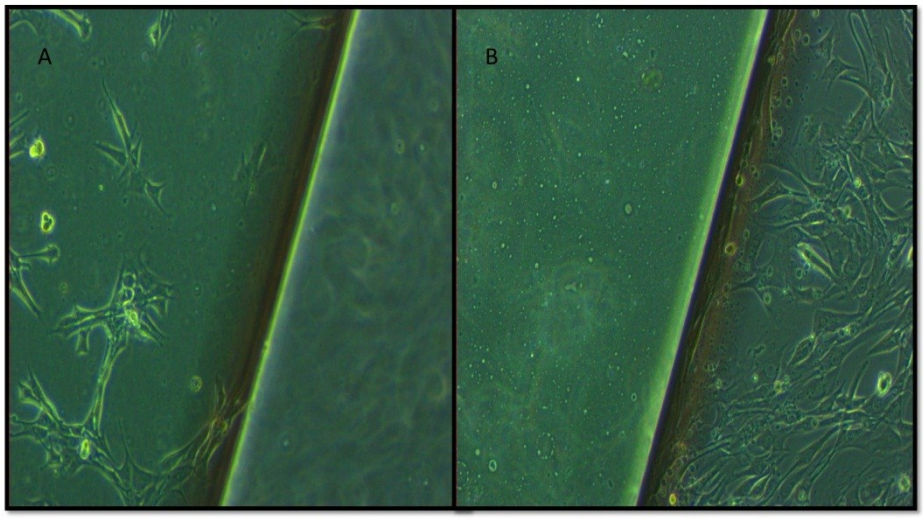


Figure 2-5 Relative growth of C2C12 cells on uncoated plastic or collagen coated plates.
A-C2C12 cells are seen proliferating more slowly on a collagen coated plate (placed at the bottom of a normal well) than on B- the uncoated plastic.

2.2.3.2 *Cell stretch using Flexcell® FX-4000™ apparatus*

Cells were stretched using Flexcell® FX-4000™ apparatus. A cell monolayer was cultured on a flexible membrane (see above). The Flexcell® apparatus allowed the application of cyclic mechanical stretch (CMS) by applying a regulated vacuum below the flexible membrane which is stretched over a loading post (Figure 2-6). The same tension was applied across the membrane and therefore equal stretch across the cell layer. The frequency, duration and degree of stretch applied can be regulated using the central Flexcell® computer (www.dunnlab.de). Stretch was applied at 15% and later 6% at a frequency of 20 cycles per minute based on (318, 319) and previous work by the group. Cells were harvested directly after the allocated stretch time.

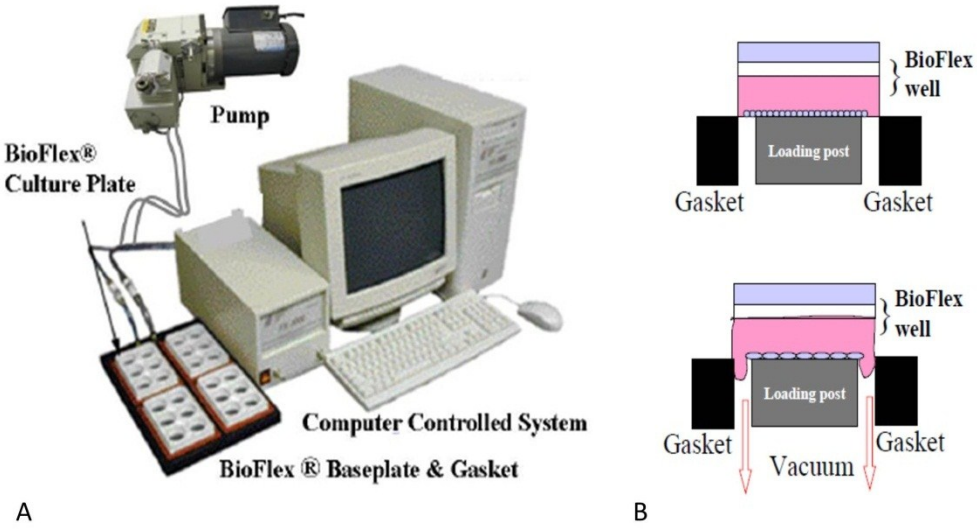


Figure 2-6 Flexcell® FX-4000™ apparatus.
A - Flexcell® FX-4000™ system. B - Diagram to illustrate the application of the vacuum to the flexible membrane over the loading post (320, 321) www.dunnlab.de.

2.2.3.3 *Cell Viability and damage assays following cell stretch.*

Cell stretch techniques can result in significant damage and loss of viability to cells, therefore cell viability and damage was assessed during the development of the methods.

Cell viability was determined with an MTT assay: 1mg of Yellow tetrazolium MTT (3-(4, 5-dimethylthiazolyl-2)-2, 5-diphenyltetrazoliumbromide) was dissolved in warmed Serum Free media. Cells were incubated for 30 minutes in 1.5mls per well of MTT media. Media was removed and 1.5mls of dimethylsulfoxide (DMSO) solution per well added. The cells were agitated for 15 minutes then 100µl of solution was transferred to a 96 well plate and absorption measured at 550nm. This assay relies on the cleavage of Yellow terrazolium MTT by viable cells into purple formazan in order to release NADPH. The amount of formazan is proportional to the number of viable cells (322).

Cell damage was determined measuring release of Lactate dehydrogenase (LDH) into the media of stretched cells. LDH was quantified using the commercially available Cytotoxicity Detection Kit (Roche, UK) according to the manufactures guidelines.

Cell viability was not decreased (MTT, p=0.70, n=1 in triplicate) and cell damage did not increase significantly (LDH, p= 0.39, n=1 x 6) following 24 hours of 15% stretch.

2.2.3.4 Method development

Cyclic mechanical stretch is an established technique used as an in vitro model of muscle activity (323). C2C12 cells were allowed to become 100% confluent prior to differentiation. This is in contrast to normal cell culture techniques which would begin the differentiation process at about 70-80% confluency. This was done as attempts to stretch cells at the start of differentiation from a lower confluency or following 3 days differentiation in differentiation media resulted in the cells peeling off the membrane. 100% confluency should ensure cell to cell contact and by starting the stretch at the start of differentiation differentiating cells may be less fragile. Furthermore although the protocols described in the literature vary substantially, it has been established that applying stretch at the start of differentiation will cause C2C12 cells to form parallel myotubes (324) . Thus each cell will be

subjected to unidirectional stretch, which may be more representative of normal physiological activity (323) and therefore the differentiating myoblasts may withstand it better.

RNA was extracted from stretched cells however the variability of the conditions resulted in extremely variable expression of target genes and house-keeping genes. Interleukin-6 (IL-6) mRNA expression was used as a positive control to demonstrate that the stretch protocol was appropriately affecting the cells (as per (318, 325)). Initially cells were stretched at 15%, but a greater increase in IL-6 mRNA was seen with 6%, however neither reached statistical significance. Choice of house-keeping genes is obviously important in these conditions as it is expected that stretch would affect both metabolic rate and cytoskeletal structure of the cell (326). GAPDH, RPLPO and 18S were found to correlate well with each other and to be stably expressed across the samples, however in preliminary experiments 18S was found to be less reliably stable between the conditions, therefore the geometric mean of GAPDH and RPLPO was used, this is also consistent with the other cell experiments in this thesis and previous experience of the group. Further analysis of mRNA expression was not attempted due to the wide variability of gene expression and the inconsistency of results of preliminary experiments. 6% stretch was used for further luciferase activity based stretch experiments.

2.2.4 GDF-15, Myostatin and TGF-β treatment

Effect of GDF-15 (50ng/ml), Myostatin (20ng/ml) and TGF-β (2.5 ng/ml) (all R&D systems, UK) were examined in different experiments. The treatment doses were based on the work carried out previously by the group. These treatments are all dissolved in 0.1% Bovine Serum Albumin (BSA) with 20mM Hydrogen chloride (HCl), a solution of which was therefore used as the control treatment.

2.2.5 Luciferase assays

SMAD activation and phosphorylation is one of the main signalling pathway mechanisms activated by the TGF-β family. Receptor binding of TGF-β ligands results in the activation of the serine/ threonine receptors: and subsequent phosphorylation of the SMAD 2/3 complex (153). This then co-localises with SMAD 4 and translocates to the nucleus where it acts as a co-transcription factor for TGF-β responsive genes. Activated SMADs bind specific nucleic acid sequences within the promoter region of the gene in order to promote the transcription of that gene; these regions have "CAGA" repeat sequences. The CAGA-(12)-luciferase assay relies on the transfection of a DNA vector plasmid which contains 12 CAGA repeats adjacent to a minimal promoter and the sequence for firefly (*Photinus pyralis*) luminescent protein. The transcription of the firefly luciferase therefore relies on the activation of SMAD proteins and their binding to the CAGA region, as there is a high repeat number of the CAGA sequence this assay should be a sensitive marker of SMAD activity. However the assay is also dependant on the transfection efficiency and the density of cells. Therefore firefly luciferase activity is normalised to the relative activity of renilla (*Renilla reniformis*) luciferase. The renilla luciferase plasmid (pRL-TK) is transfected at the same time as the reporter firefly plasmid ($p(CAGA)_{12}$–luc) and is itself under the independent control of the thymidine kinase (TK) promoter.

2.2.5.1 Preparation of DNA plasmids

All plasmids used in the current experiments were already available in the lab. Dr Paul Kemp acquired the $p(CAGA)_{12}$-luc plasmid from Prof. Susumu Itoh (sitoh@md.tsukuba.ac.jp) Faculty of Medicine, University of Tsukuba. pCDNA.3 -an empty vector control and pRL-TK were commercially available from Promega, UK.

To make plasmid stocks 40µl of competent JM 109 bacteria (Promega, UK) were mixed with 5µl of concentrated DNA plasmid and incubated for 15 minutes on ice. Subsequently they were heat-shock transformed at 42^{o}C for 90 seconds and then incubated in 500µl 2YT media (Table 2-4) at 37^{o}C for 45 minutes. Following this the bacteria were plated on ampicillin (100µg/ml) containing agar plates and cultured over night at 37^{o}C. The DNA plasmids also contain the genetic sequence for ampicillin resistance; therefore all colonies which grow will have been successfully transformed. These colonies are then picked and the bacteria allowed to multiply in 4ml 2YT media supplemented with 100ug/ml ampicillin at 37^{o}C overnight under agitation. DNA was extracted from the bacterial culture using QIAprep® Spin Miniprep kits (Qiagen, UK) as per the manufactures guidelines.

Plasmid identity was confirmed using restriction digests. This involved 1 hour incubation of 4µl of DNA with the specified restriction enzymes (see below). The digest reaction contained the restriction enzymes in a ratio of 1:1 total volume of 1µl, 2 µl 10x buffer and if a double digest was being performed - 0.5µl 0.1% BSA but not for a single digest. The final volume was then made up to 20µl per reaction with dH_2O. The products were then run on a 2% TBE- agarose gel. This was made by dissolving 2% Agarose (Bioline, UK) in 0.5xTBE (for a 75ml gel 1.5mg agarose in 75ml 0.5 TBE Table 2-4), this was then allowed to cool and 5µl ethidium bromide (10mg/ml) added. Following setting the gel was submerged in 0.5xTBE in the gel tank. Samples were mixed with 5x loading buffer (Bioline) and run for 45 minutes to 1 hour at 140V alongside standard DNA ladders (Hyperladder I and II Bioline). Appropriate band size was predicted from the known plasmid map (Table 2-5). DNA was then quantified using a NanoDrop™ machine (BioRad, UK).

Plasmid	Restriction enzymes	Predicted bands (bp)
pCDNA.3	Pst1	1356 4072
$p(CAGA)_{12}$-luc	Hindi III, BamH1	1950 >2800
pRL-TK	EcoR1, Sma1	400

Table 2-5 Restriction digests for plasmid identification

2.2.5.2 *Transfection of DNA plasmids*

C2C12 cells were seeded in the appropriate plate for the experimental protocol at a concentration of $5x10^4$ cells per ml. Cells were transfected when approximately 60% confluent on the first day after seeding. The protocol here is described per single well of a 6 well plate and volumes scaled up or down as appropriate. A total of 2µg DNA was transfected per well. The DNA mix consisted of 100µl Optimem (GIBCO, Life technologies) and a mix of plasmids as follows: $p(CAGA)_{12}$-luc - 1.45µg, pRL-TK - 0.05µg and pCDNA.3 – 0.5µg. pCDNA.3 was used as a control empty vector for another plasmid (FHL-1) which was co-transfected as part of another experiment. That experiment is not discussed further in this thesis, however these transfections were carried out at the same time and therefore in order to keep the DNA mix ratios constant the empty vector was added to all experimental wells. The DNA mix was combined with a second mix of 100µl Optimem with 10µl Lipofectamine (Invitrogen); the two were incubated together at room temperature for 15 minutes. During this time the cells were washed twice with serum free DMEM. Cells were then incubated for 4.5 hours at 37^oC with the transfection mix diluted to a volume of 1ml per well in serum free media. Subsequently the media was replaced with GM and cells returned to the incubator as normal.

2.2.5.3 *Luciferase assays*

Luciferase assays were carried out using the Dual-Luciferase® reporter assay system (Promega, UK). Following transfection and appropriate treatment cells were washed twice with PBS (Table 2-4) and lysed in passive lysis buffer (1 ml/ well of a 6 well plate, 15 minutes

incubation at room temperature under agitation). 10µl lysate was transferred to a white plastic 96 well plate and the Dual-luciferase® reporter reagents used as per the manufactures guidelines. This involved the addition of a 1st step firefly luciferase substrate and luciferase activity was read on a Luminark micro-plate spectrophotometer (BioRad) plate reader. Immediately after this the "stop and glo" reagent was added to the wells in order to read the renilla luminescence in the same way. Firefly luciferase activity was normalised to that of renilla for the same well.

2.2.5.4 Over-expression of miR-181a

To examine the effect of miR-181a on TGF-β activation of the SMAD dependant luciferase reporter discussed above, a miR-181a mirVana microRNA mimic (Invitrogen) was transfected into C2C12 myoblasts as follows. Transfection was carried out on day one post seeding C2C12 cells in 96 cells plates. Per well of a 96 well plate 0.5µl of a 20µM stock (10nmols) of mirVana mimic or negative control was mixed in 12.5µl of Optimem to make the microRNA mix. The lipofectamine mix consisted of 0.5µl of Lipofectamine 2000 (Invitrogen) was diluted separately in 12.5µl of Optimem. Following 5 minutes incubation at room temperature the two mixes were combined and incubated at room temperature for a further 20 minutes. During this time cells were washed twice with serum free DMEM. 100µl per well of serum free DMEM was then added to the transfection mix and cells incubated with 126µl per well for 4 hours at 37°C. Following which the media was changed to GM and the cells incubated overnight. The following day $p(CAGA)_{12}$-luc and pRL-TK plasmids at a ratio of 3:1 were transfected as above. TGF-β treatment occurred on the next day for 6 hours and following this, cells were lysed and luciferase activity read as described above.

2.2.6 RNA extraction

2.2.6.1 RNA extraction from Cells

Cells experiments requiring RNA extraction were carried out in 6 well plates. Cells were seeded at $5x10^4$ cell/ml (using 2 mls per well). When ready for harvesting, cells were washed twice with ice cold PBS. Cells were lysed in 1ml of Triazol (Life Technologies, UK) with vigorous scraping. The Triazol was then aspirated, transferred to a 1.5ml microcentrifuge tube and vortexed in order to facilitate further cell membrane breakdown. 200µl chloroform were then added and following thorough vortexing the sample was allowed to settle at room temperature for 2-3 minutes. Following centrifugation at 12,000x*g* for 15 minutes at 4^{o}C the supernatant, upper aqueous phase, was carefully transferred to another microcentrifuge tube without disturbing the protein layer. 500µl of isopropanol were added to the supernatant, mixed and allowed to incubate for 10 minutes at room temperature. Samples were centrifuged as above for 10 minutes and the RNA pellet precipitated onto the bottom of the tube. The supernatant was carefully removed without disturbing the pellet, which was subsequently washed twice with 75% ethanol. The ethanol was then removed and the pellet was allowed to air dry until all the remaining ethanol had evaporated. The RNA was then dissolved in 30µl of dH_2O.

RNA was quantified using a NanoDrop™ machine and absorption read at 230nm, 260nm and 280nm before storage at -80^{o}C. RNA purity was checked using the 260:280 and 230:260 ratios calculated by the NanoDrop: a ratio of 2 for both reflects pure RNA.

2.2.6.2 RNA extraction from Human Tissue

Human muscle samples were homogenised in 500ml of ice cold Triazol using a Precellys 24™ Tissue homogeniser (Stretton Scientific, UK). The technique involved the rapid agitation of the sample in tubes containing ceramic beads (CDK-14) which crush and

breakdown the tissue. Samples were homogenised with 2 x 10 second cycles at 5,500rpm on the Precellys machine – which were repeated if necessary. Following centrifugation for 3 minutes at 10,000x*g* to remove debris, the Trizol was transferred to a different microcentrifuge tube and the RNA extracted as above with adjusted volumes for 500µl of Triazol.

2.2.6.3 MicroRNA extraction from Plasma

These methods were based on those described by Kroh et al (327). As discussed in the introduction the regulation of circulating levels of microRNAs is not fully understood and as such there are presently no established "housekeeping" microRNAs that can be used to control for the efficiency of RNA extraction. Therefore this method uses an exogenous control microRNA (C-39, a microRNA from the nematode worm *c-elegans*) that is spiked it at the start of the process at a constant concentration.

4mls of Qiazol (Qiagen, UK) was vortexed thoroughly with 400µl of thawed plasma. 5µl of a 5fmol/µl stock solution of C-39 RNA (Invitrogen) was added to each sample. Following vigorous vortexing with 800µl of chloroform samples were allowed to settle for 2-3 minutes. Samples were then centrifuged at 2,500x*g* for 25 minutes at 4^{o}C and the upper aqueous phase removed. From this step onwards the Qiagen miRNAeasy RNA and small RNA extraction kit was used as per the manufacturer's guidelines (Qiagen). The final elution was carried out with 50µl volume of RNAase free water.

The above method was compared with a manual technique of RNA extraction – using isopropanol and pellet precipitation. The same sample was tested in both techniques with the same amount of C-39 control RNA. The samples were then tested for C-39 and miR-1. The Qiagen kits resulted >10-times more efficient extraction of RNA and therefore this technique was used.

2.2.7 cDNA synthesis and quantative PCR (qPCR) for mRNA.

Reverse transcription (RT) for mRNA analysis. 150ng of RNA for each sample was diluted in 11ul of RNAse- free water. The RNA was denatured at 65^{o}C or 5 minutes and then cooled on ice for 2 minutes. A 9µl reaction mix containing 1ul Omniscript (Qiagen), 2µl 10x buffer (Qiagen), 2µl- 5mM dNTPs (Qiagen), 0.5µl Random Primers (Promega, UK), 0.5µl RNAse inhibitor – (Ribolock – Thermo Scientific, UK), 1µl DTT (Qiagen) and 2µl water was then added and the samples incubated at 42^{o}C for 2 hours. The cDNA was then diluted to a final volume of 200µl and stored at -20^{o}C.

In order to test the genes of interest primers were selected from the literature. The primer sequences were run on the NCBI "primer blast" programme (www.ncbi.nlm.nih.gov/tools/primerblast) against the mRNA sequence of interest which determined the predicted size of PCR product. PCR was then carried out using a standard thermal cycler (where necessary at different annealing temperatures) and the products run on a TBE- 2% agarose gel as described above in order to identify a single product of the appropriate size.

qPCR was carried out using SYBR® green based reactions in fast optical 96 well plates (Life Technologies). Reaction mix consisted of 3µl of sample cDNA, 2µl of a 2µM primer mix containing both forward and reverse primers, 10µl of fast SYBR (Quantifast® - Qiagen) and 5µl dH_2O. Plates were sealed with MicroAmp optical adhesive film (Life Technologies) and centrifuged for 1 minute at 200x*g* to ensure mixing and removal of air bubbles. qPCR was carried out using an ABI 7500 fast thermal cycler with the following thermal profile (ABI, Life technologies): 5 minutes 95^{o}C activation step, 40 cycles of 95^{o}C for 10 seconds and 60^{o}C annealing for 30 seconds (GDF-15 primers were annealed at 65^{o}C). A melt curve was then performed to further exclude non-specific binding products. All reactions were carried out in duplicate with a negative water control. The baseline and threshold were set manually for

each gene and when appropriate kept constant across different PCR plates. The mean cycle threshold (Ct) was then taken for the duplicates and analysed using $½^{\wedge Ct}$. Samples were excluded if the melt curve showed non-specific amplification or inconsistency between duplicates. Table 2-6 lists primers used and Table 2-7 lists the housekeeping genes used for normalisation of mRNA expression in the experiments carried out in this thesis. Housekeeping genes for human mRNA normalisation were tested using NormFinder (328), this software allows both intra and inter-group variation to be assessed. GAPDH, RPLPO and 18S were assessed. The geometric mean of the three genes provided the most stable marker both between the groups and between the samples overall. For microRNA in human muscle samples U6 provided the greatest stability between and within the groups.

mRNA Sybr Green Primers		
Human	*GAPDH*	*F- GGTGGTCTCCTCTGACTTCAACA* *R – GTTGCTGTAGCCAAATTCGTTGT*
	RPLPO	*F – TCTACAACCCTGAAGTGCTTGATATC* *R – GCAGACAGACACTGGCAACATT*
	18S	*F- GTAACCCGTTGAACCCCATT* *R- CCATCCAATCGGTAGTAGCG*
	Murf-1	*F- CCTGAGAGCCATTGACTTTGG* *R -CTTCCCTTCTGTGGACTCTTCCT*
	Atrogin-1	*F- GCAGCTGAACAACATTCAGATCAC* *R -CAGCCTCTGCATGATGTTCAGT*
	CYR61	*F- ACTTCATGGTCCCAGTGCTC* *R - TGCTGCATTTCTTGCCCTTTT*
	Myostatin	*F-ACATGAACCCAGGCACTGGT* *R-GGTTGTTTGAGCCAATTTTGC*
	IGF-1	*F - CCACGATGCCTGTCTGAGG* *R - TTTCAACAAGCCCACAGGGT*
	MyoD1	*F-GACGGCATGATGGACTACAG* *R - AGGCAGTCTAGGCTCGACAC*
	MHC 1	*F - CCC TGG AGA CTT TGT CTC ATT AGG* *R - AGC TGA TGA CCA ACT TGC GC*
	MHC 2a	*F - TCA CTT ATG ACT TTT GTG TGA ACC T* *R - CAA TCT AGC TAA ATT CCG CAA GC*
	MHC 2x	*F - TGA CCT GGG ACT CAG CAA TG* *R - GGA GGA ACA ATC CAA CGT CAA*
	Myogenin	*F - ACC CTA CAG ATG CCC ACA AC* *R - GGA AGG CCA CAG ACA CAT CT*
	CTGF	*F- AACCGCAAGATCGGCGT* *R - CCGTACCACCGAAGATGCA*
	GDF-15	*F- TGCCCGCCAGCTACAATC* *R-TCTTTGGCTAACAAGTCATCATAGGT*
Mouse	*RPLPO*	*F-GGACCCGAGAAGACCTCCTT* *R-TGCTGCCGTTGTCAAACACC*
	GAPDH	*F-ACTCCACTCCACGGCAAATTCA* *R- CGCTCCTGGAAGATGGTGAT*
	Murf-1	*F-CGGGCAACGACCGAGTGCAGACGATC* *R-CCAGGATGGCGTAGAGGGTGTCAAAC*
	Atrogin	*F-TCAGCCTCTGCATGATGTTC* *R-TGGGTGTATCGGATGGAGAC*
	CYR61	*F- GGATGAATGGTGCCTTGC* *R- GTCCACATCAGCCCCTTG*
	CTGF	*F- TGGCGAGATCATGAAAAAGA* *R - AGATGTCATTGTCCCCAGGA*
	MyoD1	*F - GTGGAGATGCGCTCCACTAT* *R -CTCTGATGGCATGATGGATT*
	IL-6	*F- TAGTCCTTCCTACCCAATTTCCC* *R- TTGGTCCTTAGCCACTCCTTC*
microRNA primers		
5s		F-ATCTCGGAAGCTAAGCA R- GGTCTCCCATCCAAGTACT
U6		CTCGCTTCGGCAGCACA
miR-1		CCGGTGGAATGTAAAGAAGTATGTAT
miR-133a		GTCCCCTTCAACCAGCTG
miR-181a		ATTCAACGCTGTCGGTGAGT
miR-206		TGGAATGTAAGGAAGTGTGTGG
miR-499		GGCTTAAGACTTGCAGTGATGTTT
Universal reverse		GTACTGCGCGTGGAGAGGAAT

Table 2-6 qPCR Primers

Condition	Genes
Human mRNAs	Geomean (RPLPO, GAPDH, 18S)
Human microRNAs	U6
Mouse mRNAs	Geomean (RPLPO, GAPDH)
Mouse microRNAs	Geomean (5s,U6)

Table 2-7 Housekeeping genes.
These genes were selected on the basis of being stable between the experimental groups being compared.

2.2.8 qPCR quantification of microRNA.

Reverse transcription for microRNA quantification used in the studies presented in this thesis involves the addition of a "polyA-tail" to the cDNA template using the NCODE™ VILO™ microRNA cDNA synthesis kit (Invitrogen). The kit also includes a universal reverse primer which recognises this polyA tail and is used with a microRNA specific forward primer for qPCR. This is necessary as the microRNA are only about 22 nucleotides in length and are otherwise difficult to amplify with standard qPCR techniques.

For reverse transcription of RNA from human muscle samples 150ng of RNA was diluted in 11µl of water, however this was increased to 1000ng for cell culture RNA samples as expression of microRNA in C2C12 cells is low. RNA was again denatured at 65°C for 5 minutes and cooled for 2 minutes on ice. Following which a reaction mix of 2µl 10x superscript enzyme mix, 4µl of 5x reaction mix and 3µl of water was added and the samples incubated at 37°C for 2 hours followed by 5 minutes heat deactivation at 95°C. Sample were then diluted x10 (x5 for cell culture experiments) before storage at -20 °C. MicroRNA isolated from plasma cannot be quantified by u.v. absorption spectroscopy and concentration of some microRNA of interest was very low, therefore 14µl of RNA was added and additional water was excluded from the reaction mix.

qPCR was carried out as described above, but the reaction mix was adjusted for use of the universal reverse. The reaction mix therefore included 10µl SYBR, 0.4µl of Universal Primer (10mM) and 0.4µl specific microRNA primer (10mM) and 6.2µl of water, combined with 3µl of

appropriate cDNA. Table 2-6 lists primers used and Table 2-7 the genes used for normalisation of these qPCR data. Samples were excluded if the melt curve was showed non-specific amplification, Figure 2-7 shows example melt curves.

2.2.8.1 Across plate standardisation of microRNA qPCR data.

For the study discussed in chapter 3 (MicroRNAs as potential biomarkers of acute muscle wasting) different microRNAs in 168 separate samples, in duplicate, were quantified. In order to ensure accurate quantification between plates a standard curve for each microRNA that was quantified was generated. This was done by amplifying the specific microRNA from a plasma pool and sequentially diluting it. These standards were kindly provided by Dr Donaldson from the same group. The standards were then run alongside the samples on each plate and the results checked for linearity and compared to each other. They were then used to calculate the concentration of microRNA relative to the standards in arbitrary units (AU).

2.2.9 Protein Extraction

2.2.9.1 From Cells

Cells experiments requiring protein extraction were carried out in 6 well plates. Cells were seeded at $5x10^4$ cell/ml (using 2ml per well). When ready for harvesting cells were washed twice with ice cold PBS and then lysed in 500µl of NP40 lysis buffer (Table 2-8) with 1:100 Protease and Phosphatase inhibitors. Samples were stored at -20^{o}C

2.2.9.2 From Human Tissue

Muscle samples were homogenised in NP40 with Protease and Phosphatase (1:100) using the Precelley's methods described above. The samples were then centrifuged at 10,000x*g* to remove debris and the soluble protein fraction collected and stored at -80^{o}C.

2.2.9.3 Protein quantification

Bradford assays were used to determine protein concentration of the samples. The sample was diluted with water to ensure the NP40 did not interfere with the assay and also to ensure that the resulting concentration fell within the linear portion of the assay's standard curve. 10µl of appropriately diluted sample (5-40 times) was incubated under agitation with 90µl of Bradford reagent for 15 minutes. The absorption was then read at 620µm using a Luminark micro-plate spectrophotometer (BioRad) and the concentration calculated against the standard curve. Standards were prepared with appropriate weights of BSA dissolved in water.

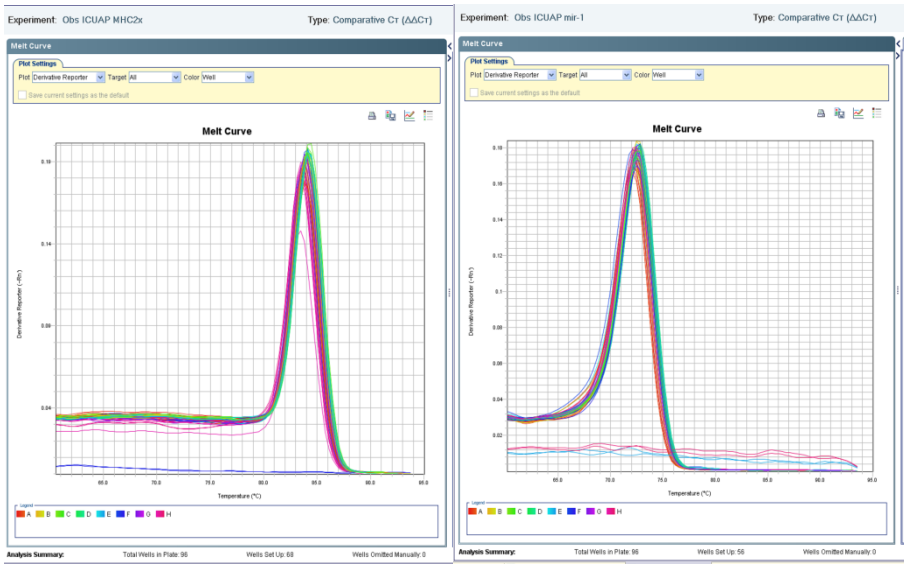


Figure 2-7 Example melt curves.

Left panel shows example melt curve from qPCR amplication of MHC2x mRNA from human ICUAP and control muscle samples, right panel shows the same for MiR-1.

2.2.10 Western Blotting

Table 2-8 describes the solutions used for western blotting.

Solution	Ingredients	Working concentration/ notes
General solutions		
NP40 lysis buffer (x2)	300mM NaCl, 20mM Tris, 10mM EDTA, 2% Igepal-NP40 In dH_2O pH7.4	1x Add protease and phosphatase inhibitors (both 1:100) before use.
RSTB sample buffer (x2)	4% SDS, 20% glycerol, 10% 2-mercaptoethanol, 10% 1M Tris (pH6.8)	1x
Running Buffer (x10)	250mM Tris, 1.9M glycine, 35mM SDS in dH_2O pH8.3	1x
Transfer Buffer (x10)	200mM Tris, 1.5M glycine in dH_2O	1x add 20% methanol at the time of use
TBS (x10)	200mM Tris, 1.4mM NaCl In dH_2O pH7.6	For TBS-T; Add 1% Tween 20 prior to dilution to 1x
Acrylamide gels		
Resolving gel (10%)	3.33ml -30% acrylamide, 2.5ml -1.5M Tris, 100µl -10% SDS, 50µl -10% APS, 5µl -TEMED, 4.02ml - dH_2O.	Enough for 2 gels
Stacking Gel	0.86ml -30% acrylamide, 1.26ml -0.5M Tris, 50µl -10% SDS, 20µl -10% APS, 5µl -TEMED, 2.11ml - dH_2O.	Enough for 2 gels

Table 2-8 Solutions for western blotting

2.2.10.1 Western blotting procedure

Protein samples were diluted 1:1 with sample buffer and heat denatured at 95^{o}C for 5 minutes. Samples were separated using SDS poly acrylamide gel electrophoresis. The resolving gel solution was poured into a glass plate cast, covered with water saturated butanol and allowed to polymerise. Following washing to remove the butanol the stacking gel was set

above the resolving gel with the appropriate comb used to produce sample loading wells. Samples were then loaded and the gel run in a BioRad gel tank at 140 volts until the standard protein ladder could be seen to have run and separated sufficiently. The protein was then transferred to a PDVF membrane (BioRad) (activated in methanol) at 14V using a semi-dry transfer technique (Semi-dry blotter - BioRad) and transfer buffer with 20% methanol (Table 2-8) which for the proteins examined required a 70 minutes transfer time.

Membranes were blocked in 5% milk-TBST (Marvel non fat milk) for 30 minutes at room temperature. Membranes were then incubated at 4^{o}C overnight (or 1 hour at room temperature) with primary antibodies prepared in 5% milk-TBST at appropriate concentrations (see Table 2-9). Prior to incubation with secondary horseradish peroxidise (HRP) conjugated antibodies (also diluted in 5% milk-TBST) membranes were washed 3 times in TBST. Following 1 hour incubation at room temperature with secondary antibody the membranes were washed as before. The blots were then imaged using ECL chemiluminescent reagents (GE Healthcare) and light sensitive Kodak film (Life technologies). The resulting image was scanned for analysis in Image J.

Primary antibody specificity was checked by ensuring that the protein band occurred at the predicted molecular weight using a standard ladder (BioRad) and also by loading a negative control (no sample) alongside the protein samples to ensure no binding. Secondary specificity was checked by incubating a membrane in secondary antibody only and ensuring no signal was created. Table 2-9 lists the antibodies used.

Normalisation for protein loading and transfer efficiency was achieved with either tublin quantification or ponceau red staining. For Ponceau red stating membranes were washed briefly with Ponceau red solution and then rinsed in TBST. The image was then scanned and analysed in Image J.

Primary Antibody	Dilution	Secondary HRP Antibody	Dilution
For human tissue			
TGFBR1 (AF-241-NA) R&D systems	1 in 500	Rabbit anti goat HRP (P0449) Dako	1 in 3000
For murine cell culture			
TGFBR1 (H-100 R) SantaCruz	1 in 400	Goat anti Rabbit HRP (P0448) Dako	1 in 6000
TGFBR2 (L21: sc-400 R) SantaCruz	1 in 400	Goat anti Rabbit HRP (P0448) Dako	1 in 3000
α-Tubulin (Ab4074) Abcam	1 in 1000	Rabbit anti goat HRP (P0449) Dako	1 in 3000

Table 2-9 Antibodies used for western blotting.
TGFBR1 and 2 – TGF-β receptor type 1 and 2 respectively, HRP – Horse Radish Peroxidase.

2.2.10.2 Quantification of protein by Western blot.

Western blot images were scanned and analysed using Image J. Appropriate bands in each lane were identified and selected with individual uniform rectangles. The pixel profile of each band was then plotted by the Image J software. Protein concentration is relative to the intensity of the signal which is represented by the area under the curve of the plot. This is manually delineated, to exclude background, and calculated for each band. For Ponceau staining the intensity of the whole lane was calculated. The target protein level was then normalised to either the Ponceau (human samples) or α-tubulin (cell culture samples).

For the quantification of the TGF-β type 2 receptor in ICUAP muscle, 26 human tissue samples were quantified. In order to standardise between gels a pool of samples at 2 different concentrations and 2 individual samples were run on each gel. These were then used to standardise the intensity of each sample relative to the other gels.

2.2.11 ELISA

Plasma levels of myostatin (Immundiagnostik, Bensheim, Germany) and GDF-15 (R&D systems, Abingdon, UK) and IGF-1 (Mediagnost, Reutlingen, Germany), were quantified using commercially available ELISA kits. These kits have all been reported as reliable in the literature and the quoted inter-plate co-efficients of variation (CV) of the ELISAs were 4.7-6.0% for GDF-

15, and 2.25-6.79% for IGF-1, the Myostatin ELISA did not report a CV. Assays were performed according to the manufacturer's instructions and ELISA plates were read on a microplate spectrometer (BioTek Powerwave XS). Results were analysed as per the manufactures guidelines using the supplied standard curve samples and all samples were analysed in duplicate.

2.2.12 Histology of muscle samples

O.C.T embedded, cork mounted quadriceps muscle biopsy specimens were sectioned (10µm) and Heamatoxylin and Eosin (H&E) stained by the histology department at Imperial College.

2.2.12.1 Muscle fibre diameter

H&E stained sections were imaged using an Olympus CKX41 microscope at 10x magnification. The fibre diameter was measured in Image J for between 33-105 fibres (depending on the quality and quantity of sample available) and the mean fibre diameter calculated for each individual. The minimal Feret's diameter of the fibre was measured, this was defined as the smallest distance between parallel edges of each fibre (http://www.curecmd.org/wp-content/uploads/scientists/sop/MDC1A_M.1.2.002.pdf). This distance should therefore reflect the true diameter if the fibre has been cut cross-sectionally or longitudinally.

2.2.12.2 Immunoflourscencent staining for fibre type

Sections were air dried and marked with a wax pen (DAXO). They were then washed briefly with PBS-1%Tween (PBST) and subsequently blocked with 5%milk-PBST for 30 minutes. Primary MHC and laminin antibodies were prepared (as per Table 2-10) in PBST and the sections incubated for 1 hour at room temperature in the antibody solution. Following 3 x 5 minute washes in PBST sections were then incubated with Alexaflor®-conjugated secondary antibodies for 1 hour at room temperature in the dark. A negative control for the secondary

antibody (i.e. no primary antibody) was included to assess secondary antibody specificity. Following repeated washing as above sections were allowed to air dry and were then fixed with Fluromount (sigma) and a glass coverslip. The immunofluorescent signal was recorded using a **Zeiss Axiovert 200 microscope** and Velocity software (Perkin Elmer, Massachusetts, USA). MHC 1, 2a, 2x (seen as unstained fibres) and hybrid fibres (stained for both MHC 1 and 2a) were then identified, counted and diameter measured using Image J software.

Primary Antibody	Dilution	Secondary Fluorescent Antibody	Dilution
MHC staining			
MHC 1 (A4.840) DSHB	1 in 25	Alexaflor® -350 anti mouse IgM (A-31552)	1 in 500
MHC 2a (N2.261) DSHB	1 in 50	Alexaflor® - 488 anti mouse IgG (A-11059)	1 in 200
Laminin (4H8-2) Abcam	1 in 500	Alexaflor® - 568 anti rat IgG (A-11079)	1 in 500
Nuclear p-SMAD 2/3 staining			
$pSMAD_{2/3}$ (11769R) Santa-Cruz	1 in 1000	Alexaflor® - 488 anti rabbit (A-11034)	1 in 500
Laminin (4H8-2) Abcam	1 in 500	Alexaflor® - 568 anti rat IgG (A-11079)	1 in 500
4', 6-diamino-2--phenylindole (DAPI) Invitrogen	1 in 10,000		NA

Table 2-10 Antibodies used for Immuno-flourescence.
DSHB - Developmental Studies Hybridoma Bank, California, Alexaflor® supplied by Life Technologies.

2.2.12.3 Localisation of pSMAD-2/3

In a separate analysis sections were stained for nuclear localisation of phosphorylated-SMAD 2/3. The protocol above was modified, sections were fixed with 4% paraformaldehyde and then permeabilised with 0.3% Triton X100 in PBS-Tween, to ensure nuclear permeability to the antibody, prior to blocking with 5% BSA in PBS-Tween. Antibodies were also prepared in BSA. Nuclei were stained with 4', 6-diamino-2--phenylindole (DAPI, Invitrogen; stock concentration at 5mg/ml diluted to 1:10000 in 1xPBS). Prior to drying and mounting slides were incubated for 2 minutes with DAPI and then washed as above. Using Velocity software all stained nuclei were counted and marked for each section. Following this, those nuclei staining for p-SMAD2/3 were also marked and the percentage of positive nuclei was calculated. The exposure, brightness and thresholds were set as the same for all images.

2.3 Statistical methods

Data were handled and analysed and figures constructed using Graphpad Prisim 6 software. For all analyses a p value of < 0.05 is taken to be statistically significant.

2.3.1 Statistical handling and analyses of demographic data and results from the clinical studies.

Statistical methods were discussed with Winston Banya (Medical statistician, NHLI, Imperial College).

Chapter 3 - Demographic data are quoted as mean ± standard deviation (SD) unless otherwise stated. Student's t-tests (for normally distributed data) or Mann-Whitney tests were used where appropriate for between group analyses. Categorical data are expressed as n or % and compared by chi-squared analyses. Myostatin, GDF-15 and IGF-1 concentrations were non-parametrically distributed and therefore the median with interquartile ranges (IQR) are used to describe the data. Repeated measures Friedman's test with Dunn's correction for comparison of all time points to the pre-operative baseline was used for within group analysis.

Chapter 4 – The control group of this study consisted of only 7 individuals and therefore the data was considered to be non-parametric. Demographic data are therefore described as median with interquartile range (IQR) unless otherwise stated. Mann-Whitney tests were used for between group comparison and Pearson's for correlation between data. Categorical data are expressed as n or % and compared by chi-squared analyses. Bonferroni correction was used where multiple tests of correlation were carried out.

Chapter 5 –There were only 12 patients included in the final analysis, demographic data were non-parametrically distributed and are described as median (IQR) unless otherwise stated. In this interventional study, which is described fully in chapter 5, one leg underwent

neuromuscular electrical stimulation (NMES) for 1 week and the other was used as a control. Change in mRNA and microRNA expression and US RF_{csa} at baseline and at the end of the study were analysed using Wilcoxon matched pairs sign rank test of the change relative to baseline. The effect of NMES compared to control was compared using Mann-Whitney U tests.

Chapter 6 – Raw and fold-change microRNA data were non-parametrically distributed and therefore expressed as median and IQR. Within group analysis was carried out as for chapter 3 and Komglov-Smirnov test used for between group analysis of microRNA fold-change as the two groups had different variance. In order to test the discriminatory value of a rise in miR-181a as a biomarker for acute muscle wasting Graphpad Prism 6 was used to generate a Receiver Operating Characteristic (ROC) curve and calculate the relative sensitivity and specificity of different fold change rises. www.medcalc.org was used to calculate the positive and negative predictive values.

2.3.1.1 Analysis of in vitro data.

Data from cell culture experiments can be considered to be parametrically distributed. Each experiment was repeated on 3 different occasions/ passages in triplicate unless otherwise stated (n=3 in triplicate). For each occasion the data was expressed relative to the mean of the control condition for that experiment and the individual un-averaged data points for each condition then analysed with a students' T-test. Data are presented as the mean and standard deviation.

Chapter 3 Investigation of circulating mediators of muscle homeostasis and Growth and Differentiation Factor-15 in acute muscle wasting following high risk cardiothoracic surgery.

3.1 Rationale

As discussed in the introduction, acute muscle wasting in critical illness is likely to be a result of a dynamic imbalance between muscle atrophy and hypertrophy pathways (40, 74). However, in part because of the heterogeneity of the ICU population and other factors such as the different lengths of stay and underlying medical problems, this has been difficult to demonstrate in human critical care models of muscle wasting. Myostatin and IGF-1 are recognised to be potent drivers of muscle atrophy and hypertrophy respectively (137, 329) and changes in the circulating levels of both have been associated with muscle wasting conditions (130, 133, 173, 330, 331). However although both increased myostatin and decreased IGF-1 have been implicated in the development of ICUAP (149, 332), the relative pattern of change in the circulating levels of these mediators during the acute development of muscle wasting has not been established.

As discussed in the introduction GDF-15 is a stress induced cytokine and a member of the TGF-β family. The rationale behind the hypothesis that GDF-15 might be a potential driver of acute muscle wasting and ICUAP is discussed fully in the introduction. Briefly this is that factors thought to aetiological in the development of ICUAP (hypoxia, inflammation etc..) are recognised to drive GDF-15 expression in other tissues (e.g. liver and heart) and that GDF-15 has been shown to drive pro-apoptotic and hypertrophy limiting molecular pathways and drive cachexia in murine models (98, 251).

Therefore in order to investigate the balance of circulating regulators of muscle homeostasis and to test the novel hypothesis that GDF-15 might be associated with acute muscle wasting, high-risk elective cardiothoracic patients were recruited pre-operatively and studied for the first post-operative week. High-risk cardiothoracic patients are at risk of prolonged ICU stay and consequently at risk of developing acute muscle wasting/ ICUAP. These patients provided a relatively homogeneous cohort to study, the opportunity to track changes in muscle bulk prospectively and measure levels of circulating mediators comparing them to "healthy" baseline. This study also had the potential to form the basis a novel human model of acute muscle wasting associated with intensive care admission.

Some of the results from this chapter have been published (Crit Care Med 2013 Apr 41(4):982-989) (333). The journal has granted permission for the reuse of all material from this paper in this thesis. See Appendix A1

3.2 Hypothesis

The above rationale led to the following hypotheses:

1) Circulating levels of known mediators of muscle homeostasis would change dynamically following cardiac surgery; specifically a rise in myostatin and fall in IGF-1 was expected. These changes would be different in those who developed muscle wasting when compared to those who did not.
2) Circulating GDF-15 levels would rise post-operatively and be associated with muscle wasting.

3.3 Patients studied and study design

The principle inclusion criterion for this study was a high-risk elective cardiothoracic surgical procedure requiring post-operative admission to adult critical care. High-risk was defined by the patient's EuroSCORE (>5) and/ or the surgical team (where the patient was deemed high risk by the surgical team despite a lower EuroSCORE – for example taking into account the cardiac anatomy, number and nature of previous surgeries or clinical rather than numeric age) (310-312). Adults undergoing elective cardiac surgery at the Royal Brompton Hospital were screened for inclusion into the study. Pre-existing muscle or neuromuscular disease, malignancy or contraindication to serial blood sampling excluded patients from the study. In order to reflect a relatively true healthy baseline, patients were only included if they were stable preoperatively and not suffering from acute illness or requiring emergency surgery. Written informed consent was obtained from all those involved and the study was approved by the local ethics committee (10/H0504/9) through the Biomedical Research Unit at the Royal Brompton Hospital.

Patients were assessed pre-operatively; this involved review of medical history, physical examination and collection of demographic data. Muscle mass was assessed by measuring the cross-sectional area of the right rectus femoris muscle by US RF_{csa}, assessment of muscle strength by MRC-SS and handheld dynamometry of QMVC. Pre-operative ("baseline") blood samples were collected. Bloods for repeat sample analysis were taken on the 1^{st} and 2^{nd} postoperative days and at day 7 (or at discharge if earlier). The latter two time points were considered identical for the purposes of analysis; only 4 patients (3 in the non-wasting patient group and 1 in the wasting group) were in fact discharged earlier than day 7. Similarly the US RF_{csa}, MRC-SS and QMVC were also repeated at day 7 or discharge. Total hospital length of stay and 30 day survival data were collected.

Patients were classified as those who developed muscle wasting or those who did not depending on the change in RF_{csa} at the end of the week. Greater than 9.24% loss of muscle bulk was classified as muscle wasting, based on the coefficient of variation of repeated measurements as described in the methods chapter.

Data were non-parametrically distributed and are therefore described as median with the interquartile range in brackets (IQR) unless otherwise stated.

3.4 Results

3.4.1 Patients and change in RF_{csa}

Cardiothoracic operating lists were screened weekly and 50 patients were identified who met the inclusion criteria. Of these 5 declined consent and 3 were retrospectively excluded due to technically inadequate muscle US images meaning that it was not possible to categorise them as having developed muscle wasting or not. Therefore, 42 patients were included in the study. Of these, 23 (55%) developed muscle wasting, as defined above, with a mean muscle loss of 24.6 ± 13.7% (paired students T-test $p<0.001$). There was no significant change in muscle bulk in those who did not develop muscle wasting (1.3 ± 5.9% $p=0.149$) (Figure 3-1).

Table 3-1 shows the demographic data, co-morbidities and critical care data for both groups of patients and demonstrates that the non-wasting and wasting patients were well matched. Not all patients underwent cardiac bypass: one patient in the non-wasting group underwent an off-pump coronary artery bypass procedure and 3 underwent transcutaneous aortic valve insertion; in the wasting group 2 patients had off-pump procedures. However circulating plasma levels for GDF-15, myostatin and IGF-1 in these patients were not different from the rest of their group. Length of stay on ICU was short in both groups and most patients had an uncomplicated recovery. At day 7, 2 patients were still on ICU. One patient's prolonged

hospital stay was due to social problems. Only one patient died at 21 days post-operatively in the wasting group; no patients died in the non-wasting group.

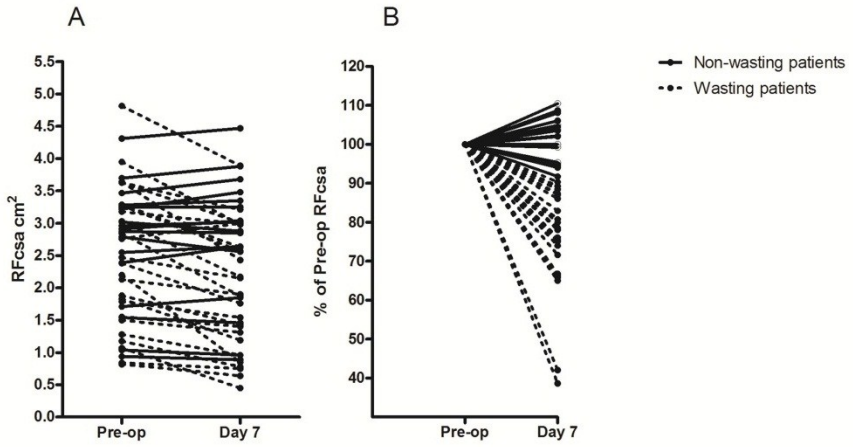


Figure 3-1 Change in Rectus Femoris Muscle Cross Sectional Area (RF_{csa}) in high-risk elective cardiothoracic patients following cardiac surgery.

A: US RF_{csa} measured in elective cardiothoracic patients pre-operatively and on the 7th post-operative day. Development of muscle wasting defined as >9.24% loss in muscle bulk. Non-wasting patients (n=19) solid lines, wasting patients (n=23) dotted lines. B: US RF_{csa} expressed as change from baseline %. Non-wasting patients change in US RF_{csa} 1.3% ± 5.9 and wasting patients 24.6% ± 13.7 (mean ± SD).

	Non-wasting patients (n=19)	Wasting patients (n=23)	pvalue (T-test, #Mann-Whitney *Chi-squared)
Demographic data			
Age (years)	65.7 ± 17.2	62.0 ± 16.2	0.47
Sex (m/f)	9/10	12/11	0.76*
BMI (kg/m^2)¥	26.6 ± 4.6	24.7 ± 4.1	0.18
EuroSCORE	5.3 ± 1.8	5.5 ±2.6	0.76
Pre-op LVEF %ǂ	60.8 ± 15.0	56.6 ± 16.4	0.41
Pre-op Creatinine (µmol/L)¥	81.3 ± 23.6	77.3 ± 17.1	0.52
Pre-op Creatinine clearance (ml/min) ¥	84.7 ± 36.1	86.8 ± 34.7	0.66
Pre operative co-morbidities (n)			
Ischaemic heart disease	10	8	0.24*
Structural heart disease	9	11	0.97*
Dysrhythmia	2	3	0.80*
Systemic hypertension	7	5	0.94*
Pulmonary hypertension	1	2	0.66*
Hypercholesterolemia	7	10	0.66*
Congenital cardiac disease	3	6	0.42*
Diabetes	3	1	0.21*
Obstructive lung disease	3	2	0.45*
Statin therapy	8	10	0.93*
ACE inhibitor or receptor blocker therapy	3	4	0.89*
Critical care data			
Total bypass time (mins)ǂǂ	115 ± 39	117 ± 35	0.91
Total cross-clamp time ǂǂ	89 ± 43	86 ±28	0.87
ICU length of stay, days (median (IQR))	1 (1-2.5)	2 (1-3)	0.62 #
Hospital length of stay, days (median (IQR))	8 (7-11)	9 (8-10.5)	0.44 #
Mean blood glucose during critical care admission (mmol/l)	7.48	7.35	0.56
IV insulin therapy whilst in critical care (n)	10	10	0.59*
Mean insulin dose during critical care admission, if treated with IV insulin (units/hr)	2.16	1.91	0.46
Exposure to NMBs (n)	0	0	NA
Exposure to corticosteroids (n)	3	4	0.89*

Table 3-1 Demographic data:

Demographic data, co-morbidities and critical care data for non-wasting (n=19) and wasting (n=23) high-risk elective cardiothoracic patients. Data presented as mean ± SD unless otherwise stated. ¥ Weight unavailable for 2 patients in the wasting group therefore n=21, ǂPre operative EF not available for 1 patient in each group. ǂǂ 4 patients in the non-wasting and 2 in the wasting group did not undergo bypass. Pre-op – preoperative, LVEF – left ventricular ejection fraction, NMBs – neuromuscular blocking agents given other than at the time of surgery. IQR – interquartile range.

3.4.2 Assessment of muscle strength

The MRC-SS was not adequately discriminatory in the elective cardiothoracic patients recruited for this study. All scored 60 at pre-operative assessment – and at follow up all but four still scored 60 despite reportedly feeling weaker and documented loss of muscle bulk on US. Of the four not scoring 60, two were still intubated and ventilated and therefore unable to complete the test and the two patients able to complete the test (one in each group) both scored 54/60.

The handheld dynamometry assessment of QMVC was unfortunately also found to have poor repeatability and reliability with a large volitional component. Furthermore for many subjects the maximum power of their quadriceps was greater than that which I, as the assessor, was able to match with my arm (this problem has also been reported by other members of our group and collaborating groups). Finally, post-operatively subjects were unable to complete the test in the majority of cases due to pain from their sternal wounds. Less than half of the patients had adequate strength measurements; therefore, these were not analysed.

3.4.3 Myostatin

Median baseline plasma myostatin did not differ significantly between groups (non-wasting patients 11.5ng/ml [IQR 8.1-18.2] and 9.3ng/ml [IQR 6.3-13.3] in those who did develop muscle wasting, p=0.29 Mann Whitney).

Repeated measures Friedman's tests (with Dunn's correction) were used to assess the change in myostatin. Contrary to our hypothesis, plasma myostatin concentration fell significantly in both groups at D1 and D2. At D1 in non-wasting patients it fell to 53% of baseline (median 7.8ng/ml [IQR4.5–11.3], P<0.0001) and wasting patients it fell to 55% of

baseline (median 5.0ng/ml [IQR 4.2 – 6.6], p<0.001). In both groups plasma myostatin returned to baseline levels at day 7 (Figure 3-2).

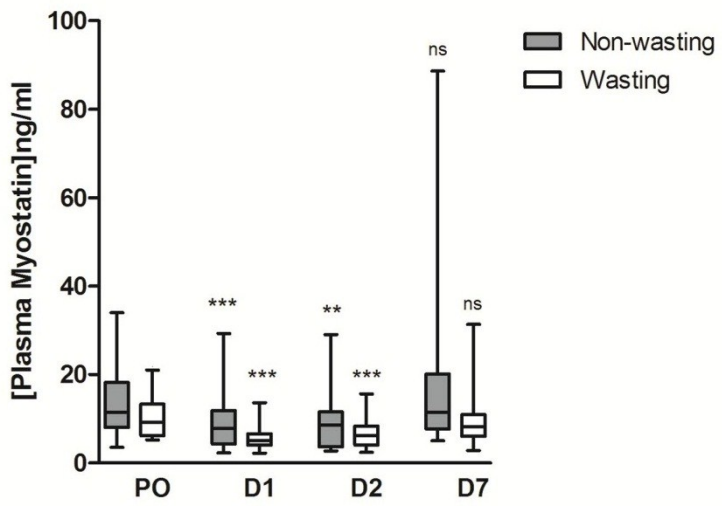


Figure 3-2 Plasma Myostatin Concentration.

Plasma Myostatin concentration (ng/ml) in non-wasting (n=19) and wasting patients (those with >9.24% muscle loss: n=23) pre-operatively (PO), on day 1 (D1), day 2 (D2) and on day 7 (D7). Data presented as box and whisker plots with median, interquartile ranges and 5-95% percentiles. * p<0.05, ** p<0.01, *** p<0.001, ns - not significant, repeated measures Freidman's test with Dunn's correction for comparison with pre-operative baseline.

3.4.4 IGF-1

Baseline plasma IGF-1 did not differ significantly between the groups (non-wasting patients, median 113.0ng/ml [IQR83.3–174.6], wasting patients median 136.5ng/ml [IQR117.9-170.4], p=0.24 Mann Whitney).

Repeated measures Friedman's tests (with Dunn's correction) were used to assess the pattern of change in IGF-1 levels after surgery. The IGF-1 plasma concentration fell significantly at D1 and D2 after surgery in both groups; non-wasting patients D1 median 90.5 ng/ml (IQR 50.4–129.7), 74% of baseline, and wasting patients D1 median 98.4 ng/ml (IQR 67.1–120.1), 75% of baseline (p<0.001 for both). In the non-wasting group the IGF-1 concentration returned to baseline by D7 median 92.9ng/ml (IQR 63.1–156.2) (p>0.05). However, in wasting patients it

remained significantly reduced at D7 median 108ng/ml (IQR 80.9 – 144.0), (p<0.01)(Figure 3-3).

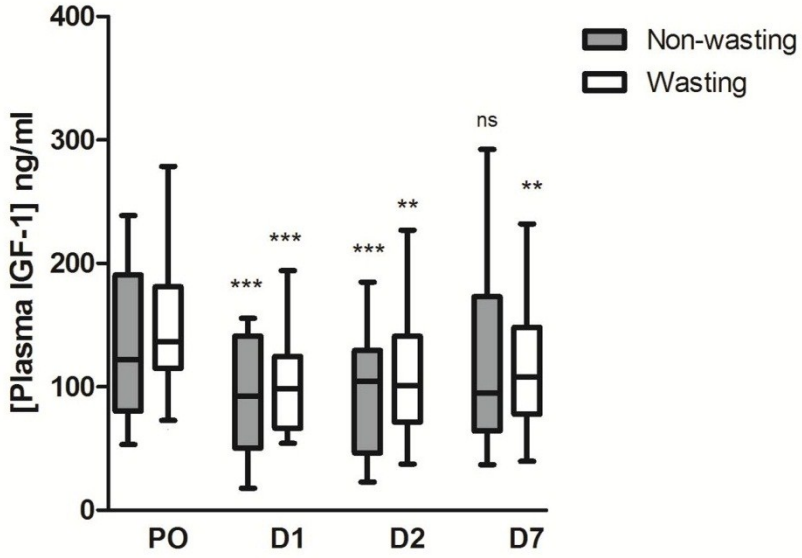


Figure 3-3 Plasma IGF-1 concentration

Plasma IGF-1 concentration (ng/ml) in non-wasting (n=19) and wasting patients (those with >9.24% muscle loss: n=23) pre-operatively (PO), on day 1 (D1), day 2 (D2) and on day 7 (D7). Data presented as box and whisker plots with median, interquartile ranges and 5-95% percentiles. *p<0.05, ** p<0.01, *** p<0.001, ns - not significant, repeated measures Freidman's test with Dunn's correction for comparison with pre-operative baseline.

3.4.5 GDF-15

Baseline plasma GDF-15 did not differ significantly between the groups; median GDF-15 in non-wasting patients 1093 pg/ml (IQR 601.5-1790) and in wasting patients 892.7 pg/ml (IQR 579.1–1560) (p=0.52 Mann Whitney).

Repeated measures Friedman's tests (with Dunn's correction) were used to assess the pattern of change in GDF-15 levels after surgery. In contrast to myostatin, GDF-15 levels increased; median GDF-15 at D2 was 4576pg/ml (IQR 3035–5238) in non-wasting patients, and 3659 pg/ml (IQR 3160-5919) in wasting patients (p<0.001 for both groups). In the non-wasting patients the increase in GDF-15 returned to baseline by D7 -median 1786pg/ml (IQR 1087–2697) (p>0.05); however in the wasting group the level remained significantly elevated at D7 -

median 2630pg/ml (IQR 1330–3797) (p<0.01), Figure 3-4. These data suggest that those who developed muscle wasting were exposed to high levels of GDF-15 for longer.

Using the fold-change from baseline GDF-15 the area under the curve of the rise in GDF-15 was calculated for each patient, this reflects the cumulative exposure to increased GDF-15 levels. The median area under the curve for wasting patients 14.1 (IQR 9.6–21.8) was higher than those without wasting 9.9 (IQR 7.2–20.4); however, this did not achieve statistical significance (p=0.12 MW), Figure 3-5.

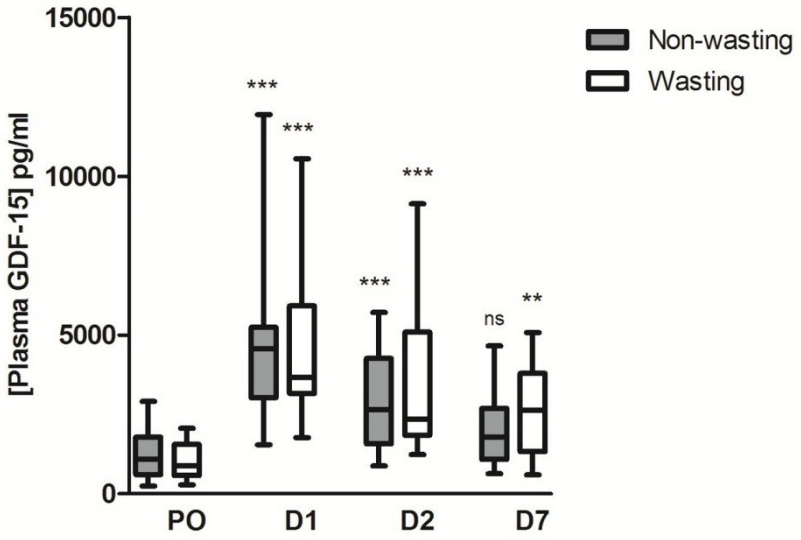


Figure 3-4 Plasma GDF-15 Concentration

Plasma GDF-15 concentration (pg/ml) in non-wasting (n=19) and wasting patients (those with >9.24% muscle loss: n=23) pre-operatively (PO), on day 1 (D1), day 2 (D2) and on day 7 (D7). Data presented as box and whisker plots with median, interquartile ranges and 5-95% percentiles. * p<0.05, ** p<0.01, *** p<0.001, ns - not significant, repeated measures Friedman's with Dunn's correction for comparison with pre-operative baseline.

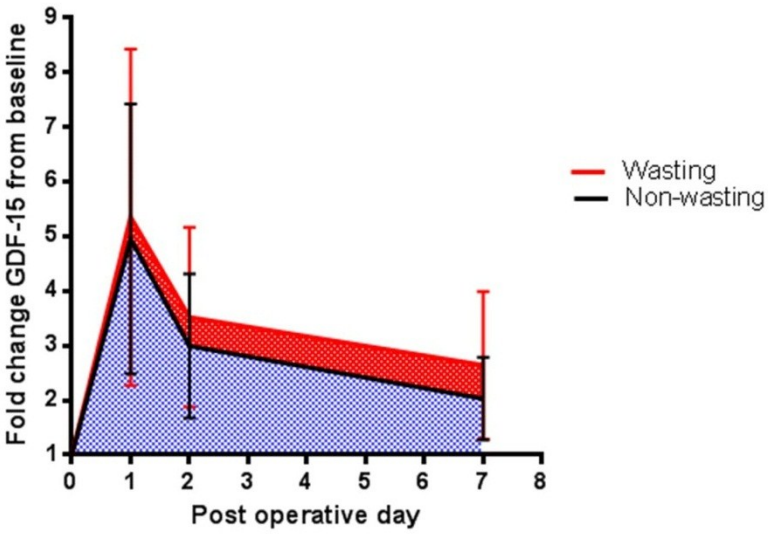


Figure 3-5 Area under the curve of rise in GDF-15.

Fold-change in GDF-15 concentration compared to baseline on days 1, 2 and 7 postoperatively. Data presented as mean and error bars represent the standard deviation of the fold-change at that time point. Area under the curve calculated from fold-change for each individual.

3.5 Discussion

3.5.1 Summary of findings

This study demonstrates that acute muscle loss detectable on US following cardiac surgery is common, being detectable in 55% of the population studied, despite the fact that these patients generally had short ICU stays and an uncomplicated post-operative course.

Secondly, these data are consistent with the hypotheses that acute muscle wasting occurs as a result of a dynamic imbalance in the regulation of muscle homeostasis and that GDF-15 may represent a novel driver of muscle wasting. A reduction in circulating IGF-1 levels that recovered to baseline by day 7 in non-wasting patients, but not in those who developed muscle wasting (Figure 3-3) was observed. However, circulating myostatin behaved in the opposite way to that expected and was suppressed in the acute phase. Furthermore, those patients who developed muscle wasting experienced a more sustained rise in GDF-15, which did not recover to baseline by day 7, when compared to those who did not (Figure 3-4).

Together these data suggest that an imbalance in GDF-15 and IGF-1 occurs in patients who develop muscle wasting and is sustained in a direction that would be expected to promote muscle wasting. In all patients the balance of regulators of muscle homeostasis is upset by the insult of cardiac surgery. In those who do not develop muscle wasting the balance is restored as levels of IGF-1 and GDF-15 return to pre-surgery levels by day 7. Conversely in those who develop muscle wasting IGF-1 remains reduced and GDF-15 remains increased at day 7 indicating that the balance of these two factors has not been restored. This lack of restoration of the normal regulation of these synthetic and atrophic factors may contribute to muscle wasting in this group (Figure 3-6).

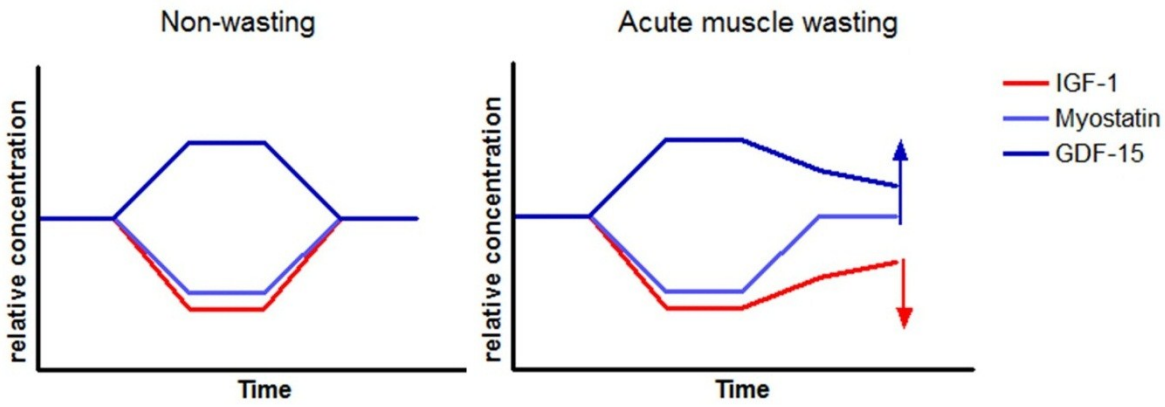


Figure 3-6 Schematic representation of the imbalance of circulating regulators of muscle mass following cardiothoracic surgery.

3.5.2 Discussion

Circulating myostatin levels changed in the direction opposite to that which was expected (329), as they were suppressed in the acute phase and recovered by day 7 in both wasting and non-wasting patients. As myostatin is a well recognised negative modulator of muscle mass (329), it would be reasonable to expect that circulating levels would be elevated in patients who developed quadriceps atrophy. However evidence to support this from the acute phase of critical illness has been contradictory despite myostatin levels (both plasma and muscle) having been elevated in a variety of muscle wasting conditions (158, 171, 329, 330,

334, 335). An example of this contradiction is that myostatin mRNA and protein from skeletal muscle of patients in the acute phase of critical illness was elevated in one study by Constantin *et al* (332), but in another study by Jespersen *et al* in fact showed lower myostatin mRNA in patients compared to controls (147). Furthermore data, from another study of a large ICU cohort (208 patients) with prolonged stays on ICU, showed different results in different muscles examined: myostatin mRNA from the rectus abdominis (taken immediately after death) of the prolonged stay ICU patients was lower than controls, but did not change in the vastus lateralis (175). Animal models have also suggested that myostatin may drive acute muscle wasting secondary to sepsis or inflammatory insult (336). A rat model, which included immobility, ventilation and neuromuscular blockade, but not sepsis, showed acute elevation of myostatin mRNA in hind-limb muscle, followed by suppression over the next week in a gene microarray analysis (337). However, consistent with data from the current study, myostatin mRNA in muscle and circulating plasma myostatin reduced significantly in rats following cecal ligation and puncture (338).

The current study suggests that GDF-15 rather than myostatin is more likely to be a driver of acute muscle atrophy in this patient cohort. GDF-15 expression is increased in response to stress, hypoxia and inflammation *in vitro* (257, 339) and in a variety of animal and human chronic disease settings (262, 339, 340). All the patients in the current study underwent the significant acute inflammatory insult of cardiac surgery and therefore it is unsurprising that all experienced an acute rise in circulating GDF-15. The findings of an association between GDF-15 and acute muscle wasting following the physiological stress of cardiac surgery are consistent with the understanding that GDF-15 is released under situations of physiological stress (257, 262). Furthermore a more prolonged exposure to elevated levels of GDF-15 was associated with the development of muscle wasting following cardiac surgery and it is possible that this reflects a driving mechanism for acute muscle wasting. This would be consistent with *in vitro* studies in which GDF-15 promoted apoptosis and suppressed

hypertrophy in cancer cells and cardiomyocytes (268, 341) and *in vivo* mouse models where mice deficient in GDF-15 showed both increased cardiac hypertrophy and loss of cardiac function in response to pressure overload compared with wild type mice. (273). These effects may in fact be beneficial in cardiac tissue. Beneficial effects of GDF-15 in cardiac tissue also include protection of the myocardium from infiltration by polymorphonuclear leukocytes and protection against myocardial rupture following infarction (278). However GDF-15 is also linked to pathological effects in cardiac tissue and its role is likely to be bidirectional depending on the environment (257). A similar situation is seen in prostate cancer cells where GDF-15 both promoted apoptosis (274, 275), and enhanced metastatic potential and angiogenesis (262). With respect to the role of GDF-15 in muscle wasting, a pathological link was first suggested when GDF-15 expressing tumours implanted into mice were found to cause cancer-related cachexia, an effect which could be reversed with GDF-15 antibodies (267). In that study a central anorexic effect of GDF-15 was suggested as the cause and thus reduced food intake was reversed by the antibodies (267). Unfortunately the food intake of patients in the current study was not recorded and it is not known if it was different between the two groups.

Data from the current study are consistent with the current understanding of the role of IGF-1 in muscle homeostasis. Muscle IGF-1 was reduced in human models of sepsis (133, 136), immobility (135), surgery (130) and in critical illness (147). Reduced plasma IGF-1 levels were also observed in acute critical illness (147), and associated with poor clinical outcome (148) and development of severe ICUAP (149).

It is important to note that in the current study these factors have been measured in plasma and not in the muscle itself. The significance of this is unknown. As discussed, variations in circulating levels of myostatin and IGF-1 have been associated with muscle wasting conditions and it is likely that these mediators and GDF-15 act in both a paracrine and endocrine manner – however the muscle concentration of these proteins cannot be known

from this study and their muscle effect is only assumed to be augmented by a raised circulating level or *vice versa*.

3.5.3 Critique of the method

The overall clinical outcome for these patients was generally good despite the high-risk nature of their surgery. They had short ICU hospital stays and mortality was very low. With this in mind it is not surprising, therefore, that these patients only really demonstrated sub-clinical wasting which was not associated with significant weakness (all but 2 post-operative MRC-SS were unchanged). This may be one of the reasons that differences in the baseline values of the myostatin, IGF-1 and GDF-15 were not detected between the two groups of patients. Of course, the study may also have been underpowered to detect a difference due to the relatively small number of patients in each group and the wide range of baseline values. Importantly the sub-clinical nature of the muscle wasting studied may mean that these patients are not truly comparable to a true weak ICUAP cohort. Nevertheless, the validity of the approach is supported by the observation that IGF-1 decreased acutely in all patients, and remained suppressed in those who developed muscle wasting, consistent with prior observations (147, 149). A larger prospective study involving more patients and particularly those with clinically obvious ICUAP would be desirable as a next step to confirm the findings.

ICUAP is a heterogeneous disorder that occurs in a very mixed cohort of patients. The advantage of the model used in the current study is that its prospective nature, the relative homogeneity of the patient cohort and the uniformity of the insult allow some of the heterogeneity to be controlled for and thus specific factors in the pathophysiology of acute muscle wasting can be considered. However it is therefore difficult to know how much can be extrapolated to a more general ICU population in whom, for example, sepsis and prolonged stays on ICU with significant prolonged immobility are common. Muscle wasting was common and therefore in the future this model may be useful in an RCT of a preventative treatment for

ICUAP. However it is important to note that although muscle wasting did develop in 55% of these patients, it could be described as subclinical - in that patients were almost all mobile and in significantly limited by the loss of muscle bulk and therefore in order to pick up a clinically significant improvement in loss of muscle bulk caused by an intervention this model may not be ideal.

Another important consideration is that bypass itself is well recognised to cause changes in the circulating levels of inflammatory molecules (342). However bypass time was not significantly different between the two groups of patients (Table 3-1). Furthermore four patients in the non-wasting group and two in the wasting group did not undergo bypass and these patients had similar circulating plasma levels of myostatin, IGF-1 and GDF-15 as the rest of the group.

Finally this study would be significantly improved by an adequate assessment of muscle strength in all patients studied and an assessment of mobility and activity over the week. The former would help describe the degree of clinical injury to the muscle that occurred and potentially better characterise the patients. The latter would potentially add to our understanding of the relevant factors in the development of acute muscle wasting in this situation. Of note all but seven of the patients were out of bed by day one (5 in the wasting and 2 in the non-wasting group, which was not statistically different) and had standard physiotherapy however this was not formally quantified and their activity was not monitored (for example by a pedometer).

3.5.4 Conclusion

Despite a good clinical outcome, 55% of high-risk elective cardiothoracic patients developed measurable muscle wasting in this cohort. This was associated with a dynamic imbalance in the circulating regulators of muscle homeostasis and a sustained elevation in

GDF-15 was associated with acute muscle loss. This study identifies GDF-15 as a potential driver of muscle wasting and strengthens the hypothesis that GDF-15 will be important in the pathogenesis of ICUAP. Despite the flaws discussed above this is a valid model of acute muscle wasting with several advantages which means that it could be used in the future to further understand the pathophysiology of acute muscle wasting.

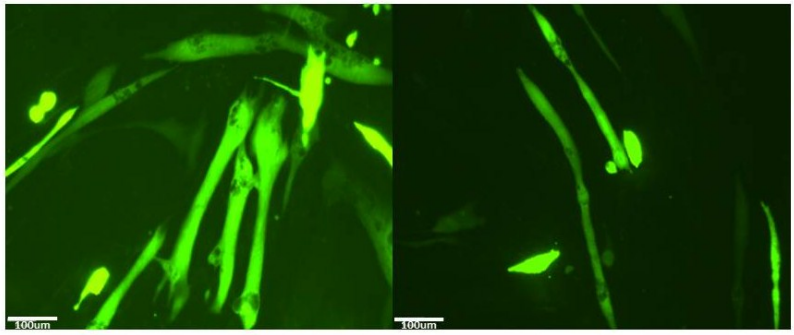
Chapter 4 GDF-15 regulation of muscle microRNAs in the pathogenesis of ICUAP

4.1 Rationale

As already discussed in the introduction there is a strong rationale for the investigation of the role of GDF-15 in the pathogenesis of ICUAP. This was strengthened by the results discussed in Chapter 3 where a sustained rise in the concentration of plasma GDF-15 was seen in those who developed muscle wasting at 1 week, but not in those who did not develop muscle wasting, where GDF-15 levels returned to baseline. Furthermore Dr Jen Lee (a member of our group) demonstrated that GDF-15 treatment of C2C12 cultured myotubes caused a 15% loss of myotube diameter (Figure 4-1) (333), suggesting that GDF-15 may indeed have a direct effect on muscle. However the potential mechanisms for this were not understood.

Acute muscle wasting is thought to occur as a result of disturbed muscle homeostasis with an imbalance between hypertrophy/protein synthesis and satellite cell recruitment and atrophy/muscle protein breakdown, apoptosis and autophagy (40). MicroRNAs are involved in the regulation of muscle cell proliferation, differentiation and regeneration and, therefore, are essential for the maintenance of normal muscle homeostasis (288). Although the regulation of microRNA expression is not fully understood, their regulation by inflammatory cytokines is recognised (301) and, in turn, microRNAs modulate inflammatory signalling (301). One important signalling pathway in muscle homeostasis which microRNAs (for example, miRs-1, 133a, 181a and 499) have been shown to interact with is the TGF-β signalling pathways (290, 343-346). This, alongside emerging evidence of their role in other myopathies (301), for example Chronic Obstructive Pulmonary Disease (COPD) (302), led to the hypothesis that the regulation of microRNA expression might be one mechanism by which GDF-15 could promote ICUAP.

In addition, hyperglycaemia is the only aetiological factor in the development of ICUAP that has been well described and demonstrated in clinical trials (48, 51). GDF-15 expression in human umbilical vein cells was up-regulated by hyperglycaemic conditions *in vitro* (347). If GDF-15 were under similar regulatory pathways in muscle, up-regulation of GDF-15 driven by hyperglycaemia might provide another mechanistic insight into the aetiology of ICUAP and therefore this was also investigated.



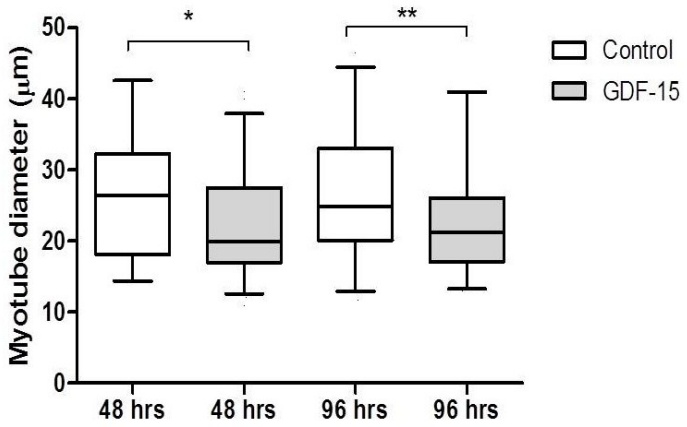


Figure 4-1 Effect of GDF-15 treatment of C2C12 myotubes.

GFP transfected myotubes following treatment with control (A) or GDF-15 50ng/ml (B) for 48 hours on day 8 of differentiation (x10 magnification – scale bar represents 100µm). (C): Box and Whisker plots show median, interquartile range and 5th and 95th centiles. Day 8 cultured myotubes were exposed to GDF-15 (50ng/ml) or vehicle control (0.1% BSA with 20mM HCL) for 48 or 96 hours. Diameter of the myotubes was then calculated. Mean control myotube diameter was 26.3 ± 9.0 µm versus 22.3 ± 7.5 µm for the GDF-15 treated myotubes at 48 hours. This equates to a 15% reduction in diameter following GDF-15 treatment; p=0.011 (Mann-Whitney). At 96 hours, mean control myotube diameter was 26.6 ± 9 µm and 22.7 ± 8 µm for GDF-15 treated myotubes (14% reduction p=0.003 Mann-Whitney) Data courtesy of Dr J Lee. Copyright permission obtained from Crit Care Med 2013 Apr 41(4):982-989, see appendix A1.

4.2 Hypothesis

The above rationale led to the following main hypotheses

1. GDF-15 plasma concentration and muscle mRNA expression would be elevated in ICUAP patients.
2. MicroRNA expression would be different in the muscle of ICUAP patients compared to controls.
3. GDF-15 treatment of C2C12 myotubes would result in increased expression of atrophy related genes and disruption of microRNA expression.
4. Hyperglycaemia would increase GDF-15 mRNA expression *in vitro* and increased GDF-15 *in vivo* would be associated with impaired glucose tolerance, diabetes or insulin resistance.

4.3 Patients studied and study design

The principle inclusion criterion for this observational study was a clinical diagnosis of ICUAP. The diagnosis was made in accordance with standard diagnostic criteria (15). Where patients were alert and cooperative this included MRC-SS evaluation (n=8), but in the majority their level of consciousness precluded MRC-SS scoring. In these cases, in line with Stevens' criteria, patients were required to have visible evidence of muscle wasting and functional evidence of muscle weakness, and other causes of muscle wasting and weakness to have been excluded. If used a MRC-SS of less than 48/60 was required. All adults admitted to ICU at the Royal Brompton Hospital for more than one week were screened. Exclusion criteria included preadmission neuromuscular disease resulting in significant wasting or weakness, malignancy or contraindications to biopsy such as extreme clotting diatheses. Control participants were elective high-risk cardiothoracic surgery patients, with MRC scores 60/60 pre-operatively, in whom a biopsy was taken at the start of surgery. This population was chosen to control for

the complex co-morbidities of the ICUAW patients. These patients were also involved in another study, which is discussed in Chapter 5 of this thesis. In these participants a biopsy was taken at the start of their surgery. Written consent was obtained from patients and controls or assent from the next of kin where the patient lacked capacity. National Research Ethics Committee approval for this study was secured (10/H0722/9). Participants underwent measurement of the mid-thigh muscle layer thickness (MLT), muscle biopsy and blood sampling (see methods Chapter 2). MLT was used for this study to enable comparison between individuals at the most standardised level of the rectus femoris muscle (i.e. 60% of the distance between the anterior superior iliac spine and supra-patella border). Despite being validated in ICU patients (306) the MLT does have potential flaws, including the impact of variable extracellular water/oedema on the measurement. However the rectus femoris cross sectional area (RF_{csa}) was not measurable in all the participants, because the whole muscle was often not visualised in a single US image and therefore the MLT was used.

Data were non-parametrically distributed and are therefore expressed as median with interquartile range (IQR) in brackets unless otherwise stated.

4.4 Results

4.4.1 Patients

Twenty-nine patients meeting the inclusion criteria (or their relatives) were approached. Four declined, 5 were too unwell and the remaining 20 consented/ assented; the Consort diagram for the study is shown in Figure 4-2. Seven control high-risk elective cardiothoracic patients were recruited, with a median euroSCORE of 9 (range 7-14). Demographic data, co-morbidities, reason for ICU admission and clinical data from their ICU stay are shown in Table 4-1. Patients and controls were well matched in terms of age and baseline body mass index, however all the controls were male. By the nature of their selection

all the control patients had either ischaemic heart disease (IHD) or other cardiac disease and no controls had a history of respiratory disease; whereas a history of cardiac disease (excluding IHD) was less common in the ICUAP patient group.

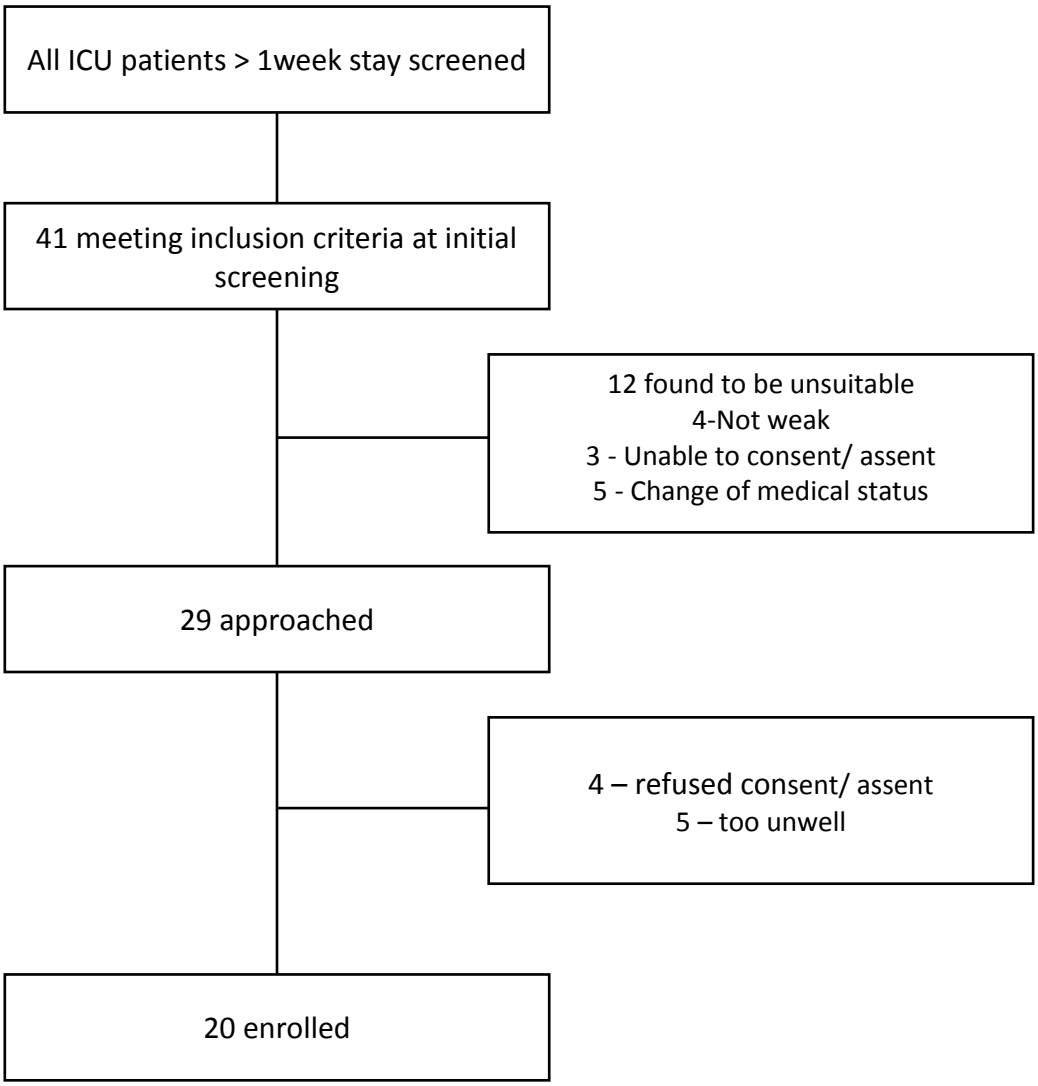


Figure 4-2 Consort diagram of recruitment of ICUAP patients into the observational study.

	Controls n=7	Patients n=20	P value (MW/ *Chi squared*)
Demographics			
Age (yrs)	69 (63-74)	64 (51-78)	0.39
Sex (m/f)	7/0	15/5	*0.14*
BMI (baseline) (kg/m^2)	24 (22-29)	27.8 (26.0-30.8)	0.21
MLT* (cm)	2.9 (2.0-3.3)	1.7 (1.4-2.5)	0.08
Co-morbidities (n)			
IHD	4 of 7	8 of 20	*0.42*
Other cardiac disease	6 of 7	6 of 20	*0.01*
Respiratory	0 of 7	6 of 20	*0.10*
COPD	0 of 7	2 of 20	
Diabetes	1 of 7	4 of 20	*0.73*
Statin use	4 of 7	6 of 20	*0.20*
Type of Cardiac surgery (n)			
CABG	1		
Valve surgery	2		
Mixed	4		
Reason for ICU admission (n)			
Post cardiac Surgery		8	
Cardiac		3	
Respiratory		9	
Pneumonia		2	
COPD		2	
ARDS/ ECMO		3	
Other respiratory		2	
ICU data			
MRC score at diagnosis [#]		36 (34 -40)	
Day on ICU of biopsy (days)		20 (15-29)	
SOFA score at time of biopsy		11 (8-14)	
Total ICU LOS (days)		42 (23-51)	
Awake at biopsy (n)		6	
Fed at time of biopsy		6	
NMB (n)		11	
Corticosteroids (n)		12	
Sepsis (n)		20	
Mean CRP (mg/l) ¥		136 (103-194)	
Mean pO2 (kPa) ¥		12.68 (12.12-14.41)	
Mean CO2 (kPa) ¥		5.7 (5.31-6.09)	
Mean pH ¥		7.41 (7.40-7.44)	
Mean Blood Glucose (mg/dl) ¥		7.6 (7.1-8.0)	
Mean Cumulative insulin dose(Units) ¥		456 (345- 894)	
Died (1yr mortality)		8	

Table 4-1 Demographics and clinical data of patients and controls in the observational study of ICUAP.

Basic baseline demographic data, co-morbidities and ICU data (where applicable) for patients with ICUAW and controls. Data presented as median (inter-quartile range) or number (n). BMI -body mass index, MLT – muscle layer thickness, IHD – ischemic heart disease, ICU – intensive care, LOS – length of stay, NMB – neuromuscular blockers. * - n=5 for controls and n=13 for patients. [#] n=8 (6 on the day of biopsy, 2 in the preceding 48 hours). ¥ during ICU stay up to the point of biopsy.

4.4.2 Muscle Layer Thickness (MLT)

Adequate US images were obtained for only 5 controls and 13 patients; this was partly due to technical factors including problems with the US machine and also oedema in patients preventing adequate visualisation of the muscle. As expected the mid-thigh MLT of patients tended to be lower than controls (Patients 1.7 [IQR 1.4-2.5] cm versus controls 2.9 [IQR 2.0-3.3] cm [p=0.079]) Figure 4-3 .

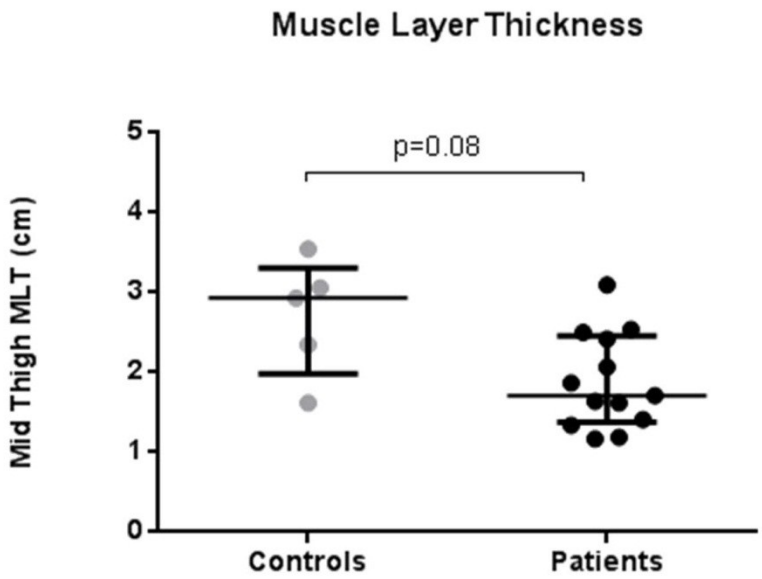


Figure 4-3 Muscle Layer Thickness (MLT).
Mid-thigh MLT measured by ultrasound for patients (n=13) and controls (n=5). Data presented as median and error bars represent interquartile range. Mann-Whitney

4.4.3 Histology

Unfortunately some O.C.T. mounted specimens were damaged by ice crystal artefact and as a result adequate muscle histology specimens were available for only 4 of 7 controls and 7 of 20 patients.

Fibre size: The mean muscle fibre diameter for each individual was calculated from 33-105 fibres per subject. Median mean fibre diameter was 56.4µm (IQR 49.5-62.2) in controls and significantly lower in patients, 47.5 µm (IQR 41.9-51.6) (p=0.042). The frequency distribution of fibre size also confirmed that the patients had smaller fibres when the

percentage of total fibres measured is considered (Figure 4-4).Fibre type: Immunofluorescent staining of histology specimens also showed fibre atrophy; the mean type 1 fibre diameter was 15% smaller in patients than controls (p<0.001 t-test) and type 2a fibres were 24% smaller (p<0.001 t-test). Fibre type staining also showed a non-significant shift in fibre proportion towards type 2 fibres; the median proportion of type 1 fibres was 44% (IQR 33-38) and 24% (IQR 21-39), p=0.109, and of type 2a fibres was 33% (IQR 28-38) and 45% (IQR 11-72), p=0.715 in controls and patients, respectively (Figure 4-5).

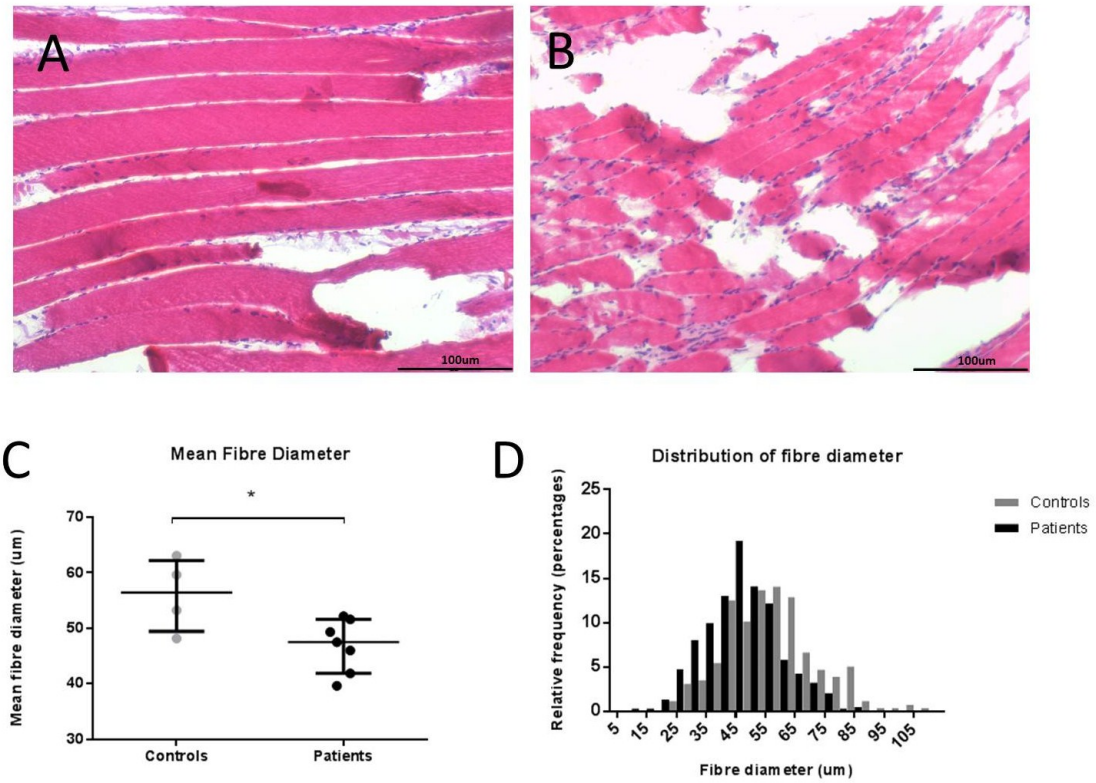


Figure 4-4 Muscle biopsy specimens from the rectus femoris of ICUAP patients (n=7) and controls (n=4).

Haematoxylin and Eosin staining of muscle biopsies from control subjects (A) and patients (B) at 10x magnification. C- mean fibre diameter of patients and controls. D – percentage distribution of all fibres measured (33-107 measured per subject). Data presented as median and error bars represent inter-quartile range, ** p<0.01 Mann Whitney.

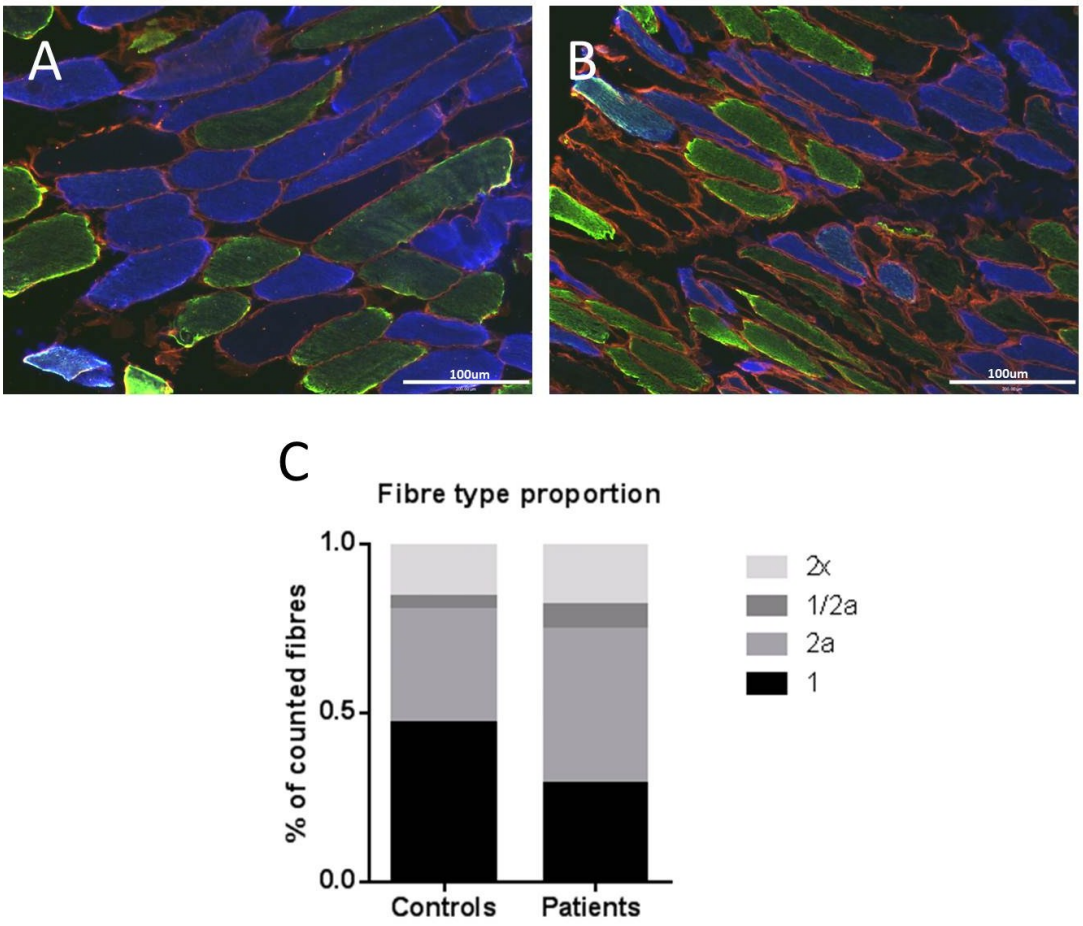


Figure 4-5 Immunostained muscle biopsy specimens for fibre typing.

Muscle biopsy specimens from the rectus femoris of ICUAP patients (n=7) and controls (n=4). Immunostaining of control (A) and patient (B) for different muscle fibre types (the same individuals as seen in the above figure). Blue – MHC 1, green – MHC 2a, red – laminin;. type 2x fibres do not stain and can be seen as black fibres (10x magnification). C - mean fibre type proportion of different MHCs 1,2a, 2x and dual staining 1/2a fibres.

4.4.4 GDF-15 in the plasma and muscle GDF-15 mRNA expression in ICUAP

Median plasma GDF-15 concentration was 2454 pg/ml (IQR 600-3118) in controls and 7239pg/ml (IQR 5613-13295) in patients (p=0.001) (Figure 4-6). At the time of biopsy, plasma GDF-15 in the patient group correlated with the patient's SOFA score, a marker of critical illness severity (r=0.64, p=0.002) (316).

Rectus femoris muscle mRNA expression of GDF-15 was higher in patients than controls (median 2.03-fold higher than controls [IQR 1.2-3.1], p=0.006, Figure 4-6).

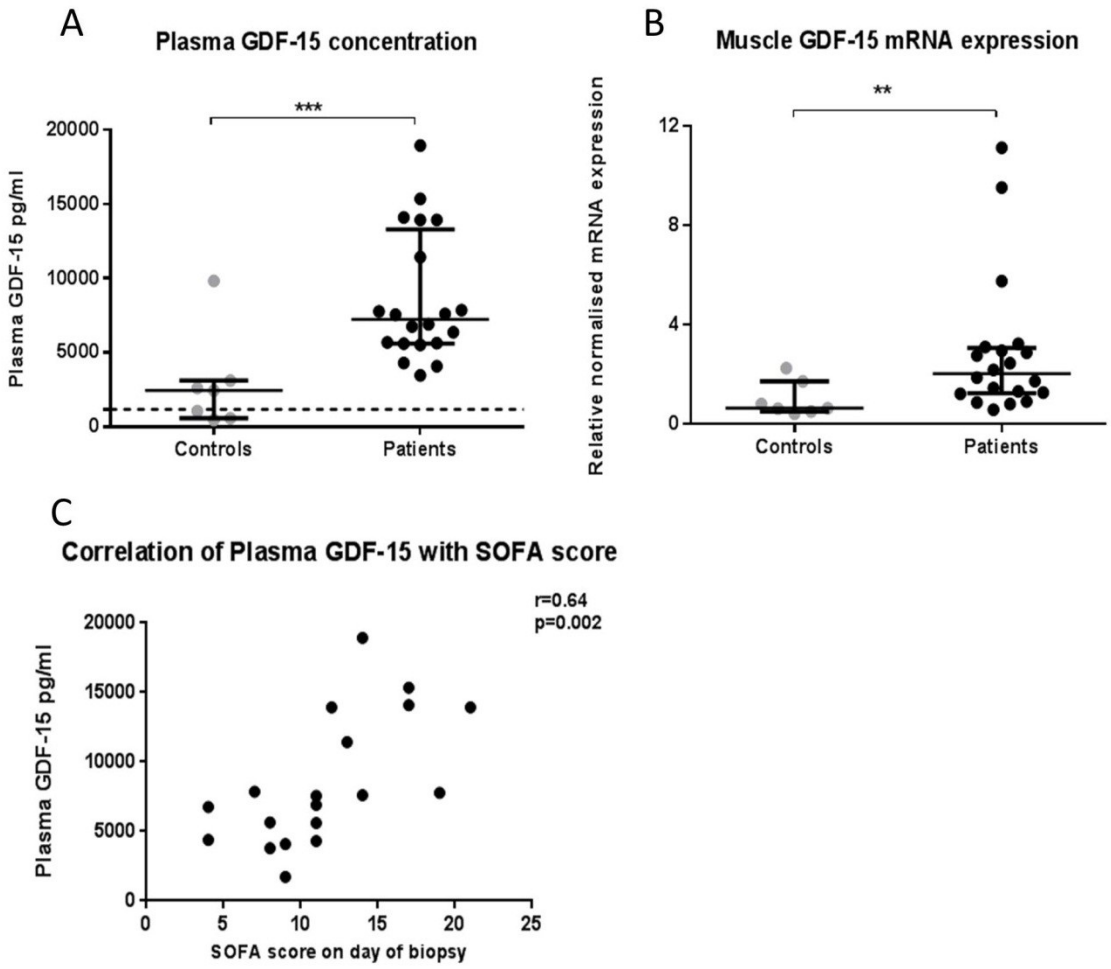


Figure 4-6 GDF-15 in ICUAP patients and controls.

GDF-15 in ICUAP patients (n=20) and controls (n=7) measured in plasma (A) and rectus femoris muscle biopsy mRNA expression (B). Dotted line figure A represents 1,200pg/ml – the upper limit of normal plasma GDF-15. ** p< 0.01, *** p<0.001 –Mann-Whitney. Correlation of plasma GDF-15 with Sequential Organ Failure Score (SOFA) at the time of sampling (C). r= Pearsons r value for correlation. Data presented as median and error bars represent interquartile range.

4.4.5 Muscle mRNA expression in ICUAP

Myostatin and IGF-1 are mediators of muscle atrophy and hypertrophy respectively (137, 329) and therefore mRNA expression of both was measured. Neither was significantly differently expressed between patients and controls (Figure 5-7). MuRF-1 and atrogin are muscle-specific ubiquitin ligases responsible for muscle protein breakdown (110, 111). Expression of atrogin was elevated significantly in the patients (median 3.42-fold higher than controls [IQR 1.7-7.9], p=0.003), but MuRF-1 was not significantly different (Figure 5-7). MyoD1 and myogenin are markers of differentiation and increased expression is seen in

regeneration (292, 348). MyoD1 was not significantly different in patients compared to controls; however, myogenin mRNA expression was significantly higher in the patients (median 2.86-fold higher [IQR 1.67-3.73], p=0.002) (Figure 4-7).Although MHC gene mRNA expression does not directly translate to protein level or muscle fibre-type microscopically, it was hypothesised that MHC gene expression would be different between patients and controls. Type 1 and 2a MHC mRNA expression was significantly lower in patients compared to controls (Figure 4-8).However, MHC type 2x mRNA expression was not significantly different.

4.4.6 microRNA expression

MicroRNA expression in the rectus femoris muscle of ICUAP patients was different from that of controls. The expression of three muscle-specific microRNAs (myomiRs), MiR-1,133a and 499, were significantly lower in patients than controls. Median patient myomiR expression as a percentage of control expression: miR-1 39% (IQR 22-69%), p=0.003; miR-133a 38% (IQR 28-47%), p<0.001; and miR-499 in ICUAP patients was 27% (IQR 17-41%) of control expression p=0.002 (Figure 4-9). MiR-206, another myoMiR, was not different between the two groups. MiR-181a (a non muscle-specific microRNA) was also significantly lower; median miR-181a expression in patients was 56% (IQR 42-77%) of control values (p=0.009; Figure 4-9).

Furthermore log [GDF-15 mRNA] showed a significant negative correlation with the log [microRNA expression] of miRs 1, 133a, 181a and 499, but not miR-206. Log [plasma GDF-15] showed a similar pattern but did not reach statistical significance for miR-181a (Figure 4-9).

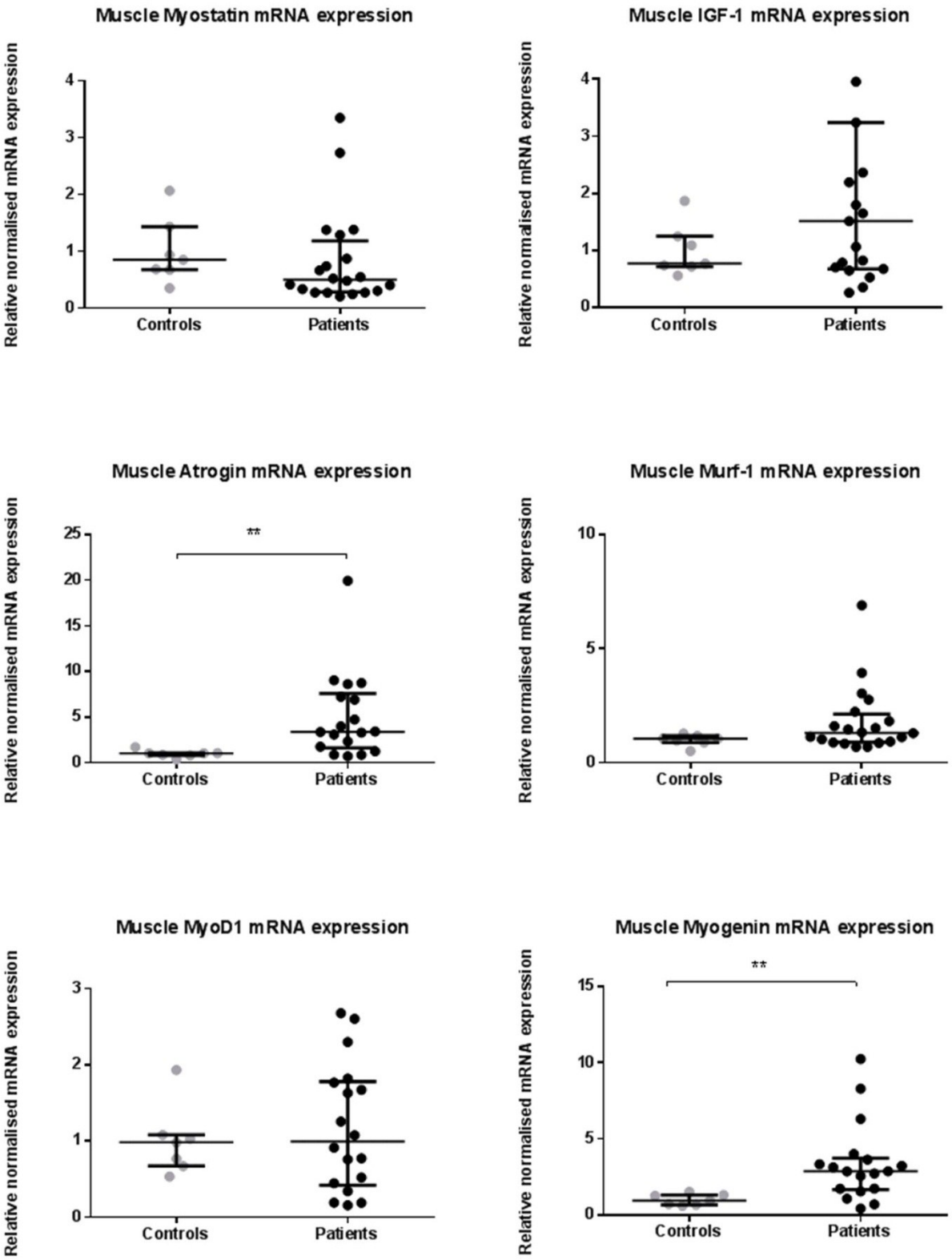


Figure 4-7 Muscle mRNA expression.

Relative normalised muscle mRNA expression of different genes in controls (n=7) and patients (n=20). Data presented as median and error bars represent interquartile range. ** p<0.01 Mann-Whitney. IGF-1 - Insulin like growth factor-1, MuRF-1 – muscle ring finger-1, MyoD1 – myogenic differentiation -1.

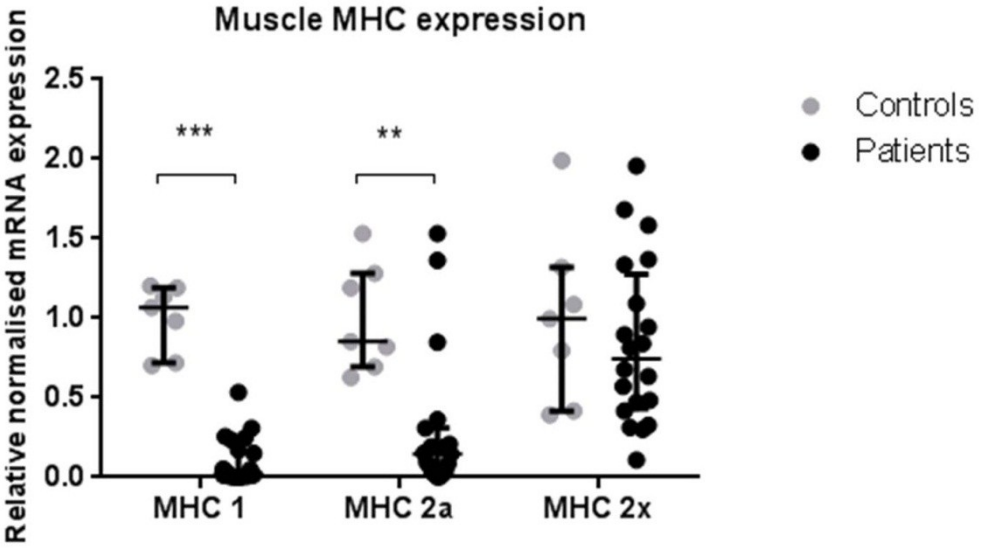
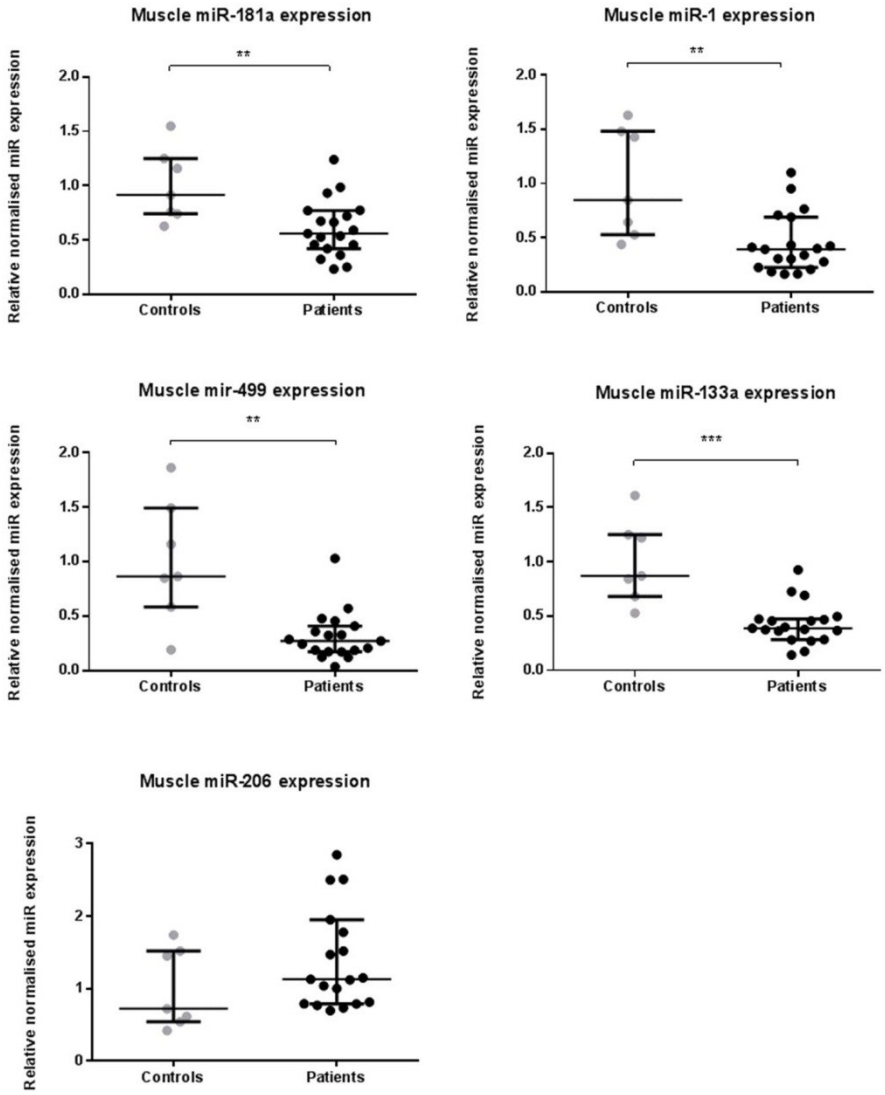


Figure 4-8 Muscle MHC expression.

Relative normalised MHC expression (Types 1, 2 and 2x) in patients (n=20) and controls (n=7). **p<0.01, *** p<0.001 Mann-Whitney. Data presented as median and error bars represent the interquartile range.



	Plasma GDF-15		Muscle mRNA GDF-15	
microRNA	R value	P value	R value	P value
1	-0.54	0.02	-0.65	0.002
133a	-0.56	0.015	-0.58	0.01
181a	-0.30	0.68	-0.50	0.045
206	0.199	0.99	0.13	0.99
499	0.54	0.025	-0.57	0.01

Figure 4-9 Rectus femoris muscle microRNA expression of different microRNA.

Rectus femoris muscle microRNA expression of different microRNA in Patients with ICUAP (n=20) and controls (n=7) .** p<0.01, ***p<0.001 Mann-Whitney. Table shows Correlation of Log [miR expression] with log [plamsa GDF-15] and log [GDF-15 mRNA expression] Pearson's r values and p values (Bonferroni-corrected for multiple testing) are listed. Data presented as median and error bars represent interquartile range.

4.4.7 TGF-β receptor type 2

TFG-β type-2 receptor (TGFBR2) protein was quantified using western blot. A prominent band was seen at the expected 65KDa level; however, a further unexpected small band was also seen. Quantification was carried out taking into account only the expected band and normalised to Ponceau staining of the membrane. There was no significant difference in the normalised TGFBR2 concentration between patients and controls.

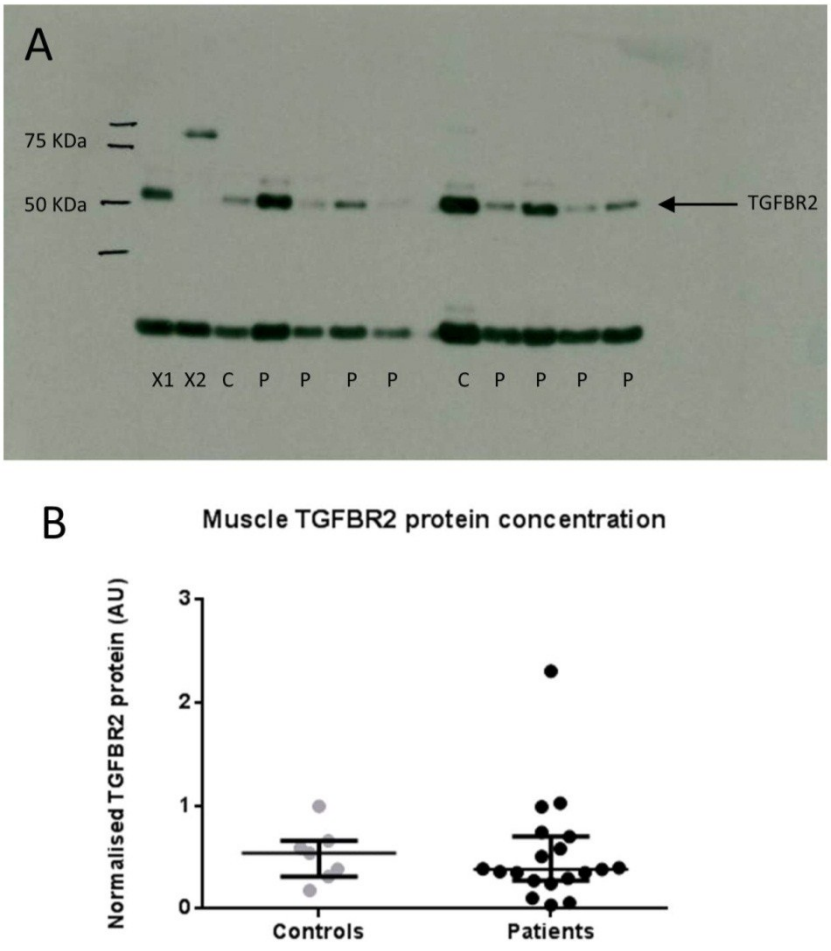


Figure 4-10 Muscle TGF-β type-2 receptor (TGFBR2) protein concentration.
(A) Representative Western blot of TGFBR2. Lanes labelled as X1,X2= protein pools for normalisation, C=control, P=patient. (B) Normalised TGFBR2 in controls (n=7) and patients (n=20) data presented as median and error bars represent interquartile range.

4.4.8 TGF -β signalling in ICUAP muscle

CYR61 (Cysteine-Rich, Angiogenic Inducer-61), is a downstream marker of TGF-β signalling (349) whose mRNA expression in ICUAP muscle was significantly higher than in control muscle (median 11.18- fold higher than controls [IQR 5.32-15.75] p=<0.0002). However CTGF (Connective Tissue Growth Factor), another TGF-β responsive gene (349), was not elevated (Figure 4-11).

TGF-β receptor activation results in SMAD2/3 phosphorylation. The phosphorylated SMAD complex then re-locates to the nucleus to act as a co-transcription factor and activate TGF-β signalling pathways (153, 154). Immuno-stained muscle sections demonstrated a higher percentage of nuclei staining positive for phosphorylated-SMAD-2/3 protein in patients (median 92% (IQR 87-95%)) than controls (median 79% (IQR 78-86%)), p=0.04 (Figure 4-11).

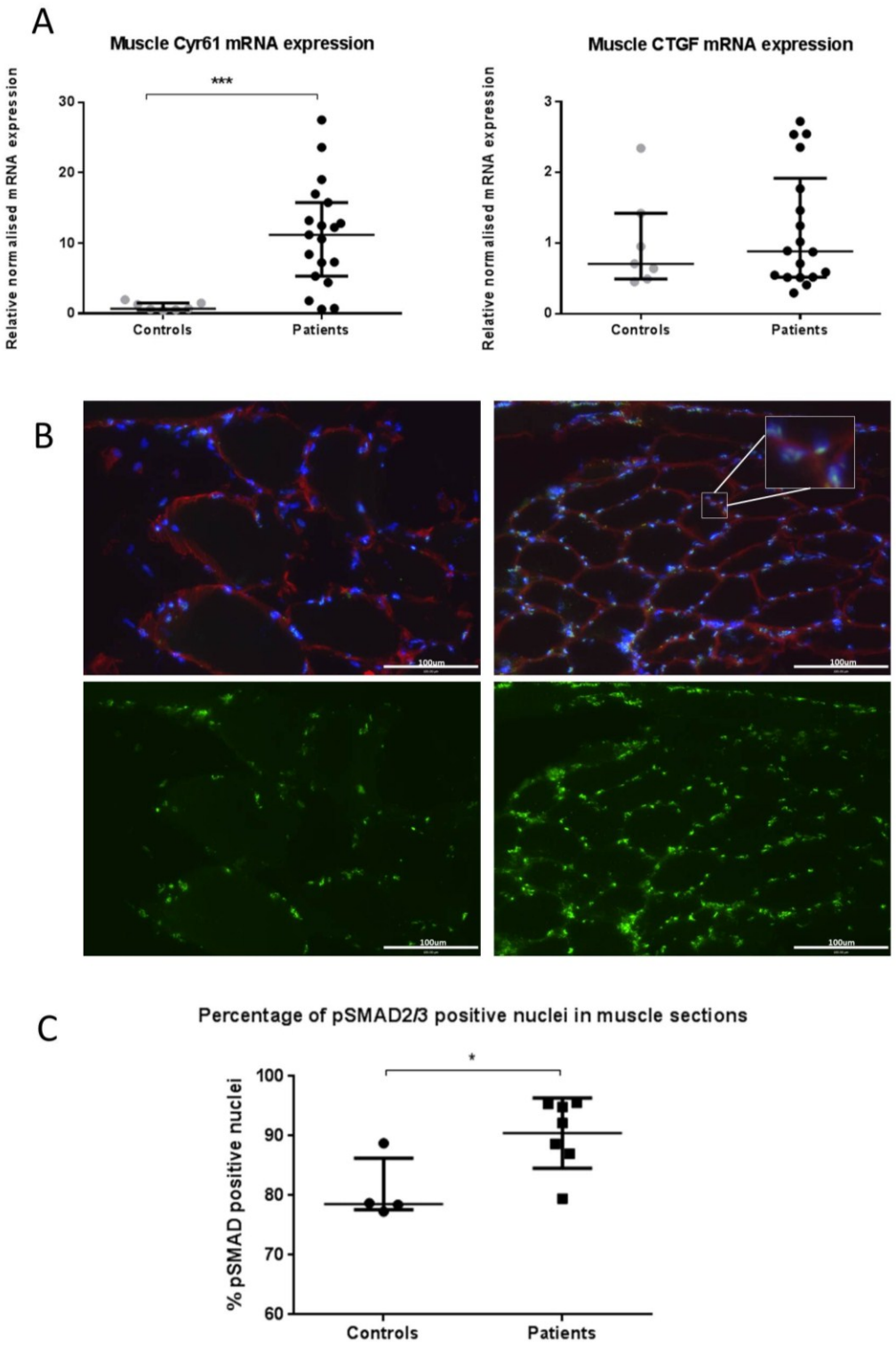


Figure 4-11 TGF-β Signalling in ICUAP muscle.

A - CYR61 (Cysteine-Rich, Angiogenic Inducer-61) and CTGF (Connective Tissue Growth Factor) mRNA expression in controls (n=7) and patients (n=20). B - Images show control (left) and patient (right) 20x magnification muscle sections stained for p-SMAD2/3 (small mothers against decapentaplegic) localisation. Blue – (DAPI) nuclear, Red – Laminin, Green - p-SMAD2/3. Expanded area demonstrates nuclear and pSMAD2/3 localisation. Lower images show p-SMAD2/3 fluorescence only of the same field of view. Graph shows percentage of pSMAD2/3 positive nuclei for controls (n=4) and patients (n=7), *p=<0.05, *** p<0.001 Mann Whitney. Data are presented as median and error bars represent interquartile range.

4.4.9 GDF-15 effects on *in vitro* C2C12 cells

In vitro data results are expressed as mean ± standard deviation.

4.4.9.1 GDF-15 did not affect SMAD-dependant luciferase activity

Treatment of C2C12 myoblasts with GDF-15 at doses from 0-100ng/ml for 24 hours from the point when they became confluent and would therefore have been starting differentiation did not activate SMAD dependant CAGA-(12)-luciferase activity. Myostatin treatment (used here as a positive control) resulted in a small but significant increase (mean 1.4±0.2-fold increase, p=0.003) Figure 4-12.

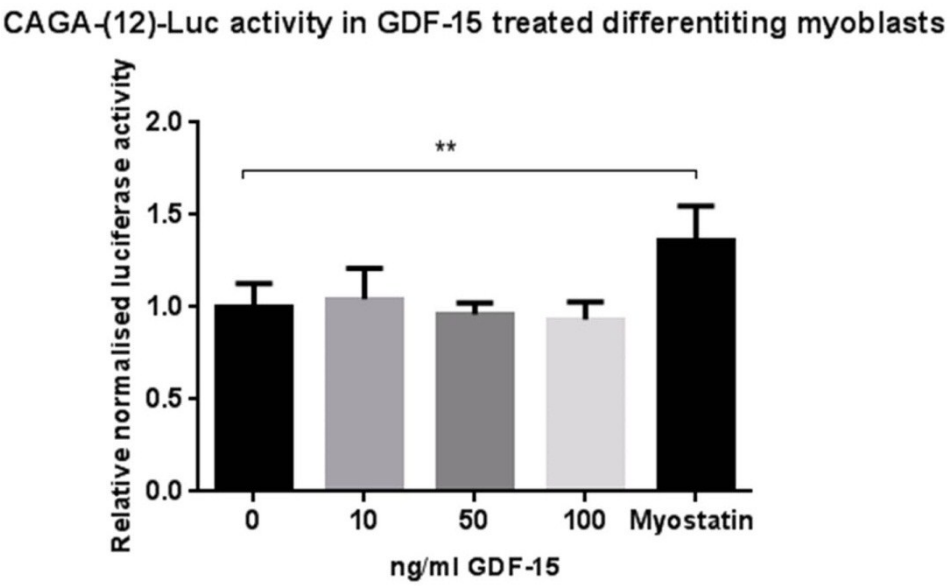


Figure 4-12 GDF-15 effects on SMAD dependant CAGA-12-driven luciferase activity.
C2C12 myoblasts were transfected with CAGA-(12) firefly and PRLTK renilla luciferase plasmids. When confluent and therefore undergoing differentiation C2C12 cells were treated with GDF-15 at increasing doses, BSA control or Myostatin as a positive control. Following 24 hours treatment, relative luciferase activity was quantified. **<0.01 T-test. Data presented as mean and error bars represent standard deviation. N=2 in triplicate.

4.4.9.2 microRNA array

The effects of GDF-15 and myostatin were tested on differentiating C2C12 myoblasts. Cells were cultured until confluent and then allowed to begin differentiation over 3 days; subsequently they were treated with control, GDF-15 (50ng/ml) or myostatin (20ng/ml) for 6

or 24 hours. No significant changes were seen in the expression of MuRF-1, atrogin-1, CYR61, CTGF, myoD1 or myogenin with either treatment or at either time point (results not shown). Therefore in order to identify the signalling pathways altered by GDF-15 which might result in the myotube atrophy that was demonstrated by Dr Lee, a microRNA array was carried out.

RNA samples from differentiating myoblasts treated for 6 and 24 hours were used; in addition, Dr Lee donated RNA from 8 day differentiated mature myotubes which had been treated for 4 days with GDF-15. The array was carried out in collaboration with the Genome Centre at St Bartholomew's and the London Hospital, London.

Appendix A2 shows the significant hits identified by the array. The results from this array suggested that GDF-15 had a more significant effect on differentiated myotubes over a longer time period and therefore these conditions were replicated for further experiments.

4.4.9.3 mRNA expression in GDF-15 treated myotubes

8 day differentiated myotubes were treated with either GDF-15 (50ng/dl), myostatin (20ng/dl) or BSA control for 4 days. GDF-15 treatment resulted in a significant rise in MuRF-1 and atrogin-1 mRNA expression with a 1.4±0.6-fold greater expression than control for each. Myostatin treatment resulted in a 1.7±0.7-fold increase in MuRF-1 mRNA expression but no significant change in atrogin-1. Neither treatment resulted in a significant change in CYR61, CTGF or MyoD1 (Figure 4-13).

4.4.9.4 microRNA expression in GDF-15 treated myotubes

GDF-15 treatment of differentiated myotubes (as above 4.4.9.3) resulted in a significant decrease in the expression of the myomiRs miR-1 and miR-133a and also in miR-181a. Myostatin treatment tended towards a similar pattern, however the reduction only reached statistical significance for miRs-133a and 181a. MiR-206 tended towards a reduction

following both treatments, but miR-499 was unchanged (Figure 4-13). Table 4-2 shows the values of expression in table form.

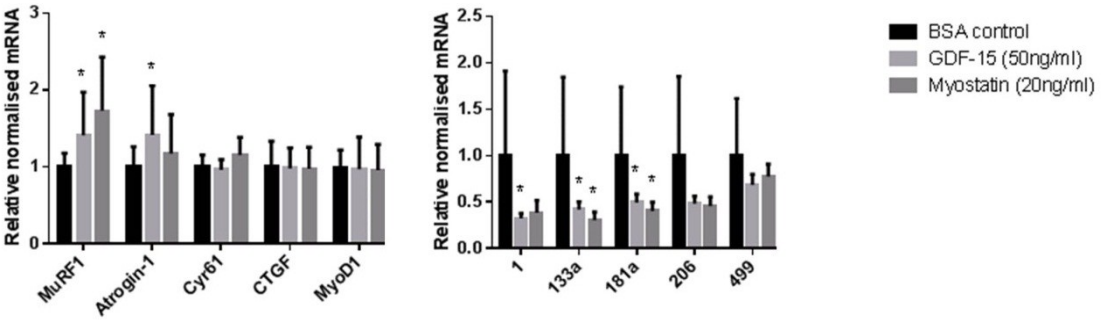


Figure 4-13 GDF-15 and myostatin effects on mRNA and microRNA expression in myotubes.
8 day differentiated myotubes were treated with control (0.1% Bovine serum albumin with 20mM HCL), GDF-15 (50ng/ml) or Myostatin (20ng/ml) in differentiation media for 4 days. Data presented as mean and error bars represent the standard deviation. *p<0.05 students t-test for comparison of treatment to control. N=4 in triplicate.

MicroRNA	Control	GDF-15	Myostatin
1	1 ± 0.92	0.32 ± 0.19 *	0.38 ± 0.40
133a	1 ± 0.85	0.42 ± 0.28 *	0.31 ± 0.27 *
181a	1 ± 0.74	0.50 ± 0.31 *	0.41 ± 0.29 *
206	1 ± 0.86	0.48 ± 0.27	0.46 ± 0.30
499	1 ± 0.62	0.69 ± 0.38	0.78 ± 0.40

Table 4-2 microRNA expression in C2C12 cells treated with GDF-15 or myotatin.
8 day differentiated myotubes were treated with control (0.1% Bovine serum albumin with 20mM HCL), GDF-15 (50ng/ml) or Myostatin (20ng/ml) in differentiation media for 4 days. Data expressed relative to control mean ± standard deviation. *p<0.05 students't-test for comparison of treatment to control. N=4 in triplicate.

4.4.9.5 TGF-β receptor type 1 and 2 protein concentration in GDF-15 treated myotubes

8 day differentiated myotubes were treated as above (4.4.9.3) and western blot for TGF-β receptors type 1 and 2 (TGFBR1 and TGFBR2) showed a possible trend towards an increase in receptor protein with myostatin (20ng/dl) and GDF-15 (50ng/dl) treatment compared to control (Figure 4-14). However the results of one experiment were not statistically significant and attempts to repeat the experiment did not show the same pattern on western blot (results of repeat experiments not shown).

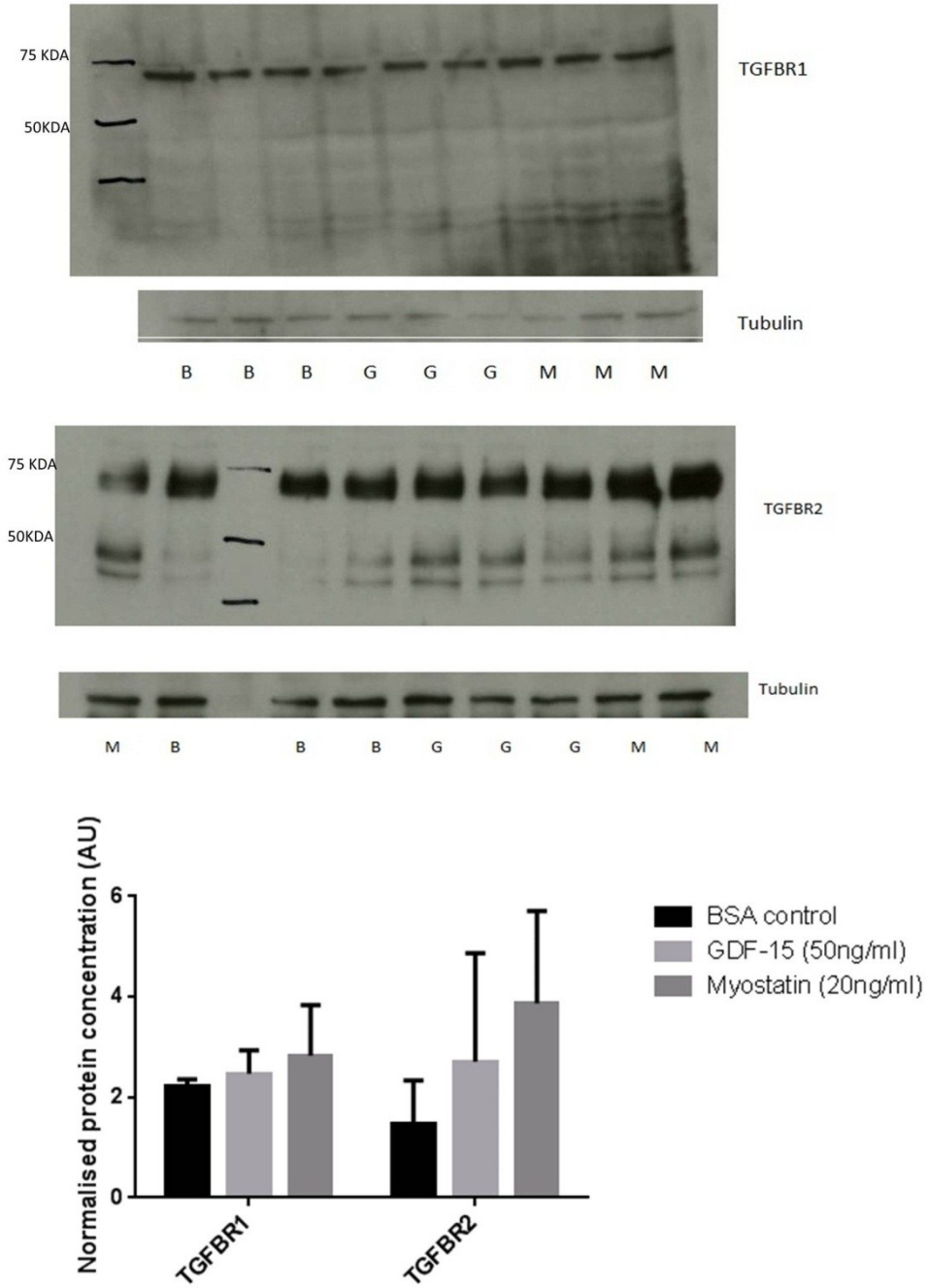


Figure 4-14 TGF-β receptor type 1 and 2 protein (TGFBR1 and 2).

Western blots to show TGFBR1 and TGFBR2 protein concentration in GDF-15 and myostatin treated C2C12 cells. 8 day differentiated myotubes were treated for 4 days with (B) vehicle control (0.1% bovine serum albumin with 20mM HCL), (G) GDF-15 (50ng/ml) or (M) myostatin (20ng/ml). Lower panel represents tubulin used as a loading control. Graph shows quantification of western blots normalised to tubulin.

4.4.10 MiR-181a over-expression reduced TGF-β signalling

Treatment of C2C12 myoblasts with TGF-β1 (2.5ng/ml) caused a 24-fold induction of CAGA-12-driven luciferase activity. Full details of this experiment can be found in the Methods

Chapter (Chapter 2). In brief, following seeding, myoblasts were transfected with mimic-miR-181a or a negative control and TGF-β signalling activation was assayed with transfected CAGA-(12)-luciferase reporter. Cells were treated with TGF β1 (2.5ng/ml) for 6 hours, harvested and assayed for luciferase activity immediately. Transfection of miR-181a into cultured myoblasts resulted in a 45% reduction in response to TGF-β treatment (Figure 4-15).

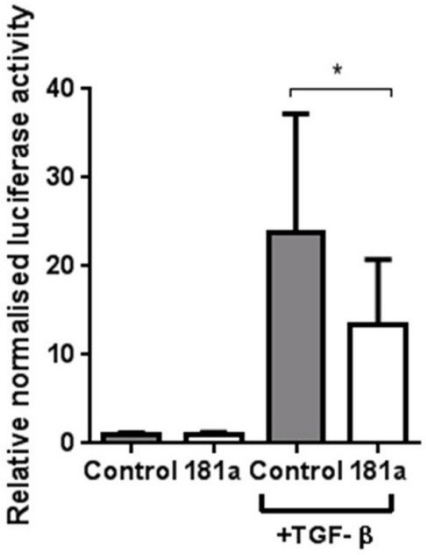


Figure 4-15 Over-expression of mir-181a reduced TGF-β signalling.
Myoblasts were transfected with miR-181a or negative control, then CAGA-12 firefly and Renilla Luciferase plasmids. Following 6 hours treatment with TGF-β (2.5ng/ml) relative luciferase activity was quantified. N=3 in triplicate and data are normalised to their contemporary control. * p=<0.05 T-test data presented as mean and error bars represent the standard deviation.

4.4.11 Investigation of the potential relationship between GDF-15 and glucose metabolism

4.4.11.1 In ICUAP patients

Plasma GDF-15 protein concentration in patients with ICUAP correlated strongly with the cumulative insulin dose received – this was corrected for length of stay (i.e. total insulin dose (units)/ ICU LOS (days)). However it did not correlate with mean blood glucose and muscle GDF-15 mRNA did not correlate with glucose or insulin (Figure 4-16).

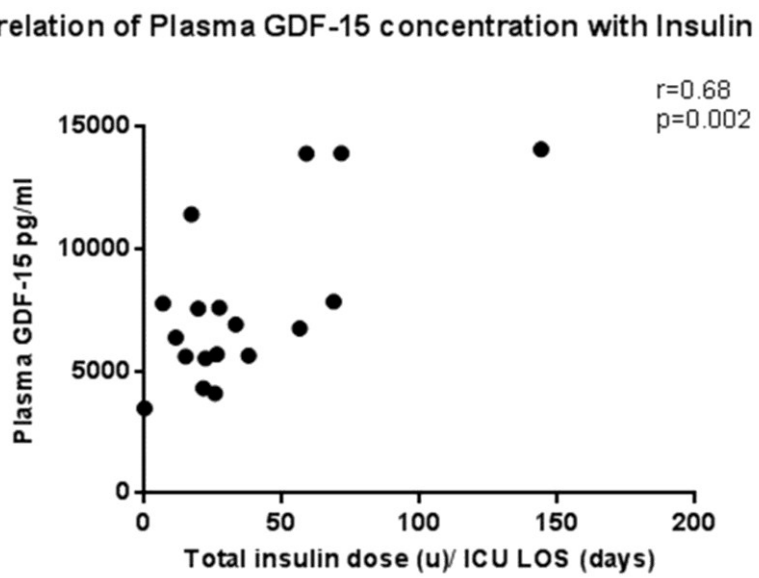


Figure 4-16 Correlation of total insulin exposure in ICUAP patients with plasma GDF-15

Graph shows correlation of total insulin dose/ ICU length of stay (LOS) with plasma GDF-15. pearsons r value and p value.

4.4.11.2 Effect of glucose concentration of GDF-15 and miR-181a expression in C2C12 myotubes

Increasing glucose concentrations in the differentiation media of 8 day differentiated myotubes for 4 days did not result in any change in either GDF-15 or miR-181a expression (data not shown). Glucose concentration was tested over a range from - 6000µg/ml (5.6 to 33 mmol/L) .

4.4.11.3 Plasma GDF-15 in COPD patients with diabetes mellitus or impaired glucose tolerance.

Plasma GDF-15 concentration was quantified in specimens donated from a cohort of 44 COPD (Chronic Obstructive Pulmonary Disease) patients by a collaborating group (Professor Emma Baker, St George's Hospital; Ethical approval was secured by the George's team 10/H0721/75). These COPD patients were taking part in another study to investigate the role of diabetes in COPD-related muscle wasting. The patients were classified according to their glucose tolerance status as normal (n=24), impaired glucose tolerance (n=8), newly diagnosed

diabetes (n=7) or established diabetes on treatment (n=5). Of this last group, one was on insulin therapy, two on metformin, one on gliclazide and one on metformin and gliclazide. The basic demographic data for the groups are described in Table 4-3. Kruskall-Wallis ANOVA test of the plasma GDF-15 concentration in the different groups revealed that they differed (p=0.037); those with established diabetes on treatment had significantly higher plasma GDF-15 concentration that all other groups (Figure 4-17). However plasma GDF-15 did not correlate with plasma glucose, HbA1c or insulin resistance (as measured by the homeostasis model assessment-2 score [HOMA2 IR]). Furthermore there was no acute change in GDF-15 during the standard glucose tolerance test in patients with or without diabetes (n=16 in total tested). However these data did confirm findings by Dr Patel (also in our group) from a separate COPD cohort that GDF-15 negatively correlated with US RF_{csa} and QMVC (data not shown).

	Normal (n=24)	**IGT (n=8)**	**New DM (n=7)**	**DM (n=5)**
Age (years)	72.5 (64.3-79.0)	67.0 (61.3-69.5)	72.0 (67.0-79.0)	81 (69.5 - 82.0)
Sex (m/f)	16/8	4/4	4/3	5/0
BMI (kg/m^2)	23.3 (19.9-27.3)	23.4(21.4-25.0)	29.0(25.3-32.1)	24.7(22.4-27.0)
FEV1 (l/s)	1.19 (1.04-1.77)	1.25 (1.12-1.65)	1.5 (0.92-1.81)	1.45 (1.04-1.64)
HbA1C (%)	39.5 (36.3-41.8)	39.5 (34.8-42.5)	49.0 (46.0-54.0)	39.0 (44.5-88.0)
HOMA2IR	0.86 (0.66-1.15)	1.06 (.74-1.62)	2.02 (1.10-3.07)	1.05(0.94-1.47)
QMVC	26.1 (22.3-36.9)	32.2 (29.1-37.3)	18.7 (12.4-25.9)	23.4 (23.0-32.1)
US RF_{csa} (cm^2)	4.10 (3.53-4.68)	4.92 (3.94-6.14)	4.13 (3.20-4.70)	3.29 (2.46-5.89)

Table 4-3 Demographic data of St George's hospital COPD patients.

IGT – impaired glucose tolerance, DM – diabetes mellitus. Data expressed as median (interquartile range). BMI-body mass index, FEV1-forced expiratory volume in 1 second, HbA1c-glycated haemoglobin, HOMA2-IR-homeostasis assessment model-2 of insulin resistance, QMVC-quadriceps maximal voluntary contraction, US RF_{csa}-rectus ultrasound femoris cross sectional area.

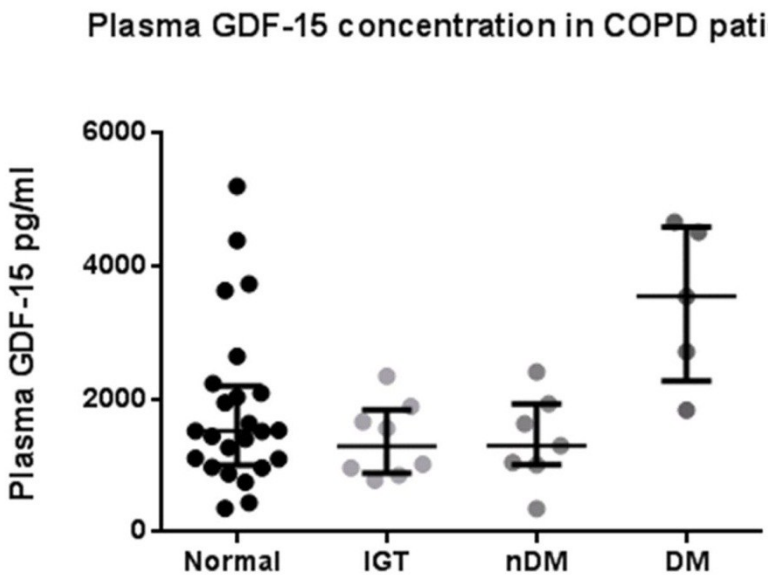


Figure 4-17 Plasma GDF-15 concentration in COPD patients classified according to glucose tolerence.
IGT – impaired glucose tolerence, nDM – new diagnosis of Diabetes Melitus (DM), DM – DM on treatment. Kruskall-Wallis ANOVA test confirms that the groups are different p=0.037

4.5 Discussion

4.5.1 Main findings

The findings of this study support the main hypothesis of this thesis and chapter, that GDF-15 and microRNAs are important in the pathogenesis of ICUAP. Firstly, both circulating GDF-15 and muscle GDF-15 mRNA expression were elevated in patients with ICUAP compared to controls (Figure 4-6). Secondly, the expression of microRNAs known to be important in muscle homeostasis and the modulation of TGF-β response were suppressed in ICUAP muscle (Figure 4-9). Thirdly, the results of stimulating differentiated myotubes in vitro demonstrated that GDF-15 can drive the reduction in these microRNAs and that suppression of miR-181a may increase tissue sensitivity to TGF-β family signalling (Figure 4-13,Figure 4-15). Taken with the increased TGF-β signalling in ICUAP muscle (Figure 4-11), these data support the hypothesis that GDF-15 is a mediator of acute muscle wasting in the critically ill and demonstrate that this activity may result from down-regulation of microRNAs leading to increased sensitivity to TGF-β signalling.

4.5.2 Discussion

GDF-15 is released from various tissues in response to stress stimuli such as hypoxia and inflammation (262); therefore the increase in circulating GDF-15 in ICUAP patients is likely in part at least to be due to their critical illness. This is consistent with the previous study (Chapter 3) (333) and is supported by the observation that patients' plasma GDF-15 correlated with their SOFA score in the current study (Figure 4-6) and that elevated GDF-15 in patients from a different study with Acute Respiratory Distress Syndrome predicted poor outcome (279). Furthermore, factors thought to be involved in the pathogenesis of ICUAP, like hyperglycaemia, inflammation and oxidative stress (74, 109), stimulated GDF-15 expression in other tissues (262, 347) and therefore also possibly drive the observed increase in GDF-15 expression in ICUAP muscle.

Dr Lee's data suggested that GDF-15 had a direct effect on muscle, which was contradictory to the hypothesis of Johnen *et al* namely that a central anorexic effect was caused GDF-15-driven muscle wasting (267). Consistent with a direct effect on muscle, in the current study GDF-15 treatment of C2C12 myotubes up-regulated the muscle specific ligases MuRF-1 and atrogin-1 (Figure 4-13) and, as previously discussed from the literature, GDF-15 was pro-apopototic and hypertrophy limiting (257, 268, 273). Furthermore, in the COPD patients studied in this analysis and in a previous analysis in our group (Dr Mehul Patel: unpublished observations) GDF-15 was associated with RF_{CSA} but not with BMI or weight, suggesting a greater effect in muscle than on lipid stores.

Atrogin-1 was also elevated in the ICUAP patients compared to controls (Figure 4-7). The rise in atrogin-1 is consistent with active muscle wasting, and both atrogin-1 and MuRF-1 have previously been proposed as mediators of ICUAP (332). MuRF-1 and atrogin-1 are responsible for muscle protein ubiquitination, a precursor event to proteolysis. MuRF-1 and atrogin expression can be driven by myostatin. However, neither MuRF-1 nor myostatin mRNA

were elevated in the patients' muscle in the current study (Figure 4-7). Human studies of short term immobilisation and acute illness (40, 350) have shown increased MuRF-1; however, this rise was lost in the longer term (175, 350) and both human and animal data concerning myostatin are inconsistent (40, 147, 175, 332, 337).

It is expected that ICUAP occurs as result of an imbalance in muscle homeostasis with a relative decrease in protein synthesis and hypertrophy pathways and a net breakdown in muscle protein/increased in atrophy. Therefore myostatin would be expected to rise and IGF-1 fall in patients compared to controls but the expression of neither mRNA differed significantly in the current study (Figure 4-7). As discussed in Chapter 3, data concerning the role of myostatin in ICUAP is often contradictory and indeed, contrary to the hypothesis, myostatin fell in the plasma of patients following cardiac surgery (Chapter 3 (333)). With respect to IGF-1, IGF-1 was *increased* in the muscle of burns patients with muscle wasting (351) and our group has previously found an *increase* in IGF-1 mRNA in COPD-related muscle wasting (302). Conversely, other groups have found *decreased* IGF-1 mRNA in human and animal muscle in response to local infection and injury (130, 133, 142). The different mRNA expression patterns seen in muscle in response to critical illness may be caused by differences in the time points examined, the muscles sampled and the injury to which the muscle was exposed. For example, it has recently been shown that after an initial period of reduced muscle protein synthesis a longer lasting phase of increased catabolism becomes predominant (40). Therefore it is important to note that the ICUAP patients in the current study had been on ICU for a median of 20 days – which represents a later time point in the disease than that assessed by the other studies mentioned above.

As a member of the TGF-β super-family it would be reasonable to suggest that GDF-15 may signal via the phosphorylation of SMAD proteins (262). However there are few data to support this (251). Treatment with GDF-15 for 24 hours did not increase activity of the SMAD-

dependant CAGA-(12)-luciferase reporter in differentiating myoblasts (Figure 4-12) and this was consistent with experiments carried out by Dr Lee in proliferating myoblasts (data not shown). However, Xu *et al* showed increased SMAD2/3 activation in neonatal cardiac myocytes following GDF-15 treatment (273) and Heger *et al* also showed SMAD activation (268). However in Herger's study, GDF-15 (3ng/ml) was found to promote hypertrophy and protect against apoptosis, which is contrary to the study by Xu *et al,* where mice over expressing GDF-15 from adenoviral vectors or exposed to GDF-15 intravenously where protected against pressure –overload induced cardiac hypertrophy. The receptor(s) through which GDF-15 acts is not yet described and although it is likely to be one of or similar to the TGF-β receptors it may be that GDF-15 mainly signals via SMAD-independent pathways. Also it is technically difficult to balance the expression of the CAGA-(12)-luciferase plasmid (which becomes weaker as the cells divide and differentiate) with the expression of TGF-β receptors on the C2C12 cells which may increase as cells mature and thus enable a response. Consistent with the suggestion that GDF-15 has a more profound *in vitro* effect on differentiated myotubes than on less mature cells were the results of the microRNA array. Very few positive targets were seen in the array overall; however, at 24 hours no targets were identified at all for GDF-15 treatment of differentiating C2C12 myoblasts, whereas at 4 days differentiated myotubes did show some interesting targets (see Appendix A2 Table A-3). The results of microRNA array gene expression experiments can be normalised and corrected in multiple ways. Individual gene expression in this array was normalised to the total background signal and the false detection rate (FDR) correction was used to correct for multiple testing. This normalisation is obviously different from that used for specific gene PCR analysis where "house-keeping genes" are used (in this case the geomean of GAPDH and RPLPO expression). It may be that this technical difference and the stringency of the correction for false positives/ detection can account for the disappointing results from the array.

Essential muscle microRNAs (288, 289, 292, 293) were significantly suppressed in the muscle of ICUAP patients when compared to controls (Figure 4-9). GDF-15 treatment of myotubes suppressed expression of the same microRNAs (with the exception of miR-499, possibly due to very low miR-499 expression in C2C12 myotubes) and log GDF-15 mRNA expression in muscle and log GDF-15 protein concentration in the plasma of ICUAP patients was inversely correlated with expression of muscle microRNAs (Figure 4-9). Therefore suppression of these microRNAs may be one mechanism by which GDF-15 disrupts normal muscle homeostasis to promote atrophy. This suggestion is also supported by several other lines of evidence. For example, knock down of these microRNAs prevented normal myoblast proliferation and myotube differentiation (289, 292, 293). MiR-1 promoted growth via targeting Histone Deacetylase-4 (HDAC4) and preventing its up-regulation of muscle-specific ligases and the ubiquitination pathway of muscle protein breakdown (290). Thus the observed reduction in miR-1 in the patients may account, in part, for the demonstrated increase in atrogin-1.

Consistent with a protective role for the microRNAs that were down regulated in the muscle of patients with ICUAP is their ability to down-regulate components of TGF-β signalling pathways. For example, miR-1 and 499 targeted and inhibited myostatin signalling; miR-1, again via inhibition of HDAC4, protects follisatin expression and thus promotes inactivation of myostatin; miR-499 targets the myostatin promoter directly and both miR-1 and 499 are predicted to target the activin IIB receptor (345, 346). MiR-133awhich is known to promote myoblast proliferation (290, 352), targeted and down regulated TGF-β family receptor type 2 and TGF-β1 itself (344). MiR-181a, promoted muscle recovery following injury (292), and also protected against TGF-β signalling via down-regulation of TGF-β type 1 receptors (343). Furthermore over-expression of miR-181a in cultured myoblasts resulted in a functional suppression of TGF-β signalling in the current study (Figure 6).

MiRWalk is an online tool which combines databases of predicted and proven microRNA targets to generate lists of potential gene targets of specific microRNAs (353). Combining all of the targets (predicted by at least 4 databases in miRwalk) of the suppressed microRNAs in our ICUAP patients in a pathway analysis using DAVID (an online tool for the functional analysis of large gene lists (354, 355)), highlights the TGF-β signalling pathway as one of the major pathways likely to be regulated. Indeed the TGF-β pathway was the third most statistically significant pathway identified with a p-value of 0.005 and a 2.2-fold enrichment score (Appendix A3 Table A-4).

The above data and results led to the hypothesis that GDF-15 dependent down-regulation of microRNA in ICUAP muscle would increase sensitivity to TGF-β signalling and thus promote muscle atrophy (Figure 4-18). Such an increase in sensitivity would result in increased downstream TGF-β signalling without an increase in the TGF-β ligands, such as myostatin, being necessary. Muscle of ICUAP patients did show features consistent with increased TGF-β signalling, such as increased expression of CYR61 (a TGF-β responsive gene, whose roles include regulation of proliferation (349) and modulation of inflammation including attracting inflammatory cells (356)) and increased proportion of nuclei containing phosphorylated SMAD-2/3 (Figure 4-11). By contrast, *in vitro* experiments in the current study in myoblasts or myotubes stimulated by GDF-15 did not show increased SMAD-dependent luciferase reporter gene activity or increased CYR61 expression (Figure 4-12, Figure 4-13). CTGF is a member of the same family of proteins as CYR61, known as the CCN family (CTGF/ CYR61/Nephroblastoma over-expressed protein family), and it too is thought to be TGF-β responsive (349). However, CTGF was not elevated in ICUAP patients' muscle. The reasons for this inconsistency are unclear and highlight the complexity of these systems and difficulties in translating bench experiments to human studies.

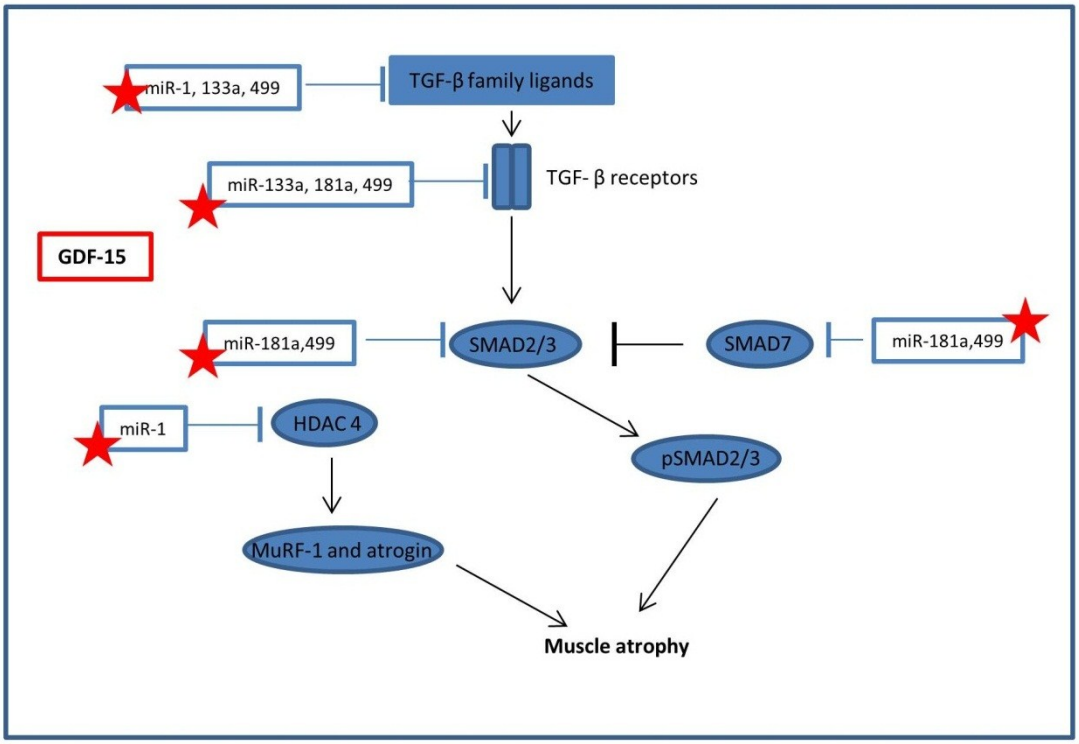


Figure 4-18 Schematic representation of the interaction between microRNAs and TGF-β (transforming growth factor-β) signalling.

Stars represent those microRNA that maybe suppressed by growth and differentiation factor -15 (GDF-15) in Intensive Care Unit Acquired Paresis resulting in a promotion of muscle atrophy. HDAC4 –Histone Deacetylase 4, MuRF-1 - Muscle Ring Finger-1, SMAD-small mothers against decapentaplegic.

It is possible that GDF-15 sensitisation of muscle to TGF-β signalling is not unique to ICUAP. Down-regulation of muscle microRNAs is consistent with changes our group have seen in COPD-associated muscle dysfunction (302) and that others have reported in inflammatory myopathies (301). Furthermore Dr Patel (also in our group) has also recently demonstrated increased GDF-15 in the plasma and muscle of COPD patients (manuscript in preparation).

Two targets identified from the literature (292, 343, 344) and the MiRWALK analysis (353) were TGFBR1 and TGFBR2. Down-regulation of the targeting microRNA (specifically miRs-133a and 181a) driven by GDF-15, should therefore result in an increase of the target protein. Attempts to demonstrate this *in vitro* were unsuccessful (Figure 4-14) and the patients did not show increased TGFBR2 protein (Figure 4-10). However Di Giovanni *et al* did demonstrate increased TGFBR2 in acute quadriplegic myopathy patients (357). Accurate protein quantification via western blot can be difficult especially from tissue samples. Further

optimisation of the *in vitro* experiments may also have achieved better results. Further work to quantify these and other potential targets of the down-regulated microRNA is needed in order to better describe the proposed mechanism.

Another important role of microRNA is in the regulation of regeneration following injury (288, 292, 358). Regeneration involves activation, proliferation and differentiation of satellite cells into myoblasts and then myoblast differentiation and incorporation into mature fibre at the same time as increased protein synthesis (292). For example, MiR-181a was highly expressed in regenerating multinucleate muscle fibres following tissue injury and up-regulated during active *in vitro* differentiation (292). Inhibition of miR-181a resulted in inhibition of myoD1 and impaired differentiation (292). Furthermore HDAC-4, an important inhibitor of skeletal muscle differentiation (359, 360), is also an established target of microRNAs 1, 133a and 206 (289, 361). Over-expression of HDAC4 inhibited myoD1 expression and impaired differentiation (360); however, despite down-regulation of microRNA-1 and 133a, no difference in myoD1 and myogenin was seen *in vitro* in response to GDF-15 treatment; and myoD1 was unchanged whilst myogenin was actually elevated in ICUAP muscle. Overall therefore the data from the current study would support a role for GDF-15 in the promotion of atrophy, but not the down-regulation of hypertrophy and regeneration. However it is important to note that myoD1 is only expressed highly in committed satellite cells and at the start of differentiation and myogenin only during active differentiation (361). Therefore mature myotubes may not have been the ideal environment to test this theory and a longer treatment of differentiating myoblasts may have had better effects. Also, satellite cells only account for a small percentage of cells in mature muscle fibres therefore changes in these cells would be difficult to detect in the background of a muscle biopsy specimen. Dr Lewis (previously in our group) demonstrated increased HDAC4 protein in the muscle of COPD patients in association with reduced miR-1 (302), but more work is needed to carefully examine these pathways in ICUAP muscle and the potential link between GDF-15 and

impairment of differentiation/regeneration via down regulation of microRNAs.. MicroRNAs are also involved in regulation of fibre type balance. MiR-499 is essential for type 1 fibre differentiation and maintenance (288). Loss of type 1 fibres has been linked to miR-499 in animal models (291) and human diseases (302). ICUAP patients showed significantly lower miR-499 compared to controls (Figure 4-9) and significantly lower MHC 1 expression (as well as type 2a) (Figure 4-8). More importantly a shift towards type 2 fibre predominance in patients was also suggested (Figure 4-5). Unfortunately this did not reach statistical significance, possibly due to the small number of subjects for whom histological analysis was possible and/or the fact that a reduction in miR-499 is likely to be an early event in the loss of type 1 fibres with a longer duration of illness needed to develop a significant fibre shift. Immobility is a contributing aetiological factor in ICUAP and reduced miR-499 was associated with low physical activity in COPD patients (302) and models of disuse atrophy also showed loss of type 1 fibres (104). Not only may immobility at least in part drive the shift in fibre type, but the loss of type 1 fibres (high endurance, slow fibres) and fibre shift towards type 2 (glycolytic, fast fibres) will contribute to the lack of muscle endurance and impaired muscle function. The only treatment interventions currently available involve increasing muscle activity (362). This impaired muscle phenotype may make rehabilitation more difficult for patients and therefore is an important aspect of the disease to address.

4.5.3 Critique of the methods

This study analysed a relatively small patient population in a specialist cardiothoracic ICU. Given the importance of GDF-15 in cardiovascular disease, caution should be exercised in generalising our data to a broader ICU population. The upper limit of normal for plasma GDF-15 is 1200pg/ml (260). It is likely that our control patients had higher plasma GDF-15 because of their underlying cardiovascular disease. This is consistent with a study of more than 1000

cardiothoracic patients where high euroSCORE was associated with raised circulating GDF-15 concentration (363).

Rather than using healthy controls, our control population was selected to match the baseline medical co-morbidities of this ICU's patient population allowing the effect of a prolonged critical illness on muscle to be examined while minimising confounding factors. However, the controls were not truly healthy and, due to the high-risk nature of their disease, were likely to have been relatively inactive and therefore potentially have some degree of muscle disuse. As a result, this choice of control group may have had the disadvantage of making it more difficult to detect a difference between them and the patients. For example, the patients clearly all had significant muscle disease resulting in ICUAP, but the US MLT was not statistically different between the two groups. This was exacerbated by the technical difficulties related to the ultrasounds themselves and, as with the O.C.T. mounted samples that had suffered ice crystal damage, the small numbers of data points available reduced the power of the study to detect true differences between the two groups.

Another important factor to consider is the feeding status of these patients, since the original effect observed in mice with tumours which over-express GDF-15 was proposed to be due to suppressed appetite (267)**.** All of the control subjects were fasted at the time of biopsy (performed during surgery) while 6 out of 20 patients (30%) were fed at the time of biopsy (2 parentrally, 4 nasogastrically). Theoretically the metabolic status of the muscle and the balance between catabolic and anabolic signalling may be different in those who are fed and those who are not. To address this concern, we reanalysed our data excluding the fed patients. No changes in the patterns of mRNA or microRNA expression that have been described were seen – except with respect to MuRF-1. When fed patients are removed from the patient cohort MuRF-1 becomes statistically significantly elevated (median MuRF-1 mRNA in starved patients 1.5-fold (SD 1.1-2.3) higher than in controls p=0.01). Starvation is thought to increase catabolic

drive (364) and it may be that MuRF-1 expression is particularly sensitive to this. Feeding in critically ill patients is currently a contentious topic. There is increasing evidence that continuous feeding is detrimental to the ability of muscle to use amino acids from the circulation and it maybe that this is an aetiological factor in the development of ICUAP (40, 365). Feeding effects cannot, of course, explain our *in vitro* observations.

As discussed, hyperglycaemia is an important aetiological factor in the development of ICUAP and it was hypothesised that hyperglycaemia might increase GDF-15 in ICUAP patients; this is potentially one way in which it might drive acute muscle wasting. However better documented outcomes for patients with tightly controlled blood glucose levels has led to ICU units adopting an "intensive insulin therapy" regime to maintain blood glucose within pre-defined levels (247). Therefore examining the relationship between blood glucose and GDF-15 in this setting is difficult. The median, mean blood glucose over the ICU stay for the patients in the current study was 7.6 with an interquartile range of 7.1-8.0, indicating that glucose was well controlled in these patients. The total cumulative insulin dose over the ICU stay has previously been reported in ICU studies (40) and may reflect insulin resistance/ glucose metabolism. However it is difficult to know what this figure really means as it could also be related to length of stay on ICU. Therefore in this study we have corrected the total cumulative insulin dose for length of stay on ICU (i.e. total insulin received in units / ICU LOS in days).

Cumulative insulin dose, corrected for length of stay, correlated strongly with plasma GDF-15, but not muscle GDF-15 mRNA expression (Figure 4-16). This might suggest that, although muscle GDF-15 is not under insulin regulation, GDF-15 release from other tissues is regulated at least in part by insulin- and glucose-dependant mechanisms. In human umbilical cells high glucose treatment elevated GDF-15 expression (347), but here treatment of C2C12 myotubes with increasing glucose concentrations did not show the same effect. One of our collaborating groups has been examining the relationship between glucose tolerance, diabetes

and muscle wasting in COPD patients and this provided the opportunity to test the hypothesis of a link between impaired glucose tolerance/ metabolism and GDF-15. Plasma GDF-15 in these patients was associated with QMVC and US RF_{csa} as previously described by Dr Patel (manuscript in preparation) but there was no association with measures of hyperglycaemia (HbA1C), insulin resistance (HOMA2 IR) or acute change during a glucose tolerance test. However, when patients were categorised according to their glucose tolerance as normal, impaired, a new diagnosis of diabetes mellitus or an established diabetic on treatment, those on treatment had significantly higher plasma GDF-15 than the other groups (Kruksall-Wallis ANOVA p=0.037). It should be noted, however, that there were only 5 individuals in the treated diabetic group and it is difficult to know how to interpret these results. The ICUAP model in patients whose glucose is so tightly controlled does not allow for full exploration of the potential link between hyperglycaemia/ insulin and GDF-15. Therefore, optimisation of the *in vitro* experiments or an animal model of hyperglycemia might provide better models in which to examine this hypothesis.

Myostatin was used in these experiments as a positive control. Myostatin is a well-established negative regulator of muscle mass, signalling via the activin IIb receptor to activate SMAD phosphorylation and drive atrophy pathways (329). As such, in the current study myostatin did increase SMAD-dependant activity of the CAGA-(12)-luciferase reporter in transfected C2C12 cells and myostatin elevated MuRF-1 expression in cultured myotubes, confirming that the model behaved as expected, with the exception that the elevation in atrogin-1 did not reach statistical significance (Figure 4-13). Myostatin has been shown to induce expression of both MuRF-1 and Atrogin-1 in various models (137, 165, 329), but not always together. These inconsistencies can probably be accounted for by the differences in the models, duration and dose of treatment, and it is likely that myostatin can drive the expression of both ubiquitin ligases in different molecular environments (137). Myostatin itself is known to be under the control of various muscle microRNAs as discussed above and a reduction in

miRs-1, 133a and 206 has previously been described in myostatin knockout mice (298). In the current experiments myostatin affected microRNA expression as expected, and in the same pattern as GDF-15, with suppression of miRs 1, 133a, 181a and 206. However the reduction in miR-206 did not reach statistical significance for either GDF-15 or myostatin and miR-1 was only reduced significantly by GDF-15 (Figure 4-13).

4.5.4 Conclusion

In conclusion, this study supports a role for GDF-15 and microRNAs in the pathogenesis of ICUAP. Furthermore, the data support the hypothesis that GDF-15 driven down-regulation of muscle microRNAs would not only disrupt muscle homeostasis, but increase sensitivity to TGF-β signalling and thus promote muscle atrophy. In ICUAP muscle there was evidence of increased activity of atrophy pathways, but not of down-regulation of hypertrophy or regeneration. This is consistent with studies demonstrating that, following the initial phase of reduced protein synthesis, muscle atrophy in clinical illness is due to a more prolonged catabolic phase (40). From a clinical perspective this study has demonstrated potential therapeutic targets in both GDF-15 and muscle microRNAs. This will be discussed further in the final discussion of this thesis.

Chapter 5 An interventional study of neuromuscular electrical stimulation in patients at risk of acute muscle wasting on the cardiothoracic ICU.

5.1 Rationale

As discussed in the introduction, early mobilisation and rehabilitation are the only treatments for ICUAP that are currently available in clinical practice (80). Studies have shown that early mobilisation can reduce length of stay and improve ICU outcomes (366). However the ability to mobilise a patient on ICU can be limited by cardiovascular instability and sedation and therefore the time at which early mobilisation is started is often delayed until the patient is medically stable and awake. Neuromuscular electrical stimulation (NMES) is an appealing option for the treatment or prevention of acute muscle wasting on the ICU as it can be delivered before the patient is awake and able to cooperate and does not result in limb movement that might compromise the patient's medical care. For this reason NMES has been included in a published guideline on rehabilitation following critical illness and the treatment and prevention of ICUAP (367); however, despite the strength of the evidence to support the intervention in healthy subjects with isolated muscle weakness (for example, following injury) (368) there is very little good evidence in the ICU setting (80). A recent systematic review identified 11 studies, only 6 of which were randomised controlled trials – three of which remain on-going and therefore have not yet published results (369). A total of 9 studies (3 randomised controlled trials, 5 contralateral-control or non-randomised and 1 crossover design trial) were included for analysis of results. The conclusions from this and a previous systematic review (96) suggest that NMES in the critical care setting is safe and may be beneficial with respect to loss of muscle function; however, they both note heterogeneity of the studies included and lack of understanding as to how these results may translate into long-

term outcomes. Furthermore, none of the completed trials in ICU patients took muscle biopsies or attempted to evaluate the molecular mechanisms involved in the muscle response to NMES.

Therefore, the rationale of the current study was to investigate the potential of NMES to modulate molecular mechanisms of muscle wasting, in particular the role of myostatin, and potentially attenuate loss of muscle mass in elective cardiothoracic patients known to be at risk of ICUAP. Unfortunately, as will be apparent from the rest of this chapter, recruitment to the study was difficult and, as a result, the final results are significantly underpowered.

Although the role of myostatin in ICUAP is unconfirmed, it is a potent negative regulator of muscle mass (329) and a member of the TGF-β superfamily known to signal via the SMAD proteins. Our group has previously shown that myostatin mRNA expression is negatively related to daily physical activity and muscle bulk in COPD patients (173). Furthermore, as discussed in previously, sensitivity to, and drivers of, TGF- β signalling are likely to be important in the development of ICUAP. Therefore, in order to complement the clinical study I aimed to investigate the effect of cyclic mechanical stretch on myostatin signalling *in vitro*.

A true *in vitro* model of physical activity is difficult to produce. Muscle cells are designed to contract in response to electrical stimuli and muscle tissue is very sensitive to changes in mechanical stimuli and force. However, even at a cellular level *in vivo* the muscle architecture is made up of multinucleate mature myotubes and these exist as part of the greater muscle fibre; these conditions are obviously difficult to reproduce in cell culture. Contraction is one part of the cycle of muscle activity; however as one muscle contracts the counteractive muscles are passively stretched, therefore stretch is also part of the normal muscular activity cycle. Stretch is sensed at a cellular level by changes in the cytoskeletal architecture. Stretch sensors are present within the myofilament and also at the membrane-membrane interface. The molecular response to stretch in muscle cells is not fully understood,

but is thought to involve activation of calcium channels in the sarcoplasmic reticulum in response to changes in the architectural interactions between the cytoskeletal elements (eg, actin:myosin, tintin and dystrophin)(370-372). Stretch of C2C12 cells *in vitro* has been widely studied and shown, amongst other things, to promote differentiation (373), increase myofibre size (374-376), alter myosin expression (319, 377), and prevent atrophy (378); these effects would potentially mimic the beneficial effects of exercise/ activity *in vivo*. Therefore, in these experiments stretch is a surrogate for activity, which, although not fully representative of an *in vivo* active muscle cell or muscle fibre, is accepted and used widely as a working model (for further examples (319, 377-380)).

5.2 Hypotheses

The above rationale led to the following main hypotheses:

1) mRNA expression of drivers of muscle atrophy, in particular myostatin and GDF-15, would be reduced by NMES in elective cardiothoracic surgical patients on ICU.
2) NMES would prevent acute muscle atrophy as measured by US RF_{csa}.
3) Cyclical mechanical stretch would protect against myostatin signalling *in vitro.*

5.3 Study design

Ethical approval for this study was secured from the National Research Ethics Committee (10/H0722/9). As an interventional trial it was registered on *clinicaltrials.gov* (NCT01321320).

5.3.1 Original protocol

An interventional, double-blind, randomised controlled trial (RCT) was designed to examine the effect of NMES or sham-NMES on a single leg in comparison to the untreated leg in high-risk elective cardiothoracic patients. Following recruitment and consent patients would

be randomised to receive either single leg NMES or sham-NMES; which leg was treated was also randomised. Randomisation lists were generated by Dr Winston Banya, NHLI medical statistician. Randomisation was to be stratified according to euroSCORE in 2 groups: EuroSCORE 6-10 or > 10. The euroSCORE takes into account age, surgical risk and co-morbidities and is known to predict ICU length of stay (311) and surgical/ peri-operative complications (312). This stratification aimed to balance groups according to these risk factors, which are suspected to increase the risk of ICUAP. This study design would allow comparison to both the patients' own untreated leg and to sham-NMES (placebo), thus potentially identifying systemic and local effects of NMES. Figure 5-1 describes the planned study design and inclusion and exclusion criteria are described in Table 5-1.

Inclusion Criteria	
Elective patients	
	Adult elective cardiothoracic patient, EuroSCORE >6, willing and able to consent
ICU patients (added later)	
	High-risk ICU patient, critically unwell, predicted to stay on ICU for a further week, willing and able to consent, or next of kin willing and able to assent
Exclusion Criteria	
All patients	
	Pre-existing neuromuscular disease, malignancy, only one leg, contraindication to biopsy, contraindication to NMES (clarified later), predicted to be anticoagulated 1 week post operatively (added later).

Table 5-1 Inclusion and exclusion criteria for the interventional study of NMES.
NMES – neuromuscular electrical stimulation.

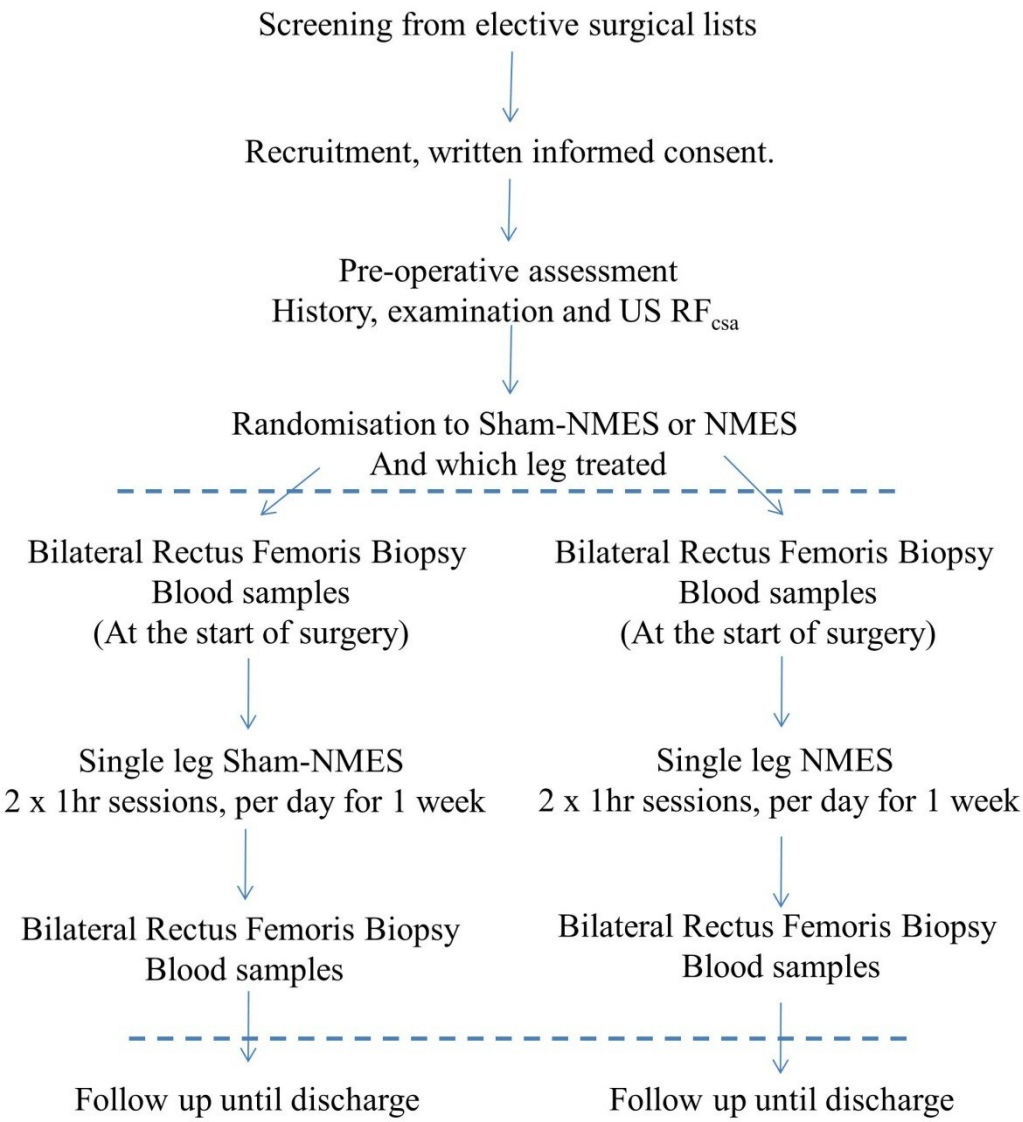


Figure 5-1 Planned study design for the interventional study of NMES in elective cardiothoracic patients.

The planned protocol is described here. Patients would be identified pre-operatively from screening of operating lists and discussion with the surgical teams. Pre-operative/ baseline assessment would be carried out prior to surgery and include history, examination and ultrasound measurement of the rectus femoris cross sectional area (US RF_{csa}) as described

in the methods chapter of this thesis. Patients would then be randomised to either NMES or sham-NMES and the leg treated also randomised. At the time of surgery, at the start of the operation, thus prior to any surgical insult, blood samples and bilateral surgical rectus femoris biopsies would be taken (as described in the methods chapter). Starting on the first post-operative day 2x 1hr sessions of NMES were to be carried out as per the protocol described below. In order for the study to remain blinded, the patients would not be told which group they were in and the sham-NMES was designed to be felt, but not sufficient to produce muscle contraction. Furthermore, the treatment would be carried out by research nurses or other colleagues in the ICU team who would not be involved in analysis of the biopsies or ultrasounds. This should continue daily for 1 week. At the end of the week US RF_{csa} would be recorded again and repeat blood samples and muscle biopsies taken. Muscle biopsies were to be either taken by the Bergstrom technique or, if this was contraindicated, open surgical biopsies would be taken (see methods chapter). Patients would then be followed up until discharge. An intention-to-treat analysis was envisaged and un-blinding would have happened once samples were processed and analysed for the primary outcome.

The primary outcome for this study was defined as a change in myostatin mRNA expression. (At the time of designing this study the group had not yet started to investigate GDF-15). Secondary outcomes included change in US RF_{csa} and change in markers of muscle synthesis and breakdown in muscle biopsy and blood samples. As such the study was powered to detect a difference in mRNA expression of myostatin.

The potential change in myostatin mRNA expression level was not known; therefore, the sample size calculation was based on data from the group's patients with COPD (data courtesy of Dr Will Man). NMES was considered as an absolute entity (i.e. active muscle with NMES or inactive muscle without NMES); the activity of the COPD patients was, however, a

spectrum. Therefore, the sample size calculation was based on the difference in myostatin mRNA expression in the most active COPD patients versus the least active.

Myostatin mRNA (qPCR data courtesy of Dr Man)

- Most active (i.e. the highest quartile of activity >90 mins/ 24 hrs) – to reflect the NMES legs – Myostatin 0.0006 (SD 0.0003) Arbitrary units (AU)
- Least active (i.e. the lowest quartile of activity <40 mins/24hrs) – to reflect the sham and untreated legs – Myostatin 0.0021 (SD 0.0029) AU

The number required in each group to detect a change in myostatin mRNA level in line with the COPD study, with power at 80% and a 5% level of significance, was 42. This calculation was carried out using Stata software (Stata Corporation, Texas, USA) and the help of Dr Jessica Harris (Medical statistician and Lecturer, NHLI, Imperial College London).

5.3.2 Amendments to the protocol

All amendments set out below were submitted to and approved by the National Research Ethics Committee.

5.3.2.1 Feasibility

In order to assess the feasibility of recruiting 84 high-risk (EuroSCORE>6) elective cardiothoracic patients to the study within the time frame of the PhD, the admission data for the main surgeon involved, Mr Mario Petrou, were reviewed. Table 5-2 shows the numbers of, and length of stay, for Mr Petrou's patients for the 6 months prior to starting the PhD (April-September 2010). A total of 53 potentially suitable patients were admitted in just 6 months from 1 surgeon. However, despite their high euroSCORE, length of stay on ICU was very short. Consequently it would not be possible to complete the study protocol during the patients' stay

on ICU. This meant that, firstly, the NMES would have to continue onto HDU and the ward; and secondly that the second biopsies would have to be done outside of the ICU setting. Bergstrom biopsies are routinely carried out in outpatient settings and therefore would not pose a problem in the ward environment. However a significant proportion of patients following surgery at RBHT require anticoagulation and Bergstrom biopsy is contraindicated in such patients. The original protocol plan, approved by the Ethics Committee, had been to carry out an open biopsy on anticoagulated patients on the ICU, with the help of the surgical team. In view of their high euroSCORE it had been expected that these patients would still be on ICU (311) and, therefore, appropriate surgical equipment, conditions and analgesia with sedation would be available and safe. However it was not deemed feasible or ethically appropriate to carry out an open biopsy once the patient had been discharged from ICU as this would involve transfer back to theatre and further anaesthetic. Therefore, as the primary outcome measure of the study was dependant on muscle biopsies, patients predicted to be anticoagulated 1 week after their operation were excluded from the study.

EuroSCORE	Number of patients	ICU LOS	Hospital LOS
<6	64	1 (1-2)	6 (5-8)
6-10	44	2 (1-4)	8 (6-13)
>10	9	2 (2-3)	9 (7-11)
Unknown	6		
Total	**123**		

Table 5-2 Surgical patients admitted under the care on Mr Petrou to the Royal Brompton Hospital between April and September 2010.

LOS – length of stay. Data presented as median full days (interquartile range).

In summary, this feasibility study resulted in 2 changes to the protocol. Firstly, in order to complete the interventional week of the study, NMES would continue after the patient was discharged from ICU, on HDU and the wards. Secondly that those patients in whom anticoagulation could be predicted would no longer be recruited, as the second set of biopsies would now take place on the ward as necessary.

5.3.2.2 Pacemakers

NMES is contraindicated in patients with permanent pacemakers. This is because of the theoretical risk of the NMES electrical current being registered by the pacemaker as cardiac electrical activity and therefore either inhibiting or disrupting the pacemaker function (381, 382). However, there is no documented occasion of such an interaction happening and certainly not any registered patient adverse events. Indeed, NMES in the outpatient setting has been tested for safety in patients with pacemakers and no adverse events were recorded (381, 382).

Following cardiac surgery a significant number of patients at the Royal Brompton hospital have temporary epicardial pacing wires in situ. Many of these are used to optimise cardiac function and protect against arrhythmia, some are for back-up pacing should the patient become bradycardic, and a small number are required because the patient's own underlying rhythm, following surgery, is asystole or complete heart block. This last group are obviously completely dependent on the epicardial pacing and it was felt that putting these patients at even theoretical risk of an interaction between their temporary pacing and the NMES was unacceptable. Therefore, the protocol was adjusted as follows: Firstly any patient with an underlying rhythm of asystole or complete heart block would not receive NMES until their rhythm had changed. Secondly any patient receiving NMES with a functioning pacing box, even if only for back-up, would be supervised by a doctor (who was qualified and able to turn off the NMES if necessary) for the duration of their NMES training session. For safety reasons the study was suspended until these changes to the protocol were approved by the Ethics Committee (January to April 2011).

5.3.2.3 Recruitment of ICU patients.

Unfortunately, shortly after restarting the study following the above ethical amendments, the lead surgeon, Mr Petrou, resigned from the Brompton (Summer 2011). This significantly reduced recruitment for the following reasons: inadequate numbers of patients with EuroSCORE>6; a high proportion of patients with mitral valve disease and atrial fibrillation and therefore requiring anticoagulation; and competition with other surgical consultants' own studies and agenda. Recruitment was on-going in this period, but very slow. However with the arrival of a new high-risk aortic surgeon, Mr Rosendahl, recruitment improved (Spring 2012).

During this time, in order to address the problems of inadequate recruitment (which was made even worse by the cancellation of surgical procedures during the swine-flu epidemic) the inclusion criteria of the study were extended to include a further group of patients. These were ICU patients who remained critically unwell and were predicted to be on the ICU for at least a further week but who were stable enough to be enrolled in the trial. It was felt that these patients would be likely to have already received a significant insult to their muscle and therefore could potentially benefit from the intervention.

Furthermore, in view of the very slow recruitment it was decided that the sham-NMES arm of the trial should be dropped, thus halving the number of patients required. However by only using the internal control of the untrained leg the ability to examine systemic effects of NMES was lost. Additionally although leg randomisation was still carried out, no stratification by euroSCORE or ICU risk was attempted.

5.3.2.4 Final protocol

Figure 5-2 shows the final protocol of the study. The principle investigators were to remain blinded as to which leg received NMES until after the principle molecular components an UF_{csa} were analysed; however, obviously the patient was no longer blinded. Therefore the

final study was a single-blinded, internally-controlled interventional trial of NMES in patients at risk of acute muscle wasting.

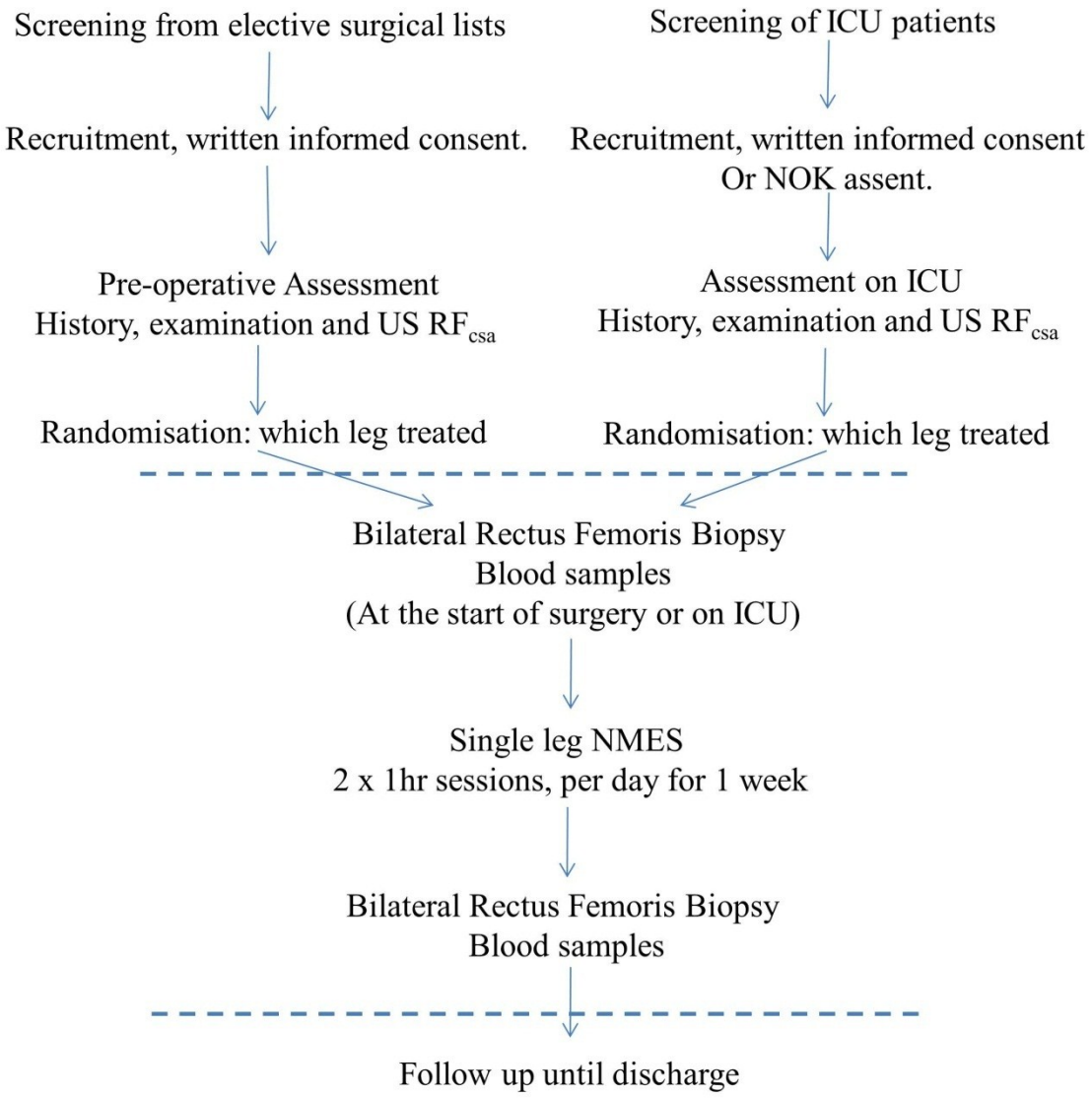


Figure 5-2 Final protocol for the interventional study of NMES in elective cardiothoracic patients and critically unwell ICU patients.

5.4 Neuromuscular electrical stimulation

Neuromuscular electrical stimulation (NMES) is the application of an electrical current over a muscle or nerve applied via skin surface electrodes. NMES aims to recruit muscle fibres and cause muscle contraction. As discussed, there is increasing interest in this technique as the

muscle contraction created could potentially have the same benefits as volitional exercise. However, the muscle fibre recruitment that results from NMES stimulation is different from that which occurs physiologically. When recruited from a motor neurone, small fibres are recruited first then sequential recruitment and de-recruitment across the muscle occurs to create a coordinated and efficient response. In the case of NMES, the recruitment depends on the strength and delivery of the current – thus larger closer fibres are recruited first and there is a sustained, but uncoordinated, response (368, 383). This can result muscle fatigue and even damage. Furthermore, there is no consensus from the literature as to a particular protocol of NMES delivery in the ICU setting and, even in other settings, a wide range of protocols are used (368, 369, 383). With this in mind, a study of 2 different devices at different settings was conducted, in 8 healthy volunteers from the muscle lab, in order to design a protocol that was comfortable for the patient and resulted in a coordinated contraction.

The conclusions from this study were as follows:

1) Skin Electrodes: Larger skin electrodes distribute the current over a wider area and, therefore, are more comfortable. In this study 10x5cm reusable long-term electrodes were used (VS.10050 Verity Medical Ltd). Electrode position can also make a difference to the efficiency and quality of contraction of the stimulated muscle. Several positions were tried and, in line with the suggestions from the device manufacturers, a horizontal position across the rectus femoris muscle was found to be the most efficient. Figure 5-3 shows the positioning of the electrodes.
2) Frequency: The frequency of the current (measured in Hertz - Hz) describes the number of pulses per second delivered. Physiological frequency is variable depending on the muscle, nerve and strength/ type of contraction being stimulated. However, physiological frequency of motor unit discharge is often around 30Hz (384). The frequency also affects the comfort of the sensation of

NMES. Lower frequencies were reported as “prickly” and higher ones “smoother”. A frequency of <10Hz was not sufficient to be felt, contraction could be stimulated at 30Hz, but higher amplitudes (see below) were tolerated at a frequency of 50Hz which was reported as more comfortable. This is in line with suggestions from the literature (384).

3) Amplitude: The amplitude (measured in milliAmperes - mA) of the current refers to the intensity or strength of the current and will affect the strength of muscle contraction produced. Ideally a strong contraction would be produced, which was comfortably tolerated by the patient so that NMES could be continued for the necessary time (384). Figure 5-4 shows the amplitudes (at 50Hz) at which the current was first felt, visible coordinated contraction could be seen and the maximum tolerated for the healthy volunteers. In the study of healthy volunteers the strength of contraction generated at the maximum tolerated amplitude (at 50Hz) was found to be only a median of 18% (interquartile range 13-25%) of the volitional QMVC (quadriceps maximal voluntary contraction) as measured by the quads chair. This is in line with what would be expected without causing pain (383).

4) NMES delivery device: Two different delivery devices were tested; the Microstim MS2v2 (Odstock Medical,UK) and the NeuroTrac® Sports XL (Verity Medical, UK). The NeuroTrac® device performed better; lower amplitudes were found to give better contraction and the delivery of current was found to be more comfortable. Furthermore it was easier to programme and cheaper.

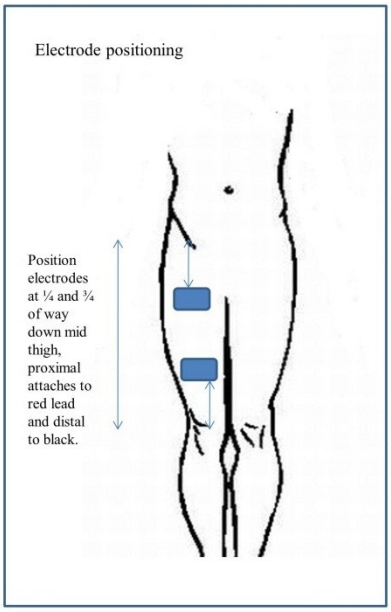


Figure 5-3 Position of electrodes for NMES.

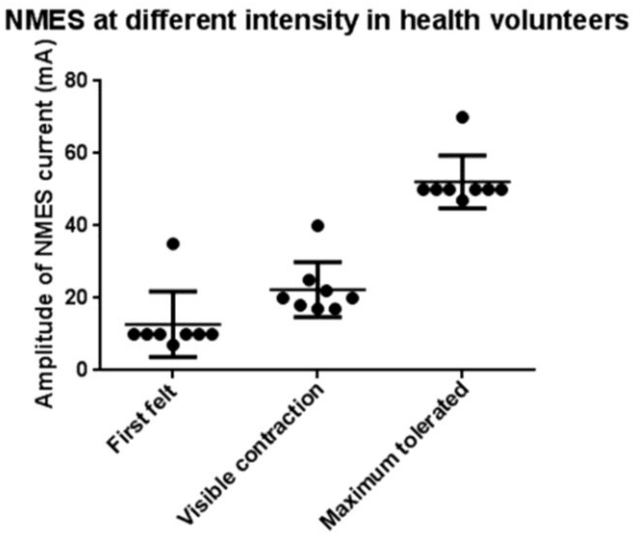


Figure 5-4 NMES in healthy volunteers.

Graph shows the first amplitude at which the current was felt, produced a visible contraction and the maximum tolerated (all at 50Hz). Data is presented as median, error bars represent the interquartile range. N=8

The protocol for NMES and Sham-NMES (with the aim that stimulation would be felt, but would not produce any functional contraction) is described in Table 5-3. A duty cycle of 6 seconds on and 4 seconds off reflected a gentle, slow, repetitive contraction (with a 0.6 second ramp speed). A symmetrical rectangular wave form, with a pulse width of 330µs was chosen as

suggested by the manufacturer's guidelines for the stimulation of large muscles like the quadriceps.

	Frequency (Hz)	Amplitude (mA)	Comment
NMES	50	>30	Starting at 20-30mA and slowly increased until a good contraction was seen.
Sham-NMES	10	10	

Table 5-3 Protocol for NMES and sham-NMES delivery.

5.5 Results

5.5.1 Effect of cyclic mechanical stretch on myostatin signalling in confluent C2C12 myoblasts.

As described in the methods chapter, C2C12 cells transfected with the SMAD driven p(CAGA)$_{12}$–luc plasmid (and control pRL-TK) were cultured on BioFlex® plates to allow cyclic mechanical stretch to be applied. Cells were cultured until confluent and then transferred to differentiation media. 24 hours of stretch, at 6% elongation and with a duty cycle of 1.5 seconds on and 1.5 seconds off was then applied. This was based on the literature (319) and experience of the group. Cells were stretched either in the presence of myostatin (20ng/ml) or BSA control (Bovine Serum Albumin 0.1% with 20mM HCl).

One-way ANOVA analysis of relative normalised luciferase activity in the different conditions confirmed that the conditions are different ($p<0.0001$) and demonstrated that stretch reduced SMAD-dependant signalling both in the presence and absence of myostatin ($p<0.001$ and 0.016 respectively, Bonferroni corrected for multiple testing) (Figure 5-5).

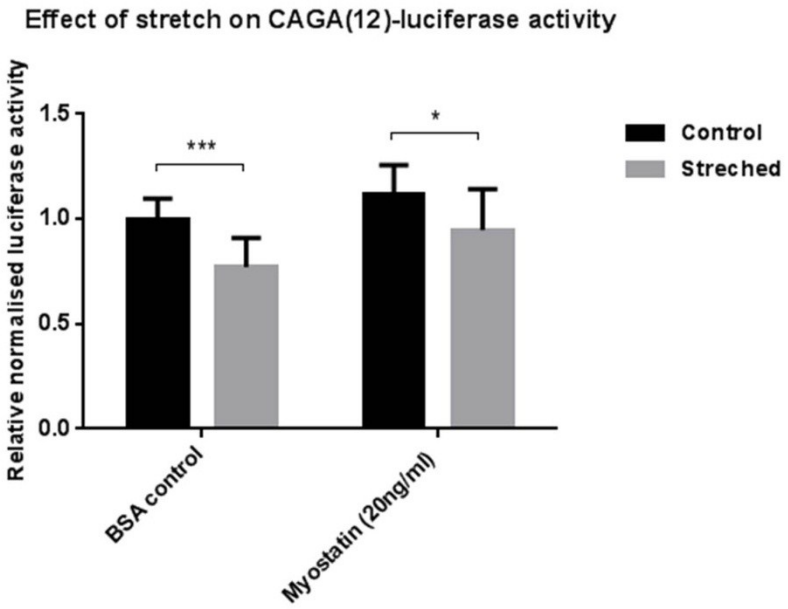


Figure 5-5 Effect of cyclic mechanical stretch on myostatin signalling in C2C12 cells.

p(CAGA)12–luc and pRL-TK transfected C2C12 cells were cultured on BioFlex® plates and at confluence were stretched for 24 hours, at 6% elongation with a duty cycle of 1.5:1.5s in the presence of myostatin (20ng/ml) or BSA control (Bovine Serum Albumin 0.1% with 20mM HCl). Relative normalised luciferase was measured. Data are presented as mean with error bars representing standard deviation. ANOVA analysis confirms that the conditions are different $p<0.0001$. $*p<0.05$, $***p<0.001$ with Bonferroni correction for multiple testing (n=4 in triplicate).

5.5.2 Patients studied

Figure 5-6 shows the consort diagram for the interventional study. After initial screening a total of 86 patients were formally screened. The most common reasons for exclusion were failure to meet the inclusion criteria; for example, 14 patients in fact did not have a euroSCORE of greater than 6 when it was recalculated. 17 patients met exclusion criteria when their history was formally reviewed; the most common reason was predicted anticoagulation (n=14), but also malignancy and previous neuromuscular disease. Finally a total of 12 patients completed the protocol, 7 elective patients and 5 ICU patients. Their demographic data, co-morbidities, surgical procedure or reason for ICU admission, interventional and outcome data are described in Table 5-4. The most striking difference between the 2 groups of patients was the length of stay both on ICU and in hospital, with the ICU patients staying much longer. This was expected as they were already prolonged stay patients having been on ICU for a median of 21 days. One patient with cystic fibrosis having

eventually recovered from her acute illness was then referred for transplant, which she received and was finally discharged from hospital 173 days after admission.

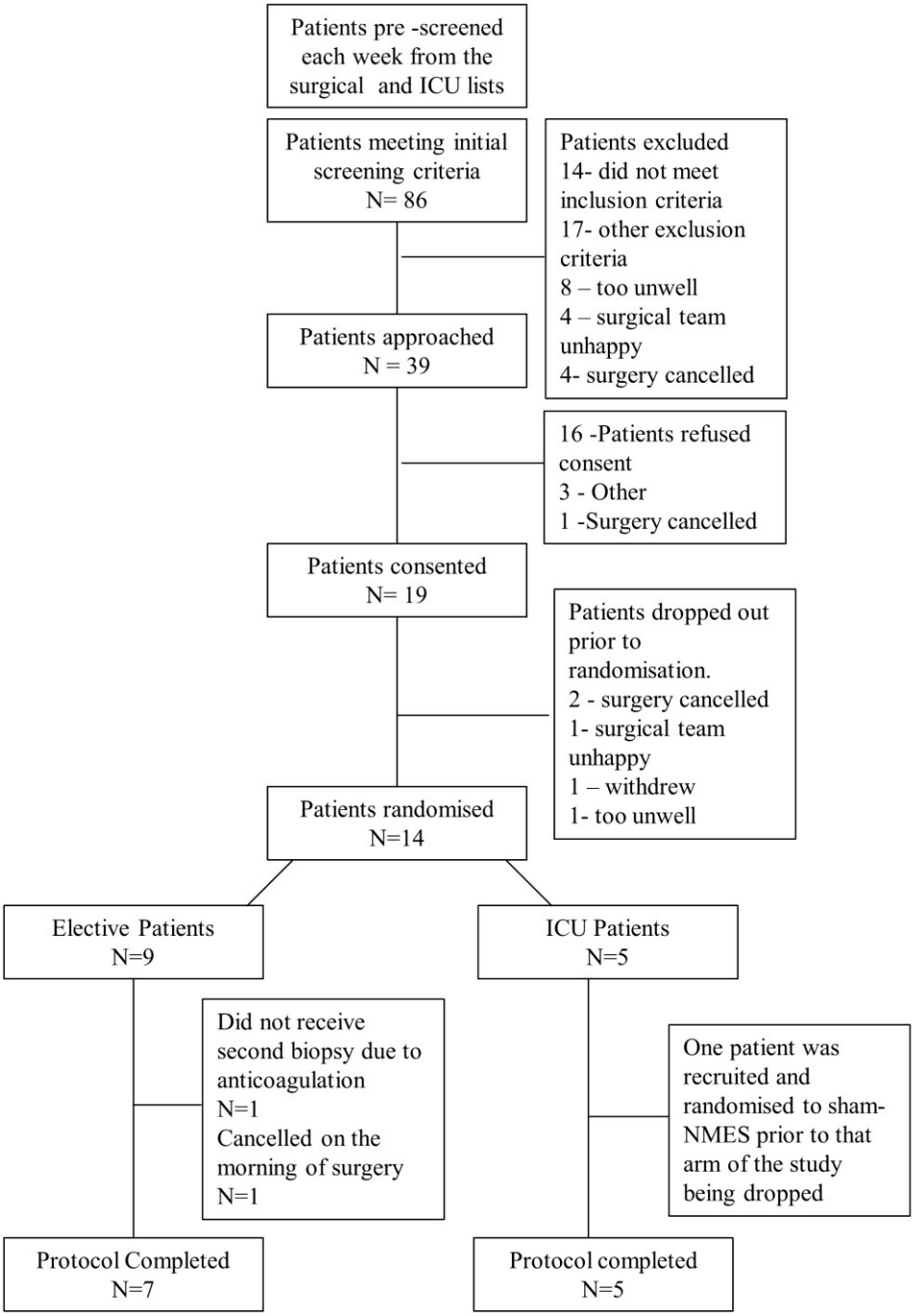


Figure 5-6 Consort diagram for the interventional study of NMES in patients at risk of acute muscle wasting on the cardiothoracic ICU.

	Elective patients (n=7)	ICU patients (n=5)	All patients (n=12)
Demographic data			
Age (yrs)	69 (64 – 73)	52 (43 – 67)	66 (51 - 71)
Sex (m/f)	7/0	4/1	11/1
BMI (kg/m^2)	24.4 (23.0 – 28.3)	27.0 (26.0 – 27.7)	26 (23.0 – 28.4)
EuroSCORE	9 (7 – 10)		
SOFA Score		9 (8 – 14)	
Co-morbidities (n)			
IHD	4	1	5
Cardiac disease	6	1	7
Respiratory	0	2	2
Diabetes	1	0	1
Statin use	4	0	4
Type of Cardiac surgery(n)			
CABG	1		
Valve surgery	2		
Mixed	4		
Reason for ICU admission (n)			
Post cardiac Surgery		1	
Cardiac		1	
Respiratory		3	
Day on ICU of biopsy		21 (8 – 29)	
Fed at first biopsies (n)	0	2	2
Fed at second biopsies (n)	3	4	7
Intervention data			
NMES leg treated (r/l)	4/3	3/1*	7/4*
Number of sessions completed	10 (5 – 10.5)	11 (10.25 – 11.25)	10 (8.5 – 11)
mAmps used (mean ± SD)	32.0 ± 10.6	40.8 ± 8.8	36.1 ± 10.7
Outcome data			
LOS on ICU after starting study protocol (d)	9 (3.5 – 15.5)	48 (32 – 54)	15.5 (8 - 44)
Total hospital LOS (d)	15 (7 – 31.5)	70 (45.5 – 121.5)	24 (7 – 52)
Died (n)	1	2	3

Table 5-4 Demograpic, intervention and outcome data for patients studied in the interventional study of NMES.
NMES- Neuromusclar electrical stimulation, BMI – body mass index, LOS – length of stay, IHD – ischaemic heart disease, CABG – coronary artery bypass grafting. Data presented as median (interquartile range) or n – number unless otherwise stated. * - please note – there are only 11 treated legs in total – please see section 5.5.3 for explanation.

5.5.3 Protocol compliance and adverse events.

One patient was recruited and randomised under the original study protocol. They were randomised to receive Sham-NMES. Therefore this leg has been excluded as it does not appropriately fit into either treated or untreated groups. Therefore there are only 11 treated legs for 12 patients.

NMES was well tolerated. No patients described pain or discomfort once they had got used to the stimulation. Patients received a median of 10 sessions (interquartile range 8.5-11) in total (Table 5-4). One patient received no NMES sessions at all and another patient received only one session as their underlying cardiac rhythm contraindicated NMES as per the study protocol. One patient terminated the study early as they were discharged from hospital at day 5. Unfortunately some sessions were missed for logistical reasons. During NMES the person applying the NMES was asked to record the quality of muscle contraction; all patients achieved good contraction except one in whom no visible contractions were seen during the final 2 sessions. During critical illness, excitability of nerve and motor units is reduced (385, 386) and this is reflected in the fact that ICU patients required a higher intensity current to achieve contraction than elective surgical patients (Table 5-4). The results are analysed as per intention-to-treat as was decided in the planning of the study.

Only one serious adverse event was reported. This was the development of a haematoma following surgical biopsy and wound infection superficial to the haematoma; However, the patient's clinical management and outcome were not altered and the situation was monitored closely by the surgical and research teams. The event was down-graded to an adverse event at closure. No adverse events were reported in relation to the NMES itself or interaction with temporary pacing boxes.

5.5.4 Primary outcome measure: change in myostatin mRNA expression

Mann-Whitney U tests were used for between group analyses (i.e. control versus NMES). Paired analysis was also conducted of the results of each leg at the two time points: pre- (baseline) and post- the study protocol (NMES or control) using Wilcoxon matched pairs ranked signed tests. This statistical design is comparable to that used by other groups (387, 388).

Relative to baseline, myostatin mRNA expression in the untreated control leg at the end of the study was median 1.03-fold (IQR 0.43-2.06). In the NMES-treated leg myostatin mRNA expression was 1.87-fold higher than baseline (IQR 0.65 – 2.44). This demonstrated a statistically significant rise in myostatin mRNA with NMES treatment, but no change over the week in the control leg (p=0.032 and 0.569 respectively Wilcoxon matched pairs ranked sign test). There was no statistical difference between the two legs at the start or end of the study in raw or relative values (Figure 5-7).

5.5.5 Secondary outcome measures

5.5.5.1 US

Due to technical issues with RF US_{csa} only 7 patients had bilateral pre- and post-paired ultrasound (5 elective patients and 2 ICU patients). RF US_{csa} did not change significantly during the study in either control or NMES legs on paired analysis. Three NMES legs and 3 control legs would have been defined as “wasting” in the previous study discussed in Chapter 3 (i.e.>9.24% muscle loss). Only one patient’s legs behaved differently from each other: the NMES leg wasted, whilst the control leg actually increased in size. The median US RF_{csa} expressed as a percentage of baseline at the end of the study was 107% (IQR 63–127) for control legs and 93% (IQR 64-104) for NMES legs, but there was no statistical difference between the two groups of legs (Figure 5-8)

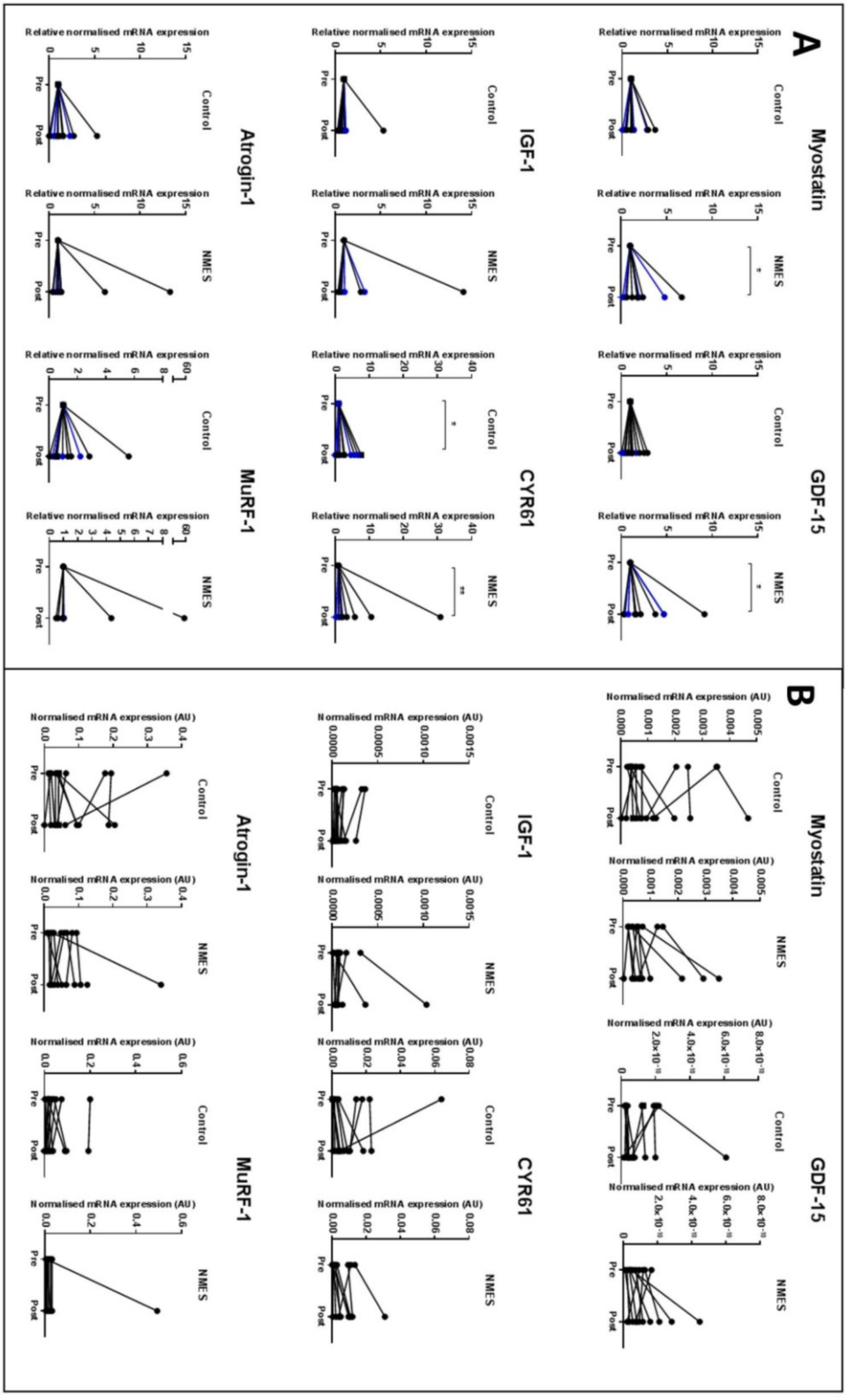


Figure 5-7 mRNA expression at baseline (pre) following 1 week (post) of single leg NMES or control.

N=12, black points represent elective cardiothoracic patients (n=7), blue –ICU patients (n=5).Panel A: Data presented relative to baseline. Statistical comparison to baseline with Wilcoxon's test *p<0.05, **<0.01. GDF-15 growth differentiation factor-15, IGF-1 Insulin like growth factor-1, CYR61 – cytesine risch protein 61, MuRF-1 mucle ring finger protein-1. Panel B: The same data, but not presented as relative to base line (AU – arbitrary units).

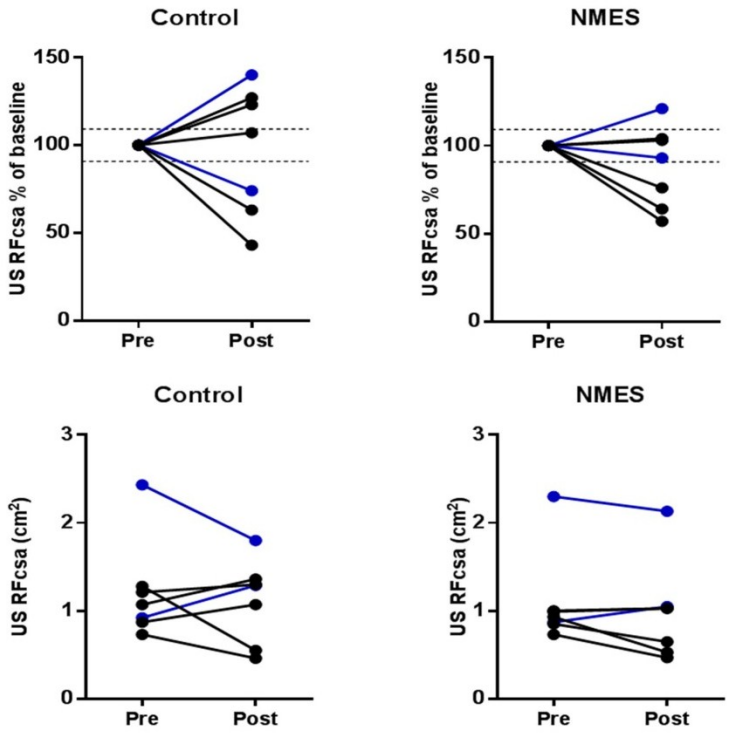


Figure 5-8 Change in US RF_{csa} following 1 week of NMES or control.

Ultrasound rectus femoris cross sectional area expressed as percentage of baseline (upper graphs) and as raw values (lower graphs), pre (baseline) and following 1 week of NMES or control. N=7, black points represent elective cardiothoracic patients (n=5), blue – ICU patients n=2).

5.5.5.2 Effect of NMES on mRNA and microRNA expression

Relative to baseline, GDF-15 mRNA expression at the end of the study was unchanged in the control leg (median 1.18-fold [IQR 0.57-1.94, p=0.339]), but 1.66-fold higher than baseline (IQR 0.80-4.71) in the NMES treated leg (p=0.042). CYR61 mRNA expression was significantly elevated in both groups of legs relative to their own baseline (control median 2.05-fold greater than baseline [IQR 0.81 – 5.49, p=0.043]; NMES 2.19 [IQR 1.2-7.07, p=0.010]), but there was no statistical difference between the groups. There was no significant change in IGF-1, atrogin or MuRF-1 mRNA expression between baseline and the end of the study and no difference between the two legs (Figure 5-7).

MiRs-1,133a, 181a, 206 and 499 were measured at baseline and at the end of the study in both legs. There were no differences between the two legs (control or NMES at either time point) and, relative to their own baseline, miR-206 was the only microRNA to change

significantly. Relative to baseline, miR-206 was significantly elevated in the NMES legs (median 2.39-fold [IQR 1.01-3.51] p=0.014), but was unchanged in the control legs (median 1.63-fold [0.81-2.14] p =0.084) (Figure 5-9). (Paired analyses – Wilcoxon matched pairs ranked signed tests; between group analyses Mann-Whitney U test).

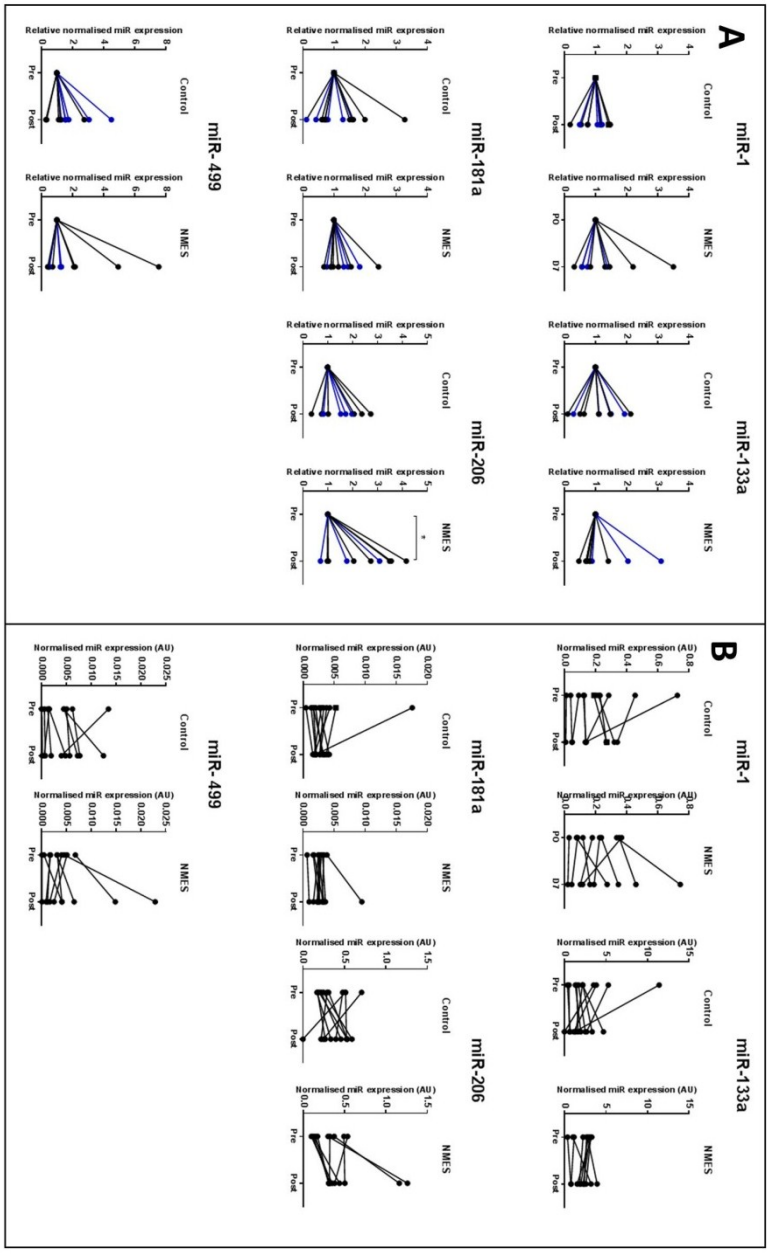


Figure 5-9 microRNA at baseline (pre) following 1 week (post) of single leg NMES or control.

N=12, black points represent elective cardiothoracic patients (n=7), blue –ICU patients (n=5). Panel A: Data presented relative to baseline. Statistical comparison to baseline with Wilcoxon's test *p<0.05.Panel B: The same data, but not presented as relative to baseline.

5.6 Discussion

5.6.1 Main findings

The *in vitro* portion of this study demonstrated that cyclical mechanical stretch, as a surrogate for physical activity, down-regulated the activity of the SMAD-2/3 driven luciferase reporter both in the presence and absence of myostatin (Figure 5-5). Potentially this might imply that activity would protect against TGF-β signalling; however, no mechanistic insight can really be drawn from this experiment alone. As discussed, TGF-β signalling is likely to be important in the development of ICUAP and from this experiment one could develop a hypothesis surrounding the effect of stretch/ activity on TGF-β pathways in ICUAP. However, rarely do *in vitro* experiments translate easily to clinical studies, as is demonstrated by the clinical component of this chapter.

Unfortunately, the current interventional study is significantly underpowered as only 12 out of a proposed 42 patients were recruited. The consequences of this are as follows. Firstly the statistically significant findings that have been detected may reflect a type 1 error (falsely rejecting the null hypothesis). As with all small studies the variance of the estimates of the parameter being measured is greater than with larger studies and therefore any effect may appear larger than it is. Secondly the study is underpowered to detect differences that may truly exist, reflecting potential type 2 error. These considerations must be taken into account when interpreting the results and their significance.

The primary outcome measure for the current interventional study was a change in myostatin mRNA following NMES treatment in elective cardiothoracic patients. It was predicted/expected that the intervention would be beneficial, potentially by preventing muscle protein breakdown. Although it was hypothesised that myostatin mRNA expression would be reduced by the intervention, on the contrary, a statistically significant rise from

baseline was observed in the NMES treated legs, whilst myostatin mRNA remained unchanged in the control legs. There was no difference in expression between the two groups of legs (NMES treated and control) either at baseline or at the end of the study. GDF-15 is also, our group believes, a potential negative regulator of muscle mass and in the current study mRNA expression of GDF-15 was also elevated from baseline in NMES treated legs, but not in control legs (Figure 5-7). Both these findings would appear to indicate that NMES in the acute phase of critical illness, either secondary to the insult of cardiothoracic surgery or whilst critically unwell on ICU, may increase the expression of molecular drivers of muscle atrophy. However these changes were not associated with any significant change in muscle mass in either treated or control legs (Figure 5-8). In addition, contrary to what might be expected based on the *in vitro* study, TGF-β signalling, as measured by CYR61 expression (349), increased relative to baseline in the NMES legs; however, it was also increased in the control leg.

5.6.2 Comment on Recruitment

Recruitment for this study was disappointing. Despite major protocol amendments in order to reduce the number of patients required from 84 to 42 and active screening efforts by myself and the ICU team, recruitment targets were still not met. In fact only 19 patients in total were recruited and only 12 successfully completed the protocol (7 elective cardiothoracic and 5 ICU). The reasons for this were two-fold: firstly logistical and secondly due to the requirements of the trial, patients and their relatives were not keen to give consent.

Considering logistical aspects, the study protocol was relatively intensive and required surgical teams to be willing and available to take biopsies and research nurses (or other members of the team including physiotherapists, ICU nurses, or other colleagues) to be available to carry out the randomised and blinded NMES. Despite starting as scheduled in the PhD plan, the study was immediately suspended whilst amendments were made concerning the locations where the NMES would take place and the issues with pacemakers (see above).

Furthermore, despite the feasibility study demonstrating that over the 2 year period there should have been sufficient suitable patients available this was not the case; due to changes in surgical personnel, the number of patients with a euroSCORE greater than 6 fell significantly and many more were excluded due to requirements for anticoagulation.

From a patient perspective the study protocol was also intensive, involving 4 biopsies and a week of single-leg NMES. Many patients felt that, in view of the fact that they were already undergoing a high-risk surgical procedure, this was too much to ask. Furthermore, relatives of critically unwell patients on ICU who were suitable for the study often felt that their relation had already "been through enough" and therefore did not want to expose them to the perceived risk of 4 biopsies and a week of NMES during their illness (which the patient may have felt, although it should not have been painful). This was in contrast to recruitment for the observational study discussed in Chapter 4, which involved a single biopsy, where relatives of ICUAP patients were generally happy to give assent (only 4 out of 24 who were approached refused). One can only speculate on the reasons for this. Perhaps one reason is that, because the relatives of patients with ICUAP or the patients themselves have close or first-hand experience of the devastating nature of the disease, they therefore understand the rationale behind the study. On the contrary, for elective cardiothoracic patients or relatives of patients in the acute phase of critical illness the rationale may not have appeared to be as relevant or important. Consistent with this suggestion is the fact that all those who were recruited to the study from the ICU already had a diagnosis of ICUAP. These patients had already been on ICU for a significant time, developed muscle wasting and remained critically unwell or had relapsed into acute critical illness; two patients were transferred into our unit for cardiothoracic surgery, having been critically unwell on other ICUs and had already developed muscle wasting and the other patients had had an acute setback (for example, a further bout of sepsis). On the contrary, those approached early in the ICU stay during the first acute phase, all declined to participate (n=5). Finally, although muscle biopsies are generally

very well tolerated and are often done in the outpatient setting, one can understand why consenting to have 4 might be daunting.

5.6.3 Critique of the method

As noted the current study was underpowered to detect differences between groups and as such no differences were detected between NMES or control legs. Differences were detected between time points of the same legs (i.e. in comparison to baseline) and the pattern of these differences in NMES legs compared to control legs were not the same. The findings might be more convincing in a true NMES versus control analysis, but the risk of a type 1 error in an underpowered study would still exist.

As discussed above recruitment for this study was very difficult and as a result the study was left with only 12 patients. Furthermore, these patients come from 2 separate cohorts of patients, those on ICU with established muscle wasting and elective cardiothoracic patients. The small numbers of the patients in each cohort do not allow a meaningful separate analysis of these groups, but visual inspection of the results suggests that the two groups do not separate obviously (Figure 5-8). Also, despite selecting elective patients with high euroSCOREs, 3 of the 7 patients were discharged from ICU before the end of the study protocol and subsequently from hospital by 1 week. Conceivably such patients might be expected to behave differently, in terms of muscle metabolism and effect of NMES, in comparison to those elective patients who remained on ICU for longer periods or the ICU patients. Gruther *et al* conducted a randomised controlled trial of NMES in acute (n=17) and long-term ICU patients (n=16) and demonstrated a beneficial effect from NMES only in the long-term patients (387). These data are consistent with the suggestion that the effect of NMES may differ at different time points in the clinical course of ICU and, therefore, it may be inappropriate to include the two heterogeneous groups of patients in the current study in the same analysis.

A significant potential confounding factor in the current study is the lack of standardisation of feeding status of patients at the time of the first and second biopsies. All elective patients were fasted for surgery at the time of their first biopsies, but some (but not all) were fed at the time of the follow-up biopsy and the feeding status of the ICU patients was variable (Table 5-4). Biopsies were taken at a convenient time for the ICU team and this was often at the time of another procedure for which the patient was fasted, for example return to theatre or tracheostomy; thus only 2 ICU patients were actually fed at the time of biopsy. Recently it has become increasingly apparent that fasting status may affect the metabolic status of muscle in the acute phase. For example Puthucheary *et al* demonstrated suppressed protein synthesis seen in fasted controls compared to fed controls (40). The degree to which feeding regime might affect the development of ICUAP is currently debated, but designing a standardised approach to the biopsies would have potentially reduced this confounding factor. Other potential confounders include prior exposure to corticosteroids (n=2 in ICU patients) and neuromuscular blocking drugs (n=3 in ICU patients). (No patient was on neuromuscular blockers during the course of the study).

A further criticism of the study is the conflicting results of the clinical study and *in vitro* experiments. Several questions arise from the *in vitro* experiment in terms of both the validity of the use of cyclic mechanical stretch as a surrogate for activity and that the SMAD-2/3 luciferase reporter only reflects one element of a complex molecular system modulating muscle mass; downstream markers or drivers of TGF-β-related muscle breakdown (e.g MuRF-1, atrogin or CYR61) or indeed myostatin itself were not measured. The reasons for this include technical difficulties with the stretch machine and the wide variability in mRNA expression between wells and conditions found in the preliminary experiments as discussed in the methods chapter.

5.6.4 Significance of the results.

It is of course essential to consider any results of the current study in view of the comments and critique above. However the data suggest that NMES may be associated with a rise in both myostatin and GDF-15 mRNA expression, whereas no change was seen in these markers over the same time period in the control legs. The significance of this is unclear as it was not associated with an appreciable difference in muscle size as measured by US RF_{csa}. Again, however, this must be considered in light of the underpowered nature of the study. NMES in ICU patients has been shown to be beneficial in terms of muscle size (387-389), strength (390-392), potential changes in the muscle microcirculation (393), circulating markers of muscle breakdown (394) and even diagnosis of ICUAP and weaning times (390). Studies resulting in positive outcomes in terms of muscle bulk or strength have generally been conducted with a longer period of NMES intervention (references (390-392)- 2 weeks, (387) – 28 days), it may be that the intervention in the current study was not long enough to be beneficial. A study of similar size (n=8) to the current one also conducted over 1 week also failed to show a change in muscle mass as measured by ultrasound (386); the patients were suffering from sepsis and in fact there was a trend towards a detrimental effect of NMES with greater loss of muscle size in the stimulated leg compared to control (386). The current study did not assess muscle strength; this is unfortunate as one study demonstrated changes in strength in the absence of changes in bulk (391), and it is possible that NMES may have a more profound effect on mechanisms related to strength rather than muscle mass (96).

The molecular effect of NMES in the ICU setting are not understood as published studies to date have not undertaken molecular analysis, although several are awaited (369). Extrapolation from other clinical scenarios and diseases may not be appropriate, as ICUAP is a complex disease that occurs at a time of systemic stress and therefore the metabolic status of the muscle is unlikely to be the same as in, for example, stable COPD or traumatic denervation.

Indeed, different molecular environments and stresses may be one of the reasons that *in vitro* results do not directly compare with those seen in the clinical situation. In COPD, NMES has been shown to be associated with a reduction in atrogin mRNA expression (395) alongside improvements in muscle physiology (muscle cross-sectional area and walking distance); however this study was over a 6 week period. Increases in oxidative enzymes, fibre cross-sectional area and a change in fibre type proportion (although this is reported in both directions) have also been shown in healthy volunteers (396). Two studies of similar design to the current one have been conducted in patients immediately after surgery, although both were in patients following abdominal surgery who were not critically unwell or admitted to ICU. Both demonstrated a favourable effect of NMES in terms of molecular markers of muscle protein breakdown. Strasser *et al* demonstrated decreased ubiquitination of sarcolemmal proteins and protease activity alongside increased total RNA and sarcoplasmatic protein content (397) associated with NMES; however, septic patients were excluded from this study and muscle mass was not assessed. In 1996 Vigne *et al* demonstrated a preservation of polyribosomes in response to NMES in patients following abdominal surgery associated with reduced loss of muscle bulk as measured by computerised tomography (CT) (398). Both these studies would suggest that following the systemic insult of surgery, which may be a model for critical illness, NMES has a beneficial effect on muscle by suppressing muscle protein breakdown. However muscle damage secondary to NMES has also been documented (399, 400) and therefore the rise in myostatin and GDF-15 seen here may reflect muscle damage in this cohort.

As far as I am aware, microRNAs have not previously been investigated in either the field of ICUAP or in response to NMES. There are, therefore, no other data with which to compare the results of the current study. Only miR-206 changed significantly in either control or NMES legs, increasing significantly from baseline in the NMES legs, but not the control legs (Figure 5-9). MiR-206 is a true myomiR and is expressed only in skeletal muscle; it is involved in

the regulation of muscle myogenesis, but is unlikely to function alone (293, 401, 402). Muscle biopsies from healthy individuals following acute and short-term endurance training showed that many muscle microRNAs are modulated by exercise, but results are often inconsistent. MiRs-1, 133a and 181a were increased following one bout of moderate intensity exercise (403-405), but only miR-1 remained elevated relative to baseline following a 10 day course of endurance training (403). Conversely, others have shown down-regulation of myomiRs following prolonged exercise (404, 406). MiR-206 was unchanged 1, 3 and 6 hours and 10 days post-exercise (403-405), but a reduction was seen following a 12 week course of exercise (404). The heterogeneity of these studies, and the current study, makes it difficult to draw conclusions. NMES affects molecular signalling in skeletal muscle (396) and, as microRNAs are an integral part of this, it is therefore probable that microRNAs will be involved in the modulation of the molecular signals, but this does not necessarily mean that this effect is independent of their role in healthy muscle homeostasis.

5.7 Conclusion

Systematic review of the literature would suggest that NMES is beneficial in terms of muscle function in critical illness (96, 369). Furthermore, early rehabilitation is now established as a means of preventing and treating ICUAP (80, 366). However, it is also plausible to suggest that the ability of muscle to respond favourably to exercise during critical illness will depend on at least the nutritional and inflammatory status of the patient. Consistent with this is not only the data from the current study, but the trend towards increased wasting seen with NMES in Poulsen *et al*'s study in septic patients (375). The current clinical trial had the potential to provide interesting insight into the molecular mechanisms behind ICUAP and the response of muscle to NMES in critical illness.

Ideally the effect of NMES on the ICU would be assessed by a double-blind, randomised, placebo-controlled trial, such as was designed for the original study protocol. This

would allow an assessment of the effects of NMES on muscle size, strength and molecular mechanisms and clinical outcome. Additionally, the design would allow the systemic effects of NMES to be measured, for example by assessing changes in circulating markers of muscle turnover. Unfortunately, I was unable to recruit the required number of patients even for the modified version of the protocol and, as a result, the conclusions are limited. With hindsight one important factor that I would change would be to make an alteration in a physiological measure (e.g. the US RF_{csa}) the primary outcome as this would have allowed the biopsies to be an optional part of the study. Although this would have potentially limited the ability of the study to answer molecular questions, it may have resulted in improved patient acceptability and hence recruitment, fewer patients excluded due to anticoagulation and fewer concerns from the medical teams. Another factor which would have improved recruitment would have been to accept patients with a lower euroSCORE. The study in Chapter 3 demonstrated that, in our surgical cohort at least, euroSCORE was not related to risk of developing muscle wasting, thus patients with a score lower than 6 were also at risk of developing measurable muscle loss that may have been modified by NMES. However, as the study stands the results are difficult to interpret in light of the small numbers of very heterogeneous patients.

Chapter 6 MiR-181a: a potential biomarker of acute muscle wasting following cardiac surgery?

6.1 Rationale

As discussed, acute muscle wasting following critical illness is a common clinical problem (180) which is associated with significant morbidity and mortality (362). Although 25% of patients who are intubated and critically unwell for more than one week develop ICUAP (3) it is often difficult to predict which these patients will be and to confidently make the diagnosis prior to the patient awakening. The ability to predict or to diagnose muscle weakness prior to awakening would enable clinicians to predict prognosis, direct early rehabilitation and guide management. Also, as drugs emerge that modify muscle metabolism (407) a predictive biomarker of acute muscle wasting would facilitate selection of high-risk patients and allow enrichment of stratified medicine trials.

Biomarkers are naturally occurring markers of disease, which provide an objective measure of the presence or progression of disease. To be clinically useful a biomarker test should be reproducible and readily available. The test should have a high specificity and sensitivity for the presence of the disease and therefore high positive and negative predictive values. Ideally the biomarker would also detect disease development prior to the onset of detectable clinical symptoms; biomarkers need not be related to the mechanism of disease, although of course they can be.

The potential of microRNAs as biomarkers in several disease areas is increasingly recognised (408). In 2008 circulating microRNAs were first reported to be reliably detectable in blood and could be used to distinguish between healthy controls and patients with B-cell lymphoma (409). The function of microRNAs in the circulation is not fully understood. They circulate in lipid exosomes, micro-vesicles or associated with HDL lipid particles. The secretion

of microRNAs from tissues is believed to be regulated and specific, as the microRNA profile within cells has been demonstrated to be different from the profile which is secreted by them (410). This has led to the hypothesis that specific profiles of circulating microRNAs may reflect disease processes and thus the interest in them as biomarkers. Furthermore microRNAs are stable in the blood and have been shown to resist multiple freeze-thaw cycles making them more attractive as clinically useful biomarkers (411). Therefore, since 2008 the investigation of microRNAs as biomarkers has rapidly developed, covering diseases from multiple organ systems (412). Two important fields in this area of research are in the diagnosis and prognosis of acute coronary syndromes (413) and in diagnosis of both solid and haematological cancers (408). Techniques used to assess and identify the microRNAs in question are also developing, from the identification of a few specific and target microRNAs to the use of microRNA array screening tools where an expression pattern of several disease-specific microRNAs can be identified and the power of the test as a diagnostic tool improved (412). With respect to muscle, muscle-specific microRNAs have been postulated as potential biomarkers of Duchene's muscular dystrophy (414), amyotrophic lateral sclerosis (415) and rhabdomyosarcoma (416). Additionally our group has shown increased circulating muscle-specific microRNAs in the blood of COPD patients related to the degree of their muscle atrophy (417).

6.2 Hypothesis

The above rationale led to the following hypothesis:

Changes in circulating levels of muscle-specific microRNAs (-1,-133,-206,-499) (289) and those involved in the regulation of muscle regeneration and inflammation (30b, -181a) (289) may reflect early development of acute muscle wasting in critically ill patients and represent potential biomarkers of ICUAP.

6.3 Patients studied

This study used plasma samples from the study discussed in Chapter 3. The elective cardiothoracic patients provide a good model of human acute muscle wasting in the critical care setting in which to investigate a potential biomarker as they are a relatively homogeneous group. The patients were categorised according to whether they developed muscle wasting or not, as defined by the US RF_{csa} (see chapter 3 for full details).

6.4 Results

6.4.1 Patients

The demographic data and clinical characteristics of this patient cohort have been previously published (333) and are described in Chapter 3 (Table 3-1). In brief, 42 patients were included in the data analysis, of whom 23 (55%) developed muscle wasting. Those who developed muscle wasting and those who did not were well matched in terms of age, sex, body mass index, co-morbidities and surgical risk (EuroSCORE)(310) at baseline, indicating that these factors cannot be used to predict skeletal muscle loss. The median length of ICU stay was 1 day for non-wasting patients and 2 for those with muscle wasting (p=0.62 Mann Whitney). Total hospital stay was also not different between the groups.

6.4.2 Circulating microRNAs in acute muscle wasting.

Samples were analysed for microRNA -1, -499, -181a, -30b and -16 in plasma samples from the pre-operative (baseline), first and second post-operative days (D1, D2) and on day seven or at discharge if earlier than day seven (D7). MiRs -133a and -206 were not detectable. MiR-16 was quantified as a control microRNA (327). Not all time points were available for each patient, because samples were excluded if the PCR melt curves suggested multiple products or inconsistency between duplicates. Excluded samples were equally distributed between the

non-wasting and wasting groups (48/380 and 57/460, respectively; p=0.91, chi-squared test). Missing time points were excluded from any repeated measures analysis. Data were non-parametrically distributed and are described as median values (interquartile range).

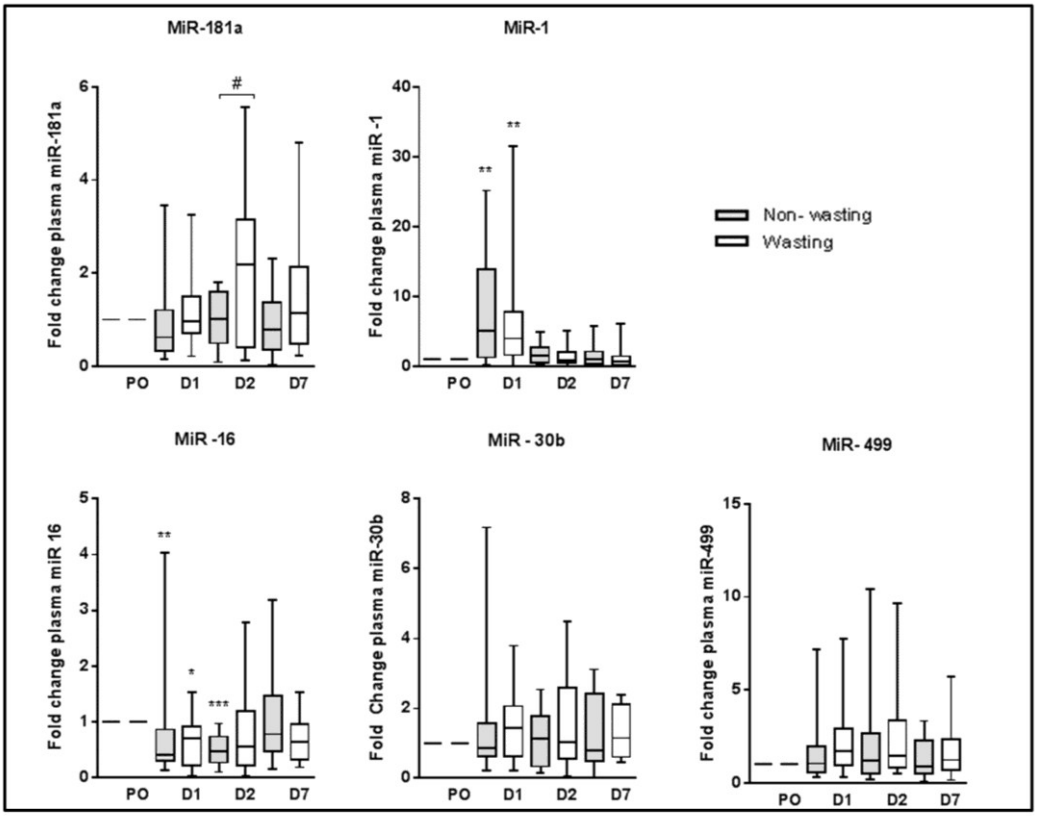


Figure 6-1 Circulating plasma microRNA following cardiothoracic surgery.

Relative plasma microRNA concentration in non-wasting (n=19) and wasting patients (those with >9.24% muscle loss: n=23) pre-operatively (PO), on day 1 (D1), day 2 (D2) and on day 7 (D7). Data presented as box and whisker plots with median, interquartile ranges and 5-95% percentiles. *p<0.05, ** p<0.01, *** p<0.001, repeated measures Freidman's test with Dunn's correction for comparison with pre-operative baseline. # p=0.03 for comparison between groups with Kolmogorov-Smirnov test.

Raw plasma concentrations of these microRNAs did not differ significantly at baseline or any time point between those who developed and those who did not develop muscle wasting. Repeated measurements were therefore expressed and analysed as relative to the patient's own baseline (fold-change). 30b and 499 remained statistically unchanged both between and within groups over time. No direction of change could be described at any time point for these microRNAs (Figure 6-1).

6.4.2.1 MiR-181a

Median plasma miR-181a at D2 was 2.15-fold greater (IQR 0.40-3.15) than baseline in those who developed muscle wasting compared to 1.02-fold (IQR 0.50-1.60) in those who did not (p=0.03 Kolmogorov-Smirnov test)[1]. ROC curve analysis for an increase in D2 miR-181a gave an area under the curve of 0.6. A rise in miR-181a at D2 of greater than 1.7-times baseline gave a specificity of 91% and sensitivity of 56% for acute muscle wasting (Figure 6-2). The positive predictive value of a rise in miR-181a >1.7-fold was 91% with a negative predictive value of 56%.[2]

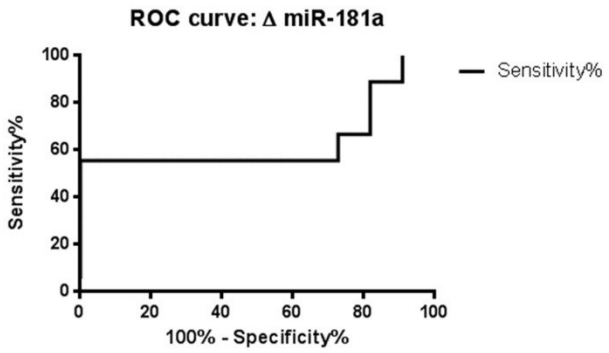


Figure 6-2 ROC curve analysis for change in circulating miR-181a of >1.7-fold following cardiothoracic surgery.

6.4.2.2 MiR-1

MiR-1 was significantly elevated at D1 compared to baseline in both those who developed muscle wasting (median 4.03-fold [IQR 1.65-7.84] higher) and those who did not (median 5.14-fold [IQR 1.31 -14.0] higher). The fold-change increase in plasma miR-1 was not statistically different between the two groups and MiR-1 returned to baseline by D2 in both groups (Figure 6-1).

[1] In this case a Kolmogorov-Smirnov test was used as the distribution of the data in the two groups was significantly different making a Mann Whitney test less reliable.

[2] Of note – in this case the positive predictive value and specificity AND the negative predictive value and sensitivity are the same numerically because the number of true positives and true negatives are numerically the same – calculated using www.medcalc.org.

6.4.2.3 MiR-16

MiR-16 was significantly reduced at D1 compared to baseline in both groups (wasting patients 0.71-fold [IQR 0.21-0.92], non-wasting 0.41 [IQR 0.31-0.87]). However, once again the fold-change reduction was not different between the groups and the levels returned to baseline in both groups (Figure 6-1).

6.5 Discussion

6.5.1 Summary of the findings

The current study shows that changes in the circulating microRNA profile occur following high-risk cardiac surgery in both patients who subsequently develop muscle wasting and those who do not. Furthermore, a 1.7-fold increase in miR-181a at D2 was 91% specific for a subsequent reduction in $RF_{CSA;}$ however, its sensitivity and negative predictive value was less striking. Obviously, as with all biomarkers, these results should be reproduced in a validation cohort. Ideally the validation cohort would be a larger cohort of patients from a wider clinical spectrum in order to truly test the hypothesis.

6.5.2 Clinical perspective

These data suggest that a rise in miR-181a early in ICU admission has a high specificity for muscle wasting at 1 week. Despite the low area under the ROC curve (0.6) of the rise in miR-181a (Figure 6-2), the high positive predictive value of this test (91%) would potentially allow it to be used to identify at-risk patients. However, due to the relatively low negative predictive value (56%), not all patients at risk of muscle wasting would be identified, so this test could not be used to exclude the development of acute muscle wasting.

The low sensitivity might be explained in a number of ways. Firstly it is accepted that the pathogenesis of ICUAP is multi-factorial and, therefore, if miR-181a does in fact have a

mechanistic role then it may be that this marker will only capture those individuals in whom this particular mechanism is the main underlying factor. Secondly, this study only measured microRNAs in the circulation on the first 2 days following surgery and it may be that this time point did not capture all individuals in whom muscle wasting would develop; it is possible that patients with wasting at D7 but only a small fold-change in miR-181a at D2 would have had a greater rise had measurements been taken over a more detailed time-course. Lastly, circulating microRNA levels depend on export of the microRNA from cells so other factors increasing cell permeability to this microRNA could contribute to the presence of miR-181a in the plasma, including potentially release of microRNA into the circulation following cell death.

As a clinical biomarker of acute muscle wasting, miR-181a would be more useful if an absolute cut-off value rather than fold-change from baseline could be applied. As, other than elective surgical patients, patients rarely present to critical care prior to becoming unwell and therefore their baseline miR-181a level would be unknown. It may be that defining baseline normal ranges would be easier in a larger cohort of patients and differences between groups in the raw values of microRNA levels in the circulation would be easier to detect. However, the data from the current study demonstrated the wide range of microRNA concentrations at baseline with raw values varying more than 100-fold between individuals. This is in line with most studies in the literature where fold-change differences in relatively small numbers of participants are also described (412). Also, it may be that as our understanding of microRNA regulation in the circulation improves, normalisation of these values, for example to body mass or circulating lipid levels, may become relevant and may allow a normal range be described.

Currently there is no effective therapy for muscle atrophy beyond ensuring adequate nutrition and facilitating early exercise and mobilisation. However, there is increasing interest in preventing muscle loss, for example, by the application of external neuromuscular electrical stimulation (discussed in chapter 5) or with early rehabilitation. Similarly, new generation

anabolic agents are presently being evaluated in animals, for example, those targeting the myostatin signalling pathway (418, 419). In developing experimental medicine studies which bring novel medicines to patients, it will be useful to stratify patients by the likelihood of developing subsequent muscle loss and circulating miR-181a could be useful for this purpose by reducing the number of participants needed for a proof of concept study.

The biological role of miR-181a is not fully understood. It is expressed in many different tissues and is not muscle-specific. However, in muscle miR-181a is essential for regeneration and differentiation after tissue injury (292) and in other tissues has been shown to be involved in the regulation of inflammatory pathways (420, 421). Both of these pathways may be relevant in the response of muscle to critical illness (109). However, miR-181b is *reduced* in blood from patients on ICU with sepsis (422). Sepsis is certainly a major aetiological factor in the development of critical illness-related acute muscle wasting (109), but the patients in the current study were not septic. MiR-181 a and b are from the same family of microRNAs. Two separate genes hold the sequences for miRs- 181a and b together and as such they are almost certainly co-transcribed. However potential differences in their function are not fully understood (292), but miR-181a is the major member of the miR-181 family that has been shown to be functional in human muscle (292).

6.5.3 Critique of the method

In order to provide a fair evaluation of a new test it is important to avoid the scenario where there is a high pre-test probability of the condition one is testing for (in this case quadriceps loss judged by RF_{CSA}). The current disease model studied patients with brief ICU stays and an uncomplicated post-operative course. Nevertheless, approximately 50% of patients developed muscle wasting by the seventh postoperative day, suggesting that the model is suitable for evaluating the test. While this model of acute muscle wasting following cardiac surgery made it possible to control for many of the other factors that occur in the

critically ill, and thus investigate a disease marker which is specific to muscle wasting, it remains to be seen whether these results are "generalisable" to a wider ICU population. It is also important to note that the observed muscle wasting could be classified as "sub-clinical". No patients developed weakness consistent with a diagnosis of ICUAP; in fact, almost all had an MRC-SS of 60 at day 7. Therefore, it is possible that larger changes in circulating microRNAs may have been seen in a sicker group of patients developing true ICUAP, which might have made between group differences easier to detect.

MiR-16 was measured in this study as a control microRNA. It is widely expressed and in plasma has previously been used to demonstrate that findings in other, more specific microRNAs do not result from general changes in microRNA levels (327, 417). However miR-16 has recently been shown to be elevated in the plasma of septic patients and is increasingly implicated in disease processes (423). Importantly, significant haemolysis of blood samples also increased circulating miR-16 (424). However the data from the current study show a reduction in miR-16 in both groups of patients. These patients were not septic, but all did experience an inflammatory insult as evidenced by a significant rise in CRP in both groups peaking at day 2. Differences between inflammation secondary to infection (sepsis) and inflammation without infection are increasingly being recognised (423) and the current data support this. In the current study, miR-16 levels in plasma changed significantly, implying that it is not an appropriate "reference" microRNA in these circumstances. Both groups showed an acute increase in miR-1 at D1 recovering to baseline on D2 after surgery; this may have been because, as well as being highly expressed in skeletal muscle (which will have been damaged by the surgical incisions), miR-1 is also expressed in cardiac muscle and all patients underwent cardiac surgery (413). However miR-499 is also present in cardiac muscle and might therefore also be expected to increase in the same way. Plasma miR-1 was elevated acutely following myocardial damage in acute coronary syndromes in several different clinical studies (413) and was predictive of outcome (425).

A potential problem of this study is that some patients received fresh frozen plasma (FFP) in their peri-operative course (11/23 wasting patients and 8/19 non-wasting on the day of surgery or the first post-operative day). The quantified microRNAs have all been measured in plasma over this time period and it is difficult to know how the donor plasma may have affected the results. FFP is known to be hyperglycaemic and hyperosmotic (426) but, because microRNA are a relatively new field of interest, it is not known if they might concentrate in FFP or if they are removed during processing and storage. The maximum volume received was 1L in a 24 hour period which conceivably could dilute the patient's own plasma. Clinically, it is standard practice to measure factors in a patient's blood (e.g., creatinine or sodium) without considering the diluting volume, or donor content, of any transfusion therapy (except of course its therapeutic content) and one could argue that, even if these factors were coming from the donor, the patient's exposure to those factors is still relevant. Additionally, one would expect donor levels to be "normal" and therefore dilute any changes detected. Importantly, however, equal numbers of patients in both groups received FFP (chi-squared $p=0.14$).

Lastly, although these microRNAs were chosen because of their roles in muscle homeostasis it is not known how the observed changes in plasma level of these microRNAs reflect the relative expression or function of these microRNAs in the patients' muscle and caution is therefore required in drawing mechanistic interpretations. MicroRNAs circulate in the blood in exosomes or bound to protein and HDL. The regulation, specificity and secretion of microRNA into the circulation is not fully understood (413). In COPD, specific microRNAs have opposite changes in muscle and plasma; for example, miR-1 was reduced in the muscle of patients with COPD and reflected muscle wasting whereas it was increased in plasma of the same patients(302, 417). If this were true of the patients in the current study (i.e. the rise in miRs-1 and 181a in the plasma reflected a fall in the microRNA level in the muscle) it would be consistent with the findings in ICUAP muscle discussed in Chapter 4.

6.6 Conclusion

In conclusion, this study evaluated the potential role of selected microRNAs for the prediction of subsequent muscle loss in patients undergoing high-risk cardiac surgery. It demonstrated that elevation of miR-181a is a highly specific marker of quadriceps wasting in these patients. However, as with all biomarkers, before miR-181a can be accepted as a potential biomarker of acute muscle wasting, it needs to be tested in a larger validation cohort including a wider range of ICU patients.

Chapter 7 General Discussion

7.1 Summary of main findings

The principle aim of the work in this thesis was to investigate the molecular mechanisms of ICUAP with a view to identifying potential therapeutic targets. GDF-15 was identified as a candidate to investigate and results from studies in two clinical models of muscle wasting in the critically ill have demonstrated that GDF-15 may at least in part drive the pathology of ICUAP. Firstly, in a novel human model of muscle wasting in the critical care setting, GDF-15 was elevated in the plasma of patients following cardio-thoracic surgery. This elevation was sustained at one week in those who developed muscle wasting, but returned to baseline in those who did not (Figure 3-4). These results were in contrast to the pattern of change in myostatin concentration, which unexpectedly fell acutely and returned to baseline in all patients (Figure 3-2). IGF-1 also fell, however in those who developed muscle wasting, IGF-1 plasma concentration did not return to baseline, but did in those who did not lose muscle bulk (Figure 3-3). Together these data suggest a dynamic imbalance in the circulating drivers of muscle homeostasis favouring muscle atrophy in those who develop muscle wasting acutely in the critical care setting. Furthermore these data support the current understanding in that GDF-15 is elevated by critical illness (279, 363) and support the hypothesis that GDF-15 may be important in the pathology of ICUAP.

In the second clinical model, plasma GDF-15 and muscle GDF-15 mRNA were elevated in patients with established ICUAP when compared to controls (Figure 4-6). This observation again supports the hypothesis that GDF-15 may be important in the pathogenesis of ICUAP. Furthermore, plasma GDF-15 correlated significantly with the patient's SOFA score, consistent with the suggestion that GDF-15 elevation is driven by critical illness. *In vitro* investigations confirmed that GDF-15 treatment could drive an increase in muscle atrophy related genes

atrogin and MuRF-1 in cultured myotubes (Figure 4-13)); significantly higher atrogin mRNA was also found in the muscle of patients with ICUAP compared to controls (Figure 4-7).

The mechanism of action of GDF-15 is not yet understood, and activation of the SMAD dependant luciferase assay (which was expected as GDF-15 is a member of the TGF-β family (427)) was not demonstrated. Muscle microRNAs are essential for muscle homeostasis and regulate many essential molecular pathways (288), dysregulation of microRNAs results in disordered growth and differentiation of muscle tissue and it was hypothesised that muscle microRNAs in patients with ICUAP would be different from controls. Significantly lower muscle microRNAs, miRs-1, -133a, -181a and -499, were found in the muscle of patients with ICUAP compared to controls (Figure 4-9). Levels of these muscle microRNAs significantly negatively correlated with both plasma GDF-15 concentration and muscle GDF-15 mRNA expression. These data suggested that GDF-15 might drive the suppression of essential microRNAs that was demonstrated in the muscle of ICUAP patients and consistent with this suggestion GDF-15 treatment of cultured myotubes *in vitro* resulted in a reduction in miRs 1, 133a and 181a (but not miR-499, which is already at a very low level in these cells and therefore further reduction may be difficult to produce) (Figure 4-13).

One action of the muscle microRNAs analysed that is thought to be important in their role as regulators/ coordinators of pathways of homeostasis is protection against TGF-β signalling (343). By targeting and down-regulating components of the TGF-β signalling pathway, a number of microRNAs have been shown to reduce the response of some cell lines to TGF-β (290, 343-346). Consistent with this mechanism, transfection of miR-181a into myoblasts significantly reduced TGF-β activation of the SMAD-dependant luciferase reporter (Figure 4-15). *In vivo,* a *suppression* of muscle microRNAs would potentially lead to *increased* sensitivity to TGF-β signalling, thus potentially augmenting, for example, myostatin driven muscle atrophy. Therefore it was hypothesised that one mechanism by which GDF-15 may drive muscle atrophy in ICUAP could be by increasing sensitivity to TGF-β signalling, via

suppression of muscle microRNAs. Supporting this hypothesis, higher CYR-61 mRNA expression and higher nuclear SMAD positivity was demonstrated in the muscle of patients with ICUAP compared to controls (Figure 4-11). However, attempts to demonstrate elevation of TGF-β receptor proteins types 1 and 2 concentration (potential targets of these muscle microRNAs) both in response to GDF-15 treatment *in vitro* and in ICUAP muscle were unsuccessful. Figure 7-1 summaries the mechanism of action of GDF-15 in ICUAP proposed as a consequence of the work in this thesis.

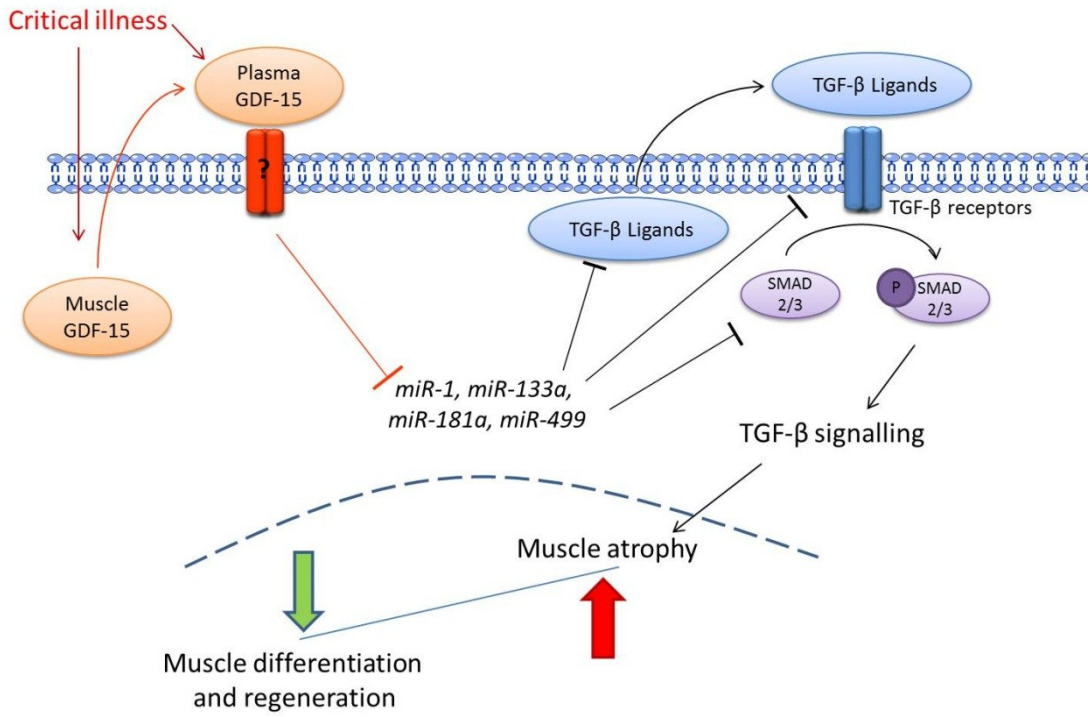


Figure 7-1 Schematic representation of the possible role of Growth and Differentiation Factor-15 (GDF-15) in the development of intensive care unit acquired paresis.

In normal muscle homeostasis muscle microRNAs (miRs 1, 133a, 181a and 499) target and down-regulate elements of the TGF-β signalling pathway. However driven by critical illness GDF-15 supresses muscle microRNAs and may result in a relative increase in elements of the TGF-β signalling pathway and increased sensitivity to TGF-β ligands. This could result in increased TGF-β signalling and TGF-β driven muscle atrophy.

Unfortunately, it is difficult to draw conclusions from the interventional study of NMES in ICU patients that was carried out as part of this thesis. As discussed in Chapter 5, this study was significantly underpowered and the results are therefore difficult to interpret and should

be taken in light of this limitation. The study demonstrated an increase in muscle expression of myostatin and GDF-15 mRNA in NMES treated legs compared to their own baseline, but no change in control legs (Figure 5-7). Although it is believed that NMES will have beneficial effects in terms of preservation of muscle function in the ICU setting (96) it is also recognised to have potential to cause muscle damage. In the setting of sedated patients who cannot report pain or those in whom the nutritional and metabolic status of the muscle may be expected to be poor, researchers should be aware that NMES *may* promote muscle breakdown.

Finally, a rise in circulating miR-181a at day 2 post cardiothoracic surgery represented a potential biomarker of acute muscle wasting (Figure 6-1). However these data need to be reproduced in a larger validation cohort of patients.

7.2 General limitations

Although the results of this work support the hypothesis that GDF-15 is important in the pathogenesis of ICUAP and provide evidence to suggest a potential mechanism, it is important to note that neither the *in vitro* work nor the clinical study can be interpreted as a definitive proof. The critique of the methods used has been discussed in each chapter, but general limitations of this work should be highlighted here to balance the above summary of findings. Firstly, the clinical studies (and in particular the interventional study) are limited by the relatively small number of participants. Furthermore, these studies were carried out in a specialist cardiothoracic ICU, and although this has the advantage of reducing patient heterogeneity, it may mean that the results do not represent a mechanism that is relevant to a wider, more general, ICU population.

The results of *in vitro* studies do not always represent what is seen when the hypothesis is tested in the clinical setting; this is a recognised limitation of translational

experiments. Although the *in vitro* results from this thesis have generally supported the hypotheses generated from the clinical/ *in vivo* data, there are some important limitations. Particularly, that although it is not possible to directly compare the use of recombinant GDF-15 protein in the *in vitro* environment with the true molecular environment within muscle cells or tissue, the dose of GDF-15 (50mg/dl) used in the cell culture experiments is significantly higher than the range seen in human plasma. As discussed in Chapter 4 attempts to demonstrate the effect of GDF-15 on protein targets (TGFBR1 and 2) were unsuccessful. This may be due to experimental design (time course etc…) and/or the fact that there are many potentially relevant targets within the TGF-β signalling system and an overall effect on the pathway may be responsible for the increased sensitivity rather than any particular single protein. Alternatively, of course the hypothesis may also be incorrect. *In vitro* GDF-15 treatment did not increase CYR-61 mRNA expression; this could be interpreted as not supporting the hypothesis that GDF-15 drives an increase in sensitivity to TGF-β signalling. In addition cyclic mechanical stretch of differentiating myoblasts caused a reduction in SMAD signalling, whereas (albeit in a significantly underpowered study) increased activity via NMES on ICU resulted in a possible increase in the expression of drivers of muscle atrophy. These inconsistencies further demonstrate the limitation of the *in vitro* experiments. The *in vitro* environment used in cell culture was designed to stimulate cell growth and differentiation (as is standard). It therefore contained a number of growth factors and similar regulators at concentrations that cells are not normally exposed to *in vivo* (e.g. Platelet derived growth factor). This did not reflect a stressed system reflective of critical illness. The concentration of TGF-β ligands in the cell culture media is not known and, if low, may not have been adequate to stimulate any TGF-β signalling. Finally the differentiation state of the myotubes is also very different from that of the developed myofibre in a mature muscle and therefore may also contribute to any differences in the response of the two systems. The response of muscle

tissue to stimuli (GDF-15 or stretch/ activity) in different molecular environments is likely to be different.

7.3 Future directions.

In order to define the mechanism of action of GDF-15-driven muscle atrophy and truly support our hypothesis, future *in vitro* experiments should aim to determine each step in the molecular pathway. For example, if GDF-15 drives myotube atrophy (as demonstrated by Dr Jen Lee in our group (333)) via suppression of muscle microRNAs, can this effect be blocked or even reversed by the transfection of exogenous microRNAs? In addition, future *in vitro* work should include attempts to identify the GDF-15 receptor(s) and the pathways involved in the regulation of microRNAs. Furthermore, in order to begin to address the problem of reflecting the physiological environment of muscle cells during the development of ICUAP, future experiments could combine GDF-15 treatment with the addition of inflammatory mediators and TGF-β ligands. Alternatively, a further potential *in vitro* experiment could include the exposure of cultured myotubes to plasma from ICUAP patients with and without the addition of neutralising GDF-15 antibodies and those to other components of the TGF-β signalling pathway; this could potentially examine the relationship between circulating factors and their effect on, for example, microRNA expression within the cells. However these experiments are difficult to adequately control as they rely on the use of mixed pools of plasma from several subjects and thus are likely to have many unquantifiable confounders (187).

The definitive experiment to prove the role of GDF-15 in the pathogenesis of ICUAP would be a randomised controlled trial of a GDF-15 antagonist in patients at risk of developing ICUAP. A first step towards such a trial might be a trial of such an anti-GDF-15 treatment in an animal model of ICUAP. Although a perfect animal model of ICUAP does not exist, various models have been used that combine critical illness with prolonged immobility and ventilation (for example (106, 113)) and might be suitable. GDF-15 blockade would demonstrate if GDF-15

is truly important in the aetiology of ICUAP and enable further examination of the potential pathways involved.

Future therapeutic options which should be explored include antibodies against GDF-15 and microRNA mimics; these options are discussed below.

7.4 Implications for the treatment of ICUAP

ICUAP is a potentially devastating consequence of critical illness for which there is currently no pharmacological treatment and management relies only on limitation of the physiological insult and active rehabilitation (74). The aim of this thesis was to better understand the molecular mechanisms of this disease as this is the key to identifying potential therapeutic targets and improving outcomes in the long run. Within the limitations discussed throughout, this work has been able to identify and mechanistically justify both GDF-15 and microRNAs as potential therapeutic targets. Many molecular pathways are described in disease. However it is rare to be able to identify a potential target and realistically envisage the method/ treatment with which to manipulate it. These targets may have significant implications in the future for the treatment of ICUAP and both anti-GDF-15 antibodies and means of delivering microRNA mimics already exist.

To date, anti-GDF-15 antibodies have not been trialled in humans. However when given to mice GDF-15 anti-bodies can reverse cachexia induced by GDF-15 expressing tumours (267) and at least one human anti-GDF-15 antibody is underdevelopment. AV-380, developed by AVEO oncology, is a new human anti-GDF-15 antibody (www.aveooncology.com). This company has developed the drug with a view to treatment of cancer-related cachexia, a condition in which plasma GDF-15 is significantly elevated and which is associated with poor prognosis (267, 280, 428). Pre-clinical results in mice have suggested that GDF-15 drives cancer-related cachexia (280, 429) and that treatment with AV-380 can reverse weight loss

and muscle weakness, restoring normal body composition (data presented at the 2nd Cachexia Conference, Montreal September 2014 by AVEO oncology). AVEO oncology plan to start first-in-man studies in the second half of 2015.

MicroRNA research is a rapidly expanding and developing field. As the understanding of the role of microRNA in the pathogenesis of disease increases so does the interest in their therapeutic potential. Manipulation of microRNA levels *in vivo* may involve the suppression of an overactive/over-expressed microRNA or the delivery and replacement of a suppressed microRNA. An antagomir is the complementary sequence of nucleotides to the target microRNA and functions by binding and inactivating the target microRNA (430). In addition, over-expression (by transfection into cells) of non-functional genes with multiple binding sites for the target microRNA, known as "miR sponges" also act to suppress microRNA activity (431). MicroRNA mimics are double-stranded nucleotides, one strand of which represents the mature target microRNA. The double-stranded nucleotide is processed in the same way as an endogenous hairpin pre-microRNA and thus results in increased concentration of the target microRNA (430, 431). It is important to note that the complementary strand of the miR-sequence may also be functional and may have divergent effects from the target microRNA. MicroRNAs may also be replaced using adenoviral vectors over-expressing the target microRNA (430).

Much of the work so far has been in the field of oncology and the manipulation of both oncogenes and tumour suppressor genes using various microRNA targets shows potential for the future treatment of cancer (430-432). For example, Let-7 and miR-34 are both tumour suppressor genes which are down regulated in lung cancer (432). MicroRNA mimics for both have been successfully shown to slow tumour growth and progression in murine models (433-435). MRX34, a miR-34 mimic, is the first microRNA mimic based drug to reach human trials (Mirna Theraputics, www.mirnarx.com). miR-34 down-regulation is found in several cancers

including, lung, liver, haematological malignancy and cervical cancer (432). An ongoing phase 1 trial in liver and haematological cancer is due to report in 2015. A further example of early human studies of microRNA therapy is Miravirsen (Santaris Pharma, www.santaris.com), an antagomir to miR-122 which has recently completed phase 2 clinical trials for the treatment of Hepatitis C infection (436). The HCV virus uses host miR-122 to enable viral replication and therefore, by targeting liver-specific miR-122 Miravirsen inhibits viral replication. Thus far no adverse effects have been reported, making microRNA-targeted therapy a viable potential therapy for the future (436).

The potential of microRNA therapy is limited by the complexity of the microRNA network and the potential for unwanted side effects due to the multiple targets of any individual microRNA. Therefore, the *in vivo* method of delivery should be carefully developed to address this. To date, several methods of microRNA mimic or antagomir delivery have been trialled, as alone the oligonucleotides are rapidly degraded and cleared and have poor tissue specificity or uptake (430). Mimics may be combined with liposome nanoparticles (437), polyethyleneimine (438) or atelocollagen (439) and these may be injected intravenously or directly into the specific tissue (for example, work to date has involved intra-tumour injection). SMARTPARTICLES® (Marina Biotech, www.marinabio.com) for example are the liposome particles used to deliver MRX34. However, these particles may be immunogenic, poorly tissue-specific and can be cytotoxic (430-432). Adenoviruses can be manipulated to have tissue-specific promoters (thus improving tissue specificity), they can be delivered intra-nasally or systemically and their use was effective in the delivery of miR-26a for the treatment of hepatocellular carcinoma in a mouse model (440) and miR-196a in the treatment of spinal and bulbar muscular atrophy (441). Importantly, adenoviral vectors have been used for some time to deliver other genetic therapies and generally are well tolerated and have a good safety profile; however they are expensive and difficult to construct (430, 431). Delivery and function of antagomirs may be enhanced by cholesterol conjugation, modification of the phosphate

backbone and/or the use of LNA (locked nucleic acids – which are chemically inaccessible RNAs) (430, 431). Mivirsen, for example, is composed of a combination of LNA and phosphate backbone modified DNA (436). Cellular uptake and distribution are poorly understood.

In muscle disease, sadly, trials of such treatments have not even reached the pre-clinical phases, but targeting muscle microRNA expression and activity has demonstrated that muscle metabolism and development can be manipulated *in vitro* and *in vivo.* For example over-expression of the muscle-specific microRNAs can reverse the negative effects seen by their knock down *in vitro*; over expression of miR-1 and 133a can protect against TNFα-induced impaired muscle differentiation *in vitro* (301); forced mir-499 over-expression in knockout mice models restore their type 1 fibres and they have better muscle endurance than wild type mice (291); and electroporation of miR-486 into the quadriceps of mice with chronic kidney disease prevented the development of muscle wasting associated with chronic disease (442).

Potentially, a combination of muscle microRNAs delivered systemically, but targeting muscle tissue, might protect against muscle damage and promote regeneration and recovery in critically unwell patients. Many muscle microRNAs are muscle specific (myomiRs) and therefore this approach may not be as limited by systemic side effects as other potential microRNA targeting therapies. However it should be remembered that just because the microRNA is not expressed in a tissue, targets of that microRNA may well be present and therefore systemic delivery of tissue-specific microRNAs may not be side effect free.

Despite the rapid recent advances in this field, we are still a long way away from the first pharmacological treatment for ICUAP, which therefore remains a potentially devastating complication of critical illness. However, the work from this thesis identifies both GDF-15 and microRNAs as potential targets that warrant further investigation in the future.

Chapter 8 References

1. Hermans G, Van Mechelen H, Clerckx B, Vanhullebusch T, Mesotten D, Wilmer A, Casaer MP, Meersseman P, Debaveye Y, Van Cromphaut S, Wouters PJ, Gosselink R, Van den Berghe G. Acute outcomes and 1-year mortality of ICU-acquired weakness: A cohort study and propensity matched analysis. *Am J Respir Crit Care Med* 2014.
2. Schweickert W, Hall J. ICU-acquired weakness. *Chest* 2007; 131: 1541-1549.
3. De Jonghe B, Sharshar T, Lefaucheur J, Authier F, Durand-Zaleski I, Boussarsar M, Cerf C, Renaud E, Mesrati F, Carlet J, Raphaël J, Outin H, Bastuji-Garin S. Paresis acquired in the intensive care unit: a prospective multicenter study. *JAMA* 2002; 288: 2859-2867.
4. Tennilä A, Salmi T, Pettilä V, Roine R, Varpula T, Takkunen O. Early signs of critical illness polyneuropathy in ICU patients with systemic inflammatory response syndrome or sepsis. *Intensive Care Med* 2000; 26: 1360-1363.
5. Fletcher S, Kennedy D, Ghosh I, Misra V, Kiff K, Coakley J, Hinds C. Persistent neuromuscular and neurophysiologic abnormalities in long-term survivors of prolonged critical illness. *Crit Care Med* 2003; 31: 1012-1016.
6. Guarneri B, Bertolini G, Latronico N. Long-term outcome in patients with critical illness myopathy or neuropathy: the Italian multicentre CRIMYNE study. *J Neurol Neurosurg Psychiatry* 2008; 79: 838-841.
7. Latronico N, Shehu I, Seghelini E. Neuromuscular sequelae of critical illness. *Curr Opin Crit Care* 2005; 11: 381-390.
8. Tan T, Brett SJ, Stokes T, Guideline Development G. Rehabilitation after critical illness: summary of NICE guidance. *Bmj* 2009; 338: b822.
9. Olsen CW. Lesions of peripheral nerves developing during coma. *JAMA* 1956; 160: 39-41.
10. MacFarlane IA, Rosenthal FD. Severe myopathy after status asthmaticus. *Lancet* 1977; 2: 615.
11. Bolton C, Gilbert J, Hahn A, Sibbald W. Polyneuropathy in critically ill patients. *J Neurol Neurosurg Psychiatry* 1984; 47: 1223-1231.
12. Latronico N, Fenzi F, Recupero D, Guarneri B, Tomelleri G, Tonin P, De Maria G, Antonini L, Rizzuto N, Candiani A. Critical illness myopathy and neuropathy. *Lancet* 1996; 347: 1579-1582.
13. Lacomis D, Zochodne D, Bird S. Critical illness myopathy. *Muscle Nerve* 2000; 23: 1785-1788.
14. Rich MM, Teener JWT, Raps EC, Schotland DL, Bird SJ. Muscle is electrically inexcitable in acute quadriplegic myopathy. *Neurology* 1996; 46: 731-736.
15. Stevens RD, Marshall SA, Cornblath DR, Hoke A, Needham DM, de Jonghe B, Ali NA, Sharshar T. A framework for diagnosing and classifying intensive care unit-acquired weakness. *Crit Care Med* 2009; 37: S299-308.
16. Bednarik J, Lukas Z, Vondracek P. Critical illness polyneuromyopathy: the electrophysiological components of a complex entity. *Intensive Care Med* 2003; 29: 1505-1514.
17. Khan J, Harrison T, Rich M. Mechanisms of neuromuscular dysfunction in critical illness. *Crit Care Clin* 2008; 24: 165-177, x.
18. De Jonghe B, Sharshar T, Hopkinson N, Outin H. Paresis following mechanical ventilation. *Curr Opin Crit Care* 2004; 10: 47-52.
19. Witt N, Zochodne D, Bolton C, Grand'Maison F, Wells G, Young G, Sibbald W. Peripheral nerve function in sepsis and multiple organ failure. *Chest* 1991; 99: 176-184.

20. De Jonghe B, Bastuji-Garin S, Durand M, Malissin I, Rodrigues P, Cerf C, Outin H, Sharshar T. Respiratory weakness is associated with limb weakness and delayed weaning in critical illness. *Crit Care Med* 2007; 35: 2007-2015.
21. Bolton C. The discovery of critical illness polyneuropathy. *Eur J Anaesthesiol Suppl* 2008; 42: 66-67.
22. Hermans G, De Jonghe B, Bruyninckx F, Van den Berghe G. Clinical review: Critical illness polyneuropathy and myopathy. *Crit Care* 2008; 12: 238.
23. Kress JP, Hall JB. ICU-acquired weakness and recovery from critical illness. *N Engl J Med* 2014; 370: 1626-1635.
24. Vanpee G, Hermans G, Segers J, Gosselink R. Assessment of limb muscle strength in critically ill patients: a systematic review. *Crit Care Med* 2014; 42: 701-711.
25. Bohannon RW. Manual muscle testing: does it meet the standards of an adequate screening test? *Clinical rehabilitation* 2005; 19: 662-667.
26. Baldwin CE, Paratz JD, Bersten AD. Muscle strength assessment in critically ill patients with handheld dynamometry: an investigation of reliability, minimal detectable change, and time to peak force generation. *Journal of critical care* 2013; 28: 77-86.
27. Vanpee G, Segers J, Van Mechelen H, Wouters P, Van den Berghe G, Hermans G, Gosselink R. The interobserver agreement of handheld dynamometry for muscle strength assessment in critically ill patients. *Crit Care Med* 2011; 39: 1929-1934.
28. Ali N, O'Brien JJ, Hoffmann S, Phillips G, Garland A, Finley J, Almoosa K, Hejal R, Wolf K, Lemeshow S, Connors AJ, Marsh C. Acquired weakness, handgrip strength, and mortality in critically ill patients. *Am J Respir Crit Care Med* 2008; 178: 261-268.
29. Hermans G, Clerckx B, Vanhullebusch T, Segers J, Vanpee G, Robbeets C, Casaer MP, Wouters P, Gosselink R, Van Den Berghe G. Interobserver agreement of Medical Research Council sum-score and handgrip strength in the intensive care unit. *Muscle Nerve* 2012; 45: 18-25.
30. Ali NA, O'Brien JM, Jr., Hoffmann SP, Phillips G, Garland A, Finley JC, Almoosa K, Hejal R, Wolf KM, Lemeshow S, Connors AF, Jr., Marsh CB. Acquired weakness, handgrip strength, and mortality in critically ill patients. *Am J Respir Crit Care Med* 2008; 178: 261-268.
31. Bittner EA, Martyn JA, George E, Frontera WR, Eikermann M. Measurement of muscle strength in the intensive care unit. *Crit Care Med* 2009; 37: S321-330.
32. Waak K, Zaremba S, Eikermann M. Muscle strength measurement in the intensive care unit: not everything that can be counted counts. *Journal of critical care* 2013; 28: 96-98.
33. Lee JJ, Waak K, Grosse-Sundrup M, Xue F, Lee J, Chipman D, Ryan C, Bittner EA, Schmidt U, Eikermann M. Global muscle strength but not grip strength predicts mortality and length of stay in a general population in a surgical intensive care unit. *Physical therapy* 2012; 92: 1546-1555.
34. Harris ML, Luo YM, Watson AC, Rafferty GF, Polkey MI, Green M, Moxham J. Adductor pollicis twitch tension assessed by magnetic stimulation of the ulnar nerve. *Am J Respir Crit Care Med* 2000; 162: 240-245.
35. Lacomis D. Electrophysiology of neuromuscular disorders in critical illness. *Muscle Nerve* 2013; 47: 452-463.
36. de Letter M, Schmitz P, Visser L, Verheul F, Schellens R, Op de Coul D, van der Meché F. Risk factors for the development of polyneuropathy and myopathy in critically ill patients. *Crit Care Med* 2001; 29: 2281-2286.
37. Morris C, Trinder JT. Electrophysiology adds little to clinical signs in critical illness polyneuropathy and myopathy. *Crit Care Med* 2002; 30: 2612.
38. Dhand U. Clinical approach to the weak patient in the intensive care unit. *Respir Care* 2006; 51: 1024-1040; discussion 1040-1021.

39. Khan J, Harrison T, Rich M, Moss M. Early development of critical illness myopathy and neuropathy in patients with severe sepsis. *Neurology* 2006; 67: 1421-1425.
40. Puthucheary ZA, Rawal J, McPhail M, Connolly B, Ratnayake G, Chan P, Hopkinson NS, Padhke R, Dew T, Sidhu PS, Velloso C, Seymour J, Agley CC, Selby A, Limb M, Edwards LM, Smith K, Rowlerson A, Rennie MJ, Moxham J, Harridge SD, Hart N, Montgomery HE. Acute skeletal muscle wasting in critical illness. *JAMA* 2013; 310: 1591-1600.
41. Ahlbeck K, Fredriksson K, Rooyackers O, Måbäck G, Remahl S, Ansved T, Eriksson L, Radell P. Signs of critical illness polyneuropathy and myopathy can be seen early in the ICU course. *Acta Anaesthesiol Scand* 2009; 53: 717-723.
42. Seymour J, Ward K, Sidhu P, Puthucheary Z, Steier J, Jolley C, Rafferty G, Polkey M, Moxham J. Ultrasound measurement of rectus femoris cross-sectional area and the relationship with quadriceps strength in COPD. *Thorax* 2009; 64: 418-423.
43. Luo Y, Moxham J, Polkey M. Diaphragm electromyography using an oesophageal catheter: current concepts. *Clin Sci (Lond)* 2008; 115: 233-244.
44. Polkey MI, Duguet A, Luo Y, Hughes PD, Hart N, Hamnegard CH, Green M, Similowski T, Moxham J. Anterior magnetic phrenic nerve stimulation: laboratory and clinical evaluation. *Intensive Care Med* 2000; 26: 1065-1075.
45. Bednarík J, Vondracek P, Dusek L, Moravcova E, Cundrle I. Risk factors for critical illness polyneuromyopathy. *J Neurol* 2005; 252: 343-351.
46. Van den Berghe G, Schoonheydt K, Becx P, Bruyninckx F, Wouters P. Insulin therapy protects the central and peripheral nervous system of intensive care patients. *Neurology* 2005; 64: 1348-1353.
47. Leijten F, Harinck-de Weerd J, Poortvliet D, de Weerd A. The role of polyneuropathy in motor convalescence after prolonged mechanical ventilation. *JAMA* 1995; 274: 1221-1225.
48. Stevens R, Dowdy D, Michaels R, Mendez-Tellez P, Pronovost P, Needham D. Neuromuscular dysfunction acquired in critical illness: a systematic review. *Intensive Care Med* 2007; 33: 1876-1891.
49. Hospital Episode Statistics Analysis. Adult Critical Care in England April 2012 to March 2013. 2014.
50. Subbe C, Criner G, Baudouin S. Weaning units: lessons from North America? *Anaesthesia* 2007; 62: 374-380.
51. Hermans G, Wilmer A, Meersseman W, Milants I, Wouters P, Bobbaers H, Bruyninckx F, Van den Berghe G. Impact of intensive insulin therapy on neuromuscular complications and ventilator dependency in the medical intensive care unit. *Am J Respir Crit Care Med* 2007; 175: 480-489.
52. Leijten F, De Weerd A, Poortvliet D, De Ridder V, Ulrich C, Harink-De Weerd J. Critical illness polyneuropathy in multiple organ dysfunction syndrome and weaning from the ventilator. *Intensive Care Med* 1996; 22: 856-861.
53. Garnacho-Montero J, Madrazo-Osuna J, García-Garmendia J, Ortiz-Leyba C, Jiménez-Jiménez F, Barrero-Almodóvar A, Garnacho-Montero M, Moyano-Del-Estad M. Critical illness polyneuropathy: risk factors and clinical consequences. A cohort study in septic patients. *Intensive Care Med* 2001; 27: 1288-1296.
54. Nanas S, Kritikos K, Angelopoulos E, Siafaka A, Tsikriki S, Poriazi M, Kanaloupiti D, Kontogeorgi M, Pratikaki M, Zervakis D, Routsi C, Roussos C. Predisposing factors for critical illness polyneuromyopathy in a multidisciplinary intensive care unit. *Acta neurologica Scandinavica* 2008; 118: 175-181.
55. Herridge MS, Cheung AM, Tansey CM, Matte-Martyn A, Diaz-Granados N, Al-Saidi F, Cooper AB, Guest CB, Mazer CD, Mehta S, Stewart TE, Barr A, Cook D, Slutsky AS, Canadian Critical Care Trials G. One-year outcomes in survivors of the acute respiratory distress syndrome. *N Engl J Med* 2003; 348: 683-693.

56. Hough CL, Steinberg KP, Taylor Thompson B, Rubenfeld GD, Hudson LD. Intensive care unit-acquired neuromyopathy and corticosteroids in survivors of persistent ARDS. *Intensive Care Med* 2009; 35: 63-68.
57. Hermans G, De Jonghe B, Bruyninckx F, Van den Berghe G. Interventions for preventing critical illness polyneuropathy and critical illness myopathy. *Cochrane Database Syst Rev* 2009: CD006832.
58. Steinberg K, Hudson L, Goodman R, Hough C, Lanken P, Hyzy R, Thompson B, Ancukiewicz M. Efficacy and safety of corticosteroids for persistent acute respiratory distress syndrome. *N Engl J Med* 2006; 354: 1671-1684.
59. Fan E, Zanni J, Dennison C, Lepre S, Needham D. Critical illness neuromyopathy and muscle weakness in patients in the intensive care unit. *AACN Adv Crit Care*; 20: 243-253.
60. Puthucheary Z, Rawal J, Ratnayake G, Harridge S, Montgomery H, Hart N. Neuromuscular blockade and skeletal muscle weakness in critically ill patients: time to rethink the evidence? *Am J Respir Crit Care Med* 2012; 185: 911-917.
61. Garnacho-Montero J, Amaya-Villar R, García-Garmendía J, Madrazo-Osuna J, Ortiz-Leyba C. Effect of critical illness polyneuropathy on the withdrawal from mechanical ventilation and the length of stay in septic patients. *Crit Care Med* 2005; 33: 349-354.
62. Papazian L, Forel JM, Gacouin A, Penot-Ragon C, Perrin G, Loundou A, Jaber S, Arnal JM, Perez D, Seghboyan JM, Constantin JM, Courant P, Lefrant JY, Guerin C, Prat G, Morange S, Roch A, Investigators AS. Neuromuscular blockers in early acute respiratory distress syndrome. *N Engl J Med* 2010; 363: 1107-1116.
63. Berg H, Larsson L, Tesch P. Lower limb skeletal muscle function after 6 wk of bed rest. *J Appl Physiol* 1997; 82: 182-188.
64. Truong AD, Fan E, Brower RG, Needham DM. Bench-to-bedside review: mobilizing patients in the intensive care unit--from pathophysiology to clinical trials. *Crit Care* 2009; 13: 216.
65. Eikermann M, Koch G, Gerwig M, Ochterbeck C, Beiderlinden M, Koeppen S, Neuhäuser M, Peters J. Muscle force and fatigue in patients with sepsis and multiorgan failure. *Intensive Care Med* 2006; 32: 251-259.
66. Fink H, Helming M, Unterbuchner C, Lenz A, Neff F, Martyn J, Blobner M. Systemic inflammatory response syndrome increases immobility-induced neuromuscular weakness. *Crit Care Med* 2008; 36: 910-916.
67. De Jonghe B, Bastuji-Garin S, Sharshar T, Outin H, Brochard L. Does ICU-acquired paresis lengthen weaning from mechanical ventilation? *Intensive Care Med* 2004; 30: 1117-1121.
68. Swallow EB, Reyes D, Hopkinson NS, Man WD, Porcher R, Cetti EJ, Moore AJ, Moxham J, Polkey MI. Quadriceps strength predicts mortality in patients with moderate to severe chronic obstructive pulmonary disease. *Thorax* 2007; 62: 115-120.
69. Herridge MS, Tansey CM, Matte A, Tomlinson G, Diaz-Granados N, Cooper A, Guest CB, Mazer CD, Mehta S, Stewart TE, Kudlow P, Cook D, Slutsky AS, Cheung AM, Canadian Critical Care Trials G. Functional disability 5 years after acute respiratory distress syndrome. *N Engl J Med* 2011; 364: 1293-1304.
70. Koch S, Spuler S, Deja M, Bierbrauer J, Dimroth A, Behse F, Spies CD, Wernecke KD, Weber-Carstens S. Critical illness myopathy is frequent: accompanying neuropathy protracts ICU discharge. *J Neurol Neurosurg Psychiatry* 2011; 82: 287-293.
71. de Sèze M, Petit H, Wiart L, Cardinaud J, Gaujard E, Joseph P, Mazaux J, Barat M. Critical illness polyneuropathy. A 2-year follow-up study in 19 severe cases. *Eur Neurol* 2000; 43: 61-69.
72. Barnato AE, Albert SM, Angus DC, Lave JR, Degenholtz HB. Disability among elderly survivors of mechanical ventilation. *Am J Respir Crit Care Med* 2011; 183: 1037-1042.

73. Unroe M, Kahn JM, Carson SS, Govert JA, Martinu T, Sathy SJ, Clay AS, Chia J, Gray A, Tulsky JA, Cox CE. One-year trajectories of care and resource utilization for recipients of prolonged mechanical ventilation: a cohort study. *Annals of internal medicine* 2010; 153: 167-175.
74. Batt J, dos Santos CC, Cameron JI, Herridge MS. Intensive care unit-acquired weakness: clinical phenotypes and molecular mechanisms. *Am J Respir Crit Care Med* 2013; 187: 238-246.
75. Annane D, Bellissant E, Bollaert P, Briegel J, Keh D, Kupfer Y. Corticosteroids for treating severe sepsis and septic shock. *Cochrane Database Syst Rev* 2004: CD002243.
76. Peter J JP, Graham P, Moran J, Adraham A, Bersten G, Bersten A. Corticosteroids in the prevention and treatment of ARDS in adults: a metanalysis. 2008; 336:1006-1009.
77. Hsu CW. Glycemic control in critically ill patients. *World journal of critical care medicine* 2012; 1: 31-39.
78. van den Berghe G, Wouters P, Weekers F, Verwaest C, Bruyninckx F, Schetz M, Vlasselaers D, Ferdinande P, Lauwers P, Bouillon R. Intensive insulin therapy in critically ill patients. *N Engl J Med* 2001; 345: 1359-1367.
79. Van den Berghe G, Wilmer A, Hermans G, Meersseman W, Wouters PJ, Milants I, Van Wijngaerden E, Bobbaers H, Bouillon R. Intensive insulin therapy in the medical ICU. *N Engl J Med* 2006; 354: 449-461.
80. Hermans G, De Jonghe B, Bruyninckx F, Van den Berghe G. Interventions for preventing critical illness polyneuropathy and critical illness myopathy. *Cochrane Database Syst Rev* 2014; 1: CD006832.
81. Van den Berghe G, Wilmer A, Milants I, Wouters P, Bouckaert B, Bruyninckx F, Bouillon R, Schetz M. Intensive insulin therapy in mixed medical/surgical intensive care units: benefit versus harm. *Diabetes* 2006; 55: 3151-3159.
82. Finney SJ, Zekveld C, Elia A, Evans TW. Glucose control and mortality in critically ill patients. *JAMA* 2003; 290: 2041-2047.
83. Finfer S, Chittock D, Su S, Blair D, Foster D, Dhingra V, Bellomo R, Cook D, Dodek P, Henderson W, Hébert P, Heritier S, Heyland D, McArthur C, McDonald E, Mitchell I, Myburgh J, Norton R, Potter J, Robinson B, Ronco J. Intensive versus conventional glucose control in critically ill patients. *N Engl J Med* 2009; 360: 1283-1297.
84. Krinsley JS, Grover A. Severe hypoglycemia in critically ill patients: risk factors and outcomes. *Crit Care Med* 2007; 35: 2262-2267.
85. Egi M, Bellomo R, Stachowski E, French CJ, Hart GK, Taori G, Hegarty C, Bailey M. Hypoglycemia and outcome in critically ill patients. *Mayo Clinic proceedings* 2010; 85: 217-224.
86. Van den Berghe G, Schetz M, Vlasselaers D, Hermans G, Wilmer A, Bouillon R, Mesotten D. Intensive insulin therapy in critically ill patients: NICE-SUGAR or Leuven blood glucose target? *J Clin Endocrinol Metab* 2009.
87. Morris PE, Goad A, Thompson C, Taylor K, Harry B, Passmore L, Ross A, Anderson L, Baker S, Sanchez M, Penley L, Howard A, Dixon L, Leach S, Small R, Hite RD, Haponik E. Early intensive care unit mobility therapy in the treatment of acute respiratory failure. *Crit Care Med* 2008; 36: 2238-2243.
88. Gosselink R, Bott J, Johnson M, Dean E, Nava S, Norrenberg M, Schonhofer B, Stiller K, van de Leur H, Vincent JL. Physiotherapy for adult patients with critical illness: recommendations of the European Respiratory Society and European Society of Intensive Care Medicine Task Force on Physiotherapy for Critically Ill Patients. *Intensive Care Med* 2008; 34: 1188-1199.
89. Lee CM, Fan E. ICU-acquired weakness: what is preventing its rehabilitation in critically ill patients? *BMC medicine* 2012; 10: 115.

90. Needham DM, Korupolu R, Zanni JM, Pradhan P, Colantuoni E, Palmer JB, Brower RG, Fan E. Early physical medicine and rehabilitation for patients with acute respiratory failure: a quality improvement project. *Archives of physical medicine and rehabilitation* 2010; 91: 536-542.
91. Bailey P, Thomsen GE, Spuhler VJ, Blair R, Jewkes J, Bezdjian L, Veale K, Rodriquez L, Hopkins RO. Early activity is feasible and safe in respiratory failure patients. *Crit Care Med* 2007; 35: 139-145.
92. Morris PE, Griffin L, Berry M, Thompson C, Hite RD, Winkelman C, Hopkins RO, Ross A, Dixon L, Leach S, Haponik E. Receiving early mobility during an intensive care unit admission is a predictor of improved outcomes in acute respiratory failure. *Am J Med Sci* 2011; 341: 373-377.
93. Stiller K. Physiotherapy in intensive care: an updated systematic review. *Chest* 2013; 144: 825-847.
94. Adler J, Malone D. Early mobilization in the intensive care unit: a systematic review. *Cardiopulmonary physical therapy journal* 2012; 23: 5-13.
95. Girard TD, Kress JP, Fuchs BD, Thomason JW, Schweickert WD, Pun BT, Taichman DB, Dunn JG, Pohlman AS, Kinniry PA, Jackson JC, Canonico AE, Light RW, Shintani AK, Thompson JL, Gordon SM, Hall JB, Dittus RS, Bernard GR, Ely EW. Efficacy and safety of a paired sedation and ventilator weaning protocol for mechanically ventilated patients in intensive care (Awakening and Breathing Controlled trial): a randomised controlled trial. *Lancet* 2008; 371: 126-134.
96. Maffiuletti NA, Roig M, Karatzanos E, Nanas S. Neuromuscular electrical stimulation for preventing skeletal-muscle weakness and wasting in critically ill patients: a systematic review. *BMC medicine* 2013; 11: 137.
97. Burtin C, Clerckx B, Robbeets C, Ferdinande P, Langer D, Troosters T, Hermans G, Decramer M, Gosselink R. Early exercise in critically ill patients enhances short-term functional recovery. *Crit Care Med* 2009; 37: 2499-2505.
98. Dos Santos CC, Batt J. ICU-acquired weakness: mechanisms of disability. *Curr Opin Crit Care* 2012; 18: 509-517.
99. Sander H, Golden M, Danon M. Quadriplegic areflexic ICU illness: selective thick filament loss and normal nerve histology. *Muscle Nerve* 2002; 26: 499-505.
100. Larsson L, Li X, Edstrom L, Eriksson LI, Zackrisson H, Argentini C, Schiaffino S. Acute quadriplegia and loss of muscle myosin in patients treated with nondepolarizing neuromuscular blocking agents and corticosteroids: mechanisms at the cellular and molecular levels. *Crit Care Med* 2000; 28: 34-45.
101. Sher JH, Shafiq SA, Schutta HS. ACUTE MYOPATHY WITH SELECTIVE LYSIS OF MYOSIN-FILAMENTS. *Neurology* 1979; 29: 100-106.
102. Friedrich O. Critical illness myopathy: sepsis-mediated failure of the peripheral nervous system. *Eur J Anaesthesiol Suppl* 2008; 42: 73-82.
103. Levine S, Nguyen T, Taylor N, Friscia M, Budak M, Rothenberg P, Zhu J, Sachdeva R, Sonnad S, Kaiser L, Rubinstein N, Powers S, Shrager J. Rapid disuse atrophy of diaphragm fibers in mechanically ventilated humans. *N Engl J Med* 2008; 358: 1327-1335.
104. Giger JM, Haddad F, Qin AX, Zeng M, Baldwin KM. Effect of unloading on type I myosin heavy chain gene regulation in rat soleus muscle. *J Appl Physiol* 2005; 98: 1185-1194.
105. Natanek SA, Gosker HR, Slot IG, Marsh GS, Hopkinson NS, Man WD, Tal-Singer R, Moxham J, Kemp PR, Schols AM, Polkey MI. Heterogeneity of quadriceps muscle phenotype in chronic obstructive pulmonary disease (Copd); implications for stratified medicine? *Muscle Nerve* 2013; 48: 488-497.

106. Ochala J, Ahlbeck K, Radell PJ, Eriksson LI, Larsson L. Factors underlying the early limb muscle weakness in acute quadriplegic myopathy using an experimental ICU porcine model. *PLoS One* 2011; 6: e20876.
107. Diaz NL, Finol HJ, Torres SH, Zambrano CI, Adjounian H. Histochemical and ultrastructural study of skeletal muscle in patients with sepsis and multiple organ failure syndrome (MOFS). *Histol Histopathol* 1998; 13: 121-128.
108. Goldberg AL. Protein turnover in skeletal muscle. II. Effects of denervation and cortisone on protein catabolism in skeletal muscle. *J Biol Chem* 1969; 244: 3223-3229.
109. Bloch S, Polkey MI, Griffiths M, Kemp P. Molecular mechanisms of intensive care unit-acquired weakness. *Eur Respir J* 2012; 39: 1000-1011.
110. Lecker SH. Ubiquitin-protein ligases in muscle wasting: multiple parallel pathways? *Curr Opin Clin Nutr Metab Care* 2003; 6: 271-275.
111. Gomes MD, Lecker SH, Jagoe RT, Navon A, Goldberg AL. Atrogin-1, a muscle-specific F-box protein highly expressed during muscle atrophy. *Proc Natl Acad Sci U S A* 2001; 98: 14440-14445.
112. Bodine SC, Latres E, Baumhueter S, Lai VK, Nunez L, Clarke BA, Poueymirou WT, Panaro FJ, Na E, Dharmarajan K, Pan ZQ, Valenzuela DM, DeChiara TM, Stitt TN, Yancopoulos GD, Glass DJ. Identification of ubiquitin ligases required for skeletal muscle atrophy. *Science* 2001; 294: 1704-1708.
113. Ochala J, Gustafson AM, Llano Diez M, Renaud G, Li M, Aare S, Qaisar R, Banduseela VC, Hedstrom Y, Tang X, Dworkin B, Ford CG, Nair SN, Perera S, Gautel M, Larsson L. Preferential skeletal muscle myosin loss in response to mechanical silencing in a novel rat intensive care unit model: Underlying mechanisms. *J Physiol* 2011.
114. Files DC, D'Alessio FR, Johnston LF, Kesari P, Aggarwal NR, Garibaldi BT, Mock JR, Simmers JL, DeGorordo A, Murdoch J, Willis MS, Patterson C, Tankersley CG, Messi ML, Liu C, Delbono O, Furlow JD, Bodine SC, Cohn RD, King LS, Crow MT. A critical role for muscle ring finger-1 in acute lung injury-associated skeletal muscle wasting. *Am J Respir Crit Care Med* 2012; 185: 825-834.
115. Tintignac LA, Lagirand J, Batonnet S, Sirri V, Leibovitch MP, Leibovitch SA. Degradation of MyoD mediated by the SCF (MAFbx) ubiquitin ligase. *J Biol Chem* 2005; 280: 2847-2856.
116. Witt SH, Granzier H, Witt CC, Labeit S. MURF-1 and MURF-2 target a specific subset of myofibrillar proteins redundantly: towards understanding MURF-dependent muscle ubiquitination. *Journal of molecular biology* 2005; 350: 713-722.
117. Ikemoto M, Nikawa T, Takeda S, Watanabe C, Kitano T, Baldwin KM, Izumi R, Nonaka I, Towatari T, Teshima S, Rokutan K, Kishi K. Space shuttle flight (STS-90) enhances degradation of rat myosin heavy chain in association with activation of ubiquitin-proteasome pathway. *FASEB J* 2001; 15: 1279-1281.
118. Wray CJ, Mammen JM, Hershko DD, Hasselgren PO. Sepsis upregulates the gene expression of multiple ubiquitin ligases in skeletal muscle. *Int J Biochem Cell Biol* 2003; 35: 698-705.
119. Li YP, Reid MB. NF-kappaB mediates the protein loss induced by TNF-alpha in differentiated skeletal muscle myotubes. *Am J Physiol Regul Integr Comp Physiol* 2000; 279: R1165-1170.
120. Zhang P, Chen X, Fan M. Signaling mechanisms involved in disuse muscle atrophy. *Med Hypotheses* 2007; 69: 310-321.
121. Cai D, Frantz JD, Tawa NE, Jr., Melendez PA, Oh BC, Lidov HG, Hasselgren PO, Frontera WR, Lee J, Glass DJ, Shoelson SE. IKKbeta/NF-kappaB activation causes severe muscle wasting in mice. *Cell* 2004; 119: 285-298.

122. Combaret L, Taillandier D, Dardevet D, Bechet D, Ralliere C, Claustre A, Grizard J, Attaix D. Glucocorticoids regulate mRNA levels for subunits of the 19 S regulatory complex of the 26 S proteasome in fast-twitch skeletal muscles. *Biochem J* 2004; 378: 239-246.
123. Helliwell TR, Wilkinson A, Griffiths RD, McClelland P, Palmer TE, Bone JM. Muscle fibre atrophy in critically ill patients is associated with the loss of myosin filaments and the presence of lysosomal enzymes and ubiquitin. *Neuropathol Appl Neurobiol* 1998; 24: 507-517.
124. Tiao G, Hobler S, Wang JJ, Meyer TA, Luchette FA, Fischer JE, Hasselgren PO. Sepsis is associated with increased mRNAs of the ubiquitin-proteasome proteolytic pathway in human skeletal muscle. *J Clin Invest* 1997; 99: 163-168.
125. Klaude M, Fredriksson K, Tjader I, Hammarqvist F, Ahlman B, Rooyackers O, Wernerman J. Proteasome proteolytic activity in skeletal muscle is increased in patients with sepsis. *Clin Sci (Lond)* 2007; 112: 499-506.
126. O'Leary MF, Hood DA. Denervation-induced oxidative stress and autophagy signaling in muscle. *Autophagy* 2009; 5: 230-231.
127. Grumati P, Coletto L, Sabatelli P, Cescon M, Angelin A, Bertaggia E, Blaauw B, Urciuolo A, Tiepolo T, Merlini L, Maraldi NM, Bernardi P, Sandri M, Bonaldo P. Autophagy is defective in collagen VI muscular dystrophies, and its reactivation rescues myofiber degeneration. *Nat Med* 2010; 16: 1313-1320.
128. Hussain SN, Mofarrahi M, Sigala I, Kim HC, Vassilakopoulos T, Maltais F, Bellenis I, Chaturvedi R, Gottfried SB, Metrakos P, Danialou G, Matecki S, Jaber S, Petrof BJ, Goldberg P. Mechanical ventilation-induced diaphragm disuse in humans triggers autophagy. *Am J Respir Crit Care Med* 2010; 182: 1377-1386.
129. Vanhorebeek I, Gunst J, Derde S, Derese I, Boussemaere M, Guiza F, Martinet W, Timmermans JP, D'Hoore A, Wouters PJ, Van den Berghe G. Insufficient activation of autophagy allows cellular damage to accumulate in critically ill patients. *J Clin Endocrinol Metab* 2011; 96: E633-645.
130. Petersson B, Wernerman J, Waller SO, von der Decken A, Vinnars E. Elective abdominal surgery depresses muscle protein synthesis and increases subjective fatigue: effects lasting more than 30 days. *Br J Surg* 1990; 77: 796-800.
131. Essen P, McNurlan MA, Gamrin L, Hunter K, Calder G, Garlick PJ, Wernerman J. Tissue protein synthesis rates in critically ill patients. *Crit Care Med* 1998; 26: 92-100.
132. Gamrin L, Essen P, Hultman E, McNurlan MA, Garlick PJ, Wernerman J. Protein-sparing effect in skeletal muscle of growth hormone treatment in critically ill patients. *Ann Surg* 2000; 231: 577-586.
133. Lang CH, Frost RA. Role of growth hormone, insulin-like growth factor-I, and insulin-like growth factor binding proteins in the catabolic response to injury and infection. *Curr Opin Clin Nutr Metab Care* 2002; 5: 271-279.
134. Lang CH, Frost RA, Nairn AC, MacLean DA, Vary TC. TNF-alpha impairs heart and skeletal muscle protein synthesis by altering translation initiation. *Am J Physiol Endocrinol Metab* 2002; 282: E336-347.
135. Hornberger TA, Hunter RB, Kandarian SC, Esser KA. Regulation of translation factors during hindlimb unloading and denervation of skeletal muscle in rats. *Am J Physiol Cell Physiol* 2001; 281: C179-187.
136. Vesali RF, Cibicek N, Jakobsson T, Klaude M, Wernerman J, Rooyackers O. Protein metabolism in leg muscle following an endotoxin injection in healthy volunteers. *Clin Sci (Lond)* 2010; 118: 421-427.
137. Otto A, Patel K. Signalling and the control of skeletal muscle size. *Exp Cell Res* 2010; 316: 3059-3066.
138. Bodine SC, Stitt TN, Gonzalez M, Kline WO, Stover GL, Bauerlein R, Zlotchenko E, Scrimgeour A, Lawrence JC, Glass DJ, Yancopoulos GD. Akt/mTOR pathway is a crucial

regulator of skeletal muscle hypertrophy and can prevent muscle atrophy in vivo. *Nat Cell Biol* 2001; 3: 1014-1019.
139. Glass DJ. Molecular mechanisms modulating muscle mass. *Trends Mol Med* 2003; 9: 344-350.
140. Sacheck JM, Ohtsuka A, McLary SC, Goldberg AL. IGF-I stimulates muscle growth by suppressing protein breakdown and expression of atrophy-related ubiquitin ligases, atrogin-1 and MuRF1. *Am J Physiol Endocrinol Metab* 2004; 287: E591-601.
141. Stitt TN, Drujan D, Clarke BA, Panaro F, Timofeyva Y, Kline WO, Gonzalez M, Yancopoulos GD, Glass DJ. The IGF-1/PI3K/Akt pathway prevents expression of muscle atrophy-induced ubiquitin ligases by inhibiting FOXO transcription factors. *Mol Cell* 2004; 14: 395-403.
142. Lin MC, Leung SY, Fang WF, Chin CH, Chung KF. Down-regulation of insulin-like growth factor I (IGF-I) in the mouse diaphragm during sepsis. *Chang Gung Med J* 2010; 33: 501-508.
143. Nystrom G, Pruznak A, Huber D, Frost RA, Lang CH. Local insulin-like growth factor I prevents sepsis-induced muscle atrophy. *Metabolism* 2009; 58: 787-797.
144. Lang CH, Frost RA. Sepsis-induced suppression of skeletal muscle translation initiation mediated by tumor necrosis factor alpha. *Metabolism* 2007; 56: 49-57.
145. Crossland H, Constantin-Teodosiu D, Gardiner SM, Constantin D, Greenhaff PL. A potential role for Akt/FOXO signalling in both protein loss and the impairment of muscle carbohydrate oxidation during sepsis in rodent skeletal muscle. *J Physiol* 2008; 586: 5589-5600.
146. West DW, Burd NA, Staples AW, Phillips SM. Human exercise-mediated skeletal muscle hypertrophy is an intrinsic process. *Int J Biochem Cell Biol* 2010; 42: 1371-1375.
147. Jespersen JG, Nedergaard A, Reitelseder S, Mikkelsen UR, Dideriksen KJ, Agergaard J, Kreiner F, Pott FC, Schjerling P, Kjaer M. Activated protein synthesis and suppressed protein breakdown signaling in skeletal muscle of critically ill patients. *PLoS One* 2011; 6: e18090.
148. Sharshar T, Bastuji-Garin S, Polito A, De Jonghe B, Stevens RD, Maxime V, Rodriguez P, Cerf C, Outin H, Touraine P, Laborde K. Hormonal status in protracted critical illness and in-hospital mortality. *Crit Care* 2011; 15: R47.
149. Sharshar T, Bastuji-Garin S, De Jonghe B, Stevens RD, Polito A, Maxime V, Rodriguez P, Cerf C, Outin H, Touraine P, Laborde K. Hormonal status and ICU-acquired paresis in critically ill patients. *Intensive Care Med* 2010; 36: 1318-1326.
150. Rennie MJ. Anabolic resistance in critically ill patients. *Crit Care Med* 2009; 37: S398-399.
151. Clark MG, Rattigan S, Barrett EJ. Nutritive blood flow as an essential element supporting muscle anabolism. *Curr Opin Clin Nutr Metab Care* 2006; 9: 185-189.
152. Massague J. TGFbeta signalling in context. *Nature reviews Molecular cell biology* 2012; 13: 616-630.
153. Shi Y, Massague J. Mechanisms of TGF-beta signaling from cell membrane to the nucleus. *Cell* 2003; 113: 685-700.
154. Attisano L, Wrana JL. Smads as transcriptional co-modulators. *Current opinion in cell biology* 2000; 12: 235-243.
155. Derynck R, Zhang YE. Smad-dependent and Smad-independent pathways in TGF-beta family signalling. *Nature* 2003; 425: 577-584.
156. McPherron AC, Lawler AM, Lee SJ. Regulation of skeletal muscle mass in mice by a new TGF-beta superfamily member. *Nature* 1997; 387: 83-90.
157. McPherron AC, Lee SJ. Double muscling in cattle due to mutations in the myostatin gene. *Proc Natl Acad Sci U S A* 1997; 94: 12457-12461.

158. Schuelke M, Wagner KR, Stolz LE, Hubner C, Riebel T, Komen W, Braun T, Tobin JF, Lee SJ. Myostatin mutation associated with gross muscle hypertrophy in a child. *N Engl J Med* 2004; 350: 2682-2688.
159. Lee SJ, McPherron AC. Regulation of myostatin activity and muscle growth. *Proc Natl Acad Sci U S A* 2001; 98: 9306-9311.
160. Huang Z, Chen X, Chen D. Myostatin: A novel insight into its role in metabolism, signal pathways, and expression regulation. *Cell Signal* 2011; 23: 1441-1446.
161. Sartori R, Gregorevic P, Sandri M. TGFbeta and BMP signaling in skeletal muscle: potential significance for muscle-related disease. *Trends in endocrinology and metabolism: TEM* 2014.
162. Elkina Y, von Haehling S, Anker SD, Springer J. The role of myostatin in muscle wasting: an overview. *Journal of cachexia, sarcopenia and muscle* 2011; 2: 143-151.
163. Lee SJ, Reed LA, Davies MV, Girgenrath S, Goad ME, Tomkinson KN, Wright JF, Barker C, Ehrmantraut G, Holmstrom J, Trowell B, Gertz B, Jiang MS, Sebald SM, Matzuk M, Li E, Liang LF, Quattlebaum E, Stotish RL, Wolfman NM. Regulation of muscle growth by multiple ligands signaling through activin type II receptors. *Proc Natl Acad Sci U S A* 2005; 102: 18117-18122.
164. Winbanks CE, Weeks KL, Thomson RE, Sepulveda PV, Beyer C, Qian H, Chen JL, Allen JM, Lancaster GI, Febbraio MA, Harrison CA, McMullen JR, Chamberlain JS, Gregorevic P. Follistatin-mediated skeletal muscle hypertrophy is regulated by Smad3 and mTOR independently of myostatin. *The Journal of cell biology* 2012; 197: 997-1008.
165. McFarlane C, Plummer E, Thomas M, Hennebry A, Ashby M, Ling N, Smith H, Sharma M, Kambadur R. Myostatin induces cachexia by activating the ubiquitin proteolytic system through an NF-kappaB-independent, FoxO1-dependent mechanism. *J Cell Physiol* 2006; 209: 501-514.
166. Lee JY, Hopkinson NS, Kemp PR. Myostatin induces autophagy in skeletal muscle in vitro. *Biochemical and biophysical research communications* 2011; 415: 632-636.
167. Amirouche A, Durieux AC, Banzet S, Koulmann N, Bonnefoy R, Mouret C, Bigard X, Peinnequin A, Freyssenet D. Down-regulation of Akt/mammalian target of rapamycin signaling pathway in response to myostatin overexpression in skeletal muscle. *Endocrinology* 2009; 150: 286-294.
168. Morissette MR, Cook SA, Buranasombati C, Rosenberg MA, Rosenzweig A. Myostatin inhibits IGF-I-induced myotube hypertrophy through Akt. *Am J Physiol Cell Physiol* 2009; 297: C1124-1132.
169. Lenk K, Schur R, Linke A, Erbs S, Matsumoto Y, Adams V, Schuler G. Impact of exercise training on myostatin expression in the myocardium and skeletal muscle in a chronic heart failure model. *Eur J Heart Fail* 2009; 11: 342-348.
170. Liu CM, Yang Z, Liu CW, Wang R, Tien P, Dale R, Sun LQ. Myostatin antisense RNA-mediated muscle growth in normal and cancer cachexia mice. *Gene Ther* 2008; 15: 155-160.
171. Gonzalez-Cadavid NF, Taylor WE, Yarasheski K, Sinha-Hikim I, Ma K, Ezzat S, Shen R, Lalani R, Asa S, Mamita M, Nair G, Arver S, Bhasin S. Organization of the human myostatin gene and expression in healthy men and HIV-infected men with muscle wasting. *Proc Natl Acad Sci U S A* 1998; 95: 14938-14943.
172. Ma K, Mallidis C, Bhasin S, Mahabadi V, Artaza J, Gonzalez-Cadavid N, Arias J, Salehian B. Glucocorticoid-induced skeletal muscle atrophy is associated with upregulation of myostatin gene expression. *Am J Physiol Endocrinol Metab* 2003; 285: E363-371.
173. W DCM, Natanek SA, Riddoch-Contreras J, Lewis A, Marsh GS, Kemp PR, Polkey MI. Quadriceps myostatin expression in COPD. *Eur Respir J* 2010; 36: 686-688.
174. Constantin D, McCullough J, Mahajan R, Greenhaff PL. Novel events in the molecular regulation of muscle mass in critically-ill patients. *J Physiol* 2011.

175. Derde S, Hermans G, Derese I, Guiza F, Hedstrom Y, Wouters PJ, Bruyninckx F, D'Hoore A, Larsson L, Van den Berghe G, Vanhorebeek I. Muscle atrophy and preferential loss of myosin in prolonged critically ill patients. *Crit Care Med* 2012; 40: 79-89.
176. Leon A, Boczkowski J, Dureuil B, Desmonts JM, Aubier M. Effects of endotoxic shock on diaphragmatic function in mechanically ventilated rats. *J Appl Physiol* 1992; 72: 1466-1472.
177. Lanone S, Taille C, Boczkowski J, Aubier M. Diaphragmatic fatigue during sepsis and septic shock. *Intensive Care Med* 2005; 31: 1611-1617.
178. Supinski G, Nethery D, Stofan D, DiMarco A. Comparison of the effects of endotoxin on limb, respiratory, and cardiac muscles. *J Appl Physiol* 1996; 81: 1370-1378.
179. Supinski GS, Callahan LA. Caspase activation contributes to endotoxin-induced diaphragm weakness. *J Appl Physiol* 2006; 100: 1770-1777.
180. Polkey MI, Moxham J. Clinical aspects of respiratory muscle dysfunction in the critically ill. *Chest* 2001; 119: 926-939.
181. Massa R, Carpenter S, Holland P, Karpati G. Loss and renewal of thick myofilaments in glucocorticoid-treated rat soleus after denervation and reinnervation. *Muscle Nerve* 1992; 15: 1290-1298.
182. Angel MJ, Bril V, Shannon P, Herridge MS. Neuromuscular function in survivors of the acute respiratory distress syndrome. *The Canadian journal of neurological sciences Le journal canadien des sciences neurologiques* 2007; 34: 427-432.
183. Latronico N, Bertolini G, Guarneri B, Botteri M, Peli E, Andreoletti S, Bera P, Luciani D, Nardella A, Vittorielli E, Simini B, Candiani A. Simplified electrophysiological evaluation of peripheral nerves in critically ill patients: the Italian multi-centre CRIMYNE study. *Crit Care* 2007; 11: R11.
184. Hermans G, Vanhorebeek I, Derde S, Van den Berghe G. Metabolic aspects of critical illness polyneuromyopathy. *Crit Care Med* 2009; 37: S391-397.
185. Fenzi F, Latronico N, Refatti N, Rizzuto N. Enhanced expression of E-selectin on the vascular endothelium of peripheral nerve in critically ill patients with neuromuscular disorders. *Acta neuropathologica* 2003; 106: 75-82.
186. Z'Graggen W, Lin C, Howard R, Beale R, Bostock H. Nerve excitability changes in critical illness polyneuropathy. *Brain* 2006; 129: 2461-2470.
187. Druschky A, Herkert M, Radespiel-Tröger M, Druschky K, Hund E, Becker C, Hilz M, Erbguth F, Neundörfer B. Critical illness polyneuropathy: clinical findings and cell culture assay of neurotoxicity assessed by a prospective study. *Intensive Care Med* 2001; 27: 686-693.
188. Jaber S, Jung B, Matecki S, Petrof BJ. Clinical review: Ventilator-induced diaphragmatic dysfunction - human studies confirm animal model findings! *Crit Care* 2011; 15: 206.
189. Mills GH, Ponte J, Hamnegard CH, Kyroussis D, Polkey MI, Moxham J, Green M. Tracheal tube pressure change during magnetic stimulation of the phrenic nerves as an indicator of diaphragm strength on the intensive care unit. *Br J Anaesth* 2001; 87: 876-884.
190. Hermans G, Agten A, Testelmans D, Decramer M, Gayan-Ramirez G. Increased duration of mechanical ventilation is associated with decreased diaphragmatic force: a prospective observational study. *Crit Care* 2011; 14: R127.
191. Jung B, Constantin JM, Rossel N, Le Goff C, Sebbane M, Coisel Y, Chanques G, Futier E, Hugon G, Capdevila X, Petrof B, Matecki S, Jaber S. Adaptive support ventilation prevents ventilator-induced diaphragmatic dysfunction in piglet: an in vivo and in vitro study. *Anesthesiology* 2011; 112: 1435-1443.
192. Gayan-Ramirez G, Testelmans D, Maes K, Racz GZ, Cadot P, Zador E, Wuytack F, Decramer M. Intermittent spontaneous breathing protects the rat diaphragm from mechanical ventilation effects. *Crit Care Med* 2005; 33: 2804-2809.

193. Reid MB, Lannergren J, Westerblad H. Respiratory and limb muscle weakness induced by tumor necrosis factor-alpha: involvement of muscle myofilaments. *Am J Respir Crit Care Med* 2002; 166: 479-484.
194. Smith IJ, Lecker SH, Hasselgren PO. Calpain activity and muscle wasting in sepsis. *Am J Physiol Endocrinol Metab* 2008; 295: E762-771.
195. Callahan LA, Supinski GS. Sepsis-induced myopathy. *Crit Care Med* 2009; 37: S354-367.
196. Supinski GS, Wang W, Callahan LA. Caspase and calpain activation both contribute to sepsis-induced diaphragmatic weakness. *J Appl Physiol* 2009; 107: 1389-1396.
197. Sandri M. Apoptotic signaling in skeletal muscle fibers during atrophy. *Curr Opin Clin Nutr Metab Care* 2002; 5: 249-253.
198. Williams AB, Decourten-Myers GM, Fischer JE, Luo G, Sun X, Hasselgren PO. Sepsis stimulates release of myofilaments in skeletal muscle by a calcium-dependent mechanism. *FASEB J* 1999; 13: 1435-1443.
199. Smith IJ, Dodd SL. Calpain activation causes a proteasome-dependent increase in protein degradation and inhibits the Akt signalling pathway in rat diaphragm muscle. *Exp Physiol* 2007; 92: 561-573.
200. Stockholm D, Herasse M, Marchand S, Praud C, Roudaut C, Richard I, Sebille A, Beckmann JS. Calpain 3 mRNA expression in mice after denervation and during muscle regeneration. *Am J Physiol Cell Physiol* 2001; 280: C1561-1569.
201. Siu PM, Pistilli EE, Alway SE. Apoptotic responses to hindlimb suspension in gastrocnemius muscles from young adult and aged rats. *Am J Physiol Regul Integr Comp Physiol* 2005; 289: R1015-1026.
202. Bartoli M, Richard I. Calpains in muscle wasting. *Int J Biochem Cell Biol* 2005; 37: 2115-2133.
203. Benson DW, Hasselgren PO, Hiyama DT, James JH, Li S, Rigel DF, Fischer JE. Effect of sepsis on calcium uptake and content in skeletal muscle and regulation in vitro by calcium of total and myofibrillar protein breakdown in control and septic muscle: results from a preliminary study. *Surgery* 1989; 106: 87-93.
204. Enns DL, Raastad T, Ugelstad I, Belcastro AN. Calpain/calpastatin activities and substrate depletion patterns during hindlimb unweighting and reweighting in skeletal muscle. *Eur J Appl Physiol* 2007; 100: 445-455.
205. Liu SH, Lai JL, Yang RS, Lin-Shiau SY. Nitric oxide is not involved in the endotoxemia-induced alterations in Ca2+ and ryanodine responses in mouse diaphragms. *Naunyn Schmiedebergs Arch Pharmacol* 2002; 366: 327-334.
206. Zink W, Kaess M, Hofer S, Plachky J, Zausig YA, Sinner B, Weigand MA, Fink RH, Graf BM. Alterations in intracellular Ca2+-homeostasis of skeletal muscle fibers during sepsis. *Crit Care Med* 2008; 36: 1559-1563.
207. Friedrich O, Hund E, Weber C, Hacke W, Fink RH. Critical illness myopathy serum fractions affect membrane excitability and intracellular calcium release in mammalian skeletal muscle. *J Neurol* 2004; 251: 53-65.
208. Lefaucheur JP, Nordine T, Rodriguez P, Brochard L. Origin of ICU acquired paresis determined by direct muscle stimulation. *J Neurol Neurosurg Psychiatry* 2006; 77: 500-506.
209. Lin MC, Ebihara S, El Dwairi Q, Hussain SN, Yang L, Gottfried SB, Comtois A, Petrof BJ. Diaphragm sarcolemmal injury is induced by sepsis and alleviated by nitric oxide synthase inhibition. *Am J Respir Crit Care Med* 1998; 158: 1656-1663.
210. Rich MM, McGarvey ML, Teener JW, Frame LH. ECG changes during septic shock. *Cardiology* 2002; 97: 187-196.
211. Rich M, Pinter M, Kraner S, Barchi R. Loss of electrical excitability in an animal model of acute quadriplegic myopathy. *Ann Neurol* 1998; 43: 171-179.

212. Kraner SD, Novak KR, Wang Q, Peng J, Rich MM. Altered sodium channel-protein associations in critical illness myopathy. *Skeletal muscle* 2012; 2: 17.
213. Teener J, Rich M. Dysregulation of sodium channel gating in critical illness myopathy. *J Muscle Res Cell Motil* 2006; 27: 291-296.
214. Rossignol B, Gueret G, Pennec JP, Morel J, Giroux-Metges MA, Talarmin H, Arvieux CC. Effects of chronic sepsis on the voltage-gated sodium channel in isolated rat muscle fibers. *Crit Care Med* 2007; 35: 351-357.
215. Haeseler G, Foadi N, Wiegand E, Ahrens J, Krampfl K, Dengler R, Leuwer M. Endotoxin reduces availability of voltage-gated human skeletal muscle sodium channels at depolarized membrane potentials. *Crit Care Med* 2008; 36: 1239-1247.
216. Teener JW, Rich MM. Dysregulation of sodium channel gating in critical illness myopathy. *J Muscle Res Cell Motil* 2006; 27: 291-296.
217. Friedrich O. Critical illness myopathy: what is happening? *Curr Opin Clin Nutr Metab Care* 2006; 9: 403-409.
218. Caquelard F, Burnet H, Tagliarini F, Cauchy E, Richalet JP, Jammes Y. Effects of prolonged hypobaric hypoxia on human skeletal muscle function and electromyographic events. *Clin Sci (Lond)* 2000; 98: 329-337.
219. Hoppeler H, Kleinert E, Schlegel C, Claassen H, Howald H, Kayar SR, Cerretelli P. Morphological adaptations of human skeletal muscle to chronic hypoxia. *Int J Sports Med* 1990; 11 Suppl 1: S3-9.
220. Gosker HR, van Mameren H, van Dijk PJ, Engelen MP, van der Vusse GJ, Wouters EF, Schols AM. Skeletal muscle fibre-type shifting and metabolic profile in patients with chronic obstructive pulmonary disease. *Eur Respir J* 2002; 19: 617-625.
221. Vianna LG, Koulouris N, Lanigan C, Moxham J. Effect of acute hypercapnia on limb muscle contractility in humans. *J Appl Physiol* 1990; 69: 1486-1493.
222. Juan G, Calverley P, Talamo C, Schnader J, Roussos C. Effect of carbon dioxide on diaphragmatic function in human beings. *N Engl J Med* 1984; 310: 874-879.
223. Rafferty GF, Lou Harris M, Polkey MI, Greenough A, Moxham J. Effect of hypercapnia on maximal voluntary ventilation and diaphragm fatigue in normal humans. *Am J Respir Crit Care Med* 1999; 160: 1567-1571.
224. Callahan LA, Stofan DA, Szweda LI, Nethery DE, Supinski GS. Free radicals alter maximal diaphragmatic mitochondrial oxygen consumption in endotoxin-induced sepsis. *Free Radic Biol Med* 2001; 30: 129-138.
225. Callahan LA, Supinski GS. Sepsis induces diaphragm electron transport chain dysfunction and protein depletion. *Am J Respir Crit Care Med* 2005; 172: 861-868.
226. Callahan LA, Supinski GS. Downregulation of diaphragm electron transport chain and glycolytic enzyme gene expression in sepsis. *J Appl Physiol* 2005; 99: 1120-1126.
227. Brealey D, Brand M, Hargreaves I, Heales S, Land J, Smolenski R, Davies NA, Cooper CE, Singer M. Association between mitochondrial dysfunction and severity and outcome of septic shock. *Lancet* 2002; 360: 219-223.
228. Vanhorebeek I, De Vos R, Mesotten D, Wouters PJ, De Wolf-Peeters C, Van den Berghe G. Protection of hepatocyte mitochondrial ultrastructure and function by strict blood glucose control with insulin in critically ill patients. *Lancet* 2005; 365: 53-59.
229. Fareed MU, Evenson AR, Wei W, Menconi M, Poylin V, Petkova V, Pignol B, Hasselgren PO. Treatment of rats with calpain inhibitors prevents sepsis-induced muscle proteolysis independent of atrogin-1/MAFbx and MuRF1 expression. *Am J Physiol Regul Integr Comp Physiol* 2006; 290: R1589-1597.
230. Li YP, Chen Y, Li AS, Reid MB. Hydrogen peroxide stimulates ubiquitin-conjugating activity and expression of genes for specific E2 and E3 proteins in skeletal muscle myotubes. *Am J Physiol Cell Physiol* 2003; 285: C806-812.

231. Shang F, Gong X, Taylor A. Activity of ubiquitin-dependent pathway in response to oxidative stress. Ubiquitin-activating enzyme is transiently up-regulated. *J Biol Chem* 1997; 272: 23086-23093.
232. Pickering AM, Koop AL, Teoh CY, Ermak G, Grune T, Davies KJ. The immunoproteasome, the 20S proteasome and the PA28alphabeta proteasome regulator are oxidative-stress-adaptive proteolytic complexes. *Biochem J* 2010; 432: 585-594.
233. Supinski GS, Callahan LA. Calpain activation contributes to endotoxin-induced diaphragmatic dysfunction. *Am J Respir Cell Mol Biol* 2010; 42: 80-87.
234. McClung JM, Judge AR, Talbert EE, Powers SK. Calpain-1 is required for hydrogen peroxide-induced myotube atrophy. *Am J Physiol Cell Physiol* 2009; 296: C363-371.
235. Jiang B, Xiao W, Shi Y, Liu M, Xiao X. Role of Smac/DIABLO in hydrogen peroxide-induced apoptosis in C2C12 myogenic cells. *Free Radic Biol Med* 2005; 39: 658-667.
236. Supinski GS, Callahan LA. Free radical-mediated skeletal muscle dysfunction in inflammatory conditions. *J Appl Physiol* 2007; 102: 2056-2063.
237. Reid MB, Andrade FH, Balke CW, Esser KA. Redox mechanisms of muscle dysfunction in inflammatory disease. *Phys Med Rehabil Clin N Am* 2005; 16: 925-949, ix.
238. Javesghani D, Magder SA, Barreiro E, Quinn MT, Hussain SN. Molecular characterization of a superoxide-generating NAD(P)H oxidase in the ventilatory muscles. *Am J Respir Crit Care Med* 2002; 165: 412-418.
239. Boveris A, Alvarez S, Navarro A. The role of mitochondrial nitric oxide synthase in inflammation and septic shock. *Free Radic Biol Med* 2002; 33: 1186-1193.
240. Buck M, Chojkier M. Muscle wasting and dedifferentiation induced by oxidative stress in a murine model of cachexia is prevented by inhibitors of nitric oxide synthesis and antioxidants. *EMBO J* 1996; 15: 1753-1765.
241. Supinski G, Nethery D, Nosek TM, Callahan LA, Stofan D, DiMarco A. Endotoxin administration alters the force vs. pCa relationship of skeletal muscle fibers. *Am J Physiol Regul Integr Comp Physiol* 2000; 278: R891-896.
242. Callahan LA, Supinski GS. Hyperglycemia-induced diaphragm weakness is mediated by oxidative stress. *Crit Care* 2014; 18: R88.
243. Bonetto A, Penna F, Muscaritoli M, Minero VG, Rossi Fanelli F, Baccino FM, Costelli P. Are antioxidants useful for treating skeletal muscle atrophy? *Free Radic Biol Med* 2009; 47: 906-916.
244. Lawler JM, Song W, Demaree SR. Hindlimb unloading increases oxidative stress and disrupts antioxidant capacity in skeletal muscle. *Free Radic Biol Med* 2003; 35: 9-16.
245. Gore DC, Wolf SE, Sanford AP, Herndon DN, Wolfe RR. Extremity hyperinsulinemia stimulates muscle protein synthesis in severely injured patients. *Am J Physiol Endocrinol Metab* 2004; 286: E529-534.
246. Cleveland BM, Weber GM. Effects of insulin-like growth factor-I, insulin, and leucine on protein turnover and ubiquitin ligase expression in rainbow trout primary myocytes. *Am J Physiol Regul Integr Comp Physiol* 2010; 298: R341-350.
247. Hansen TK, Thiel S, Wouters PJ, Christiansen JS, Van den Berghe G. Intensive insulin therapy exerts antiinflammatory effects in critically ill patients and counteracts the adverse effect of low mannose-binding lectin levels. *J Clin Endocrinol Metab* 2003; 88: 1082-1088.
248. Mesotten D, Swinnen JV, Vanderhoydonc F, Wouters PJ, Van den Berghe G. Contribution of circulating lipids to the improved outcome of critical illness by glycemic control with intensive insulin therapy. *J Clin Endocrinol Metab* 2004; 89: 219-226.
249. Ishii DN, Lupien SB. Insulin-like growth factors protect against diabetic neuropathy: effects on sensory nerve regeneration in rats. *J Neurosci Res* 1995; 40: 138-144.

250. Biolo G, De Cicco M, Lorenzon S, Dal Mas V, Fantin D, Paroni R, Barazzoni R, Zanetti M, Iapichino G, Guarnieri G. Treating hyperglycemia improves skeletal muscle protein metabolism in cancer patients after major surgery. *Crit Care Med* 2008; 36: 1768-1775.
251. Unsicker K, Spittau B, Krieglstein K. The multiple facets of the TGF-beta family cytokine growth/differentiation factor-15/macrophage inhibitory cytokine-1. *Cytokine & growth factor reviews* 2013; 24: 373-384.
252. Bootcov MR, Bauskin AR, Valenzuela SM, Moore AG, Bansal M, He XY, Zhang HP, Donnellan M, Mahler S, Pryor K, Walsh BJ, Nicholson RC, Fairlie WD, Por SB, Robbins JM, Breit SN. MIC-1, a novel macrophage inhibitory cytokine, is a divergent member of the TGF-beta superfamily. *Proc Natl Acad Sci U S A* 1997; 94: 11514-11519.
253. Lawton LN, Bonaldo MF, Jelenc PC, Qiu L, Baumes SA, Marcelino RA, de Jesus GM, Wellington S, Knowles JA, Warburton D, Brown S, Soares MB. Identification of a novel member of the TGF-beta superfamily highly expressed in human placenta. *Gene* 1997; 203: 17-26.
254. Hromas R, Hufford M, Sutton J, Xu D, Li Y, Lu L. PLAB, a novel placental bone morphogenetic protein. *Biochimica et biophysica acta* 1997; 1354: 40-44.
255. Baek SJ, Kim KS, Nixon JB, Wilson LC, Eling TE. Cyclooxygenase inhibitors regulate the expression of a TGF-beta superfamily member that has proapoptotic and antitumorigenic activities. *Molecular pharmacology* 2001; 59: 901-908.
256. Bottner M, Suter-Crazzolara C, Schober A, Unsicker K. Expression of a novel member of the TGF-beta superfamily, growth/differentiation factor-15/macrophage-inhibiting cytokine-1 (GDF-15/MIC-1) in adult rat tissues. *Cell and tissue research* 1999; 297: 103-110.
257. Xu X, Li Z, Gao W. Growth differentiation factor 15 in cardiovascular diseases: from bench to bedside. *Biomarkers* 2011; 16: 466-475.
258. Wang X, Baek SJ, Eling TE. The diverse roles of nonsteroidal anti-inflammatory drug activated gene (NAG-1/GDF15) in cancer. *Biochemical pharmacology* 2013; 85: 597-606.
259. Wu Q, Jiang D, Chu HW. Cigarette smoke induces growth differentiation factor 15 production in human lung epithelial cells: implication in mucin over-expression. *Innate immunity* 2012; 18: 617-626.
260. Nickel N, Kempf T, Tapken H, Tongers J, Laenger F, Lehmann U, Golpon H, Olsson K, Wilkins MR, Gibbs JS, Hoeper MM, Wollert KC. Growth differentiation factor-15 in idiopathic pulmonary arterial hypertension. *Am J Respir Crit Care Med* 2008; 178: 534-541.
261. Breit SN, Carrero JJ, Tsai VW, Yagoutifam N, Luo W, Kuffner T, Bauskin AR, Wu L, Jiang L, Barany P, Heimburger O, Murikami MA, Apple FS, Marquis CP, Macia L, Lin S, Sainsbury A, Herzog H, Law M, Stenvinkel P, Brown DA. Macrophage inhibitory cytokine-1 (MIC-1/GDF15) and mortality in end-stage renal disease. *Nephrology, dialysis, transplantation : official publication of the European Dialysis and Transplant Association - European Renal Association* 2012; 27: 70-75.
262. Mimeault M, Batra SK. Divergent molecular mechanisms underlying the pleiotropic functions of macrophage inhibitory cytokine-1 in cancer. *J Cell Physiol* 2010; 224: 626-635.
263. Khaled YS, Elkord E, Ammori BJ. Macrophage inhibitory cytokine-1: a review of its pleiotropic actions in cancer. *Cancer biomarkers : section A of Disease markers* 2012; 11: 183-190.
264. Eggers KM, Kempf T, Wallentin L, Wollert KC, Lind L. Change in growth differentiation factor 15 concentrations over time independently predicts mortality in community-dwelling elderly individuals. *Clinical chemistry* 2013; 59: 1091-1098.

265. Tan M, Wang Y, Guan K, Sun Y. PTGF-beta, a type beta transforming growth factor (TGF-beta) superfamily member, is a p53 target gene that inhibits tumor cell growth via TGF-beta signaling pathway. *Proc Natl Acad Sci U S A* 2000; 97: 109-114.
266. Mimeault M, Johansson SL, Batra SK. Marked improvement of cytotoxic effects induced by docetaxel on highly metastatic and androgen-independent prostate cancer cells by downregulating macrophage inhibitory cytokine-1. *British journal of cancer* 2013; 108: 1079-1091.
267. Johnen H, Lin S, Kuffner T, Brown DA, Tsai VW, Bauskin AR, Wu L, Pankhurst G, Jiang L, Junankar S, Hunter M, Fairlie WD, Lee NJ, Enriquez RF, Baldock PA, Corey E, Apple FS, Murakami MM, Lin EJ, Wang C, During MJ, Sainsbury A, Herzog H, Breit SN. Tumor-induced anorexia and weight loss are mediated by the TGF-beta superfamily cytokine MIC-1. *Nat Med* 2007; 13: 1333-1340.
268. Heger J, Schiegnitz E, von Waldthausen D, Anwar MM, Piper HM, Euler G. Growth differentiation factor 15 acts anti-apoptotic and pro-hypertrophic in adult cardiomyocytes. *J Cell Physiol* 2010; 224: 120-126.
269. Subramaniam S, Strelau J, Unsicker K. Growth differentiation factor-15 prevents low potassium-induced cell death of cerebellar granule neurons by differential regulation of Akt and ERK pathways. *J Biol Chem* 2003; 278: 8904-8912.
270. Donnelly SM, Paplomata E, Peake BM, Sanabria E, Chen Z, Nahta R. P38 MAPK contributes to resistance and invasiveness of HER2- overexpressing breast cancer. *Current medicinal chemistry* 2014; 21: 501-510.
271. Choi HJ, Kim J, Do KH, Park SH, Moon Y. Prolonged NF-kappaB activation by a macrophage inhibitory cytokine 1-linked signal in enteropathogenic Escherichia coli-infected epithelial cells. *Infection and immunity* 2013; 81: 1860-1869.
272. Smith RC, Lin BK. Myostatin inhibitors as therapies for muscle wasting associated with cancer and other disorders. *Current opinion in supportive and palliative care* 2013; 7: 352-360.
273. Xu J, Kimball TR, Lorenz JN, Brown DA, Bauskin AR, Klevitsky R, Hewett TE, Breit SN, Molkentin JD. GDF15/MIC-1 functions as a protective and antihypertrophic factor released from the myocardium in association with SMAD protein activation. *Circ Res* 2006; 98: 342-350.
274. Kim KS, Baek SJ, Flake GP, Loftin CD, Calvo BF, Eling TE. Expression and regulation of nonsteroidal anti-inflammatory drug-activated gene (NAG-1) in human and mouse tissue. *Gastroenterology* 2002; 122: 1388-1398.
275. Liu T, Bauskin AR, Zaunders J, Brown DA, Pankhurst S, Russell PJ, Breit SN. Macrophage inhibitory cytokine 1 reduces cell adhesion and induces apoptosis in prostate cancer cells. *Cancer Res* 2003; 63: 5034-5040.
276. de Jager SC, Bermudez B, Bot I, Koenen RR, Bot M, Kavelaars A, de Waard V, Heijnen CJ, Muriana FJ, Weber C, van Berkel TJ, Kuiper J, Lee SJ, Abia R, Biessen EA. Growth differentiation factor 15 deficiency protects against atherosclerosis by attenuating CCR2-mediated macrophage chemotaxis. *The Journal of experimental medicine* 2011; 208: 217-225.
277. Schlittenhardt D, Schober A, Strelau J, Bonaterra GA, Schmiedt W, Unsicker K, Metz J, Kinscherf R. Involvement of growth differentiation factor-15/macrophage inhibitory cytokine-1 (GDF-15/MIC-1) in oxLDL-induced apoptosis of human macrophages in vitro and in arteriosclerotic lesions. *Cell and tissue research* 2004; 318: 325-333.
278. Kempf T, Zarbock A, Widera C, Butz S, Stadtmann A, Rossaint J, Bolomini-Vittori M, Korf-Klingebiel M, Napp LC, Hansen B, Kanwischer A, Bavendiek U, Beutel G, Hapke M, Sauer MG, Laudanna C, Hogg N, Vestweber D, Wollert KC. GDF-15 is an inhibitor of leukocyte integrin activation required for survival after myocardial infarction in mice. *Nat Med* 2011; 17: 581-588.

279. Clark BJ, Bull TM, Benson AB, Stream AR, Macht M, Gaydos J, Meadows C, Burnham EL, Moss M, the ANI. Growth differentiation factor-15 and prognosis in acute respiratory distress syndrome: a retrospective cohort study. *Crit Care* 2013; 17: R92.
280. Tsai VW, Husaini Y, Manandhar R, Lee-Ng KK, Zhang HP, Harriott K, Jiang L, Lin S, Sainsbury A, Brown DA, Breit SN. Anorexia/cachexia of chronic diseases: a role for the TGF-beta family cytokine MIC-1/GDF15. *Journal of cachexia, sarcopenia and muscle* 2012; 3: 239-243.
281. Lee RC, Feinbaum RL, Ambros V. The C. elegans heterochronic gene lin-4 encodes small RNAs with antisense complementarity to lin-14. *Cell* 1993; 75: 843-854.
282. Pasquinelli AE, Reinhart BJ, Slack F, Martindale MQ, Kuroda MI, Maller B, Hayward DC, Ball EE, Degnan B, Muller P, Spring J, Srinivasan A, Fishman M, Finnerty J, Corbo J, Levine M, Leahy P, Davidson E, Ruvkun G. Conservation of the sequence and temporal expression of let-7 heterochronic regulatory RNA. *Nature* 2000; 408: 86-89.
283. Lewis BP, Burge CB, Bartel DP. Conserved seed pairing, often flanked by adenosines, indicates that thousands of human genes are microRNA targets. *Cell* 2005; 120: 15-20.
284. Tetreault N, De Guire V. miRNAs: their discovery, biogenesis and mechanism of action. *Clinical biochemistry* 2013; 46: 842-845.
285. Lewis BP, Shih IH, Jones-Rhoades MW, Bartel DP, Burge CB. Prediction of mammalian microRNA targets. *Cell* 2003; 115: 787-798.
286. Bartel DP. MicroRNAs: genomics, biogenesis, mechanism, and function. *Cell* 2004; 116: 281-297.
287. O'Rourke JR, Georges SA, Seay HR, Tapscott SJ, McManus MT, Goldhamer DJ, Swanson MS, Harfe BD. Essential role for Dicer during skeletal muscle development. *Developmental biology* 2007; 311: 359-368.
288. Guller I, Russell AP. MicroRNAs in skeletal muscle: their role and regulation in development, disease and function. *J Physiol* 2010; 588: 4075-4087.
289. Chen JF, Callis TE, Wang DZ. microRNAs and muscle disorders. *Journal of cell science* 2009; 122: 13-20.
290. Chen JF, Mandel EM, Thomson JM, Wu Q, Callis TE, Hammond SM, Conlon FL, Wang DZ. The role of microRNA-1 and microRNA-133 in skeletal muscle proliferation and differentiation. *Nature genetics* 2006; 38: 228-233.
291. van Rooij E, Quiat D, Johnson BA, Sutherland LB, Qi X, Richardson JA, Kelm RJ, Jr., Olson EN. A family of microRNAs encoded by myosin genes governs myosin expression and muscle performance. *Developmental cell* 2009; 17: 662-673.
292. Naguibneva I, Ameyar-Zazoua M, Polesskaya A, Ait-Si-Ali S, Groisman R, Souidi M, Cuvellier S, Harel-Bellan A. The microRNA miR-181 targets the homeobox protein Hox-A11 during mammalian myoblast differentiation. *Nat Cell Biol* 2006; 8: 278-284.
293. Wang XH. MicroRNA in myogenesis and muscle atrophy. *Curr Opin Clin Nutr Metab Care* 2013; 16: 258-266.
294. Goljanek-Whysall K, Sweetman D, Abu-Elmagd M, Chapnik E, Dalmay T, Hornstein E, Munsterberg A. MicroRNA regulation of the paired-box transcription factor Pax3 confers robustness to developmental timing of myogenesis. *Proc Natl Acad Sci U S A* 2011; 108: 11936-11941.
295. Elia L, Contu R, Quintavalle M, Varrone F, Chimenti C, Russo MA, Cimino V, De Marinis L, Frustaci A, Catalucci D, Condorelli G. Reciprocal regulation of microRNA-1 and insulin-like growth factor-1 signal transduction cascade in cardiac and skeletal muscle in physiological and pathological conditions. *Circulation* 2009; 120: 2377-2385.
296. Winbanks CE, Beyer C, Hagg A, Qian H, Sepulveda PV, Gregorevic P. miR-206 represses hypertrophy of myogenic cells but not muscle fibers via inhibition of HDAC4. *PLoS One* 2013; 8: e73589.

297. Clop A, Marcq F, Takeda H, Pirottin D, Tordoir X, Bibe B, Bouix J, Caiment F, Elsen JM, Eychenne F, Larzul C, Laville E, Meish F, Milenkovic D, Tobin J, Charlier C, Georges M. A mutation creating a potential illegitimate microRNA target site in the myostatin gene affects muscularity in sheep. *Nature genetics* 2006; 38: 813-818.
298. Rachagani S, Cheng Y, Reecy JM. Myostatin genotype regulates muscle-specific miRNA expression in mouse pectoralis muscle. *BMC research notes* 2010; 3: 297.
299. Eisenberg I, Eran A, Nishino I, Moggio M, Lamperti C, Amato AA, Lidov HG, Kang PB, North KN, Mitrani-Rosenbaum S, Flanigan KM, Neely LA, Whitney D, Beggs AH, Kohane IS, Kunkel LM. Distinctive patterns of microRNA expression in primary muscular disorders. *Proc Natl Acad Sci U S A* 2007; 104: 17016-17021.
300. McCarthy JJ, Esser KA, Andrade FH. MicroRNA-206 is overexpressed in the diaphragm but not the hindlimb muscle of mdx mouse. *Am J Physiol Cell Physiol* 2007; 293: C451-457.
301. Georgantas RW, Streicher K, Greenberg SA, Greenlees L, Zhu W, Brohawn P, Higgs BW, Czapiga M, Morehouse C, Amato A, Richman L, Jallal B, Yao Y, Ranade K. Inhibition of myogenic MicroRNAs-1, 133, and 206 by inflammatory cytokines links inflammation and muscle degeneration in adult inflammatory myopathies. *Arthritis and rheumatism* 2013.
302. Lewis A, Riddoch-Contreras J, Natanek SA, Donaldson A, Man WD, Moxham J, Hopkinson NS, Polkey MI, Kemp PR. Downregulation of the serum response factor/miR-1 axis in the quadriceps of patients with COPD. *Thorax* 2012; 67: 26-34.
303. Greco S, De Simone M, Colussi C, Zaccagnini G, Fasanaro P, Pescatori M, Cardani R, Perbellini R, Isaia E, Sale P, Meola G, Capogrossi MC, Gaetano C, Martelli F. Common micro-RNA signature in skeletal muscle damage and regeneration induced by Duchenne muscular dystrophy and acute ischemia. *FASEB J* 2009; 23: 3335-3346.
304. Gambardella S, Rinaldi F, Lepore SM, Viola A, Loro E, Angelini C, Vergani L, Novelli G, Botta A. Overexpression of microRNA-206 in the skeletal muscle from myotonic dystrophy type 1 patients. *Journal of translational medicine* 2010; 8: 48.
305. Hu J, Kong M, Ye Y, Hong S, Cheng L, Jiang L. Serum miR-206 and other muscle-specific microRNAs as non-invasive biomarkers for Duchenne muscular dystrophy. *Journal of neurochemistry* 2014; 129: 877-883.
306. Campbell IT, Watt T, Withers D, England R, Sukumar S, Keegan MA, Faragher B, Martin DF. Muscle Thickness, Measured with Ultrasound, May Be an Indicator of Lean Tissue Wasting in Multiple Organ Failure in the Presence of Edema. *Am J Clin Nutr* 1995; 62: 533-539.
307. Shrikrishna D, Patel M, Tanner RJ, Seymour JM, Connolly BA, Puthucheary ZA, Walsh SL, Bloch SA, Sidhu PS, Hart N, Kemp PR, Moxham J, Polkey MI, Hopkinson NS. Quadriceps wasting and physical inactivity in patients with COPD. *Eur Respir J* 2012.
308. Connolly BA, Jones GD, Curtis AA, Murphy PB, Douiri A, Hopkinson NS, Polkey MI, Moxham J, Hart N. Clinical predictive value of manual muscle strength testing during critical illness: an observational cohort study. *Crit Care* 2013; 17: R229.
309. Edwards RH, Young A, Hosking GP, Jones DA. Human skeletal muscle function: description of tests and normal values. *Clinical science and molecular medicine* 1977; 52: 283-290.
310. Nashef SA, Roques F, Michel P, Gauducheau E, Lemeshow S, Salamon R. European system for cardiac operative risk evaluation (EuroSCORE). *Eur J Cardiothorac Surg* 1999; 16: 9-13.
311. Messaoudi N, De Cocker J, Stockman BA, Bossaert LL, Rodrigus IE. Is EuroSCORE useful in the prediction of extended intensive care unit stay after cardiac surgery? *Eur J Cardiothorac Surg* 2009; 36: 35-39.
312. Roques F, Nashef SA, Michel P, Gauducheau E, de Vincentiis C, Baudet E, Cortina J, David M, Faichney A, Gabrielle F, Gams E, Harjula A, Jones MT, Pintor PP, Salamon R, Thulin L. Risk factors and outcome in European cardiac surgery: analysis of the EuroSCORE

multinational database of 19030 patients. *Eur J Cardiothorac Surg* 1999; 15: 816-822; discussion 822-813.
313. Vincent JL, de Mendonca A, Cantraine F, Moreno R, Takala J, Suter PM, Sprung CL, Colardyn F, Blecher S. Use of the SOFA score to assess the incidence of organ dysfunction/failure in intensive care units: results of a multicenter, prospective study. Working group on "sepsis-related problems" of the European Society of Intensive Care Medicine. *Crit Care Med* 1998; 26: 1793-1800.
314. Minne L, Abu-Hanna A, de Jonge E. Evaluation of SOFA-based models for predicting mortality in the ICU: A systematic review. *Crit Care* 2008; 12: R161.
315. Niewinski G. Prognostic scoring systems for mortality in intensive care units - the APACHE model. *Anaesthesiology intensive therapy* 2014; 46: 46-49.
316. Ferreira FL, Bota DP, Bross A, Melot C, Vincent JL. Serial evaluation of the SOFA score to predict outcome in critically ill patients. *JAMA* 2001; 286: 1754-1758.
317. Bergstrom J. Percutaneous needle biopsy of skeletal muscle in physiological and clinical research. *Scand J Clin Lab Invest* 1975; 35: 609-616.
318. Kumar A, Murphy R, Robinson P, Wei L, Boriek AM. Cyclic mechanical strain inhibits skeletal myogenesis through activation of focal adhesion kinase, Rac-1 GTPase, and NF-kappaB transcription factor. *FASEB J* 2004; 18: 1524-1535.
319. Chandran R, Knobloch TJ, Anghelina M, Agarwal S. Biomechanical signals upregulate myogenic gene induction in the presence or absence of inflammation. *Am J Physiol Cell Physiol* 2007; 293: C267-276.
320. Schaffer JL, Rizen M, L'Italien GJ, Benbrahim A, Megerman J, Gerstenfeld LC, Gray ML. Device for the application of a dynamic biaxially uniform and isotropic strain to a flexible cell culture membrane. *Journal of orthopaedic research : official publication of the Orthopaedic Research Society* 1994; 12: 709-719.
321. Gilbert JA, Weinhold PS, Banes AJ, Link GW, Jones GL. Strain profiles for circular cell culture plates containing flexible surfaces employed to mechanically deform cells in vitro. *Journal of biomechanics* 1994; 27: 1169-1177.
322. Mosmann T. Rapid colorimetric assay for cellular growth and survival: application to proliferation and cytotoxicity assays. *Journal of immunological methods* 1983; 65: 55-63.
323. Passey S, Martin N, Player D, Lewis MP. Stretching skeletal muscle in vitro: does it replicate in vivo physiology? *Biotechnology letters* 2011; 33: 1513-1521.
324. Burkholder TJ. Permeability of C2C12 myotube membranes is influenced by stretch velocity. *Biochemical and biophysical research communications* 2003; 305: 266-270.
325. Serrano A, Baeza-Raja B, Perdiguero E, Jardí M, Muñoz-Cánoves P. Interleukin-6 is an essential regulator of satellite cell-mediated skeletal muscle hypertrophy. *Cell Metab* 2008; 7: 33-44.
326. Pinhu L, Park JE, Yao W, Griffiths MJ. Reference gene selection for real-time polymerase chain reaction in human lung cells subjected to cyclic mechanical strain. *Respirology* 2008; 13: 990-999.
327. Kroh EM, Parkin RK, Mitchell PS, Tewari M. Analysis of circulating microRNA biomarkers in plasma and serum using quantitative reverse transcription-PCR (qRT-PCR). *Methods* 2010; 50: 298-301.
328. Andersen CL, Jensen JL, Orntoft TF. Normalization of real-time quantitative reverse transcription-PCR data: a model-based variance estimation approach to identify genes suited for normalization, applied to bladder and colon cancer data sets. *Cancer Res* 2004; 64: 5245-5250.
329. Elliott B, Renshaw D, Getting S, Mackenzie R. The central role of myostatin in skeletal muscle and whole body homeostasis. *Acta Physiol (Oxf)* 2012; 205: 324-340.

330. Gruson D, Ahn SA, Ketelslegers JM, Rousseau MF. Increased plasma myostatin in heart failure. *Eur J Heart Fail* 2011; 13: 734-736.
331. Garcia PS, Cabbabe A, Kambadur R, Nicholas G, Csete M. Brief-reports: elevated myostatin levels in patients with liver disease: a potential contributor to skeletal muscle wasting. *Anesth Analg* 2010; 111: 707-709.
332. Constantin D, McCullough J, Mahajan RP, Greenhaff PL. Novel events in the molecular regulation of muscle mass in critically ill patients. *J Physiol* 2011; 589: 3883-3895.
333. Bloch SA, Lee JY, Wort SJ, Polkey MI, Kemp PR, Griffiths MJ. Sustained elevation of circulating growth and differentiation factor-15 and a dynamic imbalance in mediators of muscle homeostasis are associated with the development of acute muscle wasting following cardiac surgery. *Crit Care Med* 2013; 41: 982-989.
334. Han DS, Chen YM, Lin SY, Chang HH, Huang TM, Chi YC, Yang WS. Serum myostatin levels and grip strength in normal subjects and patients on maintenance haemodialysis. *Clin Endocrinol (Oxf)* 2011; 75: 857-863.
335. Ju CR, Chen RC. Serum myostatin levels and skeletal muscle wasting in chronic obstructive pulmonary disease. *Respir Med* 2012; 106: 102-108.
336. Lang CH, Silvis C, Nystrom G, Frost RA. Regulation of myostatin by glucocorticoids after thermal injury. *FASEB J* 2001; 15: 1807-1809.
337. Llano-Diez M, Gustafson AM, Olsson C, Goransson H, Larsson L. Muscle wasting and the temporal gene expression pattern in a novel rat intensive care unit model. *BMC Genomics* 2011; 12: 602.
338. Smith IJ, Aversa Z, Alamdari N, Petkova V, Hasselgren PO. Sepsis downregulates myostatin mRNA levels without altering myostatin protein levels in skeletal muscle. *J Cell Biochem* 2010; 111: 1059-1073.
339. Vanhara P, Hampl A, Kozubik A, Soucek K. Growth/differentiation factor-15: prostate cancer suppressor or promoter? *Prostate Cancer Prostatic Dis* 2012 Epub date 2012/03/01.
340. Meadows CA, Risbano MG, Zhang L, Geraci MW, Tuder RM, Collier DH, Bull TM. Increased expression of growth differentiation factor-15 in systemic sclerosis-associated pulmonary arterial hypertension. *Chest* 2011; 139: 994-1002.
341. Schiegnitz E, Kammerer PW, Koch FP, Kruger M, Berres M, Al-Nawas B. GDF 15 as an anti-apoptotic, diagnostic and prognostic marker in oral squamous cell carcinoma. *Oral Oncol* 2012; 48: 608-614.
342. Anselmi A, Abbate A, Girola F, Nasso G, Biondi-Zoccai GG, Possati G, Gaudino M. Myocardial ischemia, stunning, inflammation, and apoptosis during cardiac surgery: a review of evidence. *Eur J Cardiothorac Surg* 2004; 25: 304-311.
343. Bhushan R, Grunhagen J, Becker J, Robinson PN, Ott CE, Knaus P. miR-181a promotes osteoblastic differentiation through repression of TGF-beta signaling molecules. *Int J Biochem Cell Biol* 2013; 45: 696-705.
344. Shan H, Zhang Y, Lu Y, Zhang Y, Pan Z, Cai B, Wang N, Li X, Feng T, Hong Y, Yang B. Downregulation of miR-133 and miR-590 contributes to nicotine-induced atrial remodelling in canines. *Cardiovascular research* 2009; 83: 465-472.
345. Sun Y, Ge Y, Drnevich J, Zhao Y, Band M, Chen J. Mammalian target of rapamycin regulates miRNA-1 and follistatin in skeletal myogenesis. *The Journal of cell biology* 2010; 189: 1157-1169.
346. McCarthy JJ, Esser KA, Peterson CA, Dupont-Versteegden EE. Evidence of MyomiR network regulation of beta-myosin heavy chain gene expression during skeletal muscle atrophy. *Physiological genomics* 2009; 39: 219-226.
347. Li J, Yang L, Qin W, Zhang G, Yuan J, Wang F. Adaptive induction of growth differentiation factor 15 attenuates endothelial cell apoptosis in response to high glucose stimulus. *PLoS One* 2013; 8: e65549.

348. Fuchtbauer EM, Westphal H. MyoD and myogenin are coexpressed in regenerating skeletal muscle of the mouse. *Developmental dynamics : an official publication of the American Association of Anatomists* 1992; 193: 34-39.
349. Parisi MS, Gazzerro E, Rydziel S, Canalis E. Expression and regulation of CCN genes in murine osteoblasts. *Bone* 2006; 38: 671-677.
350. de Boer MD, Selby A, Atherton P, Smith K, Seynnes OR, Maganaris CN, Maffulli N, Movin T, Narici MV, Rennie MJ. The temporal responses of protein synthesis, gene expression and cell signalling in human quadriceps muscle and patellar tendon to disuse. *J Physiol* 2007; 585: 241-251.
351. Biolo G, Fleming RY, Maggi SP, Nguyen TT, Herndon DN, Wolfe RR. Inverse regulation of protein turnover and amino acid transport in skeletal muscle of hypercatabolic patients. *J Clin Endocrinol Metab* 2002; 87: 3378-3384.
352. Huang MB, Xu H, Xie SJ, Zhou H, Qu LH. Insulin-like growth factor-1 receptor is regulated by microRNA-133 during skeletal myogenesis. *PLoS One* 2011; 6: e29173.
353. Dweep H, Sticht C, Pandey P, Gretz N. miRWalk--database: prediction of possible miRNA binding sites by "walking" the genes of three genomes. *Journal of biomedical informatics* 2011; 44: 839-847.
354. Huang da W, Sherman BT, Lempicki RA. Systematic and integrative analysis of large gene lists using DAVID bioinformatics resources. *Nature protocols* 2009; 4: 44-57.
355. Huang da W, Sherman BT, Lempicki RA. Bioinformatics enrichment tools: paths toward the comprehensive functional analysis of large gene lists. *Nucleic acids research* 2009; 37: 1-13.
356. Lobel M, Bauer S, Meisel C, Eisenreich A, Kudernatsch R, Tank J, Rauch U, Kuhl U, Schultheiss HP, Volk HD, Poller W, Scheibenbogen C. CCN1: a novel inflammation-regulated biphasic immune cell migration modulator. *Cellular and molecular life sciences : CMLS* 2012; 69: 3101-3113.
357. Di Giovanni S, Molon A, Broccolini A, Melcon G, Mirabella M, Hoffman EP, Servidei S. Constitutive activation of MAPK cascade in acute quadriplegic myopathy. *Ann Neurol* 2004; 55: 195-206.
358. Nakasa T, Ishikawa M, Shi M, Shibuya H, Adachi N, Ochi M. Acceleration of muscle regeneration by local injection of muscle-specific microRNAs in rat skeletal muscle injury model. *Journal of cellular and molecular medicine* 2010; 14: 2495-2505.
359. Sibley CR, Wood MJ. The miRNA pathway in neurological and skeletal muscle disease: implications for pathogenesis and therapy. *Journal of molecular medicine* 2011; 89: 1065-1077.
360. Lu J, McKinsey TA, Zhang CL, Olson EN. Regulation of skeletal myogenesis by association of the MEF2 transcription factor with class II histone deacetylases. *Mol Cell* 2000; 6: 233-244.
361. Buckingham M, Rigby PW. Gene regulatory networks and transcriptional mechanisms that control myogenesis. *Developmental cell* 2014; 28: 225-238.
362. Latronico N, Bolton CF. Critical illness polyneuropathy and myopathy: a major cause of muscle weakness and paralysis. *Lancet Neurol* 2011; 10: 931-941.
363. Heringlake M, Charitos EI, Gatz N, Kabler JH, Beilharz A, Holz D, Schon J, Paarmann H, Petersen M, Hanke T. Growth differentiation factor 15: a novel risk marker adjunct to the EuroSCORE for risk stratification in cardiac surgery patients. *Journal of the American College of Cardiology* 2013; 61: 672-681.
364. Li JB, Goldberg AL. Effects of food deprivation on protein synthesis and degradation in rat skeletal muscles. *The American journal of physiology* 1976; 231: 441-448.
365. Bohe J, Low A, Wolfe RR, Rennie MJ. Human muscle protein synthesis is modulated by extracellular, not intramuscular amino acid availability: a dose-response study. *J Physiol* 2003; 552: 315-324.

366. Schweickert WD, Pohlman MC, Pohlman AS, Nigos C, Pawlik AJ, Esbrook CL, Spears L, Miller M, Franczyk M, Deprizio D, Schmidt GA, Bowman A, Barr R, McCallister KE, Hall JB, Kress JP. Early physical and occupational therapy in mechanically ventilated, critically ill patients: a randomised controlled trial. *Lancet* 2009; 373: 1874-1882.
367. Hanekom S, Gosselink R, Dean E, van Aswegen H, Roos R, Ambrosino N, Louw Q. The development of a clinical management algorithm for early physical activity and mobilization of critically ill patients: synthesis of evidence and expert opinion and its translation into practice. *Clinical rehabilitation* 2011; 25: 771-787.
368. Maffiuletti NA, Minetto MA, Farina D, Bottinelli R. Electrical stimulation for neuromuscular testing and training: state-of-the art and unresolved issues. *Eur J Appl Physiol* 2011; 111: 2391-2397.
369. Edwards Jea. Electrcial muscle stimulation in the intensive care unit: an integrative review. *Journal of intensive care society* 2014; 15.
370. Goldspink G. Changes in muscle mass and phenotype and the expression of autocrine and systemic growth factors by muscle in response to stretch and overload. *J Anat* 1999; 194 (Pt 3): 323-334.
371. Ottenheijm CA, Granzier H. Role of titin in skeletal muscle function and disease. *Adv Exp Med Biol* 2010; 682: 105-122.
372. Ottenheijm CA, van Hees HW, Heunks LM, Granzier H. Titin-based mechanosensing and signaling: role in diaphragm atrophy during unloading? *American journal of physiology Lung cellular and molecular physiology* 2011; 300: L161-166.
373. Abe S, Rhee S, Iwanuma O, Hiroki E, Yanagisawa N, Sakiyama K, Ide Y. Effect of mechanical stretching on expressions of muscle specific transcription factors MyoD, Myf-5, myogenin and MRF4 in proliferated myoblasts. *Anatomia, histologia, embryologia* 2009; 38: 305-310.
374. Vandenburgh H, Kaufman S. In vitro model for stretch-induced hypertrophy of skeletal muscle. *Science* 1979; 203: 265-268.
375. Powell CA, Smiley BL, Mills J, Vandenburgh HH. Mechanical stimulation improves tissue-engineered human skeletal muscle. *Am J Physiol Cell Physiol* 2002; 283: C1557-1565.
376. Sasai N, Agata N, Inoue-Miyazu M, Kawakami K, Kobayashi K, Sokabe M, Hayakawa K. Involvement of PI3K/Akt/TOR pathway in stretch-induced hypertrophy of myotubes. *Muscle Nerve* 2010; 41: 100-106.
377. Rauch C, Loughna PT. Cyclosporin-A inhibits stretch-induced changes in myosin heavy chain expression in C2C12 skeletal muscle cells. *Cell Biochem Funct* 2006; 24: 55-61.
378. Soltow QA, Zeanah EH, Lira VA, Criswell DS. Cessation of cyclic stretch induces atrophy of C2C12 myotubes. *Biochemical and biophysical research communications* 2013; 434: 316-321.
379. Nakai N, Kawano F, Oke Y, Nomura S, Ohira T, Fujita R, Ohira Y. Mechanical stretch activates signaling events for protein translation initiation and elongation in C2C12 myoblasts. *Mol Cells* 2010; 30: 513-518.
380. Chambers MA, Moylan JS, Smith JD, Goodyear LJ, Reid MB. Stretch-stimulated glucose uptake in skeletal muscle is mediated by reactive oxygen species and p38 MAP-kinase. *J Physiol* 2009; 587: 3363-3373.
381. Crevenna R, Mayr W, Keilani M, Pleiner J, Nuhr M, Quittan M, Pacher R, Fialka-Moser V, Wolzt M. Safety of a combined strength and endurance training using neuromuscular electrical stimulation of thigh muscles in patients with heart failure and bipolar sensing cardiac pacemakers. *Wiener klinische Wochenschrift* 2003; 115: 710-714.
382. Wiesinger GF, Crevenna R, Nuhr MJ, Huelsmann M, Fialka-Moser V, Quittan M. Neuromuscular electric stimulation in heart transplantation candidates with cardiac pacemakers. *Archives of physical medicine and rehabilitation* 2001; 82: 1476-1477.

383. Maffiuletti NA. Physiological and methodological considerations for the use of neuromuscular electrical stimulation. *Eur J Appl Physiol* 2010; 110: 223-234.
384. Doucet BM, Lam A, Griffin L. Neuromuscular electrical stimulation for skeletal muscle function. *The Yale journal of biology and medicine* 2012; 85: 201-215.
385. Weber-Carstens S, Koch S, Spuler S, Spies CD, Bubser F, Wernecke KD, Deja M. Nonexcitable muscle membrane predicts intensive care unit-acquired paresis in mechanically ventilated, sedated patients. *Crit Care Med* 2009; 37: 2632-2637.
386. Poulsen JB, Moller K, Jensen CV, Weisdorf S, Kehlet H, Perner A. Effect of transcutaneous electrical muscle stimulation on muscle volume in patients with septic shock. *Crit Care Med* 2011; 39: 456-461.
387. Gruther W, Kainberger F, Fialka-Moser V, Paternostro-Sluga T, Quittan M, Spiss C, Crevenna R. Effects of neuromuscular electrical stimulation on muscle layer thickness of knee extensor muscles in intensive care unit patients: a pilot study. *Journal of rehabilitation medicine* 2010; 42: 593-597.
388. Gerovasili V, Stefanidis K, Vitzilaios K, Karatzanos E, Politis P, Koroneos A, Chatzimichail A, Routsi C, Roussos C, Nanas S. Electrical muscle stimulation preserves the muscle mass of critically ill patients: a randomized study. *Crit Care* 2009; 13: R161.
389. Meesen RL, Dendale P, Cuypers K, Berger J, Hermans A, Thijs H, Levin O. Neuromuscular electrical stimulation as a possible means to prevent muscle tissue wasting in artificially ventilated and sedated patients in the intensive care unit: A pilot study. *Neuromodulation : journal of the International Neuromodulation Society* 2010; 13: 315-320; discussion 321.
390. Routsi C, Gerovasili V, Vasileiadis I, Karatzanos E, Pitsolis T, Tripodaki E, Markaki V, Zervakis D, Nanas S. Electrical muscle stimulation prevents critical illness polyneuromyopathy: a randomized parallel intervention trial. *Crit Care* 2010; 14: R74.
391. Rodriguez PO, Setten M, Maskin LP, Bonelli I, Vidomlansky SR, Attie S, Frosiani SL, Kozima S, Valentini R. Muscle weakness in septic patients requiring mechanical ventilation: protective effect of transcutaneous neuromuscular electrical stimulation. *Journal of critical care* 2012; 27: 319 e311-318.
392. Karatzanos E, Gerovasili V, Zervakis D, Tripodaki ES, Apostolou K, Vasileiadis I, Papadopoulos E, Mitsiou G, Tsimpouki D, Routsi C, Nanas S. Electrical muscle stimulation: an effective form of exercise and early mobilization to preserve muscle strength in critically ill patients. *Critical care research and practice* 2012; 2012: 432752.
393. Gerovasili V, Tripodaki E, Karatzanos E, Pitsolis T, Markaki V, Zervakis D, Routsi C, Roussos C, Nanas S. Short-term systemic effect of electrical muscle stimulation in critically ill patients. *Chest* 2009; 136: 1249-1256.
394. Bouletreau P, Patricot MC, Saudin F, Guiraud M, Mathian B. Effects of intermittent electrical stimulations on muscle catabolism in intensive care patients. *JPEN Journal of parenteral and enteral nutrition* 1987; 11: 552-555.
395. Vivodtzev I, Debigare R, Gagnon P, Mainguy V, Saey D, Dube A, Pare ME, Belanger M, Maltais F. Functional and muscular effects of neuromuscular electrical stimulation in patients with severe COPD: a randomized clinical trial. *Chest* 2012; 141: 716-725.
396. Sillen MJ, Franssen FM, Gosker HR, Wouters EF, Spruit MA. Metabolic and structural changes in lower-limb skeletal muscle following neuromuscular electrical stimulation: a systematic review. *PLoS One* 2013; 8: e69391.
397. Strasser EM, Stattner S, Karner J, Klimpfinger M, Freynhofer M, Zaller V, Graf A, Wessner B, Bachl N, Roth E, Quittan M. Neuromuscular electrical stimulation reduces skeletal muscle protein degradation and stimulates insulin-like growth factors in an age- and current-dependent manner: a randomized, controlled clinical trial in major abdominal surgical patients. *Ann Surg* 2009; 249: 738-743.

398. Vinge O, Edvardsen L, Jensen F, Jensen FG, Wernerman J, Kehlet H. Effect of transcutaneous electrical muscle stimulation on postoperative muscle mass and protein synthesis. *Br J Surg* 1996; 83: 360-363.
399. Jubeau M, Sartorio A, Marinone PG, Agosti F, Van Hoecke J, Nosaka K, Maffiuletti NA. Comparison between voluntary and stimulated contractions of the quadriceps femoris for growth hormone response and muscle damage. *Journal of applied physiology* 2008; 104: 75-81.
400. Mackey AL, Bojsen-Moller J, Qvortrup K, Langberg H, Suetta C, Kalliokoski KK, Kjaer M, Magnusson SP. Evidence of skeletal muscle damage following electrically stimulated isometric muscle contractions in humans. *Journal of applied physiology* 2008; 105: 1620-1627.
401. van Rooij E, Liu N, Olson EN. MicroRNAs flex their muscles. *Trends in genetics : TIG* 2008; 24: 159-166.
402. Townley-Tilson WH, Callis TE, Wang D. MicroRNAs 1, 133, and 206: critical factors of skeletal and cardiac muscle development, function, and disease. *Int J Biochem Cell Biol* 2010; 42: 1252-1255.
403. Russell AP, Lamon S, Boon H, Wada S, Guller I, Brown EL, Chibalin AV, Zierath JR, Snow RJ, Stepto N, Wadley GD, Akimoto T. Regulation of miRNAs in human skeletal muscle following acute endurance exercise and short-term endurance training. *J Physiol* 2013; 591: 4637-4653.
404. Nielsen S, Scheele C, Yfanti C, Akerstrom T, Nielsen AR, Pedersen BK, Laye MJ. Muscle specific microRNAs are regulated by endurance exercise in human skeletal muscle. *J Physiol* 2010; 588: 4029-4037.
405. Drummond MJ, McCarthy JJ, Fry CS, Esser KA, Rasmussen BB. Aging differentially affects human skeletal muscle microRNA expression at rest and after an anabolic stimulus of resistance exercise and essential amino acids. *Am J Physiol Endocrinol Metab* 2008; 295: E1333-1340.
406. Keller P, Vollaard NB, Gustafsson T, Gallagher IJ, Sundberg CJ, Rankinen T, Britton SL, Bouchard C, Koch LG, Timmons JA. A transcriptional map of the impact of endurance exercise training on skeletal muscle phenotype. *Journal of applied physiology* 2011; 110: 46-59.
407. Steiner MC, Roubenoff R, Tal-Singer R, Polkey MI. Prospects for the development of effective pharmacotherapy targeted at the skeletal muscles in chronic obstructive pulmonary disease: a translational review. *Thorax* 2012; 67: 1102-1109.
408. Van Roosbroeck K, Pollet J, Calin GA. miRNAs and long noncoding RNAs as biomarkers in human diseases. *Expert review of molecular diagnostics* 2013; 13: 183-204.
409. Lawrie CH, Gal S, Dunlop HM, Pushkaran B, Liggins AP, Pulford K, Banham AH, Pezzella F, Boultwood J, Wainscoat JS, Hatton CS, Harris AL. Detection of elevated levels of tumour-associated microRNAs in serum of patients with diffuse large B-cell lymphoma. *British journal of haematology* 2008; 141: 672-675.
410. Hu G, Drescher KM, Chen XM. Exosomal miRNAs: Biological Properties and Therapeutic Potential. *Frontiers in genetics* 2012; 3: 56.
411. Mitchell PS, Parkin RK, Kroh EM, Fritz BR, Wyman SK, Pogosova-Agadjanyan EL, Peterson A, Noteboom J, O'Briant KC, Allen A, Lin DW, Urban N, Drescher CW, Knudsen BS, Stirewalt DL, Gentleman R, Vessella RL, Nelson PS, Martin DB, Tewari M. Circulating microRNAs as stable blood-based markers for cancer detection. *Proc Natl Acad Sci U S A* 2008; 105: 10513-10518.
412. De Guire V, Robitaille R, Tetreault N, Guerin R, Menard C, Bambace N, Sapieha P. Circulating miRNAs as sensitive and specific biomarkers for the diagnosis and monitoring of human diseases: promises and challenges. *Clinical biochemistry* 2013; 46: 846-860.

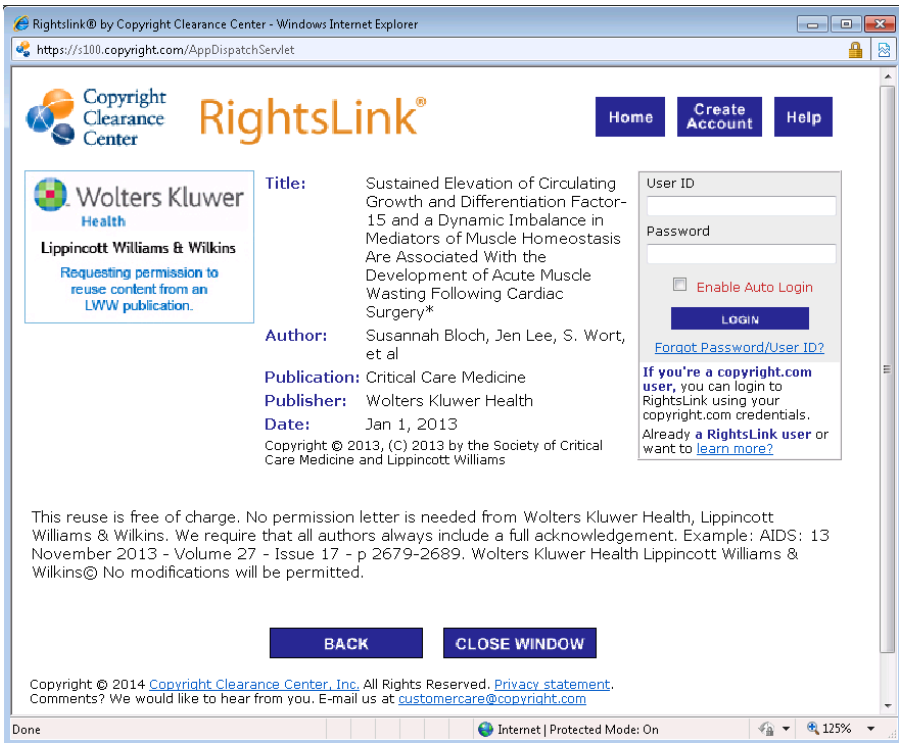
413. Deddens JC, Colijn JM, Oerlemans MI, Pasterkamp G, Chamuleau SA, Doevendans PA, Sluijter JP. Circulating MicroRNAs as Novel Biomarkers for the Early Diagnosis of Acute Coronary Syndrome. *Journal of cardiovascular translational research* 2013; 6: 884-898.
414. Perfetti A, Greco S, Bugiardini E, Cardani R, Gaia P, Gaetano C, Meola G, Martelli F. Plasma microRNAs as biomarkers for myotonic dystrophy type 1. *Neuromuscular disorders : NMD* 2014; 24: 509-515.
415. Toivonen JM, Manzano R, Olivan S, Zaragoza P, Garcia-Redondo A, Osta R. MicroRNA-206: a potential circulating biomarker candidate for amyotrophic lateral sclerosis. *PLoS One* 2014; 9: e89065.
416. Miyachi M, Tsuchiya K, Yoshida H, Yagyu S, Kikuchi K, Misawa A, Iehara T, Hosoi H. Circulating muscle-specific microRNA, miR-206, as a potential diagnostic marker for rhabdomyosarcoma. *Biochemical and biophysical research communications* 2010; 400: 89-93.
417. Donaldson A, Natanek SA, Lewis A, Man WD, Hopkinson NS, Polkey MI, Kemp PR. Increased skeletal muscle-specific microRNA in the blood of patients with COPD. *Thorax* 2013; 68: 1140-1149.
418. Zhou X, Wang JL, Lu J, Song Y, Kwak KS, Jiao Q, Rosenfeld R, Chen Q, Boone T, Simonet WS, Lacey DL, Goldberg AL, Han HQ. Reversal of cancer cachexia and muscle wasting by ActRIIB antagonism leads to prolonged survival. *Cell* 2010; 142: 531-543.
419. Cadena SM, Tomkinson KN, Monnell TE, Spaits MS, Kumar R, Underwood KW, Pearsall RS, Lachey JL. Administration of a soluble activin type IIB receptor promotes skeletal muscle growth independent of fiber type. *Journal of applied physiology* 2010; 109: 635-642.
420. Hutchison ER, Kawamoto EM, Taub DD, Lal A, Abdelmohsen K, Zhang Y, Wood WH, 3rd, Lehrmann E, Camandola S, Becker KG, Gorospe M, Mattson MP. Evidence for miR-181 involvement in neuroinflammatory responses of astrocytes. *Glia* 2013; 61: 1018-1028.
421. Sun X, Sit A, Feinberg MW. Role of miR-181 family in regulating vascular inflammation and immunity. *Trends in cardiovascular medicine* 2013.
422. Sun X, Icli B, Wara AK, Belkin N, He S, Kobzik L, Hunninghake GM, Vera MP, Registry M, Blackwell TS, Baron RM, Feinberg MW. MicroRNA-181b regulates NF-kappaB-mediated vascular inflammation. *J Clin Invest* 2012; 122: 1973-1990.
423. Wang H, Zhang P, Chen W, Feng D, Jia Y, Xie LX. Evidence for serum miR-15a and miR-16 levels as biomarkers that distinguish sepsis from systemic inflammatory response syndrome in human subjects. *Clinical chemistry and laboratory medicine : CCLM / FESCC* 2012; 50: 1423-1428.
424. McDonald JS, Milosevic D, Reddi HV, Grebe SK, Algeciras-Schimnich A. Analysis of circulating microRNA: preanalytical and analytical challenges. *Clinical chemistry* 2011; 57: 833-840.
425. Ai J, Zhang R, Li Y, Pu J, Lu Y, Jiao J, Li K, Yu B, Li Z, Wang R, Wang L, Li Q, Wang N, Shan H, Li Z, Yang B. Circulating microRNA-1 as a potential novel biomarker for acute myocardial infarction. *Biochemical and biophysical research communications* 2010; 391: 73-77.
426. Ewalenko P, Deloof T, Peeters J. Composition of fresh frozen plasma. *Crit Care Med* 1986; 14: 145-146.
427. Heldin CH, Miyazono K, ten Dijke P. TGF-beta signalling from cell membrane to nucleus through SMAD proteins. *Nature* 1997; 390: 465-471.
428. Jatoi A. Weight loss in patients with advanced cancer: effects, causes, and potential management. *Current opinion in supportive and palliative care* 2008; 2: 45-48.
429. Ebner N, Steinbeck L, Doehner W, Anker SD, von Haehling S. Highlights from the 7th Cachexia Conference: muscle wasting pathophysiological detection and novel treatment strategies. *Journal of cachexia, sarcopenia and muscle* 2014; 5: 27-34.

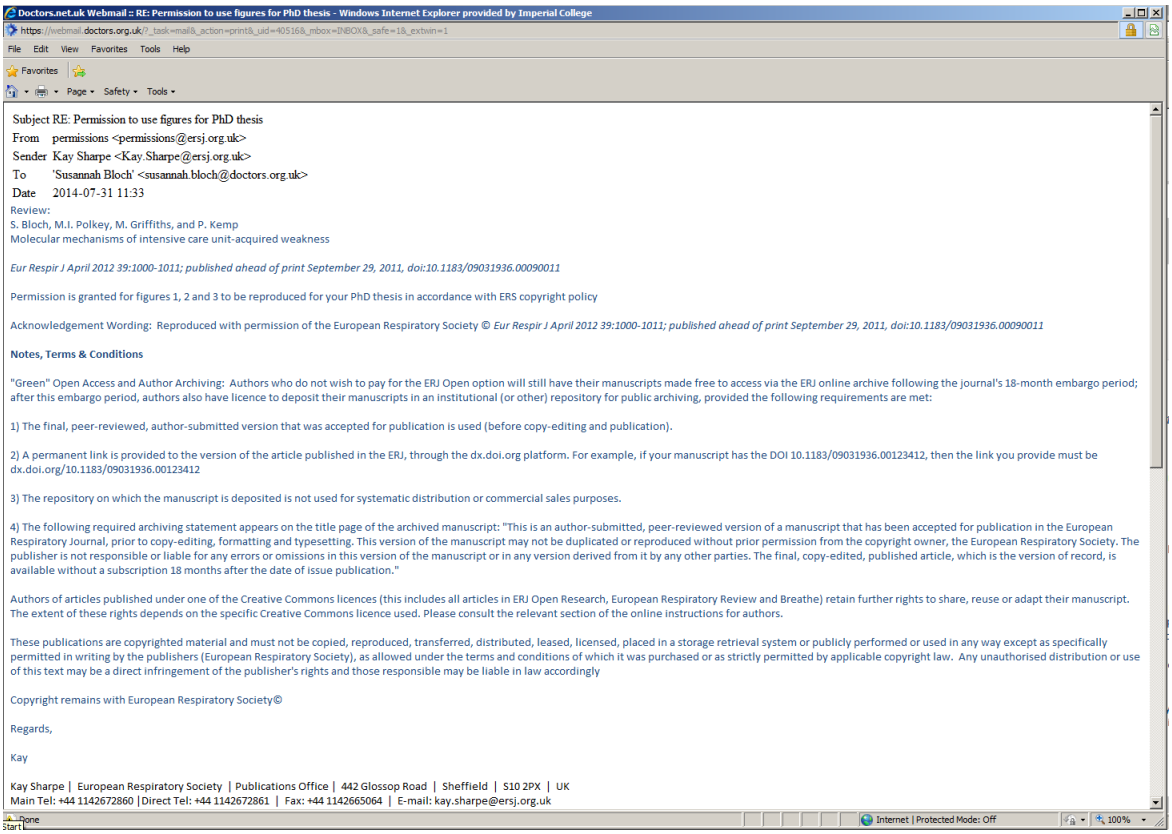
430. van Rooij E, Kauppinen S. Development of microRNA therapeutics is coming of age. *EMBO molecular medicine* 2014; 6: 851-864.
431. Maqbool R, Hussain MU. MicroRNAs and human diseases: diagnostic and therapeutic potential. *Cell and tissue research* 2014.
432. Fortunato O, Boeri M, Verri C, Moro M, Sozzi G. Therapeutic Use of MicroRNAs in Lung Cancer. *BioMed research international* 2014; 2014: 756975.
433. Trang P, Wiggins JF, Daige CL, Cho C, Omotola M, Brown D, Weidhaas JB, Bader AG, Slack FJ. Systemic delivery of tumor suppressor microRNA mimics using a neutral lipid emulsion inhibits lung tumors in mice. *Molecular therapy : the journal of the American Society of Gene Therapy* 2011; 19: 1116-1122.
434. Trang P, Medina PP, Wiggins JF, Ruffino L, Kelnar K, Omotola M, Homer R, Brown D, Bader AG, Weidhaas JB, Slack FJ. Regression of murine lung tumors by the let-7 microRNA. *Oncogene* 2010; 29: 1580-1587.
435. Esquela-Kerscher A, Trang P, Wiggins JF, Patrawala L, Cheng A, Ford L, Weidhaas JB, Brown D, Bader AG, Slack FJ. The let-7 microRNA reduces tumor growth in mouse models of lung cancer. *Cell cycle* 2008; 7: 759-764.
436. van der Ree MH, van der Meer AJ, de Bruijne J, Maan R, van Vliet A, Welzel TM, Zeuzem S, Lawitz EJ, Rodriguez-Torres M, Kupcova V, Wiercinska-Drapalo A, Hodges MR, Janssen HL, Reesink HW. Long-term safety and efficacy of microRNA-targeted therapy in chronic hepatitis C patients. *Antiviral research* 2014; 111C: 53-59.
437. Pramanik D, Campbell NR, Karikari C, Chivukula R, Kent OA, Mendell JT, Maitra A. Restitution of tumor suppressor microRNAs using a systemic nanovector inhibits pancreatic cancer growth in mice. *Molecular cancer therapeutics* 2011; 10: 1470-1480.
438. Ibrahim AF, Weirauch U, Thomas M, Grunweller A, Hartmann RK, Aigner A. MicroRNA replacement therapy for miR-145 and miR-33a is efficacious in a model of colon carcinoma. *Cancer Res* 2011; 71: 5214-5224.
439. Takeshita F, Patrawala L, Osaki M, Takahashi RU, Yamamoto Y, Kosaka N, Kawamata M, Kelnar K, Bader AG, Brown D, Ochiya T. Systemic delivery of synthetic microRNA-16 inhibits the growth of metastatic prostate tumors via downregulation of multiple cell-cycle genes. *Molecular therapy : the journal of the American Society of Gene Therapy* 2010; 18: 181-187.
440. Kota J, Chivukula RR, O'Donnell KA, Wentzel EA, Montgomery CL, Hwang HW, Chang TC, Vivekanandan P, Torbenson M, Clark KR, Mendell JR, Mendell JT. Therapeutic microRNA delivery suppresses tumorigenesis in a murine liver cancer model. *Cell* 2009; 137: 1005-1017.
441. Miyazaki Y, Adachi H, Katsuno M, Minamiyama M, Jiang YM, Huang Z, Doi H, Matsumoto S, Kondo N, Iida M, Tohnai G, Tanaka F, Muramatsu S, Sobue G. Viral delivery of miR-196a ameliorates the SBMA phenotype via the silencing of CELF2. *Nat Med* 2012; 18: 1136-1141.
442. Xu J, Li R, Workeneh B, Dong Y, Wang X, Hu Z. Transcription factor FoxO1, the dominant mediator of muscle wasting in chronic kidney disease, is inhibited by microRNA-486. *Kidney international* 2012; 82: 401-411.

Appendixes

Appendix A1 – Copy right permissions.

Some of the data and figures in this thesis have been published. I am the first author of all the manuscripts. I was responsible for writing the papers and I produced the figures. The copy right permission for the use of these materials is included below. Where relevant the use of this material is clearly acknowledged in the thesis.





Doctors.net.uk Webmail :: RE: Permission to use figures for PhD thesis - Windows Internet Explorer provided by Imperial College

https://webmail.doctors.org.uk/?_task=mail&_action=print&_uid=40516&_mbox=INBOX&_safe=1&_extwin=1

File Edit View Favorites Tools Help

Favorites

Page Safety Tools

Subject RE: Permission to use figures for PhD thesis
From permissions <permissions@ersj.org.uk>
Sender Kay Sharpe <Kay.Sharpe@ersj.org.uk>
To 'Susannah Bloch' <susannah.bloch@doctors.org.uk>
Date 2014-07-31 11:33

Review:
S. Bloch, M.I. Polkey, M. Griffiths, and P. Kemp
Molecular mechanisms of intensive care unit-acquired weakness

Eur Respir J April 2012 39:1000-1011; published ahead of print September 29, 2011, doi:10.1183/09031936.00090011

Permission is granted for figures 1, 2 and 3 to be reproduced for your PhD thesis in accordance with ERS copyright policy

Acknowledgement Wording: Reproduced with permission of the European Respiratory Society © *Eur Respir J April 2012 39:1000-1011; published ahead of print September 29, 2011, doi:10.1183/09031936.00090011*

Notes, Terms & Conditions

"Green" Open Access and Author Archiving: Authors who do not wish to pay for the ERJ Open option will still have their manuscripts made free to access via the ERJ online archive following the journal's 18-month embargo period; after this embargo period, authors also have licence to deposit their manuscripts in an institutional (or other) repository for public archiving, provided the following requirements are met:

1) The final, peer-reviewed, author-submitted version that was accepted for publication is used (before copy-editing and publication).

2) A permanent link is provided to the version of the article published in the ERJ, through the dx.doi.org platform. For example, if your manuscript has the DOI 10.1183/09031936.00123412, then the link you provide must be dx.doi.org/10.1183/09031936.00123412

3) The repository on which the manuscript is deposited is not used for systematic distribution or commercial sales purposes.

4) The following required archiving statement appears on the title page of the archived manuscript: "This is an author-submitted, peer-reviewed version of a manuscript that has been accepted for publication in the European Respiratory Journal, prior to copy-editing, formatting and typesetting. This version of the manuscript may not be duplicated or reproduced without prior permission from the copyright owner, the European Respiratory Society. The publisher is not responsible or liable for any errors or omissions in this version of the manuscript or in any version derived from it by any other parties. The final, copy-edited, published article, which is the version of record, is available without a subscription 18 months after the date of issue publication."

Authors of articles published under one of the Creative Commons licences (this includes all articles in ERJ Open Research, European Respiratory Review and Breathe) retain further rights to share, reuse or adapt their manuscript. The extent of these rights depends on the specific Creative Commons licence used. Please consult the relevant section of the online instructions for authors.

These publications are copyrighted material and must not be copied, reproduced, transferred, distributed, leased, licensed, placed in a storage retrieval system or publicly performed or used in any way except as specifically permitted in writing by the publishers (European Respiratory Society), as allowed under the terms and conditions of which it was purchased or as strictly permitted by applicable copyright law. Any unauthorised distribution or use of this text may be a direct infringement of the publisher's rights and those responsible may be liable in law accordingly

Copyright remains with European Respiratory Society©

Regards,

Kay

Kay Sharpe | European Respiratory Society | Publications Office | 442 Glossop Road | Sheffield | S10 2PX | UK
Main Tel: +44 1142672860 | Direct Tel: +44 1142672861 | Fax: +44 1142665064 | E-mail: kay.sharpe@ersj.org.uk

Done

Internet | Protected Mode: Off

100%



Rightslink® by Copyright Clearance Center - Windows Internet Explorer provided by Imperial College Healthcare

Copyright Clearance Center RightsLink®

Home Create Account Help Live Chat

BMJ

Title: Increased expression of GDF-15 may mediate ICU-acquired weakness by down-regulating muscle microRNAs

Author: S A A Bloch, J Y Lee, T Syburra, U Rosendahl, M J D Griffiths, P R Kemp, M I Polkey

Publication: Thorax

Publisher: BMJ Publishing Group Ltd.

Date: Dec 16, 2014

Copyright © 2014, BMJ Publishing Group Ltd and the British Thoracic Society

LOGIN

If you're a copyright.com user, you can login to RightsLink using your copyright.com credentials.

Already a RightsLink user or want to learn more?

Welcome to Rightslink

Important notice – please read.
This article is Open Access, published under the terms of a Creative Commons licence. Please refer back to the article to check the applicable licence (details are in the article Footnotes). Articles published under CC-BY-NC permit non-commercial use, distribution and reproduction in any medium, provided the original work is properly cited. Permission only needs to be obtained for commercial use and can be done via the RightsLink system below. Articles published under the CC-BY permit unrestricted use, distribution and reproduction in any medium, provided the original work is properly cited.

BMJ Publishing Group Ltd. has partnered with Copyright Clearance Center's Rightslink service to offer a variety of options for reusing BMJ Publishing Group content. Select the "I would like to ..." drop-down menu to view the many reuse options available to you.

I would like to... make a selection

Done

Internet | Protected Mode: Off

100%

Appendix A2 – MicroRNA Array Results

Differentiating myoblasts - 6 hour microRNA Array results

Significant hits from the microRNA Array of treatment of differentiating C2C12 myotblasts with GDF-15 and myostatin for 6 hours. (See Chapter 4 for more details).

GDF-15 (50ng/ml)			Myostatin (20ng/ml)		
Gene	Ratio	p val diff	Gene	Ratio	p val diff
Arpc1b	1.46357	0.000178	Smarcd3	0.760198	0.004177
Tsc22d1	1.282381	0.000729	Ch25h	1.383599	0.004441
Mmp15	0.778498	0.001069	**Ctgf ***	1.308946	0.022152
Adamts4	0.804531	0.002023	Fus	1.503563	0.022152
Eif4ebp2 *	0.782102	0.002023	Yrdc	1.350923	0.028957
Lig3	0.802163	0.004549	Myh1	0.720727	0.044779
Bicd2	0.814289	0.005154			
Ch25h	1.312247	0.005405			
Nedd9	0.816245	0.005405			
Osbpl2	0.813058	0.00692			
Pls3	0.819058	0.00692			
Dtx4	0.781917	0.023557			
Id2 *	1.368282	0.026093			
Mcf2l	1.210003	0.027656			
Slc38a2	0.736603	0.027698			
Twist2	1.262217	0.035958			
Tpcn1	0.836711	0.040962			

Table A-1 Significant hits from differentiating myoblasts - 6 hour microRNA Array results.
Ratio compared to control and p val diff = p value of the difference between treatment and control. * see below

* potential genes of interest.

Eif4ebp2	Negative regulator of translation
Id2	Inhibitor of differentiation
CTGF	TGF-β responsive gene

Differentiating myoblasts - 24 hour microRNA Array results

Significant hits from the microArray of treatment of differentiating C2C12 myotblasts with myostatin for 24 hours. (See Chapter 4 for more details).

Gene	Ratio	P val diff
Hes6 *	0.67077	1.93E-09
Ddx58	0.68241	2.04E-07
Edg5	1.505408	2.04E-07
Mtap7d1	1.486597	2.04E-07
Mcm6	0.694128	6.39E-07
Cdca8	0.68199	1.13E-06
Gyg	0.713219	1.13E-06
Suclg1	0.641688	1.13E-06
Nol5a	0.653888	1.38E-06
Cybasc3	1.43205	3.30E-06
Ywhaq	1.454017	3.30E-06
Eef2	0.6418	4.63E-06
Ankrd1	0.67338	6.45E-06
Nipsnap3a	0.658705	7.98E-06
1110038F14Rik	1.455819	9.08E-06
2500002L14Rik	0.725426	1.55E-05
Ndufs2	0.701354	1.62E-05
4933426M11Rik	1.451476	2.34E-05
LOC100044862	1.390789	2.34E-05
Tsc22d1	0.552042	2.57E-05
Cct3	0.679166	2.62E-05
Tmem63a	1.384494	2.93E-05
BC038286	1.376224	4.73E-05
Surf2	0.750129	5.76E-05
Ppp3ca	1.369708	6.35E-05
Dap3	0.701214	7.69E-05
2700062C07Rik	0.753319	8.18E-05
Acaa2	1.467964	0.000157
Chrnd	0.73235	0.000174
Mxra8	0.718393	0.000175
St3gal4	1.361602	0.000205
Srm	0.730111	0.000237
Oprs1	0.748927	0.000249
Polr2d	0.709624	0.000256
Slc12a3	1.342407	0.000264
Atp5j	0.76499	0.000281
Tef	1.733794	0.000281
Srpx2	0.737354	0.000298
Gpr108	0.763175	0.000487
Lrrfip1	1.38352	0.000505
Phf13	1.34181	0.000548
Iap	1.332438	0.000609
Kdelc1	1.328012	0.000609
1110059P08Rik	1.362805	0.000699
Gnas	0.708594	0.000799
Stx8	0.698921	0.000873
Ddb1	1.509062	0.000906
Mlf2	0.702553	0.000906
3000004C01Rik	0.775027	0.000909

Birc5	0.599834	0.00102
Fblim1	1.314092	0.00105
Rem1	1.33028	0.001129
Pitpnm1	1.37564	0.001142
Gmppa	0.73778	0.001253
Tssc1	0.739146	0.001253
Dnajb6	1.391504	0.00128
Atg2a	1.417639	0.001328
Ppp2r4	1.40567	0.001328
Eef1e1	0.711894	0.001336
Wipf2	1.432789	0.001417
Gtf3a	0.753687	0.001541
Arl2bp	0.728577	0.001778
Ccng1	1.407205	0.001912
Trpc4ap	0.773971	0.001912
Golga2	1.429314	0.001925
Ing4	1.461826	0.001925
Islr	1.50628	0.001925
P4ha1	1.306324	0.002001
Tmem85	0.784032	0.00201
Gpx1	0.780481	0.002145
BC085271	0.787181	0.002178
Cacnb1	1.320822	0.002178
Crebl1	1.304464	0.002178
Ltbp3	0.697225	0.002178
Rsn	1.325749	0.002178
Myg1	0.775934	0.002263
Nudt5	0.787838	0.002263
Prnpip1	0.760466	0.002263
2610019P18Rik	1.301281	0.002315
2500003M10Rik	1.383181	0.002526
Nudc	0.784613	0.002526
Ptrh2	1.330816	0.002526
B020018G12Rik	1.295865	0.00254
Polr2d	0.749141	0.002728
Itgb1	1.522977	0.002835
Raly	0.769651	0.002835
Eif4a1	0.790795	0.002858
Oas2	0.631732	0.002916
Adh5	0.721364	0.003054
LOC667609	0.784123	0.003054
Rnpc2	1.310011	0.003054
Klhl21	1.361333	0.003054
Cyb5r3	1.499971	0.003238
Flii	1.307213	0.003238
Rpl24	0.790436	0.003238
Eftud2	1.296555	0.003401
Fkbp2	0.792577	0.003401
EG433923	0.716714	0.003401
Rab24	0.755606	0.003448
Isca1	0.793662	0.003457
Nat5	0.780506	0.003457
Polr2d	0.769001	0.003457
Actn3	0.787796	0.003517
Stx12	1.280777	0.003761
Tpm3	0.663675	0.004766
Spc25	0.796372	0.00508
Ankrd1	1.285208	0.005151

Egln2	1.35971	0.005798
Med10	0.753269	0.005864
Polr2e	0.800055	0.005904
Hes6	0.754804	0.005946
Mrpl43	0.753826	0.006039
Plscr2	1.302347	0.006363
Ibtk	1.281455	0.006556
Nt5c3l	0.768689	0.007036
Sumo3	0.791385	0.007725
Nsdhl	0.591592	0.008154
Bcap29	0.771979	0.008941
Pmp22	0.65942	0.008941
Pmm2	0.715132	0.009022
LOC100047856	1.55964	0.009096
Ric8b	1.396726	0.009096
Sharpin	1.264366	0.009096
Tipin	0.754773	0.009096
Apip	0.77211	0.009343
Prr3	1.322145	0.009343
Stat2	0.803049	0.009467
Calm3	1.268908	0.009971
Golga7	0.74175	0.009971

Table 8-2 Significant hits from differentiating myoblasts treated with myostatin - 24 hour microRNA Array results. Ratio compared to control and p val diff = p value of the difference between treatment and control. There were no significant hits for GDF-15 treatment.* see below.

*potential genes of interest

HES6 Transcription factor involved in the regulation of differentiation**.**

4 day GDF-15 treatment of differentiated myotubes – microRNA Array results.

Significant hits from the microRNA Array of 4 day treatment of differentiated myotubes with GDF-15. (See Chapter 4 for more details).

Gene	Ratio	p value diff
Dhcr24	1.41646	2.96E-06
Slc2a6	1.277148	2.96E-06
Cyr61 *	0.774207	1.93E-05
AI837181	1.45115	0.000221
Slc30a6	0.794853	0.000221
Suox	1.237391	0.000372
Trim54	1.240558	0.000372
Cav1	0.808125	0.000379
Glt8d3	1.387861	0.000484
Gpr176	0.711665	0.000604
Igf2*	0.792035	0.000779
Ccl25	1.277468	0.001198

Tspan32	1.240218	0.001198
Itga3	0.77767	0.001777
Tnni1	1.392912	0.002812
Myh8	0.825201	0.003422
Rtkn	1.213962	0.004767
Uba1*	1.216063	0.004845
8030451F13Rik	0.80211	0.008073
Acta2	0.836448	0.010137
Xist	0.809834	0.010137
Cbr1	1.203184	0.010552
Cox7a2	0.78909	0.010552
Nqo2	1.191264	0.010552
9130005N14Rik	0.804467	0.010813
Mxra7	1.338052	0.017653
Emp3	1.177319	0.018464
Gcnt2	0.840984	0.019639
Smpdl3b	0.777131	0.022591
Tax1bp1*	0.848191	0.028922
Dstn	0.848682	0.029607
Myh8	0.754609	0.03196
Hist1h2bk	1.170608	0.033829
Shisa4	1.283352	0.034776
Nrbp2	0.829223	0.036241
Cmtm6	1.177944	0.046605
Prpf38b	0.804518	0.046605
2410129H14Rik	1.170109	0.047856
Gosr2	0.847394	0.047856
LOC545013	1.263417	0.049198

Table 8-3 4 day GDF-15 treatment of differentiated myotubes – microRNA Array results.
Ratio compared to control and p val diff = p value of the difference between treatment and control. * see below.

*potential genes of interest

CYR61	TGF-β responsive gene
IGF-2	Insulin-like growth factor – 2
Uba-1	Ubiquitin cycle protein
Tax1bp1	antiapoptotic

Appendix A3 – David analysis of MiRWALK microRNA targets.

	Term	Count	%	PValue	Fold Enrichment	Bonferroni	Benjamini	FDR
KEGG_PATHWAY	hsa04320:Dorso-ventral axis formation	9	0.6	0.0007	4.31	0.11	0.11	0.81
KEGG_PATHWAY	hsa04310:Wnt signalling pathway	24	1.59	0.0031	1.9	0.43	0.13	3.77
KEGG_PATHWAY	**hsa04350:TGF-beta signalling pathway**	**16**	**1.06**	**0.005**	**2.2**	**0.59**	**0.14**	**5.97**
BIOCARTA	h_ck1Pathway:Regulation of ck1/cdk5 by type 1 glutamate receptors	6	0.4	0.0086	4.25	0.89	0.89	10.62
KEGG_PATHWAY	hsa04114:Oocyte meiosis	18	1.2	0.009	1.96	0.8	0.15	10.5
BIOCARTA	h_pmlPathway: Regulation of transcriptional activity by PML	6	0.4	0.0168	3.68	0.99	0.88	19.75
KEGG_PATHWAY	hsa04520:Adherens junction	13	0.86	0.0244	2.02	0.99	0.21	26.23
KEGG_PATHWAY	hsa04510:Focal adhesion	26	1.73	0.0267	1.55	0.99	0.21	28.3
KEGG_PATHWAY	hsa04010:MAPK signalling pathway	32	2.13	0.0342	1.43	1	0.24	34.85
KEGG_PATHWAY	hsa04062:Chemokine signalling pathway	24	1.59	0.0366	1.54	1	0.24	36.76
BIOCARTA	h_telPathway: Telomeres, Telomerase, Cellular Aging, and Immortality	6	0.4	0.0366	3.07	1	0.96	38.48
KEGG_PATHWAY	hsa04360:Axon guidance	18	1.2	0.0382	1.67	1	0.24	38.08
KEGG_PATHWAY	hsa04512:ECM-receptor interaction	13	0.86	0.0444	1.85	1	0.27	42.83

Table 8-4 to show results of DAVID analysis. Predicted targets of miRs 1, 133a, 181a and 499 from mirWALK were combined to generate significant analysis for significant pathways

Appendix A4 – Publications, presentations and prizes.

Publications

Molecular Mechanisms of Intensive Care Unit-Acquired Paresis

Bloch S, Polkey MI, Griffiths M, Kemp P

European Respiratory Journal 2012 Apr;39(4):1000-11

Sustained elevation of circulating growth and differentiation factor-15 and a dynamic imbalance in mediators of muscle homeostasis are associated with the development of acute muscle wasting following cardiac surgery.

Bloch SA, Lee JY, Wort SJ, Polkey MI, Kemp PR, Griffiths MJ.

Critical Care Medicine. 2013 Apr;41(4):982-9.

Increased expression of GDF-15 may mediate ICU-acquired weakness by down-regulating muscle microRNAs.

Bloch SA, Lee JY, Syburra T, Rosendahl U, Griffiths MJ, Kemp PR, Polkey MI.

Thorax. 2014 Dec 16. pii: thoraxjnl-2014-206225

MiR-181a: a potential biomarker of acute muscle wasting following elective high-risk cardiothoracic surgery.

Bloch SA, Donaldson AV, Lewis A, Banya W, Polkey MI, Griffiths MJ, Kemp PR

Re-submitted to Critical Care January 2015 under review.

Quadriceps wasting and physical inactivity in patients with COPD.

Shrikrishna D, Patel M, Tanner RJ, Seymour JM, Connolly BA, Puthucheary ZA, Walsh SL, Bloch SA, Sidhu PS, Hart N, Kemp PR, Moxham J, Polkey MI, Hopkinson NS.

Eur Respir J. 2012 Nov;40(5):1115-22.

Presentations

Circulating regulators of acute muscle wasting in the critically ill: GDF-15 a potential novel driver of acute muscle wasting

Bloch S**,** Lee J, Wort S, Polkey M, Kemp P, Griffiths M

British Thoracic Society Winter 2012

Mir-181: a potential biomarker of acute muscle wasting

Bloch S, Griffiths M, Kemp P, Polkey M

British Thoracic Society Winter 2013

GDF-15 regulation of microRNAs; A Novel Mechanism of Intensive Care Unit Acquired Paresis?

Bloch S, Lee J, Griffiths M, Kemp P, Polkey M,

American Thoracic Society May 2014

GDF-15 down-regulation of muscle microRNA drives increased sensitivity to TGF-β signalling; a novel mechanism in intensive care unit acquired weakness.

Bloch SA, Lee JY, Syburra T, Rosendahl U, Griffiths MJ, Kemp PR, Polkey MI.

British Thoracic Society Winter 2014

A paradoxical rise in rectus femoris myostatin (GDF-8) and GDF-15 in response to neuromuscular electrical stimulation in critical care.

Bloch SA, Syburra T, Rosendahl U, Griffiths MJ, Kemp PR, Polkey MI.

British Thoracic Society Winter 2014

GDF-15 driven down-regulation of muscle microRNA drives increased sensitivity to TGF-β signalling; a novel mechanism in intensive care unit acquired weakness.

Bloch SA, Lee JY, Syburra T, Rosendahl U, Griffiths MJ, Kemp PR, Polkey MI.

Intensive Care Society State of the Art meeting – Gold medal presentation 2014

Prizes

American Thoracic Society International Travel Scholarship – 2014

British Lung Foundation Travel Award – 2014

Intensive Care Society State of the Art Meeting – shortlisted for the Gold Medal Award – 2014

Appendix A5 – Medical Research Council Grant Details

Medical Research Council - Clinical Training Fellowship

Awarded February 2010

G0901955